Study of serpins and antifungal peptides in *Manduca sexta*

by

Miao Li

B.S., China Agricultural University, 2014

AN ABSTRACT OF A DISSERTATION

submitted in partial fulfillment of the requirements for the degree

DOCTOR OF PHILOSOPHY

Biochemistry and Molecular Biophysics Graduate Group

KANSAS STATE UNIVERSITY
Manhattan, Kansas

2019

Abstract

Insects initiate innate immune responses after microbial infection. Extracellular proteolytic cascades lead to melanization of pathogens and parasites present in the hemocoel, as well as production of antimicrobial peptides to combat foreign microbes. Serpins are a superfamily of serine protease inhibitors, which regulate the proteolytic cascades by blocking activity of proteases. An antifungal peptide, diapausin, is among the induced antimicrobial peptides in *M. sexta* hemolymph, helping to protect this insect from fungal infection.

Thirty-two serpin genes identified from *M. sexta* genome were characterized. The number of exons in serpin genes varies from 1 to 10, with some conserved intron positions providing evidence of patterns of serpin gene evolution. *MsSerpin-15* and *28* encode 2 and 3 splicing isoforms respectively, with different reactive center loop sequences. Twenty-seven serpin gene products were predicted to be secretory, with amino-terminal signal peptides. An analysis of conserved amino acid residues in the gate, shutter and breach regions of serpins and the pattern of residues in the reactive center loop hinge region suggested that approximately three quarters of *M. sexta* serpin proteins (including splicing isoforms) are functional protease inhibitors. This work benefits the future investigation regarding the evolution, structure, and function of serpins in *M. sexta* and other insects.

Synthetic peptides with the sequences derived from part of the *M. sexta* serpin-3 reactive center loop (RCL) were used to test the hypothesis that they may inactivate serpin-3 by mimicking the insertion of the RCL that occurs during the protease inhibition reaction. Among four RCL-derived peptides with sizes of 5-9 amino acid residues, the shortest peptide, Ac-SVAFS-NH_2, demonstrated the greatest effect on blocking the inhibitory activity of recombinant serpin-3 by enhancing the conversion of serpin-3 from inhibitor to substrate for prophenoloxidase-activating protease-3. Ac-SVAFS-COO^- with improved solubility showed the same effects on serpin-3 as Ac-SVAFS-NH_2. Addition of Ac-SVAFS-COO^--treated recombinant serpin-3 to plasma led to elevated levels of prophenoloxidase activation, suggesting that the serpin in complex with the peptide could not regulate prophenoloxidase-activating proteases. Similar results were observed when the RCL-derived peptide was mixed with plasma, to allow it to interact with endogenous serpin-3. Circular dichroism analysis showed that serpin-3 complexed with Ac-SVAFS-COO^- has a deeper trough at 215 nm compared with the free serpin-3, consistent with a slight difference in secondary structure upon interaction with Ac-SVAFS-

COO^-. Furthermore, the complex of serpin-3 and Ac-SVAFS-COO^- displayed greater heat stability than free serpin-3, which is consistent with the predicted peptide insertion into β-sheet A.

Recombinant diapausin-1 and diapausin-2 blocked growth of *Saccharomyces cerevisiae*, with IC_{50} of 30 μM and 60 μM, respectively. Observation of the cell morphology revealed the disruption of daughter cell separation after cell division, resulting in cell clusters in the presence of diapausin. Morphological analysis revealed that diapausin-1 causes appearance of an elongated mother cell with a small, flattened bud and wider neck, as well as less elliptical shape. The growth of *Candida albicans* and *Candida krusei* was inhibited by diapausin-1, with IC_{50} of 60 μM and 20 μM respectively. Furthermore, diapausin-1 impaired the germination of conidia and hyphal growth of *Beauveria bassiana*, an insect pathogenic fungus. FITC-labeled diapausin-1 bound to the surface of *S. cerevisiae*, and pull-down experiments showed that diapausin-1 binds to β-1,3-glucan, a primary component of fungal cell walls. This study advances our understanding of an insect immune response to fungal infections and may contribute to the identification of new targets for the development of antifungal drugs.

Study of serpins and antifungal peptides in *Manduca sexta*

by

Miao Li

B.S., China Agricultural University, 2014

A DISSERTATION

submitted in partial fulfillment of the requirements for the degree

DOCTOR OF PHILOSOPHY

Biochemistry and Molecular Biophysics Graduate Group

KANSAS STATE UNIVERSITY
Manhattan, Kansas

2019

Approved by:

Major Professor
Michael R. Kanost

Copyright

Abstract

Insects initiate innate immune responses after microbial infection. Extracellular proteolytic cascades lead to melanization of pathogens and parasites present in the hemocoel, as well as production of antimicrobial peptides to combat foreign microbes. Serpins are a superfamily of serine protease inhibitors, which regulate the proteolytic cascades by blocking activity of proteases. An antifungal peptide, diapausin, is among the induced antimicrobial peptides in *M. sexta* hemolymph, helping to protect this insect from fungal infection.

Thirty-two serpin genes identified from *M. sexta* genome were characterized. The number of exons in serpin genes varies from 1 to 10, with some conserved intron positions providing evidence of patterns of serpin gene evolution. *MsSerpin-15* and *28* encode 2 and 3 splicing isoforms respectively, with different reactive center loop sequences. Twenty-seven serpin gene products were predicted to be secretory, with amino-terminal signal peptides. An analysis of conserved amino acid residues in the gate, shutter and breach regions of serpins and the pattern of residues in the reactive center loop hinge region suggested that approximately three quarters of *M. sexta* serpin proteins (including splicing isoforms) are functional protease inhibitors. This work benefits the future investigation regarding the evolution, structure, and function of serpins in *M. sexta* and other insects.

Synthetic peptides with the sequences derived from part of the *M. sexta* serpin-3 reactive center loop (RCL) were used to test the hypothesis that they may inactivate serpin-3 by mimicking the insertion of the RCL that occurs during the protease inhibition reaction. Among four RCL-derived peptides with sizes of 5-9 amino acid residues, the shortest peptide, Ac-SVAFS-NH_2, demonstrated the greatest effect on blocking the inhibitory activity of recombinant serpin-3 by enhancing the conversion of serpin-3 from inhibitor to substrate for prophenoloxidase-activating protease-3. Ac-SVAFS-COO^- with improved solubility showed the same effects on serpin-3 as Ac-SVAFS-NH_2. Addition of Ac-SVAFS-COO^--treated recombinant serpin-3 to plasma led to elevated levels of prophenoloxidase activation, suggesting that the serpin in complex with the peptide could not regulate prophenoloxidase-activating proteases. Similar results were observed when the RCL-derived peptide was mixed with plasma, to allow it to interact with endogenous serpin-3. Circular dichroism analysis showed that serpin-3 complexed with Ac-SVAFS-COO^- has a deeper trough at 215 nm compared with the free serpin-3, consistent with a slight difference in secondary structure upon interaction with Ac-SVAFS-

COO^-. Furthermore, the complex of serpin-3 and Ac-SVAFS-COO^- displayed greater heat stability than free serpin-3, which is consistent with the predicted peptide insertion into β-sheet A.

Recombinant diapausin-1 and diapausin-2 blocked growth of *Saccharomyces cerevisiae*, with IC_{50} of 30 μM and 60 μM, respectively. Observation of the cell morphology revealed the disruption of daughter cell separation after cell division, resulting in cell clusters in the presence of diapausin. Morphological analysis revealed that diapausin-1 causes appearance of an elongated mother cell with a small, flattened bud and wider neck, as well as less elliptical shape. The growth of *Candida albicans* and *Candida krusei* was inhibited by diapausin-1, with IC_{50} of 60 μM and 20 μM respectively. Furthermore, diapausin-1 impaired the germination of conidia and hyphal growth of *Beauveria bassiana*, an insect pathogenic fungus. FITC-labeled diapausin-1 bound to the surface of *S. cerevisiae*, and pull-down experiments showed that diapausin-1 binds to β-1,3-glucan, a primary component of fungal cell walls. This study advances our understanding of an insect immune response to fungal infections and may contribute to the identification of new targets for the development of antifungal drugs.

Table of Contents

List of Figures

List of Tables

Acknowledgements

I would like to express my great appreciation for my major professor, Dr. Michael Kanost for his support, suggestions and encouragement throughout my program. I also thank my committee members Dr. Michal Zolkiewski for his advice on protein structures, Dr. Kristin Michel for her knowledge on serpins and fungi, and Dr. Maureen Gorman for her generous help with protein purification. And I appreciate Dr. Philip Hardwidge for serving as chair for my doctoral defense.

My thanks is expressed to my current and previous lab members. I appreciate Dr. Neal Dittmer for his help in experiments, as well as his wonderful jokes. I thank Lisa Brummet for her supply of *M. sexta* larvae whenever my experiments needed them, and I really appreciate her birthday cakes every year to cure my homesickness. I also want to thank Jake Weber for being supportive and helpful in the lab. Those people who had already left the group should be thanked no matter where they are now. I appreciate Dr. Qasim Al Souhail for always sparing time for me when I had questions. I want to give my special thanks to Dr. Daisuke Takahashi for his career guidance and his humor. My special thanks is expressed to Dr. Hiroko Tabunoki for being around and bringing me motivation during her short visit. Appreciation is expressed to Alex Garcia for helping me through the difficulties with his big heart and optimistic attitudes towards life. I want to thank Dr. Zeyu (Sara) Peng for her encouragement during my first year at KSU.

I want to extend my thanks to my collaborators and researchers who provided assistance for my projects. My appreciation is expressed to Dr. Haobo Jiang's group at Oklahoma State University for their help with serpin genes. I thank Susan Whitaker for her help with peptide synthesis and mass spectrometry. My thanks is expressed to Dr. Govind Vediyappan from the Division of Biology, KSU, for helping with *Candida* assays. Joel Sanneman from KSU CVM Confocal Facility for training and assistance on use of confocal microscope.

My friends gave me great support when my family was not here with me. I want to thank Xiaorong Liu, Haoyu Zhang. Chenshuang Lu, Zhenhua Sun, Hao Xu, Ye Zou, Taihao Yang, Yu Song for their friendship, outgoing support and making me not feel alone. My special thanks is expressed to my best friend, Yujing Wang, for always being with me and sharing my happiness and sorrows, even she lives across the ocean.

At last, I want to thank my parents, who never doubt my ability and always give me trust, support, encouragement and unconditional love. I could not have gone so far without them.

Dedication

I dedicate this dissertation to my parents, Qiong Xia and Suigong Li, for their unconditional love and support in the past 28 years.

Chapter 1 - Literature Review

Innate Immune Responses in Insect

In order to survive different kinds of invading pathogens, organisms have evolved efficient and robust defense mechanisms to protect themselves by suppressing or killing infectious microbes (Buchmann, 2014). The innate immune system uses natural barriers, phagocytes, and soluble mediators to take immediate effect upon invasion of foreign microorganisms. In contrast, the adaptive immune system tailors the response towards specific antigens and produces corresponding antibodies to attack foreign invaders (Delves et al., 2017; Coico and Sunshine, 2015). Innate immune responses are extensively relied on by invertebrates which lack adaptive immunity. Vertebrates, with powerful and specific adaptive elements, still retain the innate immune functions, which prompt self-defense immediately upon infection. Potentially constituting 90% of the animal life forms on earth, insects have adapted to most environments on land (Erwin, 1997), which, to some extent, must benefit from the vital role that innate immune responses play throughout the insect lifetime.

Recognition of foreign bacteria, fungi or parasites in the hemolymph is carried out by various pattern recognition receptors (Hoffmann et al., 1999). Downstream protective responses are triggered by the binding of pattern recognition receptors to pathogen associated molecular patterns absent in insects, such as lipopolysaccharide on Gram-negative bacteria, peptidoglycan on most bacteria, and β-1,3-glucan on fungi (Kanost et al., 2004). Fat body and humoral effectors in the hemocoel coordinately mediate a series of defense actions, including phagocytosis, encapsulation and nodulation, melanization and synthesis of antimicrobial peptides/proteins (Horohov and Dunn, 1983; Hughes et al., 1983; Zhu et al., 2003a).

Prophenoloxidase activation, a proteolytic cascade leading to melanization of pathogens and parasites, is one of the most important defensive components in insects (Ashida, 1998; Kanost and Gorman, 2008). In *M. sexta*, it was discovered that binding of β-1,3-glucan to β-1,3-glucan recognition protein induces autoactivation of hemolymph protease14 (HP14), followed by activation of hemolymph protease 21 (HP21) and hemolymph protease 2 (HP2) by HP14 (Wang and Jiang, 2006; Wang and Jiang, 2010; Takahashi et al., 2015; Wang and Jiang, 2007; He et al., 2018; Gorman et al., 2007). Prophenoloxidase-activating protease 2 and 3 (PAP2, PAP3) are then activated by HP21 and/or HP2. The PAPs then cleave and activate prophenoloxidase

(proPO), the enzyme responsible for initiating melanin production (Wang and Jiang, 2007; Gorman et al., 2007; He et al., 2018; Gupta, et al., 2005; Wang et al., 2014; Jiang et al., 1998).

Another hemolymph protease cascade induced by microbes leads to activation of the cytokine Spätzle and expression of antimicrobial genes via activation of Toll pathway or Imd pathway (An et al., 2009; An et al., 2010; Myllymaki et al., 2014). Genomic annotation in many insects, such as *D. melanogaster*, *M. sexta*, *Bombyx mori*, *Anopheles gambiae*, and *Apis mellifera*, leads to the expectation that more serine proteases and serine protease homologs are likely to be involved in the activation of immune cascades (Cao et al., 2015b; Kanost and Jiang 2015; Cao et al., 2017; Zhao et al., 2010; Veillard et al., 2016; Zou et al., 2006). Serine protease cascades must be regulated to prevent damage caused by immune factors in tissues. A superfamily of serine protease inhibitors, serpins, is well characterized to be critical in the regulation of extracellular proteolytic cascades in insects (Jiang et al., 2003; Jiang et al., 2009; Park et al., 2011; Levashina et al., 1999; Ahmad et al., 2009; Zou and Jiang, 2005; An and Kanost, 2010; An et al., 2011c; Zou et al., 2010; Abraham et al., 2005; Michel et al., 2006; An et al., 2011a; Ligoxygakis et al., 2002; De Gregorio et al., 2002; Scherfer et al., 2008; Tong et al., 2005; Tong and Kanost, 2005; Tang et al., 2008; Zhu et al., 2003b; Wang and Jiang, 2004; Wang and Jiang, 2006; He et al., 2017b; Yang et al., 2018).

Toll and Imd signaling pathways, which transduce extracellular messages of foreign invasion into the nuclei of cells, trigger the transcriptional activation of immune-related genes (Gillespie et al., 1997; Cao et al., 2015a; Buchon et al., 2014). In *D. melanogaster*, the Toll signaling pathway is active in fat body and induces expression of antimicrobial peptides, such as drosomycin, through translocation to the nucleus of NF-κB transcription factor Dif, while the Imd signaling pathway is active particularly in gut and induces the expression of antimicrobial peptides, such as diptericin, through the NF-κB transcription factor Relish (Buchon et al., 2014). More antimicrobial peptides and proteins from diverse insect species have been discovered and characterized, such as defensins from Diptera, Hymenoptera, Coleoptera, Lepidoptera, Hemiptera, Isoptera, and Odonata, cecropins from Diptera, Coleoptera, Lepidoptera, and Isoptera, proline-rich antimicrobial peptides from Hemiptera, Hymenoptera, Lepidoptera, and Diptera, and moricins and gloverins from Lepidoptera (Yi et al., 2014).

Serpins

Serpins are a superfamily of proteins with conserved tertiary structure, containing three β-sheets, 8-9 α-helices and a solvent-exposed reactive center loop (RCL) (Silverman et al., 2001). The distribution of serpins is broad, present in viruses, unicellular prokaryotes, unicellular eukaryotes, archaea, plants, invertebrates, and vertebrates (Turner et al., 2007; Irving et al., 2002; Gettins, 2002; Roberts and Hejgaard, 2008; Meekins et al., 2017; Gettins and Olson, 2016). Most serpins act as serine protease inhibitors, whereas some are non-inhibitory serpins with various physiological functions, including acting as storage proteins, hormone transporters and molecular chaperones (Gettins and Olson, 2016; Huntington and Stein, 2001; Carrell and Read, 2017; Widmer et al., 2012). Mammalian serpins regulate proteases in vital physiological processes, such as hemostasis, fibrinolysis, blood clotting and inflammation (Rau et al., 2007).

More novel functions of serpins were investigated in the past decades. For example, some serpins expressed by orthopox viruses were discovered to be caspase inhibitors, regulating the apoptotic response (Pickup, 1994; Dobbelstein and Shenk, 1996). Human maspin is a well-known tumor suppressor and a potential prognostic indicator for various types of cancers (Zhou et al., 1994; Berardi et al., 2013). High abundance of human α_1-antichymotrypsin and its direct interaction with Aβ in Alzheimer's plaques imply certain functions in Alzheimer's pathogenesis (Baker et al., 2007). Some mutations can lead to the polymerization of serpin molecules, resulting from aberrant conformational changes by misplacing the RCL in an adjacent serpin molecule (Gooptu and Lomas, 2009). Serpinopathy was designated to describe the diseases caused by serpin polymerization.

Serpin conformations

Many crystal structures of serpins are available with various conformational forms in PDB (http://www.rcsb.org). Slight folding differences, especially the status and relative positions of the RCL, define several serpin forms with particular properties. The native form features a complete solvent-exposed RCL with potential inhibitory activity against serine proteases. The RCL in this state is usually not structurally characterized due to its flexibility. Two residues flanking the scissile bond cut by a protease in the inhibition reaction are designated as P1 and P1'. Residues on the amino-terminal side of scissile bond are numbered in a direction of C- to N-terminus: P2, P3, P4…and so on. Residues on the carboxyl-terminal side of the scissile bond are

numbered in a direction of N- to C- terminus: P2', P3', P4'…and so on. A determined native structure of *M. sexta* serpin-1K is shown in Figure 1-1A (Li et al., 1999). The native form of serpins is quite vulnerable and least stable among all forms, with average melting temperature of 58°C (Kaslik et al., 1997).

The cleaved form of serpin is the product of proteolysis at the scissile bond of the native form. The N-terminal part of the RCL is inserted into β-sheet A as the 4th strand (Fig. 1-1B). The cleaved form is the most stable serpin conformation, with melting temperature >110°C (Bruch et al., 1988; Hervé and Ghélis, 1990).

The latent serpin form is recognized by the insertion of the intact RCL into β-sheet A as the 4th strand (Fig. 1-1C). The difference between the latent and cleaved forms is the stretch of β-sheet C 1st strand following RCL due to relocalization of the entire RCL (Stout et al., 2000). The resulting absence of exposed RCL as a bait deprives the inhibitory function of the serpin, while significantly stabilizing the conformation, with a melting temperature of 85-90°C (Onda et al., 2005).

The delta form of serpin is only characterized in α_1-antichymotrypsin as one naturally occurring variant (Gooptu et al., 2000). As shown in Figure 1-1D, partial incorporation of the intact RCL occurs up to P12 into β-sheet A, while the last turn of helix F and the loop connecting s3A unwind and are recruited to β-sheet A as well. This inactive form is believed to be an intermediate conformation during folding or misfolding (Gooptu et al., 2000).

The "polymer" form of serpin results from insertion of the RCL into β-sheet A of another serpin molecule, known also as the "loop-sheet" model or "domain-swapping" model (Fig 1-1E) (Ekeowa et al., 2010; Santangelo et al., 2012; Yamasaki et al., 2010; Yamasaki et al., 2011; Huntington and Whisstock, 2010). Serpinopathies refer to those diseases that arise from serpin aberrant polymerization, as a consequence of point mutation in a serpin gene that favors the polymeric form. For example, the Z-variant of α_1-antitrypsin has a substitution of glutamate 342 to lysine, which results in accumulation of polymerized α_1-antitrypsin within hepatocytes and lung (Lomas et al., 1992; Elliott et al., 1998). Pathogenesis of cirrhosis, hepatocellular carcinoma, neonatal hepatitis and emphysema are associated with Z-variant polymerization (Gooptu et al., 2014).

Mechanism of serpin inhibition

Unlike canonical serine protease inhibitors, such as Kazal, Kunitz and Bowman-Birk inhibitors, serpins adopt a so-called "suicide" mechanism to inhibit serine proteases (Bode and Huber, 1992). The inhibition of a protease by a serpin includes cleavage by the protease of a specific "scissile" bond between residues designated P1-P1' in the serpin RCL (Loebermann et al., 1984). A noncovalent complex between the protease and serpin is formed though interaction of the protease active site and the serpin RCL (Ye et al., 2001). After the P1 residue is correctly positioned in the primary specificity pocket of the protease, the serine in the active site attacks and cleaves the scissile bond, leading to the formation of a covalent acyl complex of protease and serpin. This cleavage triggers a dramatic conformational change, in which the RCL is incorporated into β-sheet A as a new strand (s4A) (Stratikos and Gettins, 1999; Huntington et al., 2000). Translocation of the protease is accompanied by permanent distortion of the protease active site, such that the second half of the hydrolysis reaction does not occur. The protease is trapped in a covalent complex with the serpin (Gettins and Olson, 2016).

Formation of the non-covalent Michaelis complex is the first step for irreversible inhibition of a protease by a serpin. Structures of 11 serpin-protease Michaelis complexes have been investigated by NMR or X-ray crystallography so far (Peterson et al., 2000; Ye et al., 2001; Baglin et al., 2002; Dementiev et al., 2003; Dementiev et al., 2004; Li et al., 2004; Johnson et al., 2006; Li et al., 2008; Lin et al., 2011; Gong et al., 2015). It was revealed from the determined structures that the non-covalent Michaelis complex formation does not cause the tertiary structure change to either protease or serpin main body. The conformation of the serpin RCL in the Michaelis complex resembles that of small canonical inhibitors (Pearce et al., 2007). The P1 residue of the serpin RCL fits in the active site of the protease, with the aid from contacts of subsites on protease and residues flanking the RCL scissile bond (Peterson et al., 2000; Ye et al., 2001; Baglin et al., 2002; Dementiev et al., 2003; Dementiev et al., 2004; Li et al., 2004; Johnson et al., 2006; Li et al., 2008; Lin et al., 2011; Gong et al., 2015).

Through formation of the acyl intermediate between protease and serpin, hydrolysis of the scissile bond on a serpin RCL occurs, immediately followed by RCL insertion into β-sheet A as a new strand between s3A and s5A, resulting in the translocation of protease by over 70 Å (Stratikos and Gettins, 1998; Stratikos and Gettins, 1999; Fa et al., 2000). Rapid insertion of the cleaved RCL is critical for efficient inhibition. A serpin acts as predominately a substrate rather

than inhibitor if the overall rate of proteolysis and subsequent release of cleaved serpin is greater than that of loop insertion and subsequent distortion of the protease active site (Gettins, 2002).

Rapid loop insertion requires the coordination of several flexible regions in the serpin, named the hinge, shutter, breach, and gate (Stein and Carrell, 1995; Whisstock et al., 2000). The breach, at the entrance where cleaved RCL begins to insert, has highly conserved residues allowing a hydrophobic core to accept a new strand. The shutter region, the main part on β-sheet A that opens and accepts the cleaved RCL, is essential for promoting the inhibition reaction. The gate region is responsible for accommodating the dramatic translocation of the protease. The hinge region (P17-P9) of inhibitory serpins is typically composed of residues with small side chains, which contribute to the mobility for conformational change of the RCL (Hopkins et al., 1993). A consensus pattern in the hinge region is conserved in inhibitory serpins. P17 is usually glutamate, P16 is glutamate/lysine/arginine, P15 is glycine, P14 is threonine/serine, and P12-P9 are alanine/glycine/serine (Irving et al., 2000). Additionally, studies showed that mutations to place a proline in the proximal RCL prior to P2 residue disrupts the formation of a new β strand, blocking RCL incorporation (Hopkins et al., 1993; Hopkins and Stone, 1995; Gettins, 2002). Sufficient length of RCL is necessary to assist the full insertion into β-sheet A (Huntington, 2011). Determination of crystal structures of cleaved human antitrypsin (AT), serpin protein Z-dependent proteinase inhibitor (ZPI), protein C inhibitor (PCI) and plasminogen activator inhibitor-1 (PAI-1) demonstrated a requirement for at least 16 residues in the RCL prior to the scissile bond in RCL for full insertion (Schreuder et al., 1994; Huang et al., 2010; Li and Huntington, 2008; Jensen and Gettins, 2008).

Specificity of serpins as inhibitors against proteases is a topic more complicated than serine protease specificity against substrates. Though serpin specificity largely relies on the P1 residue, recent studies discovered more determinants that can provide a more complete explanation for specificity exceptions. For example, residues flanking the scissile bond contribute to complementary interactions with subsites on the target protease, which affect the selection of protease to be inhibited. Furthermore, RCL dynamics and the local electrostatics also contribute to the specificity (Gettins, 2002; Marijanovic et al., 2019).

Arthropod serpins

Sequences of serpin proteins across species may have only 20% identity in spite of common tertiary structures (Irving et al., 2000). Arthropod serpins lack orthology with mammalian serpins and there has been much less research regarding their structures and functions. Arthropod serpins, mostly with inhibitory activity, regulate a wide range of physiological processes, such as proPO activation, Toll pathway activation, development, reproduction, and host-pathogen interactions (Meekins et al., 2017). With the completion of many insect genome projects, identification of novel serpin genes and further studies regarding the evolution, structure and function are starting to thrive. There are at least 36 species from 7 insect orders with publications to describe serpins from either genome or transcriptome sequencing (Table 1-1). The total number of serpin genes in insect genomes varies from 7 (*Apis mellifera*) to 34 (*Bombyx mori*) (Zou et al., 2006; Zou et al., 2009). Eighteen anopheline mosquitoes throughout the world contain 12-23 serpin genes, implying gene expansion events after the divergence of those species (Neafsey et al., 2015).

Besides gene duplication to diversify serpin variants in a genome, mutually exclusive alternate splicing also occurs in arthropods to expand serpin protein functions. *M. sexta* serpin-1 has 14 different versions of exon 9, each encoding a different RCL, with distinct inhibitory spectra against proteases (Jiang and Kanost, 1997; Li et al., 2018; Jiang et al.,1994). Alternative exon splicing was also adopted by lepidopteran orthologs of *M. sexta* serpin-1 at the same position. *Bombyx mori*, diverged 84 million years ago from *M. sexta* (Wahlberg et al., 2013), has only 3 exon 9 duplicates in its serpin-1 gene, encoding 3 isoforms by using exon 9a, 9b or 9c (Liu et al., 2011). Serpin-1 from *Choristoneura fumiferana* generates 4 isoforms via alternative exons encoding the RCL (Zheng et al., 2009). The *Mamestra configurata* serpin-1 gene encodes 9 variants through alternative exon 9 usage (Hegedus et al., 2008). Additionally, by using alternative splicing exons, *Pteromalus puparum* serpin-1, *Anopheles gambiae* SRPN10 and *Drosophila melanogaster* Spn4 are able to express RCL variants (Yan et al., 2017; Danielli et al., 2003; Börner and Ragg 2008).

There are 14 serpin structures from 6 arthropod species that have been solved by X-ray crystallography (Table 1-2). Most structures are in native form with exposed RCL, while *D. melanogaster* Spn42Da and *Ixodes ricinus* IRS-2 were in cleaved form with proximal RCL incorporated as a strand in β-sheet A (Ellisdon et al., 2014; Kovarova et al., 2010). *M. sexta*

serpin-1B was crystalized in Michaelis complex with rat trypsin, showing the interaction of P3-P3' residues of the RCL with the trypsin active site (Ye et al., 2001). *A. gambiae* SRPN2 and *T. molitor* serpin-48 have a partial insertion of the hinge RCL into β-sheet A, which also occurs in human antithrombin III (An et al., 2011b; Park et al., 2011; Zhang et al., 2015b). However, the partial insertion in SRPN2 did not show the allosteric activation that is associated with partial insertion of hinge RCL in antithrombin (Zhang et al., 2015b). Thus, the function of the short inserted hinge observed in some insect serpins still remains intriguing. Latent form has not been reported in arthropod serpins yet, perhaps because they still remain undiscovered or they are absent in arthropods.

One of the most studied functions of arthropod serpins is regulating proteolytic cascades in the hemolymph. Upon the invasion of foreign organisms, pattern recognition proteins present in hemolymph initiate immune responses by amplifying the infection signal through proteolytic cascades such as the proPO activation pathway. *D. melanogaster* deficient for spn27A was reported to exhibit spontaneous melanization associated with elevated activity of PO, indicating unregulated proPO activation in the absence of spn27A (De Gregorio et al., 2002; Ligoxygakis et al., 2002). A characterized target protease of spn27A in *D. melanogaster* proPO activation cascade is MP2 (Tang et al., 2006). Comparably, knockdown of A. gambiae SRPN2 also resulted in appearance of melanotic pseudotumors on internal tissues (Michel et al., 2005). Biochemical results revealed that activation of proPO was suppressed by SRPN2 via inactivating CLIPB9, a proPO-activating protease (An et al., 2011a). In *Ostrinia furnacalis*, serpin-3 blocks the activation of proPO by irreversibly forming an inhibitory complex with proPO-activating enzyme, SP13 (Chu et al., 2015). In *Tenebrio molitor*, three pairs of serpin-protease were characterized to play important roles in melanization triggered by immune challenge (Jiang et al., 2009).

Serpins are involved in the regulation of Toll pathway as well. The recognition of invading organisms stimulates a proteolytic cascade, which leads to the proteolytic processing of proSpätzle and binding of cytokine Spätzle to the Toll receptor. Extracellular signaling is thus transduced into cells to initiate expression of antimicrobial effectors. Regulation of Toll pathway by serpins was studied in *T. molitor*. A protease MSP, activated by microbial infection, could be inhibited by SPN40, while SAE, proteolytically activated by MSP, is inhibited by SPN55 (Jiang et al., 2009). SPE, which processes proSpätzle, is inhibited by SPN48 (Jiang et al., 2009; Park et

al., 2011). *M. sexta* serpin-1J was found to suppress activation of Toll pathway by inactivating HP8, a Spätzle-processing protease (An et al., 2011c). Mass spectrometry was used to detect *M. sexta* serpin-1A, serpin-1E, serpin-3, serpin-6 and serpin-9 in complex with HP8 in the plasma as well, suggesting their possible roles in regulating HP8 *in vivo* (Ragan et al., 2010; Christen et al., 2012; Zou and Jiang, 2005; He et al., 2017b). HP6, upstream of HP8 in the Toll pathway, formed complexes in *M. sexta* plasma with serpin-4, 5, 9 and 13, which might be HP6 regulatory factors *in vivo* (An and Kanost, 2010; He et al., 2017b). In *D. melanogaster*, Spn1 (Spn42Dd) regulates the Toll pathway induced by GNBP3 over-expression (Fullaondo et al., 2011).

Besides the well-studied functions of serpins in regulating innate immune responses, serpins are also engaged in other physiological processes identified in *D. melanogaster*. *D. melanogaster* Spn27A regulates activation of the Toll pathway to control embryonic dorsal-ventral axis formation (Ligoxygakis et al., 2003; Hashimoto et al., 2003). Repression of Spn5 (Spn88Ea) expression resulted in defective wing expansion during eclosion (Charron et al., 2008). Spn76A, a non-inhibitory serpin, is accumulated in the female *Drosophila* genital tract during mating, while Spn28B and Spn28F with putative inhibitory activity, are highly expressed in the male accessory gland (Reichhart et al., 2011; Coleman et al., 1995). But the specific functions of those serpins still remain elusive.

Secretory serpins found in insect venom or saliva are likely to mediate the interactions between parasites and hosts. Parasitoid wasps contained several serpins in the venom and one of them, LbSPNy was discovered to suppress melanization in host hemolymph, possibly by interacting with serine proteases within the activation cascade (Colinet et al., 2009). Blood-feeding arthropods, such as mosquitoes and ticks, use proteins in saliva to interfere with host hemostasis and anti-inflammatory actions (Rau et al., 2007). Recombinant serpin IRS-2 from a tick, *I. Ricinus* inhibited human cathepsin G and mast cell chymase, which are proinflammatory proteases in host blood (Chmelar et al., 2011). Alboserpin from saliva of a mosquito, *Aedes albopictus*, not only tightly binds to Factor Xa in a reversible manner to inhibit its activity, but also binds to heparin and phospholipids, which might help to localize and concentrate alboserpin at proper sites to prevent clotting during mosquito feeding. The injection of recombinant alboserpin into mice significantly delayed thrombosis at the site of vascular injury (Calvo et al., 2011).

Manduca sexta serpins

Manduca sexta, commonly known as the tobacco hornworm, is a model insect for biochemical studies because of its large size, ease of rearing and short life cycle (Kanost et al., 2004). Extensive research was conducted in *M. sexta* to understand the mechanisms of insect development, reproduction, and immune responses.

Since the first serpin (serpin-1B) from *M. sexta* was isolated and characterized in 1989 (Kanost et al., 1989), biochemical studies and genetic analyses were implemented for understanding *M. sexta* serpins' roles in physiological processes, especially in humoral defensive responses. A variety of serpins were identified in *M. sexta* hemolymph and linked to roles in regulation of the proPO activation cascade and Toll pathway activation (Meekins et al., 2017). The accomplishment of *M. sexta* whole genome sequencing makes it possible to discover additional serpin genes which have not been revealed by cDNA and transcriptome sequencing (Kanost et al., 2016).

Various commercially available serine proteases have been utilized to characterize the inhibitory selectivity of *M. sexta* serpins (Kanost et al., 1989; Jiang and Kanost, 1997; Gan et al., 2001; Tong and Kanost, 2005; He et al., 2017b; Yang et al., 2018). Unfortunately, RNA interference technique for suppressing expression of plasma proteins has not been successful in our lab with *M. sexta* larvae (Terenius et al., 2011), which adds difficulties to the discovery of interactive proteases *in vivo* and roles that serpins play in particular biological processes. Therefore, generally two methods were developed, aiming at finding potential proteases inhibited by *M. sexta* serpins *in vivo*: (1) Inhibitory assays *in vitro* by using purified recombinant *Manduca* serine proteases, such as PAP1 and PAP3. (2) Immunoaffinity approach in plasma followed by mass spectrometry for identifying serpin-bound proteases. The following paragraphs will summarize the *Manduca* serpins which were hypothesized to regulate immune responses by blocking particular proteases in proPO activation and Toll pathways (Fig. 1-2, Table 1-3).

Investigation of the *M. sexta* serpins started in 1989 with serpin-1B isoform, which is inhibitory against porcine pancreatic elastase and bovine chymotrypsin (Kanost et al., 1989). Later research with other serpin-1 isoforms demonstrated the variety of inhibition selectivity caused by alternatively spliced exon 9-encoding RCL sequences (Jiang et al., 1994; Jiang and Kanost, 1997). A study taking advantage of qPCR, 2D-PAGE and mass spectrometry provided in-depth insights into 12 serpin-1 isoforms (Ragan et al., 2010). The transcripts of serpin-1

isoforms were not abundant in naïve hemocytes, and challenge of *M. luteus* did not significantly induce the expression of any isoform. In contrast, fat body was shown to highly express serpin-1 isoforms, especially serpin-1B, with significantly higher levels than the other isoforms. Serpin-1A, 1E and 1J were detected in complex with HP8 in the naïve hemolymph, and recombinant serpin-1J formed a complex with HP8 *in vitro*, indicating their putative functions in the Toll pathway by inhibiting HP8, which is a proSpätzle-activating enzyme (Ragan et al., 2010; An et al., 2011c). Serpin-1J can also inhibit PAP3 (Jiang et al., 2003). An inhibitory complex was reported to form between recombinant serpin-1I and HP14 *in vitro*, and addition of serpin-1I to plasma significantly suppressed activation of proPO (Wang and Jiang, 2006). An unknown variant of serpin-1 was found in acyl-complex with proHP1, an active conformation without proteolytic activation (He et al., 2017a).

Serpin-2 is an intracellular inhibitor present in *M. sexta* hemocytes. The mRNA level of serpin-2 was highly induced in larvae after injection with bacteria. Purified serpin-2 from hemocytes was only inhibitory against human cathepsin G among tested proteases, which is consistent with the sequence analysis of serpin-2 protein with less similarity to the consensus pattern for inhibitory serpins (Gan et al., 2001). The presence of serpin-2 in hemocytes and induced expression in response to bacterial challenge point to its participation in immune responses, but its physiological function of it still remains unclear.

Serpin-3 is the most studied serpin in *M. sext*a. Serpin-3 is constitutively expressed in hemolymph and can be induced by injection of bacteria or fungi. Recombinant serpin-3 was quite active against PAP1 and PAP3 with complete inhibition at 1.6:1 and 1.9:1 molar ratio (serpin:protease) respectively. PO activation in plasma was suppressed by recombinant serpin-3 in a dose-dependent manner (Zhu et al., 2003b). Immunoaffinity chromatography using serpin-3 antibody pulled down serpin-3 in plasma complexed with PAP1, PAP2, PAP3, and HP8, while another immunoaffinity column using HP1 antibody captured proHP1-serpin-3 complex (Christen et al., 2012). Serpin-3 is likely to modulate both proPO activation and Toll pathway by targeting distinct proteases.

Expression of serpin-4 and serpin-5 is highly induced in fat body upon injection of bacteria, but inhibitory activity of recombinant serpin-4 or serpin-5 against PAP1 or PAP3 was not as potent as that of serpin-3. Recombinant serpin-4 and serpin-5 purified from Sf9 cells blocked 50% amidase activity of PAP-1 at 25:1 and 13:1 molar ratio respectively, and PAP-3 at

40:1 and 17:1 molar ratio respectively. However, recombinant serpin-4 could completely inhibit the PO activation of bacteria-triggered plasma at 0.4 μg/μl, while addition of serpin-5 did not completely block proPO activation (Tong and Kanost, 2005). HP1 and HP6 were covalently complexed with serpin-4 and serpin-5 in plasma activated by Gram-positive or Gram-negative bacteria, but serpin-4 formed a complex with HP21 in plasma induced only by Gram-positive bacteria (Tong et al., 2005). Those results suggested multiple putative target proteases of serpin-4 in both proPO activation and Toll pathway, while serpin-5 might regulate the Toll pathway.

Serpin-6 is constitutively expressed at a low level but highly induced in hemocytes and fat body after bacterial challenge. Recombinant PAP3 was completely inhibited by recombinant serpin-6 at molar ratio of 2:1 (serpin:protease). Ninety percent inhibition of PO activation occurred when 140 μg/ml recombinant serpin-6 was added to induced plasma. Immunoaffinity chromatography using serpin-6 antibody uncovered PAP3 and HP8 in covalent complex with serpin-6 in plasma (Zou and Jiang, 2005). The presence of serpin-6 bound to proHP1 suggested one more putative protease target for serpin-6 *in vivo* (He et al., 2017a). Expression of serpin-7 is constitutive in both hemocytes and fat body, but can be significantly induced in fat body by bacterial challenge. Recombinant serpin-7 exhibited inhibitory activity against recombinant PAP3. Addition of recombinant serpin-7 to plasma resulted in the suppression of PO activation (Suwanchaichinda et al., 2013).

Transcripts of serpin-9 and serpin-13 are abundant in fat body and relatively low in hemocytes. They are the only two *M. sexta* serpins whose expression is downregulated after injection of bacteria. In fat body, serpin-9 mRNA level did not change, while serpin-13 mRNA level significantly decreased. In hemocytes, transcription of both serpin-9 and serpin-13 decreased after bacterial infection. Addition of recombinant serpin-9 or serpin-13 to plasma decreased proPO activation. ProHP1, HP6 and HP8 were discovered to form inhibitory complexes with serpin-9 in plasma, whereas serpin-13 complexes formed with ProHP1, HP2 and HP6 (He et al., 2017b).

Transcription level of serpin-12 remains low in both hemocytes and fat body, but can be significantly up-regulated by injection of bacteria. Recombinant serpin-12 added to plasma reduced the PO activation elicited by *E. coli* or *M. luteus*, as well as the proteolytic activation of several hemolymph protease precursors. Antibodies to serpin-12 pulled down an HP14-serpin-12

complex from plasma, suggesting that HP14 is a putative protease target for serpin-12 *in vivo* (Yang et al., 2018).

In summary, ten *M. sexta* serpins have been studied by biochemical approaches. Nine of them are extracellular proteins circulating in the hemolymph, and seven can be up-regulated in response to bacterial challenge. Their inhibitory activities potentially contribute to the regulation of proteolytic cascades that lead to melanization and antimicrobial peptide synthesis during defensive reactions. Putative target proteases of those *Manduca* serpins have been identified from plasma through immunoaffinity chromatography. However, the full picture of the serpin-protease system in immune responses requires more work in the future.

Serpin RCL-derived Peptides

Serine protease inhibition by serpins relies on rapid insertion of the proximal RCL after formation of the acyl complex with a protease (Loebermann et al., 1984; Carrell and Travis 1985). Therefore, reducing the overall rate of loop insertion can switch an inhibitory serpin to a protease substrate (Gettins, 2002). One approach to block serpin function is to pre-occupy the spot where the RCL will translocate. Synthetic peptides with sequences copied from serpin RCL hinge regions were discovered to be inhibitors of serpins by forming a stable complex with them and subsequently preventing RCL incorporation (Jendrny and Beck-Sickinger, 2015). Nomenclature of RCL-derived peptides simply follows the numbering rules for the RCL. For example, peptide P14-P10 stands for the sequence mimicking the P14-P10 residues of the original serpin RCL.

Structure of serpin•RCL-derived peptide binary complexes

There are several structures of serpin:RCL-derived peptide complex characterized by X-ray crystallography: PAI-1•2P14-P10, PAI-2•P14-P1, antithrombin•P14-P3, antithrombin•P14-P8•WMDF and antithrombin•P14-P9•MLF (Fig. 1-3) (Xue et al., 1998; Jankova et al., 2001; Skinner et al., 1998; Zhou et al., 2004). Crystal structures demonstrate that RCL-derived peptides are positioned as a new strand between s3A and s5A, with hydrogen bonds formed to stabilize the structure, which considerably resembles the corresponding endogenous RCL in an inhibitory complex, latent serpin form, and cleaved serpin form.

In antithrombin the hinge region is partially inserted into β-sheet A in the native state, which is associated with heparin-mediated activation of antithrombin (McCoy et al., 2003; Schreuder et al., 1994). This short insertion is believed to restrict the flexibility of the RCL and reduce its accessibility to target proteases. Conformational changes of antithrombin can be triggered by binding of heparin to helix D, leading to the extension of the hinge insertion and full expansion of the RCL. As a result, fully stretched RCL becomes more vulnerable to protease factor Xa, with rate of proteolysis increased by 265-fold (Olson et al., 1992). Once complexed with peptide P14-P3, native antithrombin extends the inserted hinge region, and the rate of factor Xa proteolysis increased by 36-fold (Skinner et al., 1998), converting antithrombin from an inhibitor to a substrate of factor Xa. The antithrombin•P14-P3 structure provides the insights of the molecular mechanism for an RCL-derived peptide acting as serpin inhibitor.

A structure of PAI-1 with two molecules of peptide P14-P10 annealing between s3A and s5A was different from the other 1:1 complexes of serpins with RCL-derived peptides (Xue et al., 1998). One of the peptides was positioned as predicted in the space where P14-P10 residues on RCL are meant to be when incorporation occurs, whereas the other peptide was found unexpectedly to be placed where P6-P2 residues are meant to be after RCL incorporation (Xue et al., 1998). It still remains unclear whether the binding of these two identical peptides is cooperative or sequential, and whether there is a significant difference in binding affinity of these two sites.

Two other serpin•RCL-derived peptide structures were formed with non-serpin derived peptides. Synthetic peptides, WMDF and formyl-MLF were found to be localized with P14-P8 and P14-P9 respectively within β-sheet A (Zhou et al., 2004). WMDF and formyl-MLF fit into the place where P6-P4 residues on RCL would anneal. The concurrence of one RCL-derived peptide and one exogenous peptide in s4A position might enlighten the design of therapeutic peptides intended to interrupt serpin functions.

Inhibitory effects of RCL-derived peptides on serpins

Structures of serpin•RCL-derived peptide complexes confirmed the insertion of synthetic peptides within β-sheet A, which abolishes the incorporation of the RCL and increases the vulnerability of the RCL to proteolysis. In agreement with structures, biochemical assays of RCL-peptide bound serpins demonstrated the transition from inhibitors to substrates (Table 1-4).

Investigations of RCL-derived peptides are performed frequently with human serpins, including α_1-antitrypsin, antithrombin, PAI-1 and PAI-2. The length of those serpin-blocking peptides varies from 15 to 5 amino acid residues, with mostly mimicking the hinge RCL, which tends to have small, hydrophobic residues, allowing this flexible sequence to drive the incorporation of the N-terminal RCL into β-sheet A during protease inhibition (Irving et al., 2000).

Synthetic peptides with sequences spanning P15 or P14 to P1 of the RCL were the first to be described as a counterpart of the incorporated strand A4. Specifically, P15-P1 from α_1-antitrypsin, P14-P1 from antithrombin, P14-P1 from PAI-1 and P14-P1 from PAI-2 were shown to convert corresponding serpins from an inhibitor to a substrate (Mast et al., 1992; Schulze et al., 1990; Björk et al., 1992; Eitzman et al., 1995; Jankova et al., 2001). Furthermore, research with human α_1-antitrypsin revealed that peptides representing the proximal RCL (P14-P4 and P14-P8) are sufficient to substantially inhibit antitrypsin activity, while those peptides representing the distal part of the RCL (P10-P1, P9-P1 and P8-P1) were much less efficient in blocking α_1-antitrypsin (Schulze et al., 1992). Similar results were observed in PAI-1 as well. PAI-1 complexed with P14-P9, lost nearly all of its inhibitory activity against uPA, whereas P8-P3 resulted in 60% reduction of inhibitory activity against uPA (D'Amico et al., 2012).

Evidence of conformational changes caused by the insertion of RCL-derived peptides was observed in α_1-antitrypsin and antithrombin by circular dichroism (CD) at 220nm (Schulze et al., 1990; Schulze et al., 1992; Carrell et al., 1991; Björk et al., 1992). Strands 3A and 5A are parallel in the native serpin before incorporation of the RCL as strand 4A, in a new antiparallel relationship with strands 3A and 5A, which increases the stability of the overall structure (Gettins and Olson, 2016). Native serpins are relatively unstable, with average melting temperature of around 58°C, while the other forms that contain strand 4A have a much higher melting temperature, such as cleaved serpins with >110°C melting temperature (Pearce et al., 2007). Significant increase of melting temperature of antithrombin from 58°C to 85°C after forming complex with peptide P14-P1 is consistent with the contribution of the peptide as strand 4A to thermostability of antithrombin (Björk et al., 1992).

The effect of RCL-derived peptides on serpins may not be very specific. It was reported that P15-P1 RCL peptide derived from α_1-antitrypsin had off-target activity on antichymotrypsin and antithrombin (Mast et al., 1992). P14-P3 peptide from antithrombin was able to inactivate

α_1-antitrypsin (Chang et al., 1996). This may be because inhibitory serpins share a sequence rich in small hydrophobic residues in the hinge region, which is used to design RCL-derived peptides. This significantly impedes the application of RCL-derived peptides in therapies for serpin related diseases. Furthermore, a few cases claimed the induction of antithrombin polymerization in the presence of P14-P8 and P14-P9, but attenuation of polymerization in the presence of longer RCL-derived peptides (Fitton et al., 1997; Chang et al., 1997). The mechanism of this discrepancy is not fully elaborated yet, but may be explained by the exposure of the lower half of the cleft caused by the insertion of a short peptide in the upper half of the cleft. The vacant site in the lower cleft between s3A and s5A becomes vulnerable to the corresponding part in another serpin RCL in proximity and easily leads to formation of linear polymers (Fitton et al., 1997; Chang et al., 1997). Modifying RCL-derived peptides and introducing assistant small molecules are being developed to optimize specificity and efficacy (Chang et al., 2009).

RCL peptides from plasminogen activator inhibitor-1 (PAI-1) suppress activity of this serpin and result in decreased blood clot lysis *in vitro* (Eitzman et al., 1995; D'Amico et al., 2012; Van De Craen et al., 2012). A series of RCL-derived peptides from mammalian neuroserpin and a myxomavirus serpin displayed anti-inflammatory, anti-atherogenic and pro-thrombotic functions in mice, indicating that RCL peptides can have biological activity *in vivo* (Ambadapadi et al., 2016). Another application of RCL-derived peptides is to depolymerize or deaccelerate aberrant polymerization of serpin monomers, as a potential treatment for human serpinopathies (Fitton et al., 1997).

Antifungal Peptides

Present widely in multicellular organisms, antimicrobial peptides (AMPs) are a group of principle effectors in innate immune systems. AMPs are diverse in size and structure, but a majority of them cause damage to pathogens by disrupting the cell membrane (Rautenbach et al., 2016). Cell wall and cytosolic molecules can also be the target for AMPs. Most of the reported AMPs found in insects are antibacterial, with only a few described as active against fungi (He et al., 2015). Those demonstrated with fungistatic or fungicidal activity are designated antifungal peptides. The number of identified antifungal peptides from diverse organisms is growing rapidly with 1127 deposited in the Antimicrobial Peptide Database (http://aps.unmc.edu/AP/main.php).

Modes of action

The fungal cell membrane is a target for most antifungal peptides (Rautenbach et al., 2016). Cell wall synthesis-related enzymes are localized at the membrane, including β-1,3-glucan synthase, 1,6-glucan synthase, and chitin synthase, which generate polymers for cell wall construction and maintenance (Lesage and Bussey, 2006). Various lipids, including glycerophospholipids, sphingolipids and sterols are components of cell membrane and also critical for cell communication and functioning (Baxter et al., 2015a). Some antifungal peptides can be against both bacteria and fungi by targeting the common lipid components of the membrane (Nguyen et al., 2011). However, fungi-specific peptides either inhibit membrane compounds only present in fungi, or use the cell wall components as target, such as mannoproteins and chitin (Rautenbach et al., 2016).

The cell wall of fungi is a cross-linked complex composed primarily of polysaccharide but also containing minor proteins (Lesage and Bussey, 2006). Chitin is a β-1,4-N-acetylglucosamine polymer anchored to a glucan network in the cell wall (Cabib, 2009). Several chitin-interacting antifungal peptides have been reported, such as defensin NP-1 from rabbit, Pp-AMP1/2 from Japanese bamboo, and Tu-AMP1/2 from bulbs of tulip (Levitz et al., 1986; Fujimura et al., 2005; Fujimura et al., 2004). Also linked to β-1,3-glucan on fungal cell wall, mannoproteins are diversely N-glycosylated or O-mannosylated and they act as structural proteins or cell adhesion proteins (Dean, 1999; Dempski and Imperiali, 2002; Ragni et al., 2007; Dranginis et al., 2007; Cappellaro et al., 1994). NaD1, a defensin from *Nicotiana alata* appears to interact with mannoproteins on the cell wall of *Fusarium oxysporum* prior to subsequent cell penetration (et al., 2010). Human histatin binds to cell wall protein Ssa1/2, and its fungicidal activity was significantly compromised in the absence of Ssa1/2 (Li et al., 2003). The above studies revealed that cell wall components, including mannoproteins and chitin, can potentially be cell receptors for anchoring antifungal peptides, which resembles the mechanism of yeast killer toxins (Breinig et al., 2004; Luksa et al., 2015).

Cell wall biogenesis enzymes, which are responsible for producing the polysaccharide network, span the fungal cell membrane, include β-1,3-glucan synthase, β-1,6-glucan synthase and chitin synthase (Lesage and Bussey, 2006). Only β-1,3-glucan synthase was found to be a target for an antifungal peptide, echinocandin (Cappelletty and Eiselstein-McKitrick, 2007).

Echinocandin is a cyclic lipopeptide that blocks the synthesis of β-1,3-glucan by non-competitively inhibiting β-1,3-glucan synthase (Sawistowskaschroder et al., 1984). Potent antifungal activity and no off-target effect has led to successful commercialization of echinocandin and its derivatives as pharmaceutical products (Sucher et al., 2009).

Neutral or negatively charged glycerophospholipids make up 55-75% of fungal membrane lipids and tend to have electrostatic interactions with cationic antifungal peptides (Daum et al., 1998; Ejsing et al., 2009; Singh and Prasad, 2011). Therefore, binding to fungal membrane and subsequently interrupting the integrity of the membrane is believed to be the most common mode of action for cationic AMPs, including the majority of antifungal peptides (Yeaman and Yount, 2003). A group of antifungal/antimicrobial peptides with single linear α-helical structure, such as cecropin A/B from *Hyalophora cecropia* and LL-37 from vertebrates, were observed to have broad spectrum antifungal/antimicrobial activities by binding to glycerophospholipids in the target membrane (DeLucca et al., 1997; De Lucca et al., 1998a; den Hertog et al., 2005). Certain cationic antifungal peptides display preference for specific lipids on the membrane. NaD1 from tobacco and TPP3 from tomato specifically bind to phosphatidylinositol(4,5)-bisphosphate (PIP_2) mediated by a binding motif (Payne et al., 2016; Baxter et al., 2015b).

Antifungal peptides in insects

Expression of diverse AMPs in response to invading bacteria and fungi apparently benefit the thriving of insects (Yi et al., 2014). Insect AMPs are typically synthesized in fat body and secreted to hemolymph upon microbial infection (Kanost et al., 2004). Most insect AMPs were isolated after injection of Gram-positive or Gram-negative bacteria, leading to the extensive discovery of antibacterial peptides rather than antifungal peptides. But some antibacterial peptides were observed to have antifungal activity because of the common modes of action on cell membrane (Faruck et al., 2016). Because modes of action for majority of insect antifungal peptides remain elusive, representative antifungal peptides from insects with proposed mechanisms are discussed below.

Cecropins, with single α-helical structure, were first isolated from *Hyalophora cecropia* (cecropia moth) and demonstrated to have inhibitory activity against a variety of fungi, including *Saccharomyces cerevisiae*, *Phytophthora infestans*, *Fusarium oxysporum*, and *Fusarium*

verticillioides (Cavallarin et al., 1998; De Lucca et al., 1998a; De Lucca et al., 1998b; Ekengren and Hultmark 1999; Vizioli et al., 2000). The mode of action for cecropins is believed to be disrupting the fungal membrane by binding to glycerophospholipids, which also explains the presence of antibacterial activity (De Lucca et al., 1998a; De Lucca et al., 1998b).

Drosomycin from *D. melanogaster* did not show any antibacterial activity, but was quite active against phytopathogenic fungi (Terras et al., 1993; Fehlbaum et al., 1994). Drosomycin is composed of one α-helix and three β-strands with four pairs of disulfide bonds to stabilize the structure (Landon et al., 1997). Potent antifungal activity of drosomycin was observed in various fungi with IC_{50} from 0.9-12 μM (Fehlbaum et al., 1994; Tian et al., 2008). Hyphal lysis caused by drosomycin was reported in susceptible fungi *Botrytis cinerea* and *Neurospora crassa* (Fehlbaum et al., 1994; Gao and Zhu 2008). The target of drosomycin on the fungal membrane remains to be identified, with possibly sphingolipids due to the similarity with plant defensin (Gao and Zhu, 2008). The recognized α-patch and γ-patch on the molecular surface of drosomycin was expected to mediate the membrane binding and permeability respectively (Tian et al., 2008).

Gloverin from *M. sexta* is a protein 177 amino acid long, rich with glycine (Xu et al., 2012). Inhibitory activity of gloverin was detected against *S. cerevisiae*, *Bacillus cereus* and *Cryptococcus neoformans*, but not *E. coli* or *S. aureus*. However, recombinant *M. sexta* gloverin was shown to bind O-specific antigen and outer core carbohydrate moieties of lipopolysaccharide, which are present in Gram-negative bacteria. Gloverin also binds to Gram-positive lipoteichoic acid and peptidoglycan and fungal laminarin (Xu et al., 2012).

A recently discovered family of antifungal peptides in *M. sexta*, designated diapausin, was active against *S. cerevisiae* but not bacteria (Al Souhail et al., 2016). Recombinant diapausin-1 caused curled germination tubes in *Magnaporthe oryzae* and reduced hyphal growth of *Fusarium culmorum* and *F. graminearum*. Diapausin-1 binds to the surface of yeast, which requires further investigation as a target for its mode of action (Al Souhail et al., 2016).

Goals of Current Research

With the completion of the *M. sexta* genome project, discovering all potential serpin genes in *M. sexta* became possible (Kanost et al., 2016). Ten *M. sexta* serpins have been identified and characterized by cDNA cloning and biochemical approaches, demonstrating the

important roles they play in regulation of innate immune responses, including proPO activation and the Toll pathway (Fig. 1-2). Having a general picture and dataset of complete serpin genes in M. sexta would benefit the future study on serpins regarding evolution, structure and physiological functions. Using both the genome database and transcription dataset, as well as the i5K database (https://i5k.nal.usda.gov), discovering and characterizing *M. sexta* serpin genes and protein products was the first goal of my research. To address this goal, I followed several specific aims:

(1) Present basic information on *M. sexta* serpin genes and proteins, such as complete sequences, the absence or presence of signal peptide, number of exons and introns of each serpin gene, location on the scaffold and so on.

(2) Look for any serpin genes with alternative splicing

(3) Characterize evolution of *M. sexta* serpins

(4) Predict inhibitory properties of serpins based on analysis of RCL sequences

Several publications reported that RCL-mimicking small peptides were able to block the inhibitory activity of human serpins, including PAI-1, PAI-2, α_1-antitrypsin and antithrombin. Crystal structures confirmed that the RCL-derived peptides insert into β-sheet A of the serpin, leading to the hindrance of endogenous RCL incorporation, which is critical for a serpin to inhibit a protease. The research on mammalian serpins stimulated my investigation to test the use of RCL-derived peptides in insects. This research would lay a foundation for future study of using small peptides to manipulate serpin actions *in vivo*. Serpin-3 is one of the well-studied serpins in *M. sexta*, so I decided to start with serpin-3 and its RCL-derived peptides. I aimed to investigate the function of serpin-3 RCL-derived peptides following the specific aims:

(1) Design and synthesize small peptides based on *M. sexta* serpin-3 RCL sequence

(2) Express and purify serpin-3 target protease PAP3 and obtain active form

(3) Determine whether the RCL-derived peptides block serpin-3 *in vitro*

(4) Test the activity of the peptides in hemolymph

(5) Verify the incorporation of peptide in serpin-3 by using circular dichroism

Diapausin-1 was isolated from *M. sexta* hemolymph, demonstrating antifungal activity against *S. cerevisiae*, *M. oryzae, F. culmorum* and *F. graminearum* in previous research. I

wanted to explore the potential use of diapausin on clinic and pest control by testing its antifungal activity against human pathogenic fungus Candida and entomopathogenic fungus Beauveria. Additionally, elucidating the specific target and mode of action of diapausin-1 would be instructive to understand the defensive mechanisms of insects against fungal infection. My specific aims regarding diapausin were:

(1) Express and purify recombinant diapausins in active form

(2) Test inhibitory activity of diapausin against pathogenic fungi, such as *Candida albicans* and *Beauveria bassiana*

(3) Reveal the potential mechanisms of diapausin-1 by morphological analysis

Figures

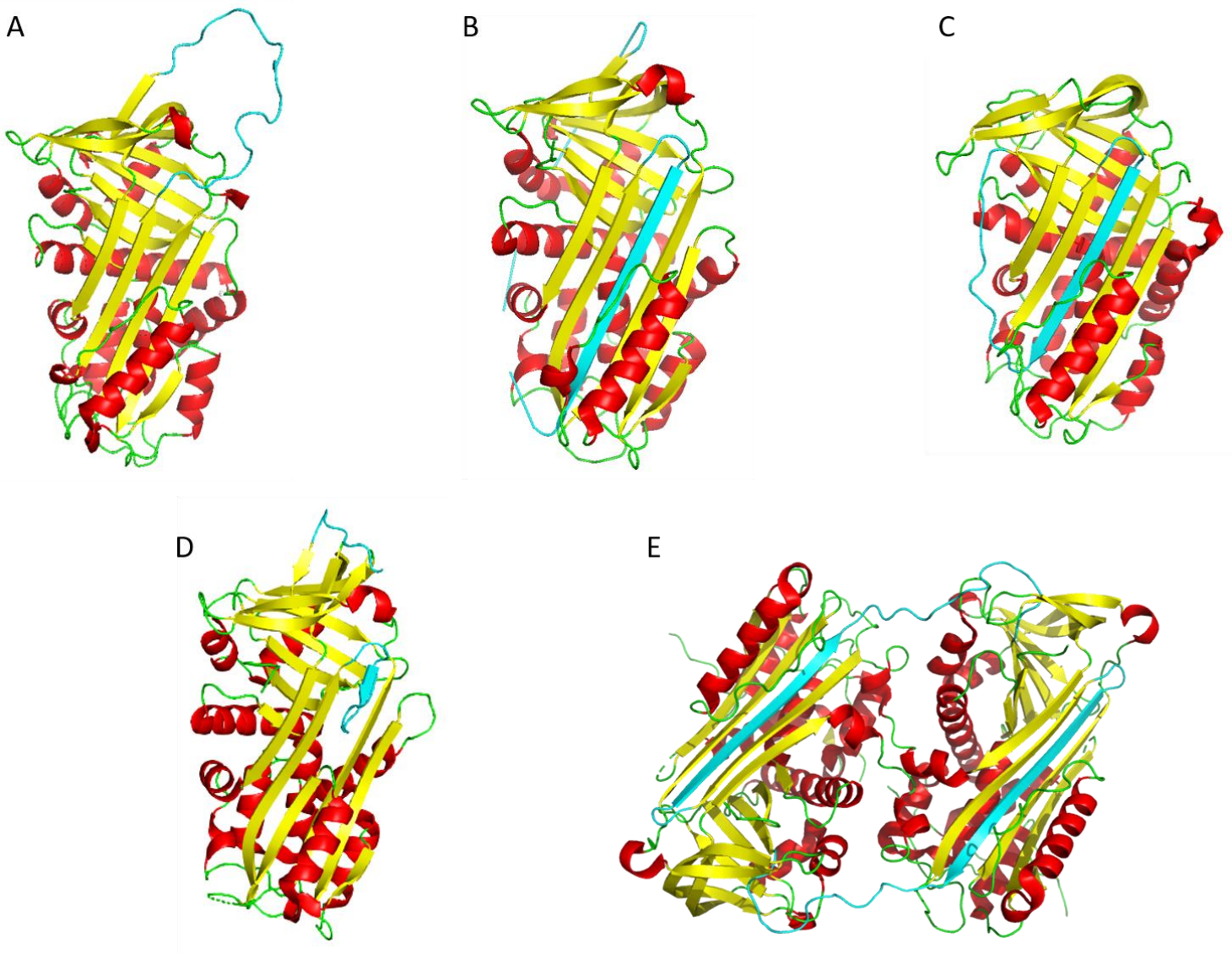

Figure 1-1. Representatives of serpin conformations.

Crystal structures of serpin proteins were from PDB and colored with PyMOL. α-helices are in red, β-sheets are in yellow, loops are in green, and RCL regions are in cyan. (A) Native serpin-1K from *M. sexta*, PDB ID: 1SEK. (B) Cleaved Spn42Da from *D. melanogaster*, PDB ID: 4P0O. (C) Latent PAI-1 from *H. sapiens*, PDB ID: 1DVN. (D) Delta antichymotrypsin from *H. sapiens*, PDB ID: 1QMN. (E) Dimer antithrombin from *H. sapiens*, PDB ID: 2ZNH.

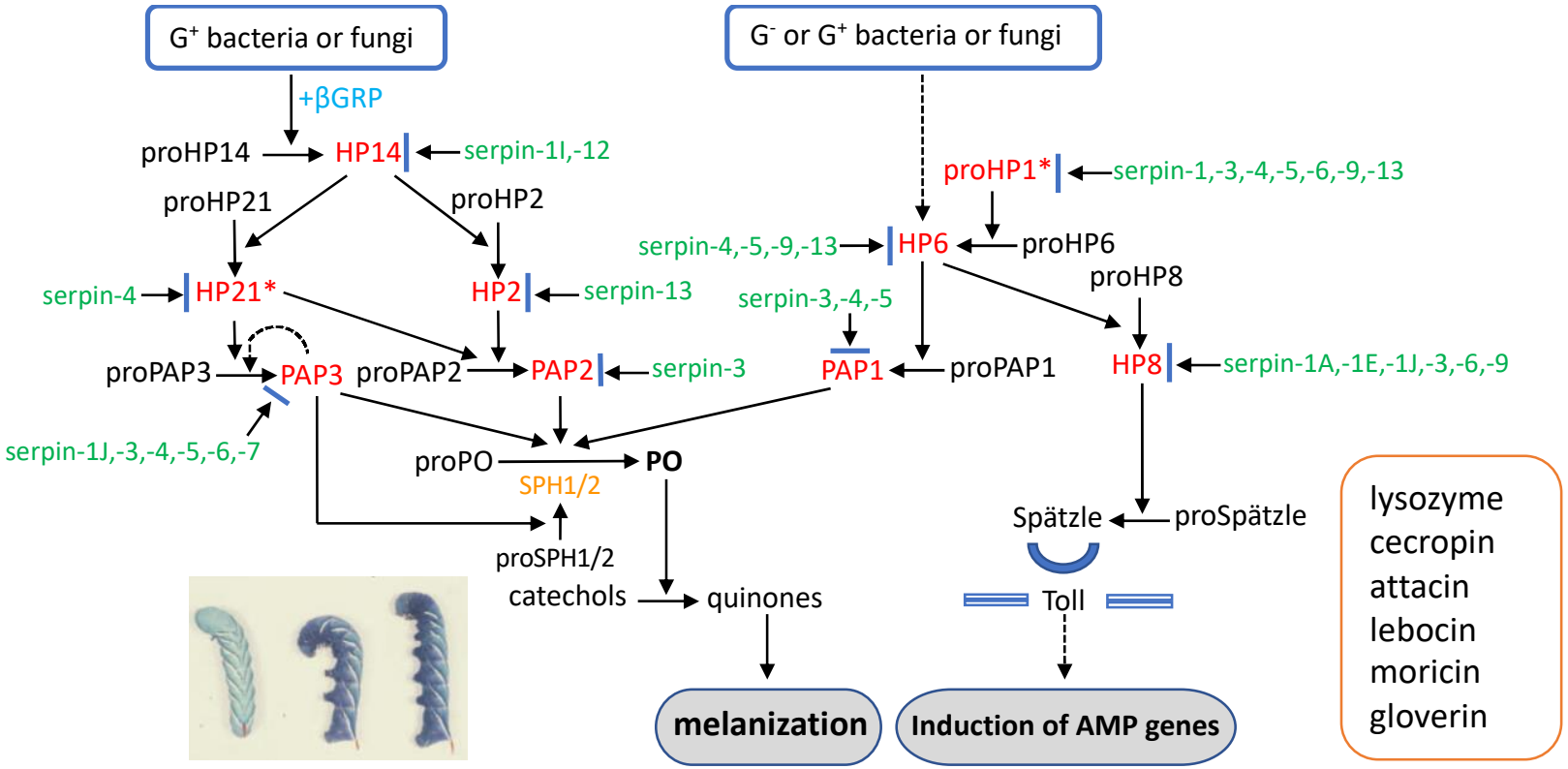

Figure 1-2. *Manduca sexta* serpins and their putative target proteases in innate immune responses.

Pattern recognition proteins are in blue, activated/active serine proteases are in red, serine protease homologs are in orange, and serpins are in green. Activation process is indicated with solid arrow, possible self-activation is indicated with dotted arrow and inhibition process is indicated with a blue bar and an arrow. Antimicrobial peptides induced are in an orange box. An asterisk indicates active serine protease without proteolytic activation.

A

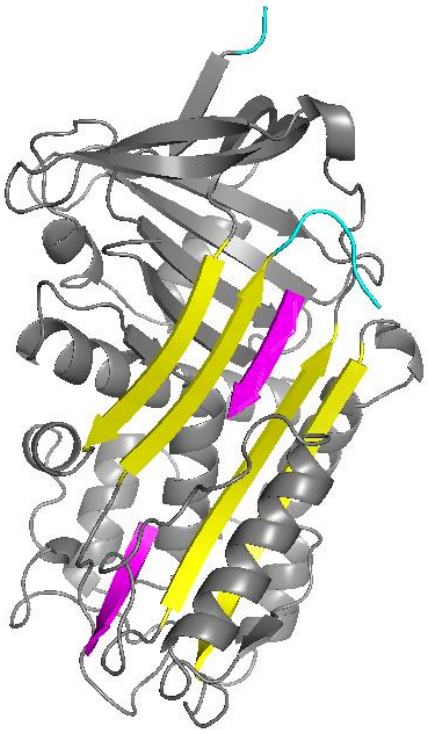

B

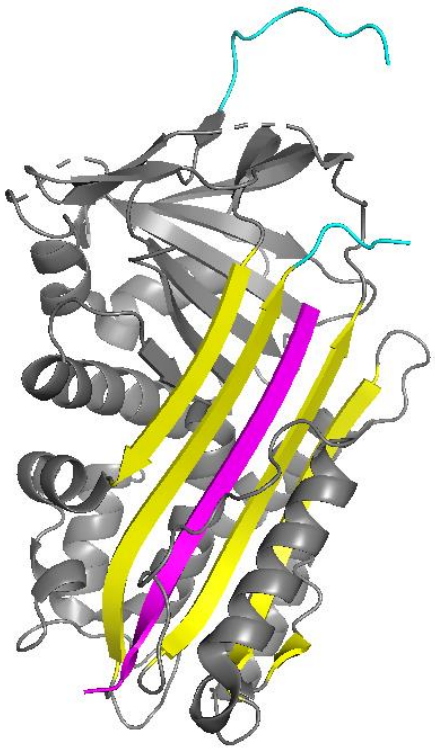

C

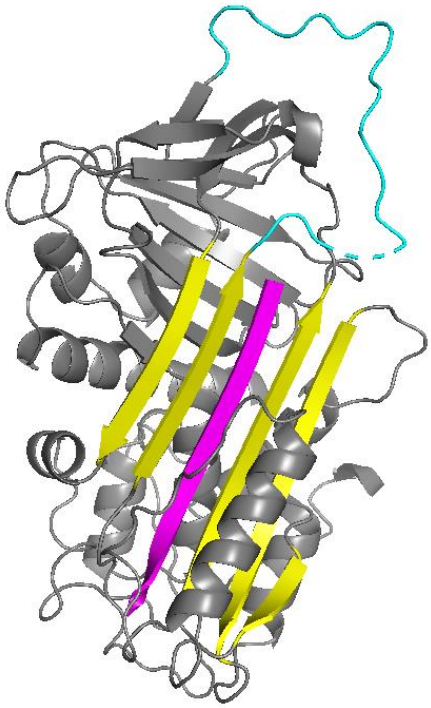

D

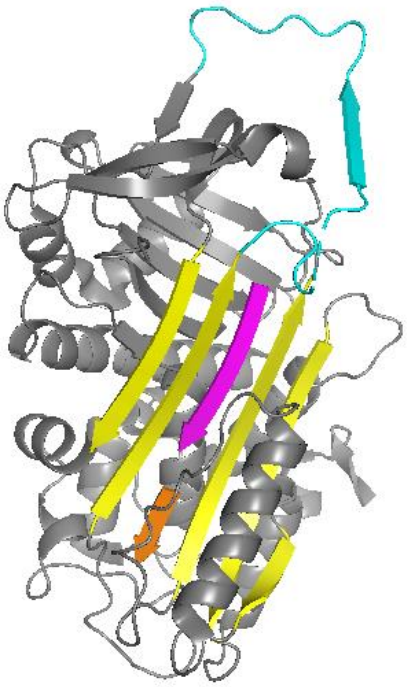

Figure 1-3. Representatives of serpin•RCL-derived peptide complex.

Structures are from PDB and colored with PyMOL. β-sheet A is in yellow, RCL is in cyan, RCL-derived peptide is in magenta and non-serpin derived peptide is in orange. (A) PAI-1•2P14-P10, PDB ID: 1A7C. (B) PAI-2•P14-P1, PDB ID: 1JRR. (C) antithrombin•P14-P3, PDB ID: 1BR8. (D) antithrombin•P14-P8•WMDF, PDB ID: 1JVQ

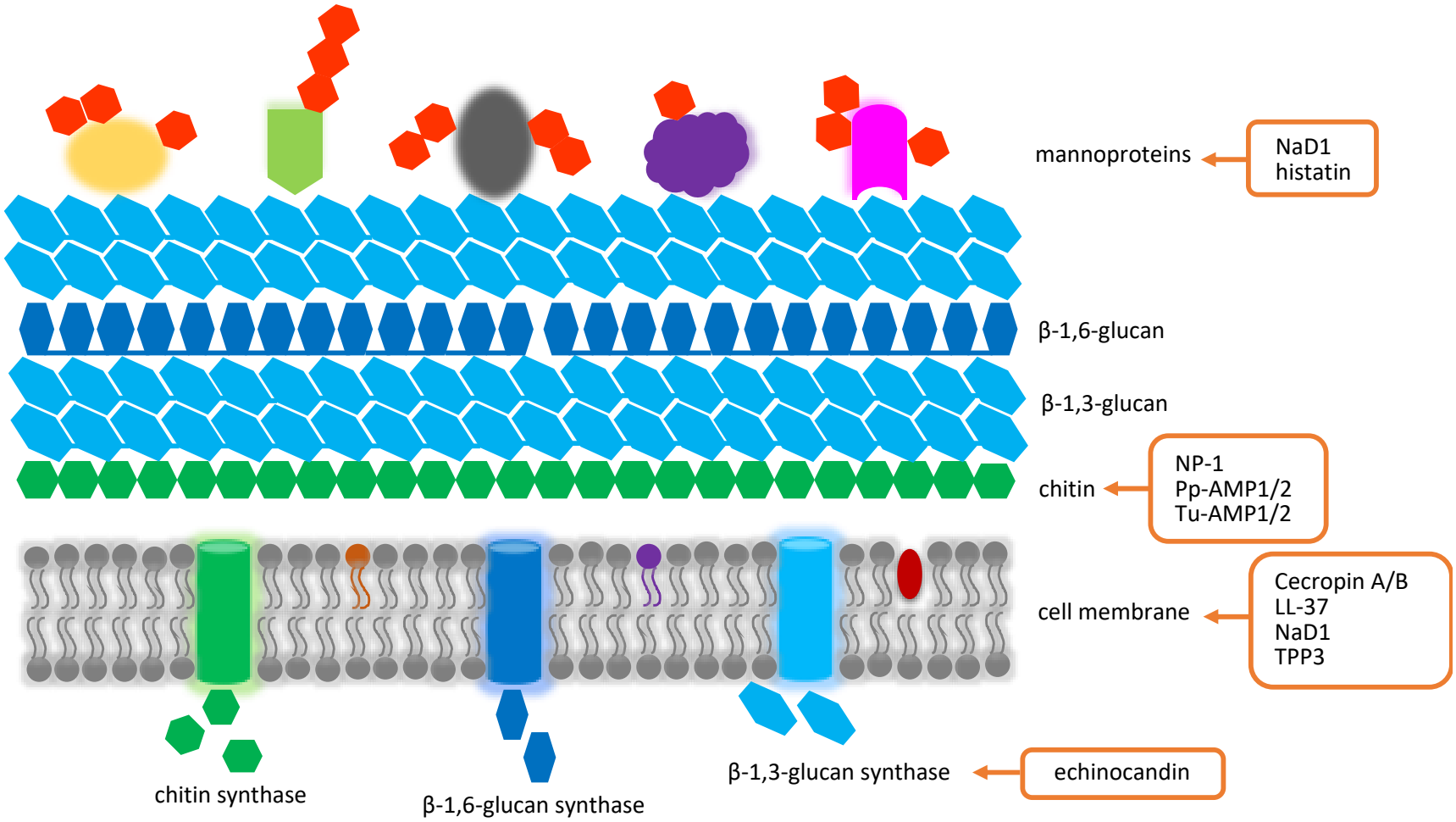

Figure 1-4. Scheme of fungal cell wall and cell membrane with examples of antifungal peptides.

Antifungal peptides are in orange boxes with arrow indicating the target in cell wall or cell membrane. This figure was modified from Marina Rautenbach *et al.*(Rautenbach et al., 2016).

Tables

Table 1-1. Arthropod serpinomes.

Class	Order	Species	Common name	Source	Number of serpin genes	Reference
Arachnida	Ixodida	*Ixodes scapularis*	deer tick	genome	45	(Mulenga et al., 2009)
		Rhipicephalus microplus	cattle tick	transcriptome	18, 22	(Tirloni et al., 2014; Rodriguez-Valle et al., 2015)
		Amblyomma americanum	lone star tick	transcriptome	30[a]	(Porter et al., 2015)
	Sarcoptiformes	*Sarcoptes scabiei*	itch mite	genome	10	(Rider et al., 2015)
Insecta	Orthoptera	*Locusta migratoria*	migratory locust	transcriptome	36	(Zhang et al., 2015a)
	Coleoptera	*Tribolium castaneum*	red flour beetle	genome	31	(Zou et al., 2007)
		Tenebrio molitor	flour beetle	transcriptome	87[b]	(Zhu et al., 2013)
	Hymenoptera	*Apis mellifera*	honeybee	genome	7	(Zou et al., 2006)
		Pteromalus puparum	endoparasitic wasp	genome	10	(Yang et al., 2017)
	Diptera	*Anopheles gambiae*	African malaria mosquito	genome+transcriptome	19	(Suwanchaichinda and Kanost, 2009; Neafsey et al., 2015)
		A. merus		genome	17	(Neafsey et al., 2015)
		A. arabiensis		genome	13	
		A. quadriannulatus		genome	13	
		A. melas		genome	19	
		A. christyi		genome	12	
		A. epiroticus		genome	15	
		A. stephensi (Indian)		genome	16	
		A. stephensi (SDA-500)		genome	17	
		A. maculatus		genome	20	
		A. culicifacies		genome	16	
		A. minimus		genome	13	
		A. funestus		genome	15	
		A. dirus		genome	15	
		A. farauti		genome	17	
		A. atroparvus		genome	23	
		A. sinensis		genome	20	
		A. albimanus		genome	19	
		A. darlingi		genome	19	

	Aedes aegypti	yellow fever mosquito	genome	23	(Gulley et al., 2013)
	Culex quinquefasciatus	southern house mosquito	genome	31	
	Drosophila melanogaster	fruit fly	genome	29	(Reichhart, 2005; Garrett et al., 2009)
	Glossina morsitans	tsetse fly	transcriptome	10	(Mwangi et al., 2011)
Lepidoptera	*Chilo suppressalis*	striped rice stem borer	transcriptome	12[c]	(Ge et al., 2013)
	Bombyx mori	silkworm	genome	34	(Zou et al., 2009)
	Ostrinia furnacalis	Asian corn borer	transcriptome	14	(Shen et al., 2014)
	Manduca sexta	tobacco hornworm	genome	32	(Li et al., 2018)

[a] This number might not be accurate because alleles and very similar genes can be distinguished in transcriptome.

[b] 57 found in male, 33 found in female and 30 found in both.

[c] 9 out of 12 with full-length sequences.

Table 1-2. Arthropod serpins with solved structures.

Species	Serpin	Form	PDB ID	Reference
M. sexta	Serpin-1K	native	1SEK	(Li et al., 1999)
	Serpin-1B	Michaelis complex with rat trypsin	1K9O	(Ye et al., 2001)
	Serpin-12	native	6CJ7	(Yang et al., 2018)
D. melanogaster	Serpin-42Da	cleaved	4P0O	(Ellisdon et al., 2014)
	Serpin-42Da	cleaved	4P0F	
A. gambiae	SRPN2	native	3PZF	(An et al., 2011b)
	SRPN2 (S358E)	native	4RO9	(Zhang et al., 2015b)
	SRPN2 (S358W)	native	4ROA	
	SRPN2 (K198C)	native	4ROB	
	SRPN2 (K198C/E359C)	native	4RSQ	
	SRPN18	native	5C98	(Meekins et al., 2016)
B. mori	Serpin-18	native	4R9I	(Guo et al., 2015)
T. molitor	Serpin-48	native	3OZQ	(Park et al., 2011)
I. ricinus	IRS-2	cleaved	3NDA	(Kovarova et al., 2010)

Table 1-3. Characterized serpins from *M. sexta.*

	Constitutive/ induced concentration in hemolymph (µg/ml)	*Protease inhibited*		non-*Manduca* target protease inhibited	References
		immunoblotting or protease activity assay	immunoaffinity		
serpin-1A	400		HP8	Tryp, Plas, PR2	(Jiang and Kanost, 1997; Ragan et al., 2010)
serpin-1B				CatG, PPE&HNE, PtK, Sub, PR1,	(Kanost et al., 1989; Jiang and Kanost, 1997)
serpin-1C				PtK, PR1	(Jiang and Kanost, 1997)
serpin-1D					(Jiang and Kanost, 1997)
serpin-1E			HP8	PR2	(Jiang and Kanost, 1997; Ragan et al., 2010)
serpin-1F				PPE&HNE, Sub	(Jiang and Kanost, 1997)
serpin-1G				Sub,	(Jiang and Kanost, 1997)
serpin-1H				Chy, CatG, PtK,	(Jiang and Kanost, 1997)
serpin-1I		HP14		Chy, CatG, PPE&HNE	(Jiang and Kanost, 1997; Wang and Jiang, 2006)
serpin-1J		PAP3	HP8	PR2	(Jiang and Kanost, 1997; Jiang et al., 2003; Ragan et al., 2010; An et al., 2011c)
serpin-1K				Chy, CatG, PtK	(Jiang and Kanost, 1997)
serpin-1Z				Chy, CatG	(Jiang and Kanost, 1997)
serpin-2				CatG,	(Gan et al., 2001)
serpin-3	5-12/30-75	PAP1, PAP3	PAP1, PAP2, PAP3, HP8, proHP1	Chyd	(Zhu et al., 2003b; Christen et al., 2012; He et al., 2017a)
serpin-4	3/7	PAP1, PAP3, HP6	proHP1, HP6, HP21	Tryp	(He et al., 2017a; Tong et al., 2005; Tong and Kanost, 2005)
serpin-5	1/3-8	PAP1, PAP3, HP6	proHP1, HP6	Tryp	(He et al., 2017a; Tong et al., 2005; Tong and Kanost, 2005; An and Kanost, 2010)
serpin-6	15/30	PAP3	PAP3, HP8		(Wang and Jiang, 2004; Zou and Jiang, 2005; He et al., 2017a)
serpin-7		PAP3			(Suwanchaichinda et al., 2013)
serpin-9			proHP1, HP6, HP8	Tryp, Chy, PPE&HNE, CatG	(He et al., 2017b; He et al., 2017a)
serpin-12			HP14	Chy, PPE, CatG	(Yang et al., 2018)
serpin-13			proHP1, HP2, HP6	Tryp, HNE, CatG	(He et al., 2017b; He et al., 2017a)

Abbreviations: Tryp, trypsin; Plas, plasmin; CatG, cathepsin G; PPE, porcine pancreatic elastase; HNE, human neutraphil elastase; PtK, protease K; Sub, subtilisin; Chy, chymotrypsin.

Table 1-4. RCL-derived peptides as serpin inhibitors.

Sequences of the RCL from the conserved glycine residue at the N-terminus to P1 on the C-terminus of each serpin are in bold. Sequences of RCL-derived peptides are aligned with the original RCL. Mutants of residues on peptides are in blue. Ac: acetyl.

Original serpin	Peptides	Sequence	Target serpin	References
α_1-antitrypsin		**N-GTEAAGAMFLEAIPM-C**		
	P15-P1	GTEAAGAMFLEAIPMY	α_1-antitrypsin	(Mast et al., 1992)
			α_1-antichymotrypsin	
			antithrombin	
	P15-P3	Ac-GTEAAGAMFLEAI	α_1-antitrypsin	(Chang et al., 1996)
			antithrombin	
	P14-P1	Ac-TEAAGAMFLEAIVM	α_1-antitrypsin	(Schulze et al., 1990)
	P14-P4	Ac-TEAAGAMFLEA	α_1-antitrypsin	(Schulze et al., 1992)
	P14-P8	Ac-TEAAGAM	α_1-antitrypsin	
	P12-P1	Ac-AAGAMFLEAIVM	α_1-antitrypsin	
antithrombin		**N-GSEAAASTAVVIAGR-C**		
	P14-P1	Ac-SEAAASTAVVIAGR	antithrombin	(Björk et al., 1992)
	P14-P2	Ac-SEAAASTAVVIAG	antithrombin	(Carrell et al., 1991)
	P14-P3	Ac-SEAAASTAVVIA	antithrombin	(Chang et al., 1996)
			α_1-antitrypsin	(Skinner et al., 1998)
	P14-P9	Ac-SEAAAS	antithrombin	(Carrell et al., 1991)
PAI-1		**N-GTVASSSTAVIVSAR-C**		
	P14-P1	Ac-TVASSSTAVIVSAR	PAI-1	(Eitzman et al., 1995)
	P14-P7	Ac-TVASSSTA	PAI-1	(Kvassman et al., 1995)
	P14-P9	TVASSS	PAI-1	(D'Amico et al., 2012)
	P14-P10	Ac-TVASS-NH_2	PAI-1	(Xue et al., 1998)
	P8-P3	TAVIVS	PAI-1	(D'Amico et al., 2012)
PAI-2		**N-GTEAAAGTGGVMTGR-C**		
	P14-P1	Ac-TEAAAGTGGVMTGR	PAI-2	(Jankova et al., 2001)
	P14-P1(TP8D)	Ac-TEAAAGDGGVMTGR	PAI-2	(Di Giusto et al., 2005)
	P14-P1(TP8M)	Ac-TEAAAGMGGVMTGR	PAI-2	

References

Abraham, E. G., S. B. Pinto, A. Ghosh, D. L. Vanlandingham, A. Budd, S. Higgs, F. C. Kafatos, M. Jacobs-Lorena & K. Michel (2005) An immune-responsive serpin, SRPN6, mediates mosquito defense against malaria parasites. *Proceedings of the National Academy of Sciences of the United States of America*, 102, 16327-16332.

Ahmad, S. T., S. T. Sweeney, J.-A. Lee, N. T. Sweeney & F.-B. Gao (2009) Genetic screen identifies serpin5 as a regulator of the toll pathway and CHMP2B toxicity associated with frontotemporal dementia. *Proceedings of the National Academy of Sciences of the United States of America*, 106, 12168-12173.

Al Souhail, Q., Y. Hiromasa, M. Rahnamaeian, M. C. Giraldo, D. Takahashi, B. Valent, A. Vilcinskas & M. R. Kanost (2016) Characterization and regulation of expression of an antifungal peptide from hemolymph of an insect, *Manduca sexta*. *Developmental & Comparative Immunology*, 61, 258-268.

Ambadapadi, S., G. Munuswamy-Ramanujam, D. Zheng, C. Sullivan, E. Dai, S. Morshed, B. McFadden, E. Feldman, M. Pinard & R. McKenna (2016) Reactive center loop (RCL) peptides derived from serpins display independent coagulation and immune modulating activities. *Journal of Biological Chemistry*, 291, 2874-2887.

An, C., A. Budd, M. R. Kanost & K. Michel (2011a) Characterization of a regulatory unit that controls melanization and affects longevity of mosquitoes. *Cellular and Molecular Life Sciences*, 68, 1929-1939.

An, C., J. Ishibashi, E. J. Ragan, H. Jiang & M. R. Kanost (2009) Functions of *Manduca sexta* hemolymph proteinases HP6 and HP8 in two innate immune pathways. *Journal of Biological Chemistry*, 284, 19716-19726.

An, C., H. Jiang & M. R. Kanost (2010) Proteolytic activation and function of the cytokine Spätzle in the innate immune response of a lepidopteran insect, *Manduca sexta*. *The FEBS journal*, 277, 148-162.

An, C. & M. R. Kanost (2010) *Manduca sexta* serpin-5 regulates prophenoloxidase activation and the Toll signaling pathway by inhibiting hemolymph proteinase HP6. *Insect biochemistry and molecular biology*, 40, 683-689.

An, C., S. Lovell, M. R. Kanost, K. P. Battaile & K. Michel (2011b) Crystal structure of native *Anopheles gambiae* serpin-2, a negative regulator of melanization in mosquitoes. *Proteins*, 79(6), 1999.

An, C., E. J. Ragan & M. R. Kanost (2011c) Serpin-1 splicing isoform J inhibits the proSpätzle-activating proteinase HP8 to regulate expression of antimicrobial hemolymph proteins in *Manduca sexta*. *Developmental and comparative immunology*, 35, 135-141.

Ashida, M. (1998) Recent advances in research on the insect prophenoloxidase cascade. *Molecular mechanisms of immune responses in insects*.

Baglin, T. P., R. W. Carrell, F. C. Church, C. T. Esmon & J. A. Huntington (2002) Crystal structures of native and thrombin-complexed heparin cofactor II reveal a multistep allosteric mechanism. *Proceedings of the National Academy of Sciences of the United States of America*, 99, 11079-11084.

Baker, C., O. Belbin, N. Kalsheker & K. Morgan (2007) SERPINA3 (aka alpha-1-antichymotrypsin). *Front Biosci*, 12, 35.

Baxter, A., M. Hulett & I. Poon (2015a) The phospholipid code: a key component of dying cell recognition, tumor progression and host-microbe interactions. *Cell Death and Differentiation*, 22, 1893-1905.

Baxter, A., V. Richter, F. Lay, I. Poon, C. Adda, P. Veneer, T. Phan, M. Bleackley, M. Anderson, M. Kvansakul & M. Hulett (2015b) The tomato defensin TPP3 binds phosphatidylinositol (4,5)-bisphosphate via a conserved dimeric cationic grip conformation to mediate cell lysis. *Molecular and Cellular Biology*, 35, 1964-1978.

Berardi, R., F. Morgese, A. Onofri, P. Mazzanti, M. Pistelli, Z. Ballatore, A. Savini, M. De Lisa, M. Caramanti & S. Rinaldi (2013) Role of maspin in cancer. *Clinical and translational medicine*, 2, 8.

Björk, I., K. Ylinenjärvi, S. T. Olson & P. E. Bock (1992) Conversion of antithrombin from an inhibitor of thrombin to a substrate with reduced heparin affinity and enhanced conformational stability by binding of a tetradecapeptide corresponding to the P1 to P14 region of the putative reactive bond loop of the inhibitor. *Journal of Biological Chemistry*, 267, 1976-1982.

Bode, W. & R. Huber (1992) Natural protein proteinase-inhibitors and their interaction with proteinases. *European Journal of Biochemistry*, 204, 433-451.

Breinig, F., K. Schleinkofer & M. Schmitt (2004) Yeast Kre1p is GPI-anchored and involved in both cell wall assembly and architecture. *Microbiology*, 150, 3209-3218.

Bruch, M., V. Weiss & J. Engel (1988) Plasma serine proteinase inhibitors (serpins) exhibit major conformational changes and a large increase in conformational stability upon cleavage at their reactive sites. *Journal of Biological Chemistry*, 263, 16626-16630.

Buchmann, K. (2014) Evolution of innate immunity: clues from invertebrates via fish to mammals. *Frontiers in Immunology*, 5, 459.

Buchon, N., N. Silverman & S. Cherry (2014) Immunity in *Drosophila melanogaster*-from microbial recognition to whole-organism physiology. *Nat Rev Immunol*, 14, 796-810.

Börner, S. & H. Ragg (2008) Functional diversification of a protease inhibitor gene in the genus *Drosophila* and its molecular basis. *Gene*, 415, 23-31.

Cabib, E. (2009) Two novel techniques for determination of polysaccharide cross-links show that Crh1p and Crh2p attach chitin to both β (1-6)-and β (1-3) glucan in the *Saccharomyces cerevisiae* cell wall. *Eukaryotic Cell*, 8, 1626-1636.

Calvo, E., D. Mizurini, A. Sa-Nunes, J. Ribeiro, J. Andersen, B. Mans, R. Monteiro, M. Kotsyfakis & I. Francischetti (2011) Alboserpin, a factor Xa inhibitor from the mosquito vector of yellow fever, binds heparin and membrane phospholipids and exhibits antithrombotic activity. *Journal of Biological Chemistry*, 286, 27998-28010.

Cao, X., M. Gulati & H. Jiang (2017) Serine protease-related proteins in the malaria mosquito, *Anopheles gambiae*. *Insect biochemistry and molecular biology*, 88, 48-62.

Cao, X., Y. He, Y. Hu, Y. Wang, Y.-R. Chen, B. Bryant, R. J. Clem, L. M. Schwartz, G. Blissard & H. Jiang (2015a) The immune signaling pathways of *Manduca sexta*. *Insect biochemistry and molecular biology*, 62, 64-74.

Cao, X., Y. He, Y. Hu, X. Zhang, Y. Wang, Z. Zou, Y. Chen, G. W. Blissard, M. R. Kanost & H. Jiang (2015b) Sequence conservation, phylogenetic relationships, and expression profiles of nondigestive serine proteases and serine protease homologs in *Manduca sexta*. *Insect biochemistry and molecular biology*, 62, 51-63.

Cappellaro, C., C. Baldermann, R. Rachel & W. Tanner (1994) Mating type-specific cell-cell recognition of *Saccharomyces cerevisiae*: cell wall attachment and active sites of a-agglutinin and alpha-agglutinin. *Embo Journal*, 13, 4737-4744.

Cappelletty, D. & K. Eiselstein-McKitrick (2007) The Echinocandins. *Pharmacotherapy*: *The Journal of Human Pharmacology and Drug Therapy*, 27, 369-388.

Carrell, R. & J. Travis (1985) α_1-Antitrypsin and the serpins: variation and countervariation. *Trends in biochemical sciences*, 10, 20-24.

Carrell, R. W., D. L. Evans & P. E. Stein (1991) Mobile reactive centre of serpins and the control of thrombosis. *Nature*, 353, 576.

Carrell, R. W. & R. J. Read. 2017. How serpins transport hormones and regulate their release. In *Seminars in cell & developmental biology*, 133-141. Elsevier.

Cavallarin, L., D. Andreu & B. Segundo (1998) Cecropin A-derived peptides are potent inhibitors of fungal plant pathogens. *Molecular Plant-Microbe Interactions*, 11, 218-227.

Chang, W. S. W., M. R. Wardell, D. A. Lomas & R. W. Carrell (1996) Probing serpin reactive-loop conformations by proteolytic cleavage. *Biochemical Journal*, 314, 647-653.

Chang, W. S. W., J. Whisstock, P. C. R. Hopkins, A. M. Lesk, R. W. Carrell & M. R. Wardell (1997) Importance of the release of strand 1C to the polymerization mechanism of inhibitory serpins. *Protein Science*, 6, 89-98.

Chang, Y. P., R. Mahadeva, W. S. W. Chang, S. C. Lin & Y. H. Chu (2009) Small-molecule peptides inhibit Z α_1-antitrypsin polymerization. *Journal of Cellular and Molecular Medicine*, 13, 2304-2316.

Charron, Y., R. Madani, C. Combepine, V. Gajdosik, Y. Hwu, G. Margaritondo & J. Vassalli (2008) The serpin Spn5 is essential for wing expansion in *Drosophila melanogaster*. *International Journal of Developmental Biology*, 52, 933-942.

Chmelar, J., C. Oliveira, P. Rezacova, I. Francischetti, Z. Kovarova, G. Pejler, P. Kopacek, J. Ribeiro, M. Mares, J. Kopecky & M. Kotsyfakis (2011) A tick salivary protein targets cathepsin G and chymase and inhibits host inflammation and platelet aggregation. *Blood*, 117, 736-744.

Christen, J. M., Y. Hiromasa, C. An & M. R. Kanost (2012) Identification of plasma proteinase complexes with serpin-3 in *Manduca sexta*. *Insect biochemistry and molecular biology*, 42, 946-955.

Chu, Y., F. Zhou, Y. Liu, F. Hong, G. Wang & C. An (2015) *Ostrinia furnacalis* serpin-3 regulates melanization cascade by inhibiting a prophenoloxidase-activating protease. *Insect biochemistry and molecular biology*, 61, 53-61.

Coico, R. & G. Sunshine. 2015. Immunology: a short course. John Wiley & Sons.

Coleman, S., B. Drahn, G. Petersen, J. Stolorov & K. Kraus (1995) A *Drosophila* male accessory-gland protein that is a member of the serpin superfamily of proteinase-inhibitors is transferred to females during mating. *Insect biochemistry and molecular biology*, 25, 203-207.

Colinet, D., A. Dubuffet, D. Cazes, S. Moreau, J. Drezen & M. Poirie (2009) A serpin from the parasitoid wasp Leptopilina boulardi targets the *Drosophila* phenoloxidase cascade. *Developmental and Comparative Immunology*, 33, 681-689.

D'Amico, S., J. A. Martial & I. Struman (2012) A peptide mimicking the C-terminal part of the reactive center loop induces the transition to the latent form of plasminogen activator inhibitor type-1. *FEBS letters*, 586, 686-692.

Danielli, A., F. C. Kafatos & T. G. Loukeris (2003) Cloning and characterization of four *Anopheles gambiae* serpin isoforms, differentially induced in the midgut by *Plasmodium berghei* invasion. *The Journal of Biological Chemistry*, 278, 4184-4193.

Daum, G., N. Lees, M. Bard & R. Dickson (1998) Biochemistry, cell biology and molecular biology of lipids of *Saccharomyces cerevisiae*. *Yeast*, 14, 1471-1510.

De Gregorio, E., S. J. Han, W. J. Lee, M. J. Baek, T. Osaki, S. I. Kawabata, B. L. Lee, S. Iwanaga, B. Lemaitre & P. T. Brey (2002) An immune-responsive Serpin regulates the melanization cascade in *Drosophila*. *Developmental cell*, 3, 581-592.

De Lucca, A., J. Bland, T. Jacks, C. Grimm & T. Walsh (1998a) Fungicidal and binding properties of the natural peptides cecropin B and dermaseptin. *Medical Mycology*, 36, 291-298.

De Lucca, A., T. Jacks & W. Broekaert (1998b) Fungicidal and binding properties of three plant peptides. *Mycopathologia*, 144, 87-91.

Dean, N. (1999) Asparagine-linked glycosylation in the yeast Golgi. *Biochimica Et Biophysica Acta-General Subjects*, 1426, 309-322.

DeLucca, A., J. Bland, T. Jacks, C. Grimm, T. Cleveland & T. Walsh (1997) Fungicidal activity of Cecropin A. *Antimicrobial Agents and Chemotherapy*, 41, 481-483.

Delves, P. J., S. J. Martin, D. R. Burton & I. M. Roitt. 2017. Essential immunology. John Wiley & Sons.

Dementiev, A., M. Petitou, J. Herbert & P. Gettins (2004) The ternary complex of antithrombin-anhydrothrombin heparin reveals the basis of inhibitor specificity. *Nature Structural & Molecular Biology*, 11, 863-867.

Dementiev, A., M. Simonovic, K. Volz & P. G. W. Gettins (2003) Canonical inhibitor-like interactions explain reactivity of α_1-proteinase inhibitor Pittsburgh and antithrombin with proteinases. *Journal of Biological Chemistry*, 278, 37881-37887.

Dempski, R. & B. Imperiali (2002) Oligosaccharyl transferase: gatekeeper to the secretory pathway. *Current Opinion in Chemical Biology*, 6, 844-850.

den Hertog, A. L., van Marle, J., Bolscher, J. G., Veerman, E. C., & Arie, V. (2005) Candidacidal effects of two antimicrobial peptides: histatin 5 causes small membrane defects, but LL-37 causes massive disruption of the cell membrane. *Biochemical Journal*, 388, 689-695.

Di Giusto, D., A. Sutherland, L. Jankova, S. Harrop, P. Curmi & G. King (2005) Plasminogen activator inhibitor-2 is highly tolerant to P8 residue substitution - Implications for serpin mechanistic model and prediction of nsSNP activities. *Journal of Molecular Biology*, 353, 1069-1080.

Dobbelstein, M. & T. Shenk (1996) Protection against apoptosis by the vaccinia virus SPI-2 (B13R) gene product. *Journal of virology*, 70, 6479-6485.

Dranginis, A., J. Rauceo, J. Coronado & P. Lipke (2007) A biochemical guide to yeast adhesins: glycoproteins for social and antisocial occasions. *Microbiology and Molecular Biology Reviews*, 71(2), 282-294.

Eitzman, D. T., W. P. Fay, D. A. Lawrence, A. M. Francis-Chmura, J. D. Shore, S. T. Olson & D. Ginsburg (1995) Peptide-mediated inactivation of recombinant and platelet plasminogen activator inhibitor-1 *in vitro*. *The Journal of clinical investigation*, 95, 2416-2420.

Ejsing, C., J. Sampaio, V. Surendranath, E. Duchoslav, K. Ekroos, R. Klemm, K. Simons & A. Shevchenko (2009) Global analysis of the yeast lipidome by quantitative shotgun mass spectrometry. *Proceedings of the National Academy of Sciences of the United States of America*, 106, 2136-2141.

Ekengren, S. & D. Hultmark (1999) *Drosophila* cecropin as an antifungal agent. *Insect biochemistry and molecular biology*, 29, 965-972.

Ekeowa, U. I., J. Freeke, E. Miranda, B. Gooptu, M. F. Bush, J. Pérez, J. Teckman, C. V. Robinson & D. A. Lomas (2010) Defining the mechanism of polymerization in the serpinopathies. *Proceedings of the National Academy of Sciences*, 107, 17146-17151.

Elliott, P. R., D. Bilton & D. A. Lomas (1998) Lung polymers in Z α_1-antitrypsin deficiency-related emphysema. *American Journal of Respiratory Cell and Molecular Biology*, 18, 670-674.

Ellisdon, A., Q. Zhang, M. Henstridge, T. Johnson, C. Warr, R. Law & J. Whisstock (2014) High resolution structure of cleaved Serpin 42 Da from *Drosophila melanogaster*. *BMC Structural Biology*, 14.

Erwin, T. L. (1997) Biodiversity at its utmost: tropical forest beetles. *Biodiversity II. Understanding and protecting our biological resources*, 27-40.

Fa, M., F. Bergstrom, P. Hagglof, M. Wilczynska, L. Johansson & T. Ny (2000) The structure of a serpin-protease complex revealed by intramolecular distance measurements using donor-donor energy migration and mapping of interaction sites. *Structure With Folding & Design*, 8, 397-405.

Faruck, M., F. Yusof & S. Chowdhury (2016) An overview of antifungal peptides derived from insect. *Peptides*, 80, 80-88.

Fehlbaum, P., P. Bulet, L. Michaut, M. Lagueux, W. Broekaert, C. Hetru & J. Hoffmann (1994) Insect immunity. Septic injury of *Drosophila* induces the synthesis of a potent antifungal peptide with sequence homology to plant antifungal peptides. *Journal of Biological Chemistry*, 269, 33159-33163.

Fitton, H. L., R. N. Pike, R. W. Carrell & W.-S. W. Chang (1997) Mechanisms of antithrombin polymerisation and heparin activation probed by the insertion of synthetic reactive loop peptides. *Biological chemistry*, 378, 1059-1064.

Fujimura, M., M. Ideguchi, Y. Minami, K. Watanabe & K. Tadera (2004) Purification, characterization, and sequencing of novel antimicrobial peptides, Tu-AMP 1 and Tu-AMP 2, from bulbs of tulip (Tulipa gesneriana L.). *Bioscience Biotechnology and Biochemistry*, 68, 571-577.

Fujimura, M., Ideguchi, M., Minami, Y., Watanabe, K., & Tadera, K. (2005) Amino acid sequence and antimicrobial activity of chitin-binding peptides, Pp-AMP 1 and Pp-AMP 2, from Japanese bamboo shoots (*Phyllostachys pubescens*). *Bioscience Biotechnology and Biochemistry*, 69, 642-645.

Fullaondo, A., S. Garcia-Sanchez, A. Sanz-Parra, E. Recio, S. Lee & D. Gubb (2011) Spn1 regulates the GNBP3-dependent Toll signaling pathway in *Drosophila melanogaster*. *Molecular and Cellular Biology*, 31, 2960-2972.

Gan, H., Y. Wang, H. Jiang, K. Mita & M. R. Kanost (2001) A bacteria-induced, intracellular serpin in granular hemocytes of *Manduca sexta*. *Insect biochemistry and molecular biology*, 31, 887-898.

Gao, B. & S. Zhu (2008) Differential potency of drosomycin to Neurospora crassa and its mutant: implications for evolutionary relationship between defensins from insects and plants. *Insect Molecular Biology*, 17, 405-411.

Garrett, M., A. Fullaondo, L. Troxler, G. Micklem & D. Gubb (2009) Identification and analysis of serpin-family genes by homology and synteny across the 12 sequenced Drosophilid genomes. *BMC Genomics*, 10(1), 489.

Ge, Z., P. Wan, X. Cheng, Y. Zhang, G. Li & Z. Han (2013) Cloning and characterization of serpin-like genes from the striped rice stem borer, Chilo suppressalis. *Genome*, 56, 359-366.

Gettins, P. G. & S. T. Olson (2016) Inhibitory serpins. New insights into their folding, polymerization, regulation and clearance. *The Biochemical journal*, 473, 2273-2293.

Gettins, P. G. W. (2002) Serpin structure, mechanism, and function. *Chemical reviews*, 102, 4751-4804.

Gillespie and, J. P., M. R. Kanost & T. Trenczek (1997) Biological mediators of insect immunity. *Annual review of entomology*, 42, 611-643.

Gong, L., M. Liu, T. Zeng, X. Shi, C. Yuan, P. Andreasen & M. Huang (2015) Crystal structure of the Michaelis complex between tissue-type plasminogen activator and plasminogen activators inhibitor-1. *Journal of Biological Chemistry*, 290, 25795-25804.

Gooptu, B., J. A. Dickens & D. A. Lomas (2014) The molecular and cellular pathology of α_1-antitrypsin deficiency. *Trends in molecular medicine*, 20, 116-127.

Gooptu, B., B. Hazes, W. S. W. Chang, T. R. Dafforn, R. W. Carrell, R. J. Read & D. A. Lomas (2000) Inactive conformation of the serpin α_1-antichymotrypsin indicates two-stage insertion of the reactive loop: implications for inhibitory function and conformational disease. *Proceedings of the National Academy of Sciences*, 97, 67-72.

Gooptu, B. & D. A. Lomas (2009) Conformational pathology of the serpins: themes, variations, and therapeutic strategies. *Annual Review of Biochemistry*, 78, 147-176.

Gorman, M. J., Y. Wang, H. Jiang & M. R. Kanost (2007) *Manduca sexta* hemolymph proteinase 21 activates prophenoloxidase-activating proteinase 3 in an insect innate immune response proteinase cascade. *Journal of Biological Chemistry*, 282, 11742-11749.

Gulley, M. M., X. Zhang & K. Michel (2013) The roles of serpins in mosquito immunology and physiology. *Journal of insect physiology*, 59, 138-147.

Guo, P., Z. Dong, P. Zhao, Y. Zhang, H. He, X. Tan, W. Zhang & Q. Xia (2015) Structural insights into the unique inhibitory mechanism of the silkworm protease inhibitor serpin18. *Scientific Reports*, 5.

Gupta, S., Y. Wang & H. Jiang (2005) *Manduca sexta* prophenoloxidase (proPO) activation requires proPO-activating proteinase (PAP) and serine proteinase homologs (SPHs) simultaneously. *Insect biochemistry and molecular biology*, 35, 241-248.

Hashimoto, C., D. Kim, L. Weiss, J. Miller & D. Morisato (2003) Spatial regulation of developmental signaling by a serpin. *Developmental Cell*, 5, 945-950.

He, Y., X. Cao, K. Li, Y. Hu, Y. R. Chen, G. Blissard, M. R. Kanost & H. Jiang (2015) A genome-wide analysis of antimicrobial effector genes and their transcription patterns in *Manduca sexta*. *Insect biochemistry and molecular biology*, 62, 23-37.

He, Y., Y. Wang, Y. Hu & H. Jiang (2018) *Manduca sexta* hemolymph protease-2 (HP2) activated by HP14 generates prophenoloxidase-activating protease-2 (PAP2) in wandering larvae and pupae. *Insect biochemistry and molecular biology*, 101, 57-65.

He, Y., Y. Wang, F. Yang & H. Jiang (2017a) *Manduca sexta* hemolymph protease-1, activated by an unconventional non-proteolytic mechanism, mediates immune responses. *Insect biochemistry and molecular biology*, 84, 23-31.

He, Y., Y. Wang, P. Zhao, S. Rayaprolu, X. Wang, X. Cao & H. Jiang (2017b) Serpin-9 and-13 regulate hemolymph proteases during immune responses of *Manduca sexta*. *Insect biochemistry and molecular biology*, 90, 71-81.

Hegedus, D. D., M. Erlandson, D. Baldwin, X. Hou & M. Chamankhah (2008) Differential expansion and evolution of the exon family encoding the Serpin-1 reactive centre loop has resulted in divergent serpin repertoires among the Lepidoptera. *Gene*, 418, 15-21.

Hervé, M. & C. Ghélis (1990) Conformational changes in intact and papain-modified α_1-proteinase inhibitor induced by guanidinium chloride. *European journal of biochemistry*, 191, 653-658.

Hoffmann, J. A., F. C. Kafatos, C. A. Janeway & R. Ezekowitz (1999) Phylogenetic perspectives in innate immunity. *Science*, 284, 1313-1318.

Hopkins, P. C. R., R. W. Carrell & S. R. Stone (1993) Effects of mutations in the hinge region of serpins. *Biochemistry*, 32, 7650-7657.

Hopkins, P. C. R. & S. R. Stone (1995) The Contribution of the conserved hinge region residues of α_1-antitrypsin to its reaction with elastase. *Biochemistry*, 34, 15872-15879.

Horohov, D. W. & P. E. Dunn (1983) Phagocytosis and nodule formation by hemocytes of *Manduca sexta* larvae following injection of *Pseudomonas aeruginosa*. *Journal of Invertebrate Pathology*, 41, 203-213.

Huang, X., A. Dementiev, S. T. Olson & P. G. W. Gettins (2010) Basis for the specificity and activation of the serpin protein Z-dependent proteinase inhibitor (ZPI) as an inhibitor of membrane-associated factor Xa. *Journal of Biological Chemistry*, 285, 20399-20409.

Hughes, J. A., R. E. Hurlbert, R. A. Rupp & K. D. Spence (1983) Bacteria-induced haemolymph proteins of *Manduca sexta* pupae and larvae. *Journal of Insect Physiology*, 29, 625-632.

Huntington, J. A. (2011) Serpin structure, function and dysfunction. *Journal of Thrombosis and Haemostasis*, 9, 26-34.

Huntington, J. A., A. McCoy, K. J. Belzar, X. Y. Pei, P. G. Gettins & R. W. Carrell (2000) The conformational activation of antithrombin. A 2.85 Å structure of a fluorescein derivative reveals an electrostatic link between the hinge and heparin binding regions. *The Journal of Biological Chemistry*, 275, 15377-15383.

Huntington, J. A. & P. E. Stein (2001) Structure and properties of ovalbumin. *Journal of Chromatography B: Biomedical Sciences and Applications*, 756, 189-198.

Huntington, J. A. & J. C. Whisstock (2010) Molecular contortionism - on the physical limits of serpin 'loop-sheet'polymers. *Biological chemistry*, 391, 973-982.

Irving, J. A., R. N. Pike, A. M. Lesk & J. C. Whisstock (2000) Phylogeny of the serpin superfamily: implications of patterns of amino acid conservation for structure and function. *Genome research*, 10, 1845-1864.

Irving, J. A., P. J. M. Steenbakkers, A. M. Lesk, H. J. M. Op den Camp, R. N. Pike & J. C. Whisstock (2002) Serpins in prokaryotes. *Molecular biology and evolution*, 19, 1881-1890.

Jankova, L., S. J. Harrop, D. N. Saunders, J. L. Andrews, K. C. Bertram, A. R. Gould, M. S. Baker & P. M. G. Curmi (2001) Crystal structure of the complex of plasminogen activator inhibitor 2 with a peptide mimicking the reactive center loop. *Journal of Biological Chemistry*, 276, 43374-43382.

Jendrny, C. & A. G. Beck-Sickinger. 2015. Peptides as modulators of serpin action. In *The Serpin Family*, 29-45. Springer.

Jensen, J. K. & P. G. W. Gettins (2008) High-resolution structure of the stable plasminogen activator inhibitor type-1 variant 14-1B in its proteinase-cleaved form: a new tool for detailed interaction studies and modeling. *Protein Science*, 17, 1844-1849.

Jiang, H. & M. R. Kanost (1997) Characterization and functional analysis of 12 naturally occurring reactive site variants of serpin-1 from *Manduca sexta*. *Journal of Biological Chemistry*, 272, 1082-1087.

Jiang, H., Y. Wang & M. R. Kanost (1994) Mutually exclusive exon use and reactive center diversity in insect serpins. *The Journal of Biological Chemistry*, 269, 55-58.

Jiang, H., Wang, Y., & Kanost, M. R. (1998) Pro-phenol oxidase activating proteinase from an insect, *Manduca sexta*: a bacteria-inducible protein similar to *Drosophila* easter. *Proceedings of the National Academy of Sciences*, 95, 12220-12225.

Jiang, H., Y. Wang, X. Q. Yu, Y. Zhu & M. Kanost (2003) Prophenoloxidase-activating proteinase-3 (PAP-3) from *Manduca sexta* hemolymph: a clip-domain serine proteinase regulated by serpin-1J and serine proteinase homologs. *Insect biochemistry and molecular biology*, 33, 1049-1060.

Jiang, R., E.-H. Kim, J. H. Gong, H. M. Kwon, C. H. Kim, K. H. Ryu, J. W. Park, K. Kurokawa, J. Zhang, D. Gubb & B. L. Lee (2009) Three pairs of protease-serpin complexes cooperatively regulate the insect innate immune responses. *Journal of Biological Chemistry*, 284, 35652-35658.

Johnson, D. J. D., W. Li, T. E. Adams & J. A. Huntington (2006) Antithrombin-S195A factor Xa-heparin structure reveals the allosteric mechanism of antithrombin activation. *Embo Journal*, 25, 2029-2037.

Kanost, M. R., E. L. Arrese, X. Cao, Y.-R. Chen, S. Chellapilla, M. R. Goldsmith, E. Grosse-Wilde, D. G. Heckel, N. Herndon, H. Jiang, A. Papanicolaou, J. Qu, J. L. Soulages, H. Vogel, J. Walters, R. M. Waterhouse, S.-J. Ahn, F. C. Almeida, C. An, P. Aqrawi, A. Bretschneider, W. B. Bryant, S. Bucks, H. Chao, G. Chevignon, J. M. Christen, D. F. Clarke, N. T. Dittmer, L. C. F. Ferguson, S. Garavelou, K. H. J. Gordon, R. T. Gunaratna, Y. Han, F. Hauser, Y. He, H. Heidel-Fischer, A. Hirsh, Y. Hu, H. Jiang, D. Kalra, C. Klinner, C. Konig, C. Kovar, A. R. Kroll, S. S. Kuwar, S. L. Lee, R. Lehman, K. Li, Z. Li, H. Liang, S. Lovelace, Z. Lu, J. H. Mansfield, K. J. McCulloch, T. Mathew, B. Morton, D. M. Muzny, D. Neunemann, F. Ongeri, Y. Pauchet, L. L. Pu, I. Pyrousis, X. J. Rao, A. Redding, C. Roesel, A. Sanchez-Gracia, S. Schaack, A. Shukla, G. Tetreau, Y. Wang, G.-H. Xiong, W. Traut, T. K. Walsh, K. C. Worley, D. Wu, W. Wu, Y.-Q. Wu, X. Zhang, Z. Zou, H. Zucker, A. D. Briscoe, T. Burmester, R. J. Clem, R. Feyereisen, C. J. P. Grimmelikhuijzen, S. J. Hamodrakas, B. S. Hansson, E. Huguet, L. S. Jermiin, Q. Lan, H. K. Lehman, M. Lorenzen, H. Merzendorfer, I. Michalopoulos, D. B. Morton, S. Muthukrishnan, J. G. Oakeshott, W. Palmer, Y. Park, A. L. Passarelli, et al., (2016) Multifaceted biological insights from a draft genome sequence of the tobacco hornworm moth, *Manduca sexta*. *Insect biochemistry and molecular biology*, 76, 118-147.

Kanost, M. R. & M. J. Gorman (2008) Phenoloxidases in insect immunity. *Insect immunology*, 1, 69-96.

Kanost, M. R. & H. Jiang (2015) Clip-domain serine proteases as immune factors in insect hemolymph. *Current opinion in insect science*, 11, 47-55.

Kanost, M. R., H. Jiang & X. Q. Yu (2004) Innate immune responses of a lepidopteran insect, *Manduca sexta*. *Immunological reviews*, 198, 97-105.

Kanost, M. R., S. V. Prasad & M. A. Wells (1989) Primary structure of a member of the serpin superfamily of proteinase inhibitors from an insect, *Manduca sexta*. *The Journal of Biological Chemistry*, 264, 965-972.

Kaslik, G., J. Kardos, E. Szabó, L. Szilágyi, P. Závodszky, W. M. Westler, J. L. Markley & L. Gráf (1997) Effects of serpin binding on the target proteinase: global stabilization, localized increased structural flexibility, and conserved hydrogen bonding at the active site. *Biochemistry*, 36, 5455-5464.

Kovarova, Z., J. Chmelar, M. Sanda, J. Brynda, M. Mares & P. Rezacova (2010) Crystallization and diffraction analysis of the serpin IRS-2 from the hard tick Ixodes ricinus. *Acta Crystallographica Section F-Structural Biology Communications*, 66, 1453-1457.

Kvassman, J., D. Lawrence & J. Shore (1995) The acid stabilization of plasminogen activator inhibitor-1 depends on protonation of a single group that affects loop insertion into β-sheet A. *Journal of Biological Chemistry*, 270, 27942-27947.

Landon, C., P. Sodano, C. Hetru, J. Hoffmann & M. Ptak (1997) Solution structure of drosomycin, the first inducible antifungal protein from insects. *Protein Science*, 6, 1878-1884.

Lesage, G. & H. Bussey (2006) Cell wall assembly in *Saccharomyces cerevisiae*. *Microbiology and Molecular Biology Reviews*, 70(2), 317-343.

Levashina, E. A., E. Langley, C. Green, D. Gubb, M. Ashburner, J. A. Hoffmann & J. M. Reichhart (1999) Constitutive activation of toll-mediated antifungal defense in serpin-deficient *Drosophila*. *Science* (New York, N.Y.), 285, 1917-1919.

Levitz, S. M., M. E. Selsted, T. Ganz, R. I. Lehrer & R. D. Diamond (1986) *In vitro* killing of spores and hyphae of *Aspergillus fumigatus* and *Rhizopus oryzae* by rabbit neutrophil cationic peptides and bronchoalveolar macrophages. *The Journal of Infectious Diseases*, 154, 483-489.

Li, J., Z. Wang, B. Canagarajah, H. Jiang, M. Kanost & E. J. Goldsmith (1999) The structure of active serpin 1K from *Manduca sexta*. Structure, 7, 103-109.

Li, M., J. M. Christen, N. T. Dittmer, X. Cao, X. Zhang, H. Jiang & M. R. Kanost (2018) The *Manduca sexta* serpinome: analysis of serpin genes and proteins in the tobacco hornworm. *Insect biochemistry and molecular biology*, 102, 21-30.

Li, W., T. Adams, J. Nangalia, C. Esmon & J. Huntington (2008) Molecular basis of thrombin recognition by protein C inhibitor revealed by the 1.6-angstrom structure of the heparin-bridged complex. *Proceedings of the National Academy of Sciences of the United States of America*, 105, 4661-4666.

Li, W. & J. A. Huntington (2008) The heparin binding site of protein C inhibitor is protease-dependent. *Journal of Biological Chemistry*, 283, 36039-36045.

Li, W., D. Johnson, C. Esmon & J. Huntington (2004) Structure of the antithrombin-thrombin-heparin ternary complex reveals the antithrombotic mechanism of heparin. *Nature Structural & Molecular Biology*, 11, 857-862.

Li, X., M. Reddy, D. Baev & M. Edgerton (2003) *Candida albicans* Ssa1/2p is the cell envelope binding protein for human salivary histatin 5. *Journal of Biological Chemistry*, 278, 28553-28561.

Ligoxygakis, P., N. Pelte, C. Ji, V. Leclerc, B. Duvic, M. Belvin, H. Jiang, J. A. Hoffmann & J. M. Reichhart (2002) A serpin mutant links Toll activation to melanization in the host defence of *Drosophila*. *The EMBO journal*, 21, 6330-6337.

Ligoxygakis, P., S. Roth & J. Reichhart (2003) A serpin regulates dorsal-ventral axis formation in the *Drosophila* embryo. *Current Biology*, 13, 2097-2102.

Lin, Z., L. Jiang, C. Yuan, J. Jensen, X. Zhang, Z. Luo, B. Furie, B. Furie, P. Andreasen & M. Huang (2011) Structural basis for recognition of urokinase-type plasminogen activator by plasminogen activator inhibitor-1. *Journal of Biological Chemistry*, 286, 7027-7032.

Liu, H. F., Y. N. Li, R. Jia, W. Z. Cui, Z. M. Mu & Z. F. Zhang (2011) Alternative splicing of the antitrypsin gene in the silkworm, *Bombyx mori*. Molecular biology reports, 38, 2793-2799.

Loebermann, H., R. Tokuoka, J. Deisenhofer & R. Huber (1984) Human α_1-proteinase inhibitor: crystal structure analysis of two crystal modifications, molecular model and preliminary analysis of the implications for function. *Journal of Molecular Biology*, 177, 531-557.

Lomas, D. A., D. L. Evans, J. T. Finch & R. W. Carrell (1992) The mechanism of Z α_1-antitrypsin accumulation in the liver. *Nature*, 357, 605-607.

Luksa, J., M. Podoliankaite, I. Vepstaite, Z. Strazdaite-Zieliene, J. Urbonavicius & E. Serviene (2015) Yeast beta-1,6-glucan is a primary target for the *Saccharomyces cerevisiae* K2 toxin. *Eukaryotic Cell*, 14, 406-414.

Marijanovic, E. M., J. Fodor, B. T. Riley, B. T. Porebski, M. G. S. Costa, I. Kass, D. E. Hoke, S. McGowan & A. M. Buckle (2019) Reactive centre loop dynamics and serpin specificity. *Scientific Reports*, 9.

Mast, A. E., J. J. Enghild & G. Salvesen (1992) Conformation of the reactive site loop of α_1-proteinase inhibitor probed by limited proteolysis. *Biochemistry*, 31, 2720-2728.

McCoy, A., X. Pei, R. Skinner, J. Abrahams & R. Carrell (2003) Structure of beta-antithrombin and the effect of glycosylation on antithrombin's heparin affinity and activity. *Journal of Molecular Biology*, 326, 823-833.

Meekins, D. A., M. R. Kanost & K. Michel. 2017. Serpins in arthropod biology. *In Seminars in cell & developmental biology*, 105-119. Elsevier.

Meekins, D. A., X. Zhang, K. P. Battaile, S. Lovell & K. Michel (2016) 1.45 angstrom resolution structure of SRPN18 from the malaria vector *Anopheles gambiae*. *Acta Crystallographica Section F-Structural Biology Communications*, 72, 853-862.

Michel, K., A. Budd, S. Pinto, T. J. Gibson & F. C. Kafatos (2005) *Anopheles gambiae* SRPN2 facilitates midgut invasion by the malaria parasite *Plasmodium berghei*. *EMBO reports*, 6, 891-897.

Michel, K., C. Suwanchaichinda, I. Morlais, L. Lambrechts, A. Cohuet, P. H. Awono-Ambene, F. Simard, D. Fontenille, M. R. Kanost & F. C. Kafatos (2006) Increased melanizing activity in *Anopheles gambiale* does not affect development of *Plasmodium falciparum*. *Proceedings of the National Academy of Sciences of the United States of America*, 103, 16858-16863.

Mulenga, A., R. Khumthong & K. Chalaire (2009) *Ixodes scapularis* tick serine proteinase inhibitor (serpin) gene family; annotation and transcriptional analysis. *BMC Genomics*, 10(1), 217.

Mwangi, S., E. Murungi, M. Jonas & A. Christoffels (2011) Evolutionary genomics of *Glossina morsitans* immune-related CLIP domain serine proteases and serine protease inhibitors. *Infection Genetics and Evolution*, 11, 740-745.

Myllymaki, H., S. Valanne & M. Ramet (2014) The *Drosophila* imd signaling pathway. *J Immunol*, 192, 3455-62.

Neafsey, D. E., R. M. Waterhouse, M. R. Abai, S. S. Aganezov, M. A. Alekseyev, J. E. Allen, J. Amon, B. Arcà, P. Arensburger, G. Artemov, L. A. Assour, H. Basseri, A. Berlin, B. W. Birren, S. A. Blandin, A. I. Brockman, T. R. Burkot, A. Burt, C. S. Chan, C. Chauve, J. C. Chiu, M. Christensen, C. Costantini, V. L. M. Davidson, E. Deligianni, T. Dottorini, V. Dritsou, S. B. Gabriel, W. M. Guelbeogo, A. B. Hall, M. V. Han, T. Hlaing, D. S. T. Hughes, A. M. Jenkins, X. Jiang, I. Jungreis, E. G. Kakani, M. Kamali, P. Kemppainen, R. C. Kennedy, I. K. Kirmitzoglou, L. L. Koekemoer, N. Laban, N. Langridge, M. K. N. Lawniczak, M. Lirakis, N. F. Lobo, E. Lowy, R. M. MacCallum, C. Mao, G. Maslen, C. Mbogo, J. McCarthy, K. Michel, S. N. Mitchell, W. Moore, K. A. Murphy, A. N. Naumenko, T. Nolan, E. M. Novoa, S. O'Loughlin, C. Oringanje, M. A. Oshaghi, N. Pakpour, P. A. Papathanos, A. N. Peery, M. Povelones, A. Prakash, D. P. Price, A. Rajaraman, L. J. Reimer, D. C. Rinker, A. Rokas, T. L. Russell, N. F. Sagnon, M. V. Sharakhova, T. Shea, F. A. Simão, F. Simard, M. A. Slotman, P. Somboon, V. Stegniy, C. J. Struchiner, G. W. C. Thomas, M. Tojo, P. Topalis, J. M. C. Tubio, M. F. Unger, J. Vontas, C. Walton, C. S. Wilding, J. H. Willis, Y.-C. Wu, G. Yan, E. M. Zdobnov, X. Zhou, F. Catteruccia, G. K. Christophides, F. H. Collins, R. S. Cornman, et al., (2015) Highly evolvable malaria vectors: the genomes of 16 *Anopheles* mosquitoes. *Science*, 347, 1258522.

Nguyen, L., E. Haney & H. Vogel (2011) The expanding scope of antimicrobial peptide structures and their modes of action. *Trends in Biotechnology*, 29, 464-472.

Olson, S., I. Bjork, R. Sheffer, P. Craig, J. Shore & J. Choay (1992) Role of the antithrombin-binding pentasaccharide in heparin acceleration of antithrombin-proteinase reactions - resolution of the antithrombin conformational change contribution to heparin rate enhancement. *Journal of Biological Chemistry*, 267, 12528-12538.

Onda, M., D. Belorgey, L. K. Sharp & D. A. Lomas (2005) Latent S49P neuroserpin forms polymers in the dementia familial encephalopathy with neuroserpin inclusion bodies. *Journal of Biological Chemistry*, 280, 13735-13741.

Park, S. H., R. Jiang, S. Piao, B. Zhang, E. H. Kim, H. M. Kwon, X. L. Jin, B. L. Lee & N. C. Ha (2011) Structural and functional characterization of a highly specific serpin in the insect innate immunity. *Journal of Biological Chemistry*, 286, 1567-1575.

Payne, J., M. Bleackley, T. Lee, T. Shafee, I. Poon, M. Hulett, M. Aguilar, N. van der Weerden & M. Anderson (2016) The plant defensin NaD1 introduces membrane disorder through a specific interaction with the lipid, phosphatidylinositol 4,5 bisphosphate. *Biochimica Et Biophysica Acta-Biomembranes*, 1858, 1099-1109.

Pearce, M. C., R. N. Pike, A. M. Lesk & S. P. Bottomley. 2007. *Serpin conformations*. World Scientific.

Peterson, F., N. Gordon & P. Gettins (2000) Formation of a noncovalent serpin-proteinase complex involves no conformational change in the serpin. Use of H-1-N-15 HSQC NMR as a sensitive nonperturbing monitor of conformation. *Biochemistry*, 39, 11884-11892.

Pickup, D. (1994) Poxviral modifiers of cytokine responses to infection. *Infectious agents and disease*, 3, 116-127.

Porter, L., Z. Radulovic, T. Kim, G. Braz, I. Vaz & A. Mulenga (2015) Bioinformatic analyses of male and female *Amblyomma americanum* tick expressed serine protease inhibitors (serpins). *Ticks and Tick-Borne Diseases*, 6, 16-30.

Ragan, E. J., C. An, C. T. Yang & M. R. Kanost (2010) Analysis of mutually exclusive alternatively spliced serpin-1 isoforms and identification of serpin-1 proteinase complexes in *Manduca sexta* hemolymph. *The Journal of Biological Chemistry*, 285, 29642-29650.

Ragni, E., M. Sipiczki & S. Strahl (2007) Characterization of Ccw12p, a major key player in cell wall stability of *Saccharomyces cerevisiae*. *Yeast*, 24, 309-319.

Rau, J., L. Beaulieu, J. Huntington & F. C. Church (2007) Serpins in thrombosis, hemostasis and fibrinolysis. *Journal of thrombosis and haemostasis*, 5, 102-115.

Rautenbach, M., A. Troskie & J. Vosloo (2016) Antifungal peptides: to be or not to be membrane active. *Biochimie*, 130, 132-145.

Reichhart, J. M. (2005) Tip of another iceberg: *Drosophila* serpins. *Trends in cell biology*, 15, 659-665.

Reichhart, J. M., D. Gubb & V. Leclerc (2011) The *Drosophila* serpins: multiple functions in immunity and morphogenesis. *Methods in Enzymology: Biology of Serpins*, 499, 205-225.

Rider, S., M. Morgan & L. Arlian (2015) Draft genome of the scabies mite. *Parasites & Vectors*, 8(1), 585.

Roberts, T. H. & J. Hejgaard (2008) Serpins in plants and green algae. *Functional & integrative genomics*, 8, 1-27.

Rodriguez-Valle, M., T. Xu, S. Kurscheid & A. Lew-Tabor (2015) *Rhipicephalus microplus* serine protease inhibitor family: annotation, expression and functional characterisation assessment. *Parasites & Vectors*, 8(1), 7.

Santangelo, M., R. Noto, M. Levantino, A. Cupane, S. Ricagno, M. Pezzullo, M. Bolognesi, M. Mangione, V. Martorana & M. Manno. 2012. On the molecular structure of human neuroserpin polymers. *Proteins: Structure, Function, and Bioinformatics*, 80(1), 8-13.

Sawistowskaschroder, E., D. Kerridge & H. Perry (1984) Echinocandin inhibition of 1,3-beta-D-glucan synthase from *Candida albicans*. *FEBS Letters*, 173, 134-138.

Scherfer, C., H. Tang, Z. Kambris, N. Lhocine, C. Hashimoto & B. Lemaitre (2008) *Drosophila* Serpin-28D regulates hemolymph phenoloxidase activity and adult pigmentation. *Developmental biology*, 323, 189-196.

Schreuder, H., B. Deboer, R. Dijkema, J. Mulders, H. Theunissen, P. Grootenhuis & W. Hol (1994) The intact and cleaved human antithrombin-III complex as a model for serpin-proteinase interactions. *Nature Structural Biology*, 1, 48-54.

Schulze, A. J., U. Baumann, S. Knof, E. Jaeger, R. Huber & C. B. Laurell (1990) Structural transition of α_1-antitrypsin by a peptide sequentially similar to β-strand s4A. *European journal of biochemistry*, 194, 51-56.

Schulze, A. J., P. W. Frohnert, R. A. Engh & R. Huber (1992) Evidence for the extent of insertion of the active site loop of intact α_1-proteinase inhibitor in β-sheet A. *Biochemistry*, 31, 7560-7565.

Shen, D., Y. Liu, F. Zhou, G. Wang & C. An (2014) Identification of immunity-related genes in *Ostrinia furnacalis* against entomopathogenic fungi by RNA-seq analysis. *Plos One*, 9(1), e86436.

Silverman, G. A., P. I. Bird, R. W. Carrell, F. C. Church, P. B. Coughlin, P. G. W. Gettins, J. A. Irving, D. A. Lomas, C. J. Luke & R. W. Moyer (2001) The serpins are an expanding superfamily of structurally similar but functionally diverse proteins evolution, mechanism of inhibition, novel functions, and a revised nomenclature. *Journal of Biological Chemistry*, 276, 33293-33296.

Singh, A. & R. Prasad (2011) Comparative lipidomics of azole sensitive and resistant clinical isolates of *Candida albicans* reveals unexpected diversity in molecular lipid imprints. *Plos One*, 6(4), e19266.

Skinner, R., W. S. W. Chang, L. Jin, X. Pei, J. A. Huntington, J.-P. Abrahams, R. W. Carrell & D. A. Lomas (1998) Implications for function and therapy of a 2.9 Å structure of binary-complexed antithrombin. *Journal of Molecular Biology*, 283, 9-14.

Stein, P. & R. Carrell (1995) What do dysfunctional serpins tell us about molecular mobility and disease. *Nature Structural Biology*, 2, 96-113.

Stout, T. J., H. Graham, D. I. Buckley & D. J. Matthews (2000) Structures of active and latent PAI-1: a possible stabilizing role for chloride ions. *Biochemistry*, 39, 8460-8469.

Stratikos, E. & P. Gettins (1998) Mapping the serpin-proteinase complex using single cysteine variants of alpha(1)-proteinase inhibitor Pittsburgh. *Journal of Biological Chemistry*, 273, 15582-15589.

Stratikos, E. & P. G. Gettins (1999) Formation of the covalent serpin-proteinase complex involves translocation of the proteinase by more than 70 Å and full insertion of the reactive center loop into beta-sheet A. *Proceedings of the National Academy of Sciences of the United States of America*, 96, 4808-4813.

Sucher, A., E. Chahine & H. Balcer (2009) Echinocandins: the newest class of antifungals. *Annals of Pharmacotherapy*, 43, 1647-1657.

Suwanchaichinda, C. & M. R. Kanost (2009) The serpin gene family in *Anopheles gambiae*. *Gene*, 442, 47-54.

Suwanchaichinda, C., R. Ochieng, S. Zhuang & M. R. Kanost (2013) *Manduca sexta* serpin-7, a putative regulator of hemolymph prophenoloxidase activation. *Insect biochemistry and molecular biology*, 43, 555-561.

Takahashi, D., B. L. Garcia & M. R. Kanost (2015) Initiating protease with modular domains interacts with β-glucan recognition protein to trigger innate immune response in insects. *Proceedings of the National Academy of Sciences*, 112, 13856-13861.

Tang, H., Z. Kambris, B. Lemaitre & C. Hashimoto (2006) Two proteases defining a melanization cascade in the immune system of *Drosophila*. *Journal of Biological Chemistry*, 281, 28097-28104.

Tang, H., Kambris, Z., Lemaitre, B., & Hashimoto, C. (2008) A serpin that regulates immune melanization in the respiratory system of *Drosophila*. *Developmental cell*, 15(4), 617-626.

Terenius, O., A. Papanicolaou, J. S. Garbutt, I. Eleftherianos, H. Huvenne, S. Kanginakudru, M. Albrechtsen, C. An, J. L. Aymeric & A. Barthel (2011) RNA interference in Lepidoptera: an overview of successful and unsuccessful studies and implications for experimental design. *Journal of insect physiology*, 57, 231-245.

Terras, F., S. Torrekens, F. Vanleuven, R. Osborn, J. Anderleyden, B. Cammue & W. Broekaert (1993) A new family of basic cysteine-rich plant antifungal proteins from Brassicaceae species. *FEBS Letters*, 316, 233-240.

Tian, C., B. Gao, M. Rodriguez, H. Lanz-Mendoza, B. Ma & S. Zhu (2008) Gene expression, antiparasitic activity, and functional evolution of the Drosomycin family. *Molecular Immunology*, 45, 3909-3916.

Tirloni, L., A. Seixas, A. Mulenga, I. Vaz & C. Termignoni (2014) A family of serine protease inhibitors (serpins) in the cattle tick *Rhipicephalus (Boophilus) microplus*. *Experimental Parasitology*, 137, 25-34.

Tong, Y., H. Jiang & M. R. Kanost (2005) Identification of plasma proteases inhibited by *Manduca sexta* serpin-4 and serpin-5 and their association with components of the prophenol oxidase activation pathway. *The Journal of Biological Chemistry*, 280, 14932-14942.

Tong, Y. & M. R. Kanost (2005) *Manduca sexta* serpin-4 and serpin-5 inhibit the prophenol oxidase activation pathway: cDNA cloning, protein expression, and characterization. *The Journal of Biological Chemistry*, 280, 14923-14931.

Turner, P. C., P. F. McAuliffe, A. L. MacNeill & R. W. Moyer (2007) New lessons from poxvirus serpins. *Molecular and Cellular Aspects of the Serpinopathies and Disorders in Serpin Activity*, 163.

Van De Craen, B., P. J. Declerck & A. Gils (2012) The biochemistry, physiology and pathological roles of PAI-1 and the requirements for PAI-1 inhibition in vivo. *Thrombosis research*, 130, 576-585.

van der Weerden, N., R. Hancock & M. Anderson (2010) Permeabilization of fungal hyphae by the plant defensin NaD1 occurs through a cell wall-dependent process. *Journal of Biological Chemistry*, 285, 37513-37520.

Veillard, F., L. Troxler & J. M. Reichhart (2016) *Drosophila melanogaster* clip-domain serine proteases: structure, function and regulation. *Biochimie*, 122, 255-69.

Vizioli, J., P. Bulet, M. Charlet, C. Lowenberger, C. Blass, H. Muller, G. Dimopoulos, J. Hoffmann, F. Kafatos & A. Richman (2000) Cloning and analysis of a cecropin gene from the malaria vector mosquito, *Anopheles gambiae*. *Insect Molecular Biology*, 9, 75-84.

Wahlberg, N., C. Wheat & C. Pena (2013) Timing and patterns in the taxonomic diversification of Lepidoptera (Butterflies and Moths). *Plos One*, 8(11), e80875.

Wang, Y. & H. Jiang (2004) Purification and characterization of *Manduca sexta* serpin-6: a serine proteinase inhibitor that selectively inhibits prophenoloxidase-activating proteinase-3. *Insect biochemistry and molecular biology*, 34, 387-395.

Wang, Y., & Jiang, H. (2006) Interaction of β-1, 3-glucan with its recognition protein activates hemolymph proteinase 14, an initiation enzyme of the prophenoloxidase activation system in *Manduca sexta*. *Journal of Biological Chemistry*, 281(14), 9271-9278.

Wang, Y., & Jiang, H. (2007) Reconstitution of a branch of the *Manduca sexta* prophenoloxidase activation cascade *in vitro*: snake-like hemolymph proteinase 21 (HP21) cleaved by HP14 activates prophenoloxidase-activating proteinase-2 precursor. *Insect biochemistry and molecular biology*, 37(10), 1015-1025.

Wang, Y., & Jiang, H. (2010) Binding properties of the regulatory domains in *Manduca sexta* hemolymph proteinase-14, an initiation enzyme of the prophenoloxidase activation system. *Developmental & Comparative Immunology*, 34(3), 316-322.

Wang, Y., Z. Lu & H. Jiang (2014) *Manduca sexta* proprophenoloxidase activating proteinase-3 (PAP3) stimulates melanization by activating proPAP3, proSPHs, and proPOs. *Insect biochemistry and molecular biology*, 50, 82-91.

Whisstock, J. C., R. Skinner, R. W. Carrell & A. M. Lesk (2000) Conformational changes in serpins: I. The native and cleaved conformations of α_1-antitrypsin. *Journal of Molecular Biology*, 295, 651-665.

Widmer, C., J. M. Gebauer, E. Brunstein, S. Rosenbaum, F. Zaucke, C. Droegemueller, T. Leeb & U. Baumann (2012) Molecular basis for the action of the collagen-specific chaperone Hsp47/SERPINH1 and its structure-specific client recognition. *Proceedings of the National Academy of Sciences of the United States of America*, 109, 13243-13247.

Xu, X., X. Zhong, H. Yi & X. Yu (2012) *Manduca sexta* gloverin binds microbial components and is active against bacteria and fungi. *Developmental and Comparative Immunology*, 38, 275-284.

Xue, Y., P. Björquist, T. Inghardt, M. Linschoten, D. Musil, L. Sjölin & J. Deinum (1998) Interfering with the inhibitory mechanism of serpins: crystal structure of a complex formed between cleaved plasminogen activator inhibitor type 1 and a reactive-centre loop peptide. *Structure*, 6, 627-636.

Yamasaki, M., T. J. Sendall, L. E. Harris, G. M. Lewis & J. A. Huntington (2010) Loop-sheet mechanism of serpin polymerization tested by reactive center loop mutations. *Journal of Biological Chemistry*, 285, 30752-30758.

Yamasaki, M., T. J. Sendall, M. C. Pearce, J. C. Whisstock & J. A. Huntington (2011) Molecular basis of α_1-antitrypsin deficiency revealed by the structure of a domain-swapped trimer. *EMBO reports*, 12, 1011-1017.

Yan, Z., Q. Fang, Y. Liu, S. Xiao, L. Yang, F. Wang, C. An, J. Werren & G. Ye (2017) A venom serpin splicing isoform of the endoparasitoid wasp *Pteromalus puparum* suppresses host prophenoloxidase cascade by forming complexes with host hemolymph proteinases. *Journal of Biological Chemistry*, 292, 1038-1051.

Yang, F., Y. Wang, N. Sumathipala, X. Cao, M. R. Kanost & H. Jiang (2018) *Manduca sexta* serpin-12 controls the prophenoloxidase activation system in larval hemolymph. *Insect biochemistry and molecular biology*.

Yang, L., Y. Mei, Q. Fang, J. Wang, Z. Yan, Q. Song, Z. Lin & G. Ye (2017) Identification and characterization of serine protease inhibitors in a parasitic wasp, *Pteromalus puparum*. *Scientific Reports*, 7(1), 15755.

Ye, S., A. L. Cech, R. Belmares, R. C. Bergstrom, Y. Tong, D. R. Corey, M. R. Kanost & E. J. Goldsmith (2001) The structure of a Michaelis serpin–protease complex. *Nature Structural & Molecular Biology*, 8, 979-983.

Yeaman, M. & N. Yount (2003) Mechanisms of antimicrobial peptide action and resistance. *Pharmacological Reviews*, 55, 27-55.

Yi, H. Y., M. Chowdhury, Y. D. Huang & X. Q. Yu (2014) Insect antimicrobial peptides and their applications. *Appl Microbiol Biotechnol*, 98, 5807-22.

Zhang, W., J. Chen, N. Keyhani, Z. Zhang, S. Li & Y. Xia (2015a) Comparative transcriptomic analysis of immune responses of the migratory locust, *Locusta migratoria*, to challenge by the fungal insect pathogen, *Metarhizium acridum*. *BMC Genomics*, 16.

Zhang, X., D. A. Meekins, C. An, M. Zolkiewski, K. P. Battaile, M. R. Kanost, S. Lovell & K. Michel (2015b) Structural and inhibitory effects of hinge loop mutagenesis in serpin-2 from the malaria vector *Anopheles gambiae*. *Journal of Biological Chemistry*, 290, 2946-2956.

Zhao, P., G. H. Wang, Z. M. Dong, J. Duan, P. Z. Xu, T. C. Cheng, Z. H. Xiang & Q. Y. Xia (2010) Genome-wide identification and expression analysis of serine proteases and homologs in the silkworm *Bombyx mori*. *BMC genomics*, 11, 405.

Zheng, Y. P., W. Y. He, C. Béliveau, A. Nisole, D. Stewart, S. C. Zheng, D. Doucet, M. Cusson & Q. L. Feng (2009) Cloning, expression and characterization of four serpin-1 cDNA variants from the spruce budworm, *Choristoneura fumiferana*. *Comparative Biochemistry and Physiology Part B: Biochemistry and Molecular Biology*, 154, 165-173.

Zhou, A., P. E. Stein, J. A. Huntington, P. Sivasothy, D. A. Lomas & R. W. Carrell (2004) How small peptides block and reverse serpin polymerisation. *Journal of Molecular Biology*, 342, 931-941.

Zhou, Z., A. Anisowicz, M. J. H. Hendrix, A. Thor, M. Neveu, S. Sheng, K. Rafidi, E. Seftor & R. Sager (1994) Maspin, a serpin with tumor-suppressing activity in human mammary epithelial cells. *Science*, 263, 526-529.

Zhu, J., P. Yang, Z. Zhang, G. Wu & B. Yang (2013) Transcriptomic immune response of *Tenebrio molitor* pupae to parasitization by *Scleroderma guani*. *Plos One*, 8(1), e54411.

Zhu, Y., T. Johnson & M. Kanost (2003a) Identification of differentially expressed genes in the immune response of the tobacco hornworm, *Manduca sexta*. *Insect Biochem Mol Biol*, 33, 541-559.

Zhu, Y., Y. Wang, M. J. Gorman, H. Jiang & M. R. Kanost (2003b) *Manduca sexta* serpin-3 regulates prophenoloxidase activation in response to infection by inhibiting prophenoloxidase-activating proteinases. *The Journal of Biological Chemistry*, 278, 46556-46564.

Zou, Z., J. D. Evans, Z. Lu, P. Zhao, M. Williams, N. Sumathipala, C. Hetru, D. Hultmark & H. Jiang (2007) Comparative genomic analysis of the Tribolium immune system. *Genome biology*, 8, R177.

Zou, Z. & H. Jiang (2005) *Manduca sexta* serpin-6 regulates immune serine proteinases PAP-3 and HP8. cDNA cloning, protein expression, inhibition kinetics, and function elucidation. *The Journal of Biological Chemistry*, 280, 14341-14348.

Zou, Z., D. L. Lopez, M. R. Kanost, J. D. Evans & H. Jiang (2006) Comparative analysis of serine protease-related genes in the honey bee genome: possible involvement in embryonic development and innate immunity. *Insect molecular biology*, 15, 603-614.

Zou, Z., Z. Picheng, H. Weng, K. Mita & H. Jiang (2009) A comparative analysis of serpin genes in the silkworm genome. *Genomics*, 93, 367-375.

Zou, Z., S. W. Shin, K. S. Alvarez, V. Kokoza & A. S. Raikhell (2010) Distinct melanization pathways in the mosquito *Aedes aegypti*. *Immunity*, 32, 41-53.

Chapter 2 - Analysis of Serpin Genes and Proteins in *Manduca sexta*

Part of this chapter has been published as a journal article:

Li, M., Christen, J. M., Dittmer, N. T., Cao, X., Zhang, X., Jiang, H., Kanost, M. R. (2018). The *Manduca sexta* serpinome: Analysis of serpin genes and proteins in the tobacco hornworm. *Insect biochemistry and molecular biology*, 102, 21-30.

Introduction

Serpins are a superfamily of proteins, many of which inhibit serine proteinases. They share a conserved tertiary structure composed of three β-sheets, 8-9 α-helices, and an exposed reactive center loop (RCL) (Silverman et al., 2001). The mechanism for proteinase inhibition by serpins includes cleavage by the proteinase of a specific peptide bond (the scissile bond) between residues designated P1-P1' in the serpin RCL. The inhibition reaction begins with the formation of a noncovalent complex between the proteinase and serpin through interaction of the proteinase active site with the serpin RCL (Ye et al., 2001). Once the P1 side chain is correctly positioned in the primary specificity pocket of the proteinase, the active site serine of the proteinase attacks and cleaves the scissile bond, resulting in formation of a covalent acyl complex of the serpin and proteinase. The serpin undergoes a large conformational change, in which the RCL inserts as the fourth strand in its β-sheet A. The proteinase is translocated by about 70 Å, and its active site catalytic triad becomes distorted, resulting in proteinase inactivation (Gettins and Olson, 2016).

Serpins have been identified in animals, plants, bacteria, archaea, and some viruses (Gettins, 2002). Insect serpins have been a subject of significant research efforts in the last three decades (Meekins et al., 2017). Biochemical studies and genetic analyses have shown that some insect serpins regulate extracellular proteinase cascades in the hemolymph, which stimulate innate immune responses, including the Toll pathway and prophenoloxidase activation (Shin et al., 2006; Jiang et al., 2009; Park et al., 2011; Levashina et al., 1999; Ahmad et al., 2009; Zou and Jiang, 2005; An and Kanost, 2010; An et al., 2011; Zou et al., 2010; Abraham et al., 2005; Michel et al., 2006; Ligoxygakis et al., 2002; De Gregorio et al., 2002; Scherfer et al., 2008; Tang et al., 2008; Jiang et al., 2003; Zhu et al., 2003; Wang and Jiang, 2004; Tong and Kanost, 2005; Tong et al., 2005; Wang and Jiang, 2006; He et al., 2017; Yang et al., 2018).

Completion of insect genome projects has revealed the presence of many previously unknown serpin genes. Thirty-four serpin genes have been identified in *Bombyx mori* (Zou et al.,

2009), thirty-one in *Culex quinquefasciatus* (Gulley et al., 2013), thirty-one in *Tribolium castaneum* (Zou et al., 2007), twenty-nine in *Drosophila melanogaster* (Reichhart, 2005; Reichhart et al., 2011), twenty-three in *Aedes aegypti* (Gulley et al., 2013), eighteen in *Anopheles gambiae* (Christophides et al., 2002; Suwanchaichinda and Kanost, 2009), ten in *Pteromalus puparum* (Yang et al., 2017), and at least seven serpin genes in *Apis mellifera* (Zou et al., 2006). However, physiological functions of most insect serpins are unknown.

The first insect serpin (serpin-1B) with a known sequence was isolated from hemolymph of the tobacco hornworm, *M. sexta* (Kanost et al., 1989). Since then, nine additional serpins from *M. sexta* have been identified and investigated through biochemical studies (Jiang et al., 1994; Gan et al., 2001; Zhu et al., 2003; Tong and Kanost, 2005; Zou and Jiang, 2005; Suwanchaichinda et al., 2013; He et al., 2017; Yang et al., 2018). In this chapter, I described the properties of serpin genes identified in the *M. sexta* genome (Kanost et al., 2016). Thirty-one genes encoding serpin proteins and one likely serpin pseudogene were characterized. Alternatively spliced isoforms were detected and demonstrated. Sequence alignment and conserved residue comparison were performed and used to make structure-function predictions.

Materials and Methods

Basic parameters of serpin genes and proteins

Searching for novel serpin genes in *M. sexta* OGS2.0 (https://i5k.nal.usda.gov/Manduca_sexta) were performed by Dr. Jayne Christen, and Dr. Michael Kanost corrected the coding sequences and protein sequences. Conversion of scaffold ID and NCBI accession number is available on ftp://ftp.ncbi.nlm.nih.gov/genomes/all/GCA/000/262/585/GCA_000262585.1_Msex_1.0/GCA_000262585.1_Msex_1.0_assembly_report.txt. Gene structure information, including alternative splicing, exons and introns was obtained from *M. sexta* JBrowse/Apollo (https://i5k.nal.usda.gov/available-genome-browsers) (Poelchau et al., 2015). Theoretical molecular weight and pI of mature serpins were calculated using ProtParam (http://us.expasy.org/) (Gasteiger et al., 2005). Signal peptides were predicted using SignalP 4.1 (http://www.cbs.dtu.dk/services/SignalP/) (Petersen et al., 2011). Multiple sequence alignments were performed using ClustalW2 (http://www.ebi.ac.uk/Tools/msa/clustalw2/) (Larkin et al.,

2007). Prediction of secondary structures in the aligned sequences was based on the crystal structure of *M. sexta* serpin-1K (Li et al., 1999) and human α_1-antitrypsin (Irving et al., 2000). Conserved residues in the shutter, breach, hinge, gate and other regions were identified as described previously (Irving et al., 2000).

Cloning of *MsSerpin-7* gene

The *MsSerpin-7* gene was found with parts in two scaffolds, 12474 and 15728. Phylogenetic analysis showed that *MsSerpin-7* was grouped with serpins that only have a single exon, so *MsSerpin-7* was suspected to have single exon as well. To test this hypothesis, the full length of *MsSerpin-7* gene from genomic DNA of *M. sexta* was amplified by PCR, using a forward primer (5'-AAC ACC CGT CCC ATG AGA ATG TGG ACT-3') that contains the start codon (underlined) and a reverse primer (5'-AAA CGT TAG CTC TCA CAC AAC TGA AGG-3') that contains the stop codon (underlined). PCR was performed using Taq DNA polymerase (Invitrogen) as follows: initial denaturation at 95 °C for 3 min followed by 30 cycles of denaturing at 95 °C for 30 seconds, annealing at 58 °C for 30 seconds, extension at 68 °C for 90 seconds, and a final extension at 68 °C for 10 min. Products were gel purified, cloned into pCR4-TOPO vector using TOPO TA Cloning Kit (Invitrogen), and used to transform competent *Escherichia coli* strain TOP10 (Invitrogen). Recombinant plasmids were extracted and subjected to EcoRI-HF digestion, and the inserted *MsSerpin-7* gene was sequenced at GENWIZ.

Analysis of serpin transcript abundance upon immune challenge

Protein sequences of *M. sexta* serpins were used as TBLASTN queries with default settings to search against RNAseq CIFH09contigs (http://darwin.biochem.okstate.edu/blast/blast.html) (Zhang et al., 2011). Hits were filtered by the following criteria: score > 100 bits, E value < 0.01, identities > 90. Reads of control hemocytes, control fat body, bacteria-induced hemocytes and bacteria-induced fat body were retrieved from previous work and normalized accordingly (Zhang et al., 2011).

Results and Discussion

Overview of serpin genes

Thirty-two serpin genes were identified in the *M. sexta* genome by Dr. Michael Kanost and Dr. Jayne Christen (Table 2-1). Complete CDS and protein sequences of 31/32 were revealed, while MsSerpin-29 lacks a significant part of the typically conserved amino-terminal region, perhaps due to incomplete genome assembly. Most of the serpin genes are located on a single genomic scaffold, but *MsSerpin-3* and *MsSerpin-7* were fragmented, with exons on more than one scaffold. MsSerpin-3 sequence was confirmed by the published cDNA sequences. Cloning of *MsSerpin-7* from genomic DNA by PCR showed single band of ~1.2 kilobases which implied no intron present (Fig. 2-1). Sequencing further confirmed the single exon structure of *MsSerpin-7* gene. *MsSerpin-22* had two apparent haplotypes on different scaffolds 00144 and 00153. Several genomic scaffolds contain multiple serpin genes within a relatively small region (Fig. 2-2, Table B-1), including 8 serpin genes located within a 20 kb segment on scaffold 00379. The *M. sexta* serpin genes vary from one exon to ten (Table 2-1 and Fig. 2-3), with most composed of 8-10 exons. *MsSerpins-4, 5, 7, 9,* and *14* contain a single exon (Table 2-1).

Alternative splicing of *MsSerpin-15* and *MsSerpin-28*

Besides MsSerpin-1 reported before, two additional *M. sexta* serpin genes, *MsSerpin-15* and *MsSerpin-28* have alternative exons encoding the carboxyl terminal ~45 residues, including the RCL (Fig. 2-4, Table B-2). *MsSerpin-15*, encodes two serpin splicing isoforms with different exon 9 sequences encoding the RCL. A closely related *B. mori* gene, *BmSerpin2*, has a similar gene structure and also encodes two splicing isoforms with different RCL sequences (Zou et al., 2009). The *MsSerpin-28* gene contains three versions of exon 7, each encoding a different RCL sequence.

MsSerpin-17 was originally thought to encode two splicing isoforms based on the OGS2.0 assembly. Isoform A contained putative consecutive exon 6A, 7A and 8A, and isoform B contained putative consecutive exon 6B, 7B and 8B. Between tentative exon 8A and 6B there are 7007 bp, which contains a 3107 bp gap. However, I found that predicted alternative splicing of *MsSerpin-17* was likely caused by assembly errors. Tentative exon 6A of *MsSerpin-17* probably missed 105 bp at the 5' end. If this 105 bp "intron" is considered as the 5' end of exon 6A, sequences of 6A and 6B would be identical. Besides, tentative exon 7A has identical

sequence with tentative exon 7B, so do tentative exon 8A with 8B. The corresponding intron sequence alignments demonstrated high similarity between tentative splicing regions. Therefore, I suspect exon 6, 7 and 8 with introns of *MsSerpin-17* were incorrectly duplicated during genome assembly, and the evidence for presence of MsSerpin-17 splicing isoforms currently is not convincing.

Analysis and comparison of serpin amino acid sequences

A majority of the *M. sexta* serpin gene products are predicted to be secreted, with amino-terminal secretion signal peptides varying from 15 to 24 residues (Table 2-1). MsSerpin-2 was reported to by cytoplasmic without signal peptide (Gan et al., 2001). MsSerpin-15, 16, and 17 lack a detected signal peptide and thus may be cytoplasmic proteins. Alignment of the amino acid sequences (Fig. B-1) indicates that although overall sequence identity between some serpins is fairly low (~35%), there are regions of identity between all of the sequences that correspond with secondary structures conserved in insect and mammalian serpin three-dimensional structures. The length of the mature serpins varies from 332 to 502 residues with a theoretical mass of 37.8-57.1 kDa (excluding MsSerpin-29, 284 residues). Notably, MsSerpin-10 has a nearly 100-amino acid insertion between helix-F and strand-3A (Fig. B-1), resulting in its greater than average length of 502 residues. The *B. mori* ortholog, BmSerpin10, has an insertion of a similar length at the same position (Zou et al., 2009). The structure and potential function of this region is not yet known, but perhaps could be a site for interaction with other proteins. The calculated isoelectric point of most of the *M. sexta* serpins varies from 4.4 to 7.3. However, MsSerpin-12, 14, 20, 21, 22, 26, 29, and 31 are more basic, with a calculated pI of approximately 8-9 (Table 2-1).

RCL region of *M. sexta* serpins

The RCL in serpins is a solvent-exposed region between strand-4A and strand-1C, consisting of 16-25 amino acid residues (Meekins et al., 2016). In the inhibition of a proteinase by a serpin, the proteinase cleaves the RCL at a specific position called the scissile bond, between two residues designated P1 and P1' (Loebermann et al., 1984). As a result, the amino-terminal segment of the RCL inserts into β-sheet A, forming a new strand between strand-3A and strand-5A, with formation of an irreversible serpin-proteinase complex (Stratikos and Gettins, 1999; Huntington et al., 2000; Dunstone and Whisstock, 2011). Some members of the serpin

superfamily, such as ovalbumin, Hsp47/SERPINH1, maspin and MENT, lack the capability for protease inhibition (Huntington and Stein, 2001; Nagata, 1996; Zhou et al., 1994; Grigoryev et al., 1999). The sequence and length of the RCL of such non-inhibitory serpins are factors that distinguish them from inhibitory serpins (Irving et al., 2000). In non-inhibitory serpins, either the length of the RCL limits the complete translocation of the protease, or the critical residues in the hinge region are not favorable for rapid loop insertion (Widmer et al., 2012; Al-Ayyoubi et al., 2004; Stein et al., 1991; McGowan et al., 2006).

In order to predict inhibitory or non-inhibitory *M. sexta* serpins, I analyzed their RCL sequences (Fig. 2-5). The hinge region (P15-P9) of inhibitory serpins is typically composed of two charged residues, followed by a series of residues with small hydrophobic side chains, which contribute to mobility for the conformational change accompanying RCL insertion into β-sheet A (Hopkins et al., 1993). A consensus pattern in the hinge region can be used as a theoretical guideline to recognize inhibitory serpins. P17 is usually glutamate, P16 is glutamate/lysine/ arginine, P15 is glycine, P14 is threonine/serine/alanine, and P12-P9 are alanine/glycine/serine (Irving et al., 2000). Additionally, the presence of proline in the proximal RCL prior to the P2 residue disrupts the formation of a new β strand, leading to failure of RCL incorporation (Hopkins et al., 1993; Hopkins and Stone, 1995; Gettins, 2002). Furthermore, conserved residues in the breach and shutter regions, which facilitate sheet opening to accept the RCL as a new strand in the β-sheet should also be considered (Whisstock et al., 2000b; Whisstock et al., 2000a). Guided by the above criteria, 16 of the 48 serpin gene products (MsSerpin-1D, 8, 10, 18-20, 22-27, 29-32) are predicted to encode non-inhibitory serpins. They lack the consensus pattern of inhibitory serpins in the hinge region, and these putative non-inhibitors are relatively rich in proline in the proximal RCL and less conserved in the breach and shutter regions (Fig. B-1). The other 32 genes encode proteins more likely to have a mobile hinge region, few proline residues in the proximal RCL, and highly conserved residues in the breach and shutter regions and thus are more likely to function as proteinase inhibitors.

The scissile bond position for some inhibitory *M. sexta* serpins were previously determined experimentally (Jiang and Kanost, 1997; Zou and Jiang, 2005; He et al., 2017; Yang et al., 2018). For the remaining serpins likely to be inhibitory, the position of their RCL scissile bond was predicted based on the distance from the hinge and previously confirmed cleavage sites of studied serpins (Gettins, 2002; Jiang and Kanost, 1997; Zou and Jiang, 2005; Reichhart et al.,

2011). Based on putative P1 residues, *M. sexta* serpins can be categorized into three groups: 1) serpins with K or R at P1, including MsSerpin-1A, 1E, 1J, 1N, 1Y, 3, 4, 5, 6, 7, 9, 13, 15B, 16, 17, and 28B; 2) serpins with Y or F at P1, including MsSerpin-1C, 1H, 1K, 1Z, 15A, and 21; and 3) serpins with small hydrophobic residues at P1, including MsSerpin-1B, 1F, 1G, 1I, 2, 11, 12, 28A, and 28C. Distinguishing inhibitory and non-inhibitory serpins and characterizing inhibitory selectivity will require future biochemical experiments using purified serpins.

Intron positions of *M. sexta* serpin genes

Intron positions are often conserved in closely related genes, including serpin genes (Roy et al., 2003; Kaiserman and Bird, 2005). Based on the number of exons and intron positions, *M. sexta* serpins can be categorized into the following groups (Fig. 2-3): I) serpin genes with a single exon (*MsSerpin-4, 5, 7, 9* and *14*); II) serpin genes with 2-3 coding exons and one intron position that is conserved (*MsSerpin-8, 23, 20, 32* and *24*); III) serpin genes with 6-8 coding exons and 2-3 intron positions conserved (*MsSerpin-3, 10, 11, 12*); IV) serpins genes with 7-10 coding exons and most intron positions are conserved (*MsSerpin-16, 29, 22, 21, 26, 31, 30, 18, 19, 25, 27, 28, 1, 2, 17, 15*). Serpin genes 6 and 13 contain multiple introns but none at conserved positions. Genes in groups I and II may be derived from a single retrotransposition event followed by several rounds of gene duplication. One series of duplications may have led to *MsSerpin-4, 5, 7, 9,* and *14*, while a second series of duplications occurring after gaining an intron led to group II genes *MsSerpin-8, 20, 23, 24*, and *32*. A similar process of serpin gene evolution was also described in *B. mori* (Zou et al., 2009). Phylogenetic analysis indicated 17 orthologous gene pairs between *M. sexta* and *B. mori* serpins (Li et al., 2018). It is interesting to note that 13 of the 16 genes in groups I, II, and III have orthologs in *B. mori*, thus these genes evolved before the divergence of these two lineages. In contrast, 12 of the 16 genes in group IV do not have an ortholog in *B. mori*, indicating that either those genes arose after the divergence or that they were lost in *B. mori*. It is intriguing that of the 13 serpin genes that appear to have evolved in *M. sexta* after its divergence from the common ancestor with *B. mori*, 10 encode proteins that are predicted to be non-inhibitory. Of the 17 orthologous gene pairs between *M. sexta* and *B. mori*, 14 are predicted to encode protease inhibitors, while only three are non-inhibitory. Thus, it appears that most of the serpin proteins present in *M. sexta* but not in *B. mori* have a function other than protease inhibition.

Differential expression of *M. sexta* serpins in response to immune challenge

Previous studies on changes of transcription level in response to immune challenge were performed in *M. sexta* day-1 fifth instar larvae, providing reference information on immune-related genes (Zhang et al., 2011; Gunaratna and Jiang, 2013). The fold change of mRNA abundance 24 h after injection of bacteria in fat body and hemocytes of MsSerpin1-7, 9, 11-15, 17-19, and 22 were derived from CIFH (Control/Induced Fat body/Hemocyte) libraries (Zhang et al., 2011) (Table B-3). The unavailability of data for other *M. sexta* serpins probably resulted from low level of transcription in chosen life stage and tissue. MsSerpin-1 and 17 exhibited >2 fold increase in mRNA level in hemocytes, but remained the same level or showed slight up-regulation in fat body. In contrast, MsSerpin-4, 7, 14, 18 and 22 displayed a significant up-regulation of transcript level in fat body but not in hemocytes. mRNA levels of MsSerpin-2, 3, 5, 6, 11, 12, 15 and 17 increased more than 2-fold in both fat body and hemocytes (Table B-3). The data of MsSerpin-3, 4, 5, 6 and 7 are consistent with RT-PCR results in published literature (Zhu et al., 2003; Tong and Kanost, 2005; Zou and Jiang, 2005; Suwanchaichinda et al., 2013; Yang et al., 2018). The only discrepancy occurs to MsSerpin-2, which did not show any presence of mRNA in fat body even after bacterial challenge in immunoblot analysis (Gan et al., 2001), but 2.8-fold increase by RNAseq was observed in CIFH libraries (Gunaratna and Jiang, 2013). Surprisingly, *MsSerpin-19* is the only gene on the list, whose transcript level decreased after injection of a mixture of *Escherichia coli*, *Micrococcus luteus* and curdlan. A similar effect has been reported in multiple lepidopterans in response to parasitoid wasps, which interfere with serpin levels by targeting transcripts with miRNA, such as miR-8 (Beckage and Kanost, 1993; Song et al., 2008; Etebari and Asgari, 2014; Lee and Hyun, 2014).

Furthermore, proteomics data and immunoblotting analysis regarding the changes in expression of several *M. sexta* serpins in hemolymph after infection of bacteria are available in previous work (He et al., 2016; Zhu et al., 2003; Tong and Kanost, 2005; Zou and Jiang, 2005). Intact protein abundance of MsSerpin-3, 4, 5, 11 and 12 significantly increased in hemolymph after infection (Zhu et al., 2003; Tong and Kanost, 2005; He et al., 2016), while intact MsSerpin-1A, 1E, 1K, 1Z, 6 and 13 remained the similar level (Zou and Jiang, 2005; He et al., 2016). However, MsSerpin-3, 4 and 12 started to prevail in the high *M*r bands once hemolymph was induced, suggesting a complex formation with serine proteases was triggered by immune challenge. MsSerpin-1A, 1K, 1Z, 6, 11, 13, 15 and 30 were not present in high *M*r bands after

infection, indicating an absence or degradation of serpin-protease complex. Surprisingly, unique spectral counts of total MsSerpin-9 decreased from 38 to 3 after immune challenge (He et al., 2016). What contributes to the degradation of MsSerpin-9 in induced hemolymph might be an appealing question to be answered.

Future Directions

Identification and characterization of *M. sexta* serpin genes provided a general picture and data set for future study regarding evolution, structure and physiological functions of serpins in *M. sexta* and other insects.

Acknowledgements

I would like to thank Dr. Michael Kanost and Dr. Jayne Christin for performing BLAST search and sequence editing. I also express thanks to Dr. Neal Dittmer and Dr. Haobo Jiang's group at Oklahoma State University, including Dr. Xiaolong Cao and Dr. Xiufeng Zhang, for collaborating on organizing the paper which contains the work presented in this chapter. And I appreciate Dr. Di Wu for providing genomic DNA of larval *M. sexta*. This work was supported by NIH grant GM041247.

Figures

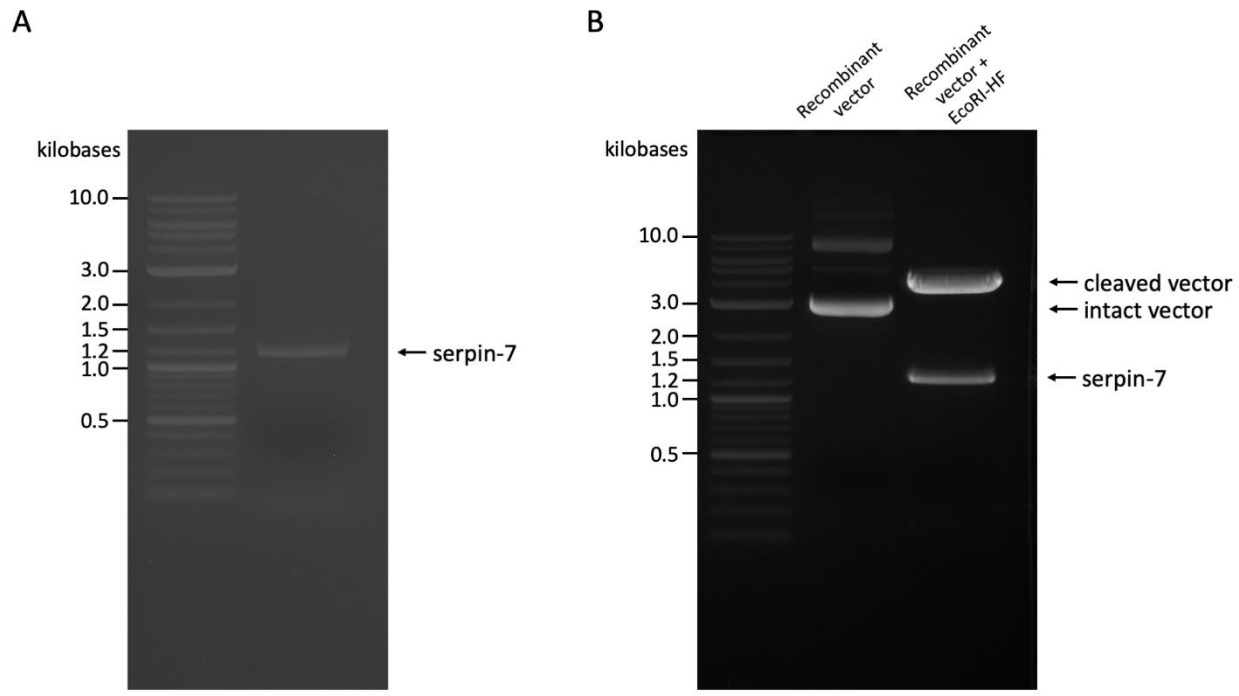

Figure 2-1. Cloning of *MsSerpin-7* gene.

(A) *MsSerpin-7* was amplified from *M. sexta* genomic DNA by PCR, followed by 1% agarose gel electrophoresis. (B) After *MsSerpin-7* fragment was cloned into pCR4-TOPO vector, the recombinant construct was verified by restriction enzyme EcoRI-HF digestion.

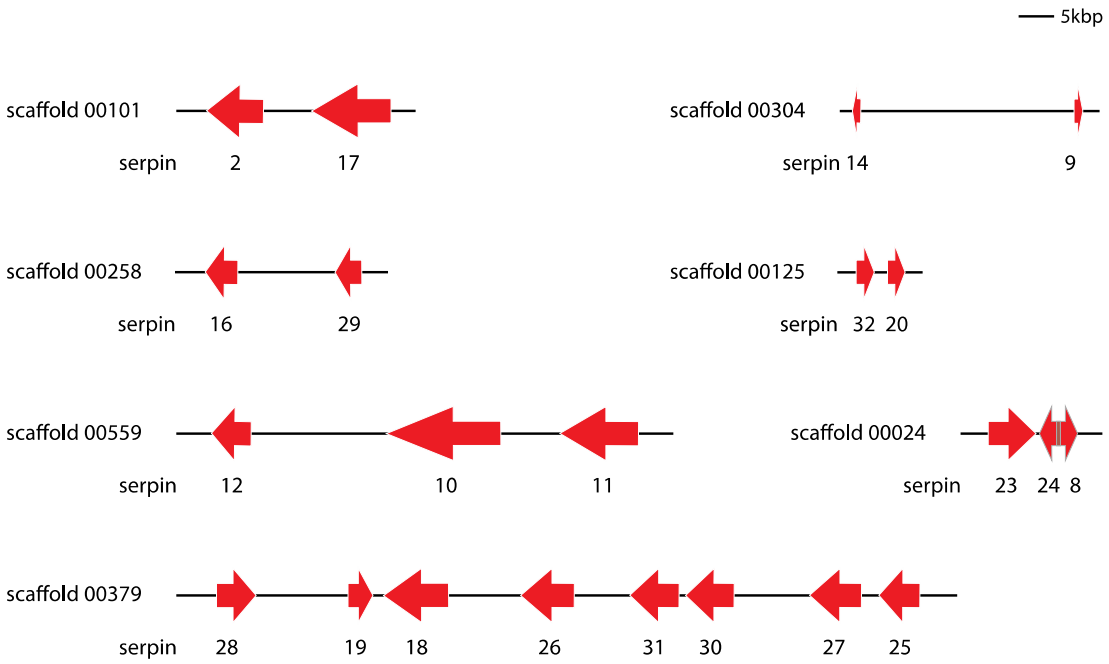

Figure 2-2. *M. sexta* serpin gene clusters.

Seven clusters of serpin genes identified on individual genomic scaffolds are shown, with length and orientations identified by red arrows. An overlapping region of oppositely directed *MsSerpin-24* and *MsSerpin-8* is indicated by brown color.

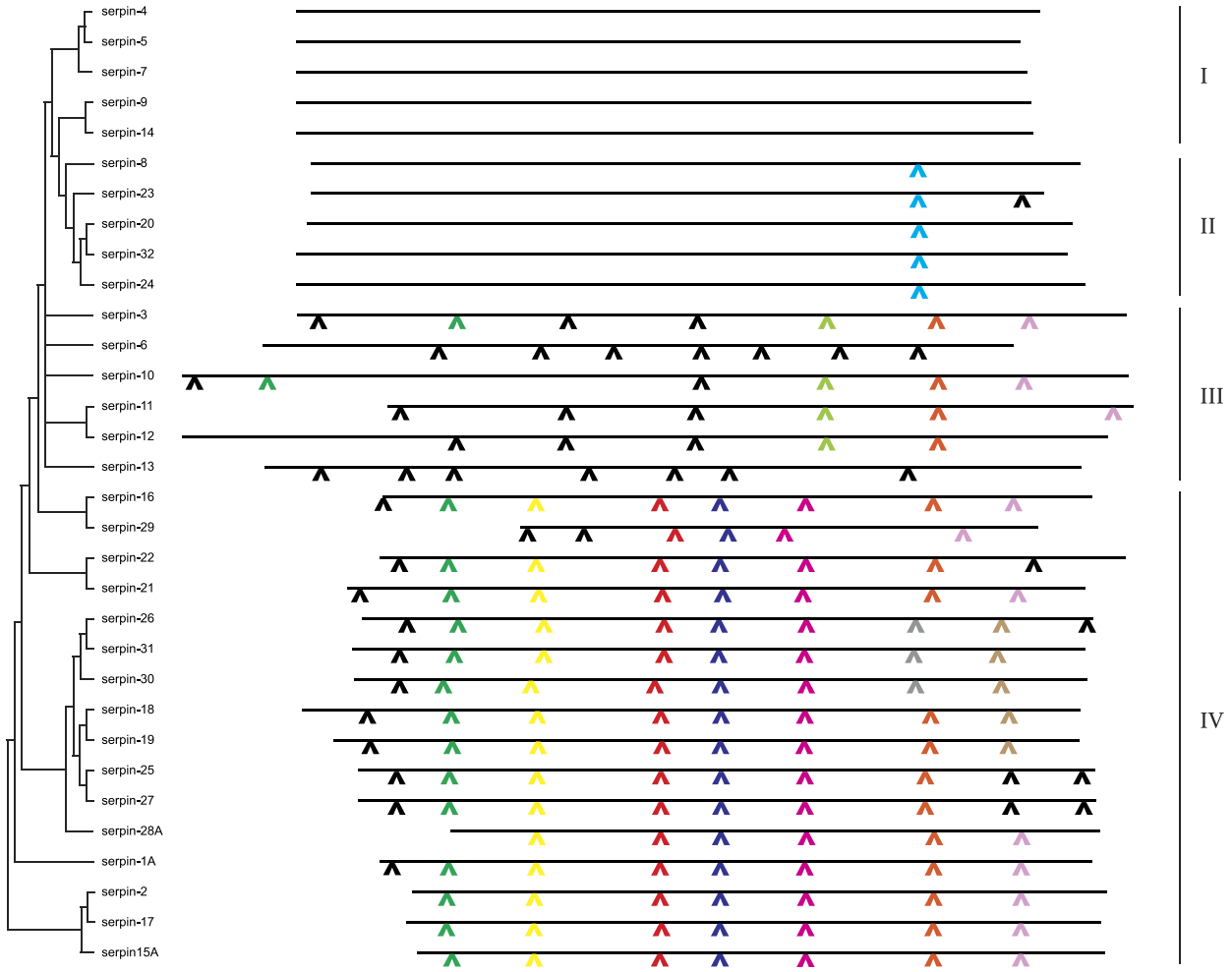

Figure 2-3. Intron positions of *M. sexta* serpin genes.

Intron positions are marked on linear maps of the serpin polypeptides, based on alignment of their amino acid sequences (Fig. B-3). Arrowheads of the same color indicate identical intron position. Unconserved intron positions are shown with black arrowheads. Serpins are organized based on the topology of a phylogenetic tree based on their amino acid sequence alignment. Serpins lacking an intron are in group I, those with one conserved intron position are in group II, with 2-3 conserved intron positions are in group III, with four or more conserved intron positions are in group IV. Ms*Serpins-6* and *13* contain multiple introns, but the intron positions are not shared with other serpin genes.

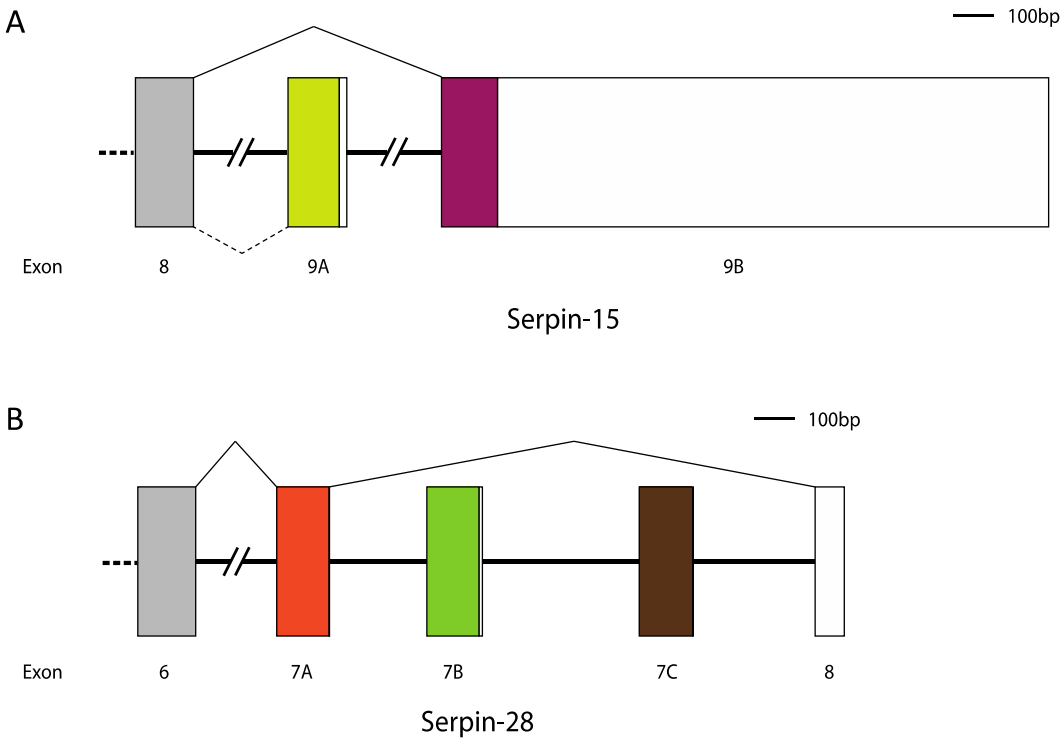

Figure 2-4. Simplified splicing variant diagrams of M. sexta serpin-15 and 28.
(A) Alternative exon 9 of MsSerpin-15 has two variants, 9A and 9B. (B) Alternate splicing to include exon 7A, 7B or 7C leads to the expression of MsSerpin-28A, 28B and 28C respectively. Alternative exons are in color, exons which are always expressed are in grey, and untranslated regions of the last exon of each gene are in white.

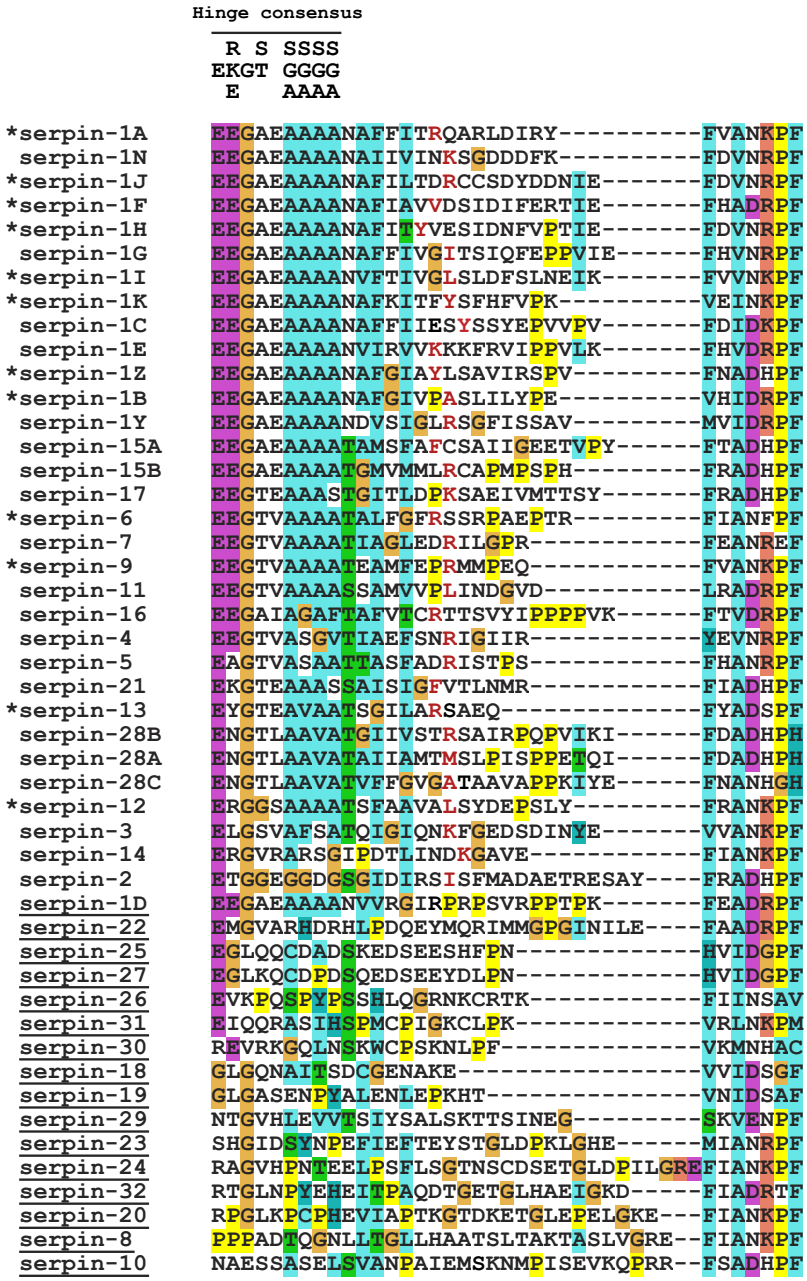

Figure 2-5. Alignment of the RCL region of *M. sexta* serpins.

The consensus sequence observed in the hinge region of inhibitory serpins is indicated above the alignment. Predicted and known P1 residues are in red. Serpins whose scissile bond has been experimentally determined are marked with an asterisk. Predicted non-inhibitory serpins are underlined. ClustalX2 was used to color amino acids based on percentage of consensus by default parameters.

Tables

Table 2-1. Summary of *M. sexta* serpins.

Gene name	Gene ID in OGS2.0	Scaffold number	NCBI accession number	Exon number[a]	B. mori serpin ortholog	protein product	GenBank ID	Protein length (residues)[b]	Signal peptide[c]	MW (kDa)[d]	pI[d]	Scissile bond determined experimentally	inhibitory[e]
serpin-1	Msex2.12851	00761	JH669038.1	10	*BmSpn1*	serpin-1A	AAC47342.1	375	1-16 (A*G)	41.9	5.46	+	+
						serpin-1B	AAC47343.1	376	1-16 (A*G)	41.9	5.01	+	+
						serpin-1C	AAC47339.1	376	1-16 (A*G)	42.3	4.95		+
						serpin-1D	AAC47341.1	379	1-16 (A*G)	42.3	5.36		-
						serpin-1E	AAC47335.1	379	1-16 (A*G)	42.4	5.70		+
						serpin-1F	AAC47333.1	381	1-16 (A*G)	42.4	5.01	+	+
						serpin-1G	AAC47336.1	380	1-16 (A*G)	42.3	5.11		+
						serpin-1H	AAC47332.1	382	1-16 (A*G)	42.7	4.96	+	+
						serpin-1I	AAC47337.1	379	1-16 (A*G)	42.3	5.11	+	+
						serpin-1J	AAC47340.1	381	1-16 (A*G)	42.7	4.88	+	+
						serpin-1K	AAC47334.1	376	1-16 (A*G)	42.1	5.44	+	+
						serpin-1N	MG753799.1	378	1-16 (A*G)	42.2	5.01		(+)
						serpin-1Y	MG753798.1	376	1-16 (A*G)	41.8	5.18		(+)
						serpin-1Z	AAC47338.1	376	1-16 (A*G)	41.8	5.17	+	+
serpin-2	Msex2.04874	00101	JH668379.1	9		serpin-2	AAB58491.1	381	none	42.2	4.99		+
serpin-3	Msex2.11872, Msex2.15169, Msex2.15173	00559, 08663, 08596	JH668837.1 AIXA01026169.1 AIXA01026102.1	7	*BmSpn3*	serpin-3	AAO21505.1	435	1-20 (A*D)	48.9	5.27		+
serpin-4	Msex2.04237	00077	JH668355.1	1	*BmSpn4*	serpin-4	AAS68503.1	391	1-16 (C*D)	44.7	5.90		+
serpin-5	Msex2.12952	00791	JH669068.1	1	*BmSpn4*	serpin-5	AAS68507.1	379	1-17 (C*D)	42.7	6.12		+
serpin-6	Msex2.06874	00170	JH668448.1	9	*BmSpn6*	serpin-6	AAV91026.1	395	1-17 (S*Q)	45.0	5.57	+	+
serpin-7	Msex2.15425, Msex2.15342	12474, 15728	AIXA01029976.1 AIXA01033229.1	1	*BmSpn32*	serpin-7	ADM86478.1	385	1-15 (G*A)	42.8	5.29		+
serpin-8	Msex2.01482	00024	JH668302.1	3	*BmSpn8*	serpin-8		401	1-21 (A*Q)	44.2	4.45		(-)
serpin-9	Msex2.09571	00304	JH668582.1	1	*BmSpn7*	serpin-9	MG732912.1	382	1-20 (A*Q)	43.3	4.89	+	+
serpin-10	Msex2.11870	00559	JH668837.1	8	*BmSpn10*	serpin-10		502	1-17 (A*R)	57.1	5.11		(-)

serpin-11	Msex2.11871	00559	JH668837.1	9	*BmSpn11*	serpin-11		391	1-18 (C*I)	44.5	6.23		(+)
serpin-12	Msex2.11869	00559	JH668837.1	6	*BmSpn12*	serpin-12	MG732913.1	467	1-18 (S*Q)	51.4	8.52	+	+
serpin-13	Msex2.06711	00158	JH668436.1	10	*BmSpn13*	serpin-13	MG732911.1	423	1-21 (A*I)	48.3	5.27	+	+
serpin-14	Msex2.09570	00304	JH668582.1	1	*BmSpn14*	serpin-14		386	1-17 (A*H)	45.0	9.52		(+)
serpin-15	Msex2.06848	00170	JH668448.1	9	*BmSpn2*	serpin-15A		377	none	41.3	4.60		(+)
						serpin-15B		373	none	41.0	4.92		(+)
serpin-16	Msex2.09066	00258	JH668536.1	9	*BmSpn9*	serpin-16		389	none	43.2	5.80		(+)
serpin-17	Msex2.15518	00101	JH668379.1	8		serpin-17		381	none	42.5	4.93		(+)
serpin-18	Msex2.10821	00379	JH668657.1	10		serpin-18		408	1-19 (A*E)	45.5	4.86		(-)
serpin-19	Msex2.10820	00379	JH668657.1	9		serpin-19		390	1-19 (G*T)	44.2	4.87		(-)
serpin-20	Msex2.15520	00125	JH668403.1	2		serpin-20		404	1-16 (S*E)	45.7	8.80		(-)
serpin-21	Msex2.09937	00316	JH668594.1	9		serpin-21		386	1-19 (A*K)	43.1	9.64		(+)
serpin-2[f]	Msex2.06154, Msex2.06167	00144, 00153	JH668422.1 JH668431.1	9	*BmSpn33*	serpin-22		387	1-22 (S*D)	46.8	9.27		(-)
serpin-23	Msex2.01480	00024	JH668302.1	3		serpin-23		375	1-16 (Q*E)	42.1	4.86		(-)
serpin-24	Msex2.01481	00024	JH668302.1	3		serpin-24		411	1-22 (A*S)	46.7	5.63		(-)
serpin-25	Msex2.10827	00379	JH668657.1	10		serpin-25		382	1-22 (G*Y)	43.9	5.96		(-)
serpin-26	Msex2.10822	00379	JH668657.1	10		serpin-26		381	1-20 (A*Y)	43.8	9.53		(-)
serpin-27	Msex2.10826	00379	JH668657.1	10		serpin-27		386	1-19 (A*F)	44.2	7.26		(-)
serpin-28	Msex2.10818	00379	JH668657.1	8	*BmSpn28*	serpin-28A		332	1-24 (L*L)	38.0	5.04		(+)
						serpin-28B		332	1-24 (L*L)	37.9	6.06		(+)
						serpin-28C		333	1-24 (L*L)	37.8	5.59		(+)
serpin-29[g]	Msex2.09069	00258	JH668536.1	7		serpin-29		284	none	31.8	8.22		(-)
serpin-30	Msex2.10824	00379	JH668657.1	9		serpin-30		379	1-23 (S*K)	44.0	6.29		(-)
serpin-31	Msex2.10823	00379	JH668657.1	10		serpin-31		382	1-20 (A*Y)	43.8	9.05		(-)
serpin-32	Msex2.05826	00125	JH668403.1	2		serpin-32		406	1-17 (A*K)	46.5	6.84		(-)

[a] Number of exons included in the mRNA after splicing
[b] Length of mature serpin was calculated after removing the putative signal peptide
[c] SignalP 4.1 was used for signal peptides prediction
[d] Theoretical molecular weight and isoelectric point were calculated by ProParam tool on the ExPASy website
[e] Confirmed inhibitory activity is indicated by + or -, predicted inhibitory activity was in brackets
[f] Serpin-22 has a haplotype without signal peptide
[g] Serpin-29 gene may be a pseudogene or an incomplete assembly

References

Abraham, E. G., S. B. Pinto, A. Ghosh, D. L. Vanlandingham, A. Budd, S. Higgs, F. C. Kafatos, M. Jacobs-Lorena & K. Michel (2005) An immune-responsive serpin, SRPN6, mediates mosquito defense against malaria parasites. *Proceedings of the National Academy of Sciences of the United States of America*, 102, 16327-16332.

Ahmad, S. T., S. T. Sweeney, J.-A. Lee, N. T. Sweeney & F.-B. Gao (2009) Genetic screen identifies serpin5 as a regulator of the toll pathway and CHMP2B toxicity associated with frontotemporal dementia. *Proceedings of the National Academy of Sciences of the United States of America*, 106, 12168-12173.

Al-Ayyoubi, M., P. G. Gettins & K. Volz (2004) Crystal structure of human maspin, a serpin with antitumor properties: reactive center loop of maspin is exposed but constrained. *The Journal of Biological Chemistry*, 279, 55540-55544.

An, C. & M. R. Kanost (2010) *Manduca sexta* serpin-5 regulates prophenoloxidase activation and the Toll signaling pathway by inhibiting hemolymph proteinase HP6. *Insect biochemistry and molecular biology*, 40, 683-689.

An, C., E. J. Ragan & M. R. Kanost (2011) Serpin-1 splicing isoform J inhibits the proSpätzle-activating proteinase HP8 to regulate expression of antimicrobial hemolymph proteins in *Manduca sexta*. Developmental and comparative immunology, 35, 135-141.

Beckage, N. E. & M. R. Kanost (1993) Effects of parasitism by the braconid wasp *Cotesia congregata* on host hemolymph proteins of the tobacco hornworm, *Manduca sexta*. *Insect biochemistry and molecular biology*, 23, 643-653.

Christophides, G. K., E. Zdobnov, C. Barillas-Mury, E. Birney, S. Blandin, C. Blass, P. T. Brey, F. H. Collins, A. Danielli, G. Dimopoulos, C. Hetru, N. T. Hoa, J. A. Hoffmann, S. M. Kanzok, I. Letunic, E. A. Levashina, T. G. Loukeris, G. Lycett, S. Meister, K. Michel, L. F. Moita, H. M. Muller, M. A. Osta, S. M. Paskewitz, J. M. Reichhart, A. Rzhetsky, L. Troxler, K. D. Vernick, D. Vlachou, J. Volz, C. von Mering, J. Xu, L. Zheng, P. Bork & F. C. Kafatos (2002) Immunity-related genes and gene families in *Anopheles gambiae*. Science (New York, N.Y.), 298, 159-165.

De Gregorio, E., S.-J. Han, W.-J. Lee, M.-J. Baek, T. Osaki, S.-I. Kawabata, B.-L. Lee, S. Iwanaga, B. Lemaitre & P. T. Brey (2002) An immune-responsive Serpin regulates the melanization cascade in *Drosophila*. Developmental cell, 3, 581-592.

Dunstone, M. A. & J. C. Whisstock (2011) Crystallography of serpins and serpin complexes. *Methods in Enzymology*, Vol 501: Serpin Structure and Evolution, 501, 63-87.

Etebari, K. & S. Asgari (2014) Accuracy of microRNA discovery pipelines in non-model organisms using closely related species genomes. PLoS One, 9, e84747.

Gan, H., Y. Wang, H. Jiang, K. Mita & M. R. Kanost (2001) A bacteria-induced, intracellular serpin in granular hemocytes of *Manduca sexta*. *Insect biochemistry and molecular biology*, 31, 887-898.

Gasteiger, E., C. Hoogland, A. Gattiker, M. R. Wilkins, R. D. Appel & A. Bairoch. 2005. Protein identification and analysis tools on the ExPASy server. In *The proteomics protocols handbook*, 571-607. Springer.

Gettins, P. G. & S. T. Olson (2016) Inhibitory serpins. New insights into their folding, polymerization, regulation and clearance. *The Biochemical journal*, 473, 2273-2293.

Gettins, P. G. W. (2002) Serpin structure, mechanism, and function. *Chemical reviews*, 102, 4751-4804.

Grigoryev, S. A., J. Bednar & C. L. Woodcock (1999) MENT, a heterochromatin protein that mediates higher order chromatin folding, is a new serpin family member. *The Journal of Biological Chemistry*, 274, 5626-5636.

Gulley, M. M., X. Zhang & K. Michel (2013) The roles of serpins in mosquito immunology and physiology. *Journal of insect physiology*, 59, 138-147.

Gunaratna, R. T. & H. Jiang (2013) A comprehensive analysis of the *Manduca sexta* immunotranscriptome. *Developmental and comparative immunology*, 39, 388-398.

He, Y., X. Cao, S. Zhang, J. Rogers, S. Hartson & H. Jiang (2016) Changes in the plasma proteome of *Manduca sexta* larvae in relation to the transcriptome variations after an immune challenge: evidence for high molecular weight immune complex formation. *Molecular & Cellular Proteomics*, 15, 1176-1187.

He, Y., Y. Wang, P. Zhao, S. Rayaprolu, X. Wang, X. Cao & H. Jiang (2017) Serpin-9 and-13 regulate hemolymph proteases during immune responses of *Manduca sexta*. *Insect biochemistry and molecular biology*, 90, 71-81.

Hopkins, P. C. R., R. W. Carrell & S. R. Stone (1993) Effects of mutations in the hinge region of serpins. *Biochemistry*, 32, 7650-7657.

Hopkins, P. C. R. & S. R. Stone (1995) The contribution of the conserved hinge region residues of α_1-antitrypsin to its reaction with elastase. *Biochemistry*, 34, 15872-15879.

Huntington, J. A., A. McCoy, K. J. Belzar, X. Y. Pei, P. G. Gettins & R. W. Carrell (2000) The conformational activation of antithrombin. A 2.85-Å structure of a fluorescein derivative reveals an electrostatic link between the hinge and heparin binding regions. *The Journal of Biological Chemistry*, 275, 15377-15383.

Huntington, J. A. & P. E. Stein (2001) Structure and properties of ovalbumin. *Journal of Chromatography B: Biomedical Sciences and Applications*, 756, 189-198.

Irving, J. A., R. N. Pike, A. M. Lesk & J. C. Whisstock (2000) Phylogeny of the serpin superfamily: implications of patterns of amino acid conservation for structure and function. *Genome research*, 10, 1845-1864.

Jiang, H. & M. R. Kanost (1997) Characterization and functional analysis of 12 naturally occurring reactive site variants of serpin-1 from *Manduca sexta*. *Journal of Biological Chemistry*, 272, 1082-1087.

Jiang, H., Y. Wang & M. R. Kanost (1994) Mutually exclusive exon use and reactive center diversity in insect serpins. *The Journal of Biological Chemistry*, 269, 55-58.

Jiang, H., Y. Wang, X. Q. Yu, Y. Zhu & M. Kanost (2003) Prophenoloxidase-activating proteinase-3 (PAP-3) from *Manduca sexta* hemolymph: a clip-domain serine proteinase regulated by serpin-1J and serine proteinase homologs. *Insect biochemistry and molecular biology*, 33, 1049-1060.

Jiang, R., E. H. Kim, J. H. Gong, H. M. Kwon, C. H. Kim, K. H. Ryu, J. W. Park, K. Kurokawa, J. Zhang, D. Gubb & B. L. Lee (2009) Three pairs of protease-serpin complexes cooperatively regulate the insect innate immune responses. *Journal of Biological Chemistry*, 284**,** 35652-35658.

Kaiserman, D. & P. I. Bird (2005) Analysis of vertebrate genomes suggests a new model for clade B serpin evolution. *BMC genomics*, 6, 167.

Kanost, M., E. Arrese, X. Cao, Y. Chen, S. Chellapilla, M. Goldsmith, E. Grosse-Wilde, D. Heckel, N. Herndon, H. Jiang, A. Papanicolaou, J. Qu, J. Soulages, H. Vogel, J. Walters, R. Waterhouse, S. Ahn, F. Almeida, C. An, P. Aqrawi, A. Bretschneider, W. Bryant, S. Bucks, H. Chao, G. Chevignon, J. Christen, D. Clarke, N. Dittmer, L. Ferguson, S. Garavelou, K. Gordon, R. Gunaratna, Y. Han, F. Hauser, Y. He, H. Heidel-Fischer, A. Hirsh, Y. Hu, D. Kalra, C. Klinner, C. Konig, C. Kovar, A. Kroll, S. Kuwar, S. Lee, R. Lehman, K. Li, Z. Li, H. Liang, S. Lovelace, Z. Lu, J. Mansfield, K. McCulloch, T. Mathew, B. Morton, D. MuznyJ, D. Muzny, D. Neunemann, F. Ongeri, Y. Pauchet, L. Pu, I. Pyrousis, X. Rao, A. Redding, C. Roesel, A. Sanchez-Gracia, S. Schaack, A. Shukla, G. Tetreau, Y. Wang, G. Xiong, W. Traut, T. Walsh, K. Worley, D. Wu, W. Wu, Y. Wu, X. Zhang, Z. Zou, H. Zucker, A. Briscoe, T. Burmester, R. Clem, R. Feyereisen, C. Grimmelikhuijzen, S. Hamodrakas, B. Hansson, E. Huguet, L. Jermiin, Q. Lan, H. Lehman, M. Lorenzen, H. Merzendorfer, I. Michalopoulos, D. Morton, S. Muthukrishnan, J. Oakeshott, W. Palmer, Y. Park, A. Passarelli, et al., (2016) Multifaceted biological insights from a draft genome sequence of the tobacco hornworm moth, *Manduca sexta*. *Insect biochemistry and molecular biology*, 76, 118-147.

Kanost, M. R., S. V. Prasad & M. A. Wells (1989) Primary structure of a member of the serpin superfamily of proteinase inhibitors from an insect, *Manduca sexta*. *The Journal of Biological Chemistry*, 264, 965-972.

Larkin, M. A., G. Blackshields, N. P. Brown, R. Chenna, P. A. McGettigan, H. McWilliam, F. Valentin, I. M. Wallace, A. Wilm, R. Lopez, J. D. Thompson, T. J. Gibson & D. G. Higgins (2007) Clustal W and Clustal X version 2.0. *Bioinformatics*, 23, 2947-2948.

Lee, G. J. & S. Hyun (2014) Multiple targets of the microRNA miR-8 contribute to immune homeostasis in *Drosophila*. *Developmental and comparative immunology*, 45, 245-251.

Levashina, E. A., E. Langley, C. Green, D. Gubb, M. Ashburner, J. A. Hoffmann & J. M. Reichhart (1999) Constitutive activation of toll-mediated antifungal defense in serpin-deficient *Drosophila*. *Science* (New York, N.Y.), 285, 1917-1919.

Li, J., Z. Wang, B. Canagarajah, H. Jiang, M. Kanost & E. J. Goldsmith (1999) The structure of active serpin 1K from *Manduca sexta*. *Structure*, 7, 103-109.

Li, M., J. M. Christen, N. T. Dittmer, X. Cao, X. Zhang, H. Jiang & M. R. Kanost (2018) The *Manduca sexta* serpinome: analysis of serpin genes and proteins in the tobacco hornworm. *Insect biochemistry and molecular biology*, 102, 21-30.

Ligoxygakis, P., N. Pelte, C. Ji, V. Leclerc, B. Duvic, M. Belvin, H. Jiang, J. A. Hoffmann & J. M. Reichhart (2002) A serpin mutant links Toll activation to melanization in the host defence of *Drosophila*. *The EMBO journal*, 21, 6330-6337.

Loebermann, H., R. Tokuoka, J. Deisenhofer & R. Huber (1984) Human α_1-proteinase inhibitor: crystal structure analysis of two crystal modifications, molecular model and preliminary analysis of the implications for function. *Journal of Molecular Biology*, 177, 531-557.

McGowan, S., A. M. Buckle, J. A. Irving, P. C. Ong, T. A. Bashtannyk-Puhalovich, W.-T. Kan, K. N. Henderson, Y. A. Bulynko, E. Y. Popova, A. I. Smith, S. P. Bottomley, J. Rossjohn, S. A. Grigoryev, R. N. Pike & J. C. Whisstock (2006) X-ray crystal structure of MENT: evidence for functional loop-sheet polymers in chromatin condensation. *EMBO Journal*, 25, 3144-3155.

Meekins, D., X. Zhang, K. Battaile, S. Lovell & K. Michel (2016) 1.45 angstrom resolution structure of SRPN18 from the malaria vector *Anopheles gambiae*. *Acta Crystallographica Section F-Structural Biology Communications*, 72, 853-862.

Meekins, D. A., M. R. Kanost & K. Michel. 2017. Serpins in arthropod biology. In *Seminars in cell & developmental biology*, 105-119. Elsevier.

Michel, K., C. Suwanchaichinda, I. Morlais, L. Lambrechts, A. Cohuet, P. H. Awono-Ambene, F. Simard, D. Fontenille, M. R. Kanost & F. C. Kafatos (2006) Increased melanizing activity in *Anopheles gambiae* does not affect development of *Plasmodium falciparum*. *Proceedings of the National Academy of Sciences of the United States of America*, 103, 16858-16863.

Nagata, K. (1996) Hsp47: a collagen-specific molecular chaperone. *Trends in biochemical sciences*, 21, 23-26.

Park, S. H., R. Jiang, S. Piao, B. Zhang, E.-H. Kim, H.-M. Kwon, X. L. Jin, B. L. Lee & N.-C. Ha (2011) Structural and functional characterization of a highly specific serpin in the insect innate immunity. *Journal of Biological Chemistry*, 286, 1567-1575.

Petersen, T. N., S. Brunak, G. von Heijne & H. Nielsen (2011) SignalP 4.0: discriminating signal peptides from transmembrane regions. *Nature Methods*, 8, 785.

Poelchau, M., C. Childers, G. Moore, V. Tsavatapalli, J. Evans, C. Y. Lee, H. Lin, J. W. Lin & K. Hackett (2015) The i5k Workspace@NAL-enabling genomic data access, visualization and curation of arthropod genomes. *Nucleic Acids Research*, 43, D714-D719.

Reichhart, J. M. (2005) Tip of another iceberg: *Drosophila* serpins. *Trends in cell biology*, 15, 659-665.

Reichhart, J. M., D. Gubb & V. Leclerc (2011) The *Drosophila* serpins: multiple functions in immunity and morphogenesis. *Methods in Enzymology: Biology of Serpins*, 499, 205-225.

Roy, S. W., A. Fedorov & W. Gilbert (2003) Large-scale comparison of intron positions in mammalian genes shows intron loss but no gain. *Proceedings of the National Academy of Sciences of the United States of America*, 100, 7158-7162.

Scherfer, C., H. Tang, Z. Kambris, N. Lhocine, C. Hashimoto & B. Lemaitre (2008) *Drosophila* Serpin-28D regulates hemolymph phenoloxidase activity and adult pigmentation. *Developmental biology*, 323, 189-196.

Shin, S. W., G. Bian & A. S. Raikhel (2006) A toll receptor and a cytokine, Toll5A and Spz1C, are involved in toll antifungal immune signaling in the mosquito *Aedes aegypti*. *Journal of Biological Chemistry*, 281, 39388-39395.

Silverman, G. A., P. I. Bird, R. W. Carrell, F. C. Church, P. B. Coughlin, P. G. Gettins, J. A. Irving, D. A. Lomas, C. J. Luke, R. W. Moyer, P. A. Pemberton, E. Remold-O'Donnell, G. S. Salvesen, J. Travis & J. C. Whisstock (2001) The serpins are an expanding superfamily of structurally similar but functionally diverse proteins. Evolution, mechanism of inhibition, novel functions, and a revised nomenclature. *The Journal of Biological Chemistry*, 276, 33293-33296.

Song, K. H., M. K. Jung, J. H. Eum, I. C. Hwang & S. S. Han (2008) Proteomic analysis of parasitized *Plutella xylostella* larvae plasma. *Journal of insect physiology*, 54, 1271-1280.

Stein, P. E., A. G. W. Leslie, J. T. Finch & R. W. Carrell (1991) Crystal structure of uncleaved ovalbumin at 1.95 Å resolution. *Journal of Molecular Biology*, 221, 941-959.

Stratikos, E. & P. G. Gettins (1999) Formation of the covalent serpin-proteinase complex involves translocation of the proteinase by more than 70 Å and full insertion of the reactive center loop into beta-sheet A. *Proceedings of the National Academy of Sciences of the United States of America*, 96, 4808-4813.

Suwanchaichinda, C. & M. R. Kanost (2009) The serpin gene family in *Anopheles gambiae*. *Gene*, 442, 47-54.

Suwanchaichinda, C., R. Ochieng, S. Zhuang & M. R. Kanost (2013) *Manduca sexta* serpin-7, a putative regulator of hemolymph prophenoloxidase activation. *Insect biochemistry and molecular biology*, 43, 555-561.

Tang, H., Z. Kambris, B. Lemaitre & C. Hashimoto (2008) A serpin that regulates immune melanization in the respiratory system of *Drosophila*. *Developmental Cell*, 15, 617-626.

Tong, Y., H. Jiang & M. R. Kanost (2005) Identification of plasma proteases inhibited by *Manduca sexta* serpin-4 and serpin-5 and their association with components of the prophenol oxidase activation pathway. *The Journal of Biological Chemistry*, 280, 14932-14942.

Tong, Y. & M. R. Kanost (2005) *Manduca sexta* serpin-4 and serpin-5 inhibit the prophenol oxidase activation pathway: cDNA cloning, protein expression, and characterization. *The Journal of Biological Chemistry*, 280, 14923-14931.

Wang, Y. & H. Jiang (2004) Purification and characterization of *Manduca sexta* serpin-6: a serine proteinase inhibitor that selectively inhibits prophenoloxidase-activating proteinase-3. *Insect biochemistry and molecular biology*, 34, 387-395.

Wang, Y., & Jiang, H. (2006) Interaction of β-1, 3-glucan with its recognition protein activates hemolymph proteinase 14, an initiation enzyme of the prophenoloxidase activation system in *Manduca sexta*. *Journal of Biological Chemistry*, 281(14), 9271-9278.

Whisstock, J. C., R. Skinner, R. W. Carrell & A. M. Lesk (2000a) Conformational changes in serpins: I. the native and cleaved conformations of α 1-antitrypsin. Journal of Molecular Biology, 296, 685-699.

Whisstock, J. C., Skinner, R., Carrell, R. W., & Lesk, A. M. (2000). Conformational changes in serpins: I. The native and cleaved conformations of α_1-antitrypsin. *Journal of molecular biology*, 295(3), 651-665.

Widmer, C., J. M. Gebauer, E. Brunstein, S. Rosenbaum, F. Zaucke, C. Droegemueller, T. Leeb & U. Baumann (2012) Molecular basis for the action of the collagen-specific chaperone Hsp47/SERPINH1 and its structure-specific client recognition. *Proceedings of the National Academy of Sciences of the United States of America*, 109, 13243-13247.

Yang, F., Y. Wang, N. Sumathipala, X. Cao, M. R. Kanost & H. Jiang (2018) *Manduca sexta* serpin-12 controls the prophenoloxidase activation system in larval hemolymph. *Insect biochemistry and molecular biology*.

Yang, L., Y. Mei, Q. Fang, J. Wang, Z. Yan, Q. Song, Z. Lin & G. Ye (2017) Identification and characterization of serine protease inhibitors in a parasitic wasp, *Pteromalus puparum*. *Scientific Reports*, 7(1), 15755.

Ye, S., A. L. Cech, R. Belmares, R. C. Bergstrom, Y. Tong, D. R. Corey, M. R. Kanost & E. J. Goldsmith (2001) The structure of a Michaelis serpin-protease complex. *Nature Structural & Molecular Biology*, 8, 979-983.

Zhang, S., R. T. Gunaratna, X. Zhang, F. Najar, Y. Wang, B. Roe & H. Jiang (2011) Pyrosequencing-based expression profiling and identification of differentially regulated genes from *Manduca sexta*, a lepidopteran model insect. *Insect biochemistry and molecular biology*, 41, 733-746.

Zhou, Z., A. Anisowicz, M. J. H. Hendrix, A. Thor, M. Neveu, S. Sheng, K. Rafidi, E. Seftor & R. Sager (1994) Maspin, a serpin with tumor-suppressing activity in human mammary epithelial cells. *Science*, 263, 526-529.

Zhu, Y., Y. Wang, M. J. Gorman, H. Jiang & M. R. Kanost (2003) *Manduca sexta* serpin-3 regulates prophenoloxidase activation in response to infection by inhibiting prophenoloxidase-activating proteinases. *The Journal of Biological Chemistry*, 278, 46556-46564.

Zou, Z., J. D. Evans, Z. Lu, P. Zhao, M. Williams, N. Sumathipala, C. Hetru, D. Hultmark & H. Jiang (2007) Comparative genomic analysis of the Tribolium immune system. *Genome biology*, 8, R177.

Zou, Z. & H. Jiang (2005) *Manduca sexta* serpin-6 regulates immune serine proteinases PAP-3 and HP8. cDNA cloning, protein expression, inhibition kinetics, and function elucidation. *The Journal of Biological Chemistry*, 280, 14341-14348.

Zou, Z., D. L. Lopez, M. R. Kanost, J. D. Evans & H. Jiang (2006) Comparative analysis of serine protease-related genes in the honey bee genome: possible involvement in embryonic development and innate immunity. *Insect molecular biology*, 15, 603-614.

Zou, Z., Z. Picheng, H. Weng, K. Mita & H. Jiang (2009) A comparative analysis of serpin genes in the silkworm genome. *Genomics*, 93, 367-375.

Zou, Z., S. W. Shin, K. S. Alvarez, V. Kokoza & A. S. Raikhell (2010) Distinct melanization pathways in the mosquito *Aedes aegypti*. *Immunity*, 32, 41-53.

Chapter 3 - Peptides Based on RCL of *Manduca sexta* Serpin-3 Block Its Protease Inhibitory Function

Introduction

Serpins have been extensively studied since the name was coined in 1985 to define a family of serine protease inhibitors with conserved tertiary structure (Carrell and Travis, 1985). Broadly distributed throughout vertebrates, invertebrates, plants, unicellular organisms and even some viruses, most serpins act as serine protease inhibitors, although some have other functions, including acting as hormone transporters and molecular chaperones (Silverman et al., 2001; Meekins et al., 2017; Roberts and Hejgaard, 2008; Irving et al., 2002; Turner et al., 2007; Gettins and Olson, 2016). The tertiary structure of serpins is comprised of three β-sheets, 8-9 α-helices, and a solvent-exposed reactive center loop (RCL) that is near the carboxyl-terminal end of the serpin sequence (Silverman et al., 2001). When a serpin encounters a target protease, the protease cleaves a specific peptide bond of the RCL (designated P1-P1', the "scissile bond") but the second half of the hydrolysis reaction does not occur, leaving the protease and serpin in an acyl-intermediate state. The amino-terminal end of the RCL rapidly inserts into serpin β-sheet A as a new strand (strand 4A), and the protease is translocated to the other side of serpin molecule, resulting in formation of an irreversible inhibitory complex, with the active site of the protease distorted (Gettins and Olson, 2016). Alternatively, the cleavage of the scissile bond can proceed as a typical protease hydrolysis reaction, producing a shortened and disabled serpin protein, with no inhibition of the protease. The balance of these two types of serpin-protease interactions determines the efficiency of a serpin as an inhibitor of a given protease (Shin and Yu, 2002).

Rapidly expanding sequence data from insect genomes and transcriptomes has resulted in discovery of thousands of insect serpins, but the physiological functions of only a few have been investigated experimentally through biochemical or genetic studies. Many insect serpins are secreted into the circulating hemolymph and regulate extracellular protease cascades, which activate innate immune responses (Meekins et al., 2017). By inactivating specific proteases, serpins suppress the immune reactions to avoid excessive production of harmful molecules, which may cause damage to host insects (Kanost and Gorman, 2008).

Immune responses mediated by hemolymph serine proteases and their regulation by serpins have been studied intensively in a model species, *M. sexta*, the tobacco hornworm (Kanost and Jiang, 2015). The *M. sexta* genome contains 32 serpin genes, and only 10 of these have been studied with regard to their function (Li et al., 2018; Yang et al., 2018). *M. sexta* serpin-3 expression increases during immune challenge, and it inhibits key proteases in two immune cascades. Serpin-3 inhibits prophenoloxidase activating proteases (PAPs), the terminal enzymes in prophenoloxidase activation leading to melanin synthesis, and it inhibits hemolymph protease 8, which cleaves proSpätzle to stimulate the toll pathway (Zhu et al., 2003; Christen et al., 2012). *M. sexta* serpin-3 is orthologous to *Drosophila melanogaster* serpin-27a and *Anopheles gambiae* SRPN2, which are also significant regulators of innate immune protease cascades (Michel et al., 2005; Michel et al., 2006).

Studies of mammalian serpins have shown that peptides with sequences derived from the RCL can modulate serpin function. A synthetic peptide with sequence of the P14-P1 residues of the human α_1-antitrypsin RCL integrated into α_1-antitrypsin, and this modified serpin exhibited properties similar to cleaved α_1-antitrypsin, including lack of inhibitory activity (Schulze et al., 1990). This finding was followed by studies investigating peptides with sequences derived from the RCL of other human serpins, such as antithrombin, antichymotrypsin, plasminogen activator inhibitor-1, and plasminogen activator inhibitor-2 (PAI-1 and PAI-2) (Carrell et al., 1991; Mast et al., 1992; Eitzman et al., 1995; Jankova et al., 2001). Characterization of crystal structures of the binary complex of serpin with RCL-derived peptide verified the insertion of the RCL-derived peptide as strand 4A in the serpins in antithrombin, PAI-1, and PAI-2 (Skinner et al., 1998; Zhou et al., 2004; Xue et al., 1998; Jankova et al., 2001). In most cases, the principle consequence of RCL-derived peptide incorporation was loss of protease inhibitory activity of the serpin, which acted instead as a substrate of the target protease (Jendrny and Beck-Sickinger, 2015; Björk et al., 1992; D'Amico et al., 2012). Research in this area has focused on interactions of human serpins and their RCL-derived peptides, because of relevance to serpinopathies, a class of conformational disorders featuring a polymer of serpins in which the RCL of one serpin is inserted into the β-sheet A of an adjacent serpin monomer (Gooptu and Lomas, 2009). There is evidence for potential therapeutic use of RCL-derived peptides to treat serpinopathies, by blocking aberrant polymerization both *in vitro* and *in vivo* (Mahadeva et al., 2002; Ambadapadi et al., 2016).

These results on mammalian serpins stimulated this investigation to test the use of RCL-derived peptides to manipulate serpin actions in insects, as reagents for experiments to provide a better understanding of serpin physiological functions, particularly for serpins with unknown roles. To test this idea, I hypothesized that serpin-3 from *M sexta* would be inactivated by synthetic peptides designed based on its RCL sequence, due to binding and insertion of the peptides between β-sheet strands A3 and A5 in place of its own RCL, thus blocking inhibition. I studied a series of peptides with sequences from the serpin-3 RCL and identified an optimum short sequence that blocked inhibition of prophenoloxidase-activating protease 3 (PAP3) by serpin-3 and also significantly diminished regulation of proPO activation in hemolymph plasma.

Materials and Methods

Insects

M. sexta eggs originally obtained from Carolina Biological Supply were used to establish a laboratory colony, which has been maintained by feeding on a wheat germ-based artificial diet, with a photoperiod of 16 h of light and 8 h of darkness at 26°C.

Synthesis of peptides

Peptides were synthesized in the KSU Biotechnology/Proteomics Core Laboratory using solid phase peptide synthesis on an ABI 431 automated peptide synthesizer (Applied Biosystems, Waltham, MA) with N-Fmoc protected amino acids (P3 Biosystems, Louisville, KY and AnaSpec, Fremont, CA). CLEAR amide resin (Peptides International, Louisville, KY) was used for synthesis of Ac-SVAFSATQ-NH_2, Ac-SVAFSAT-NH_2, Ac-SVAFSA-NH_2, and Ac-SVAFS-NH_2, while Wang resin pre-loaded with the initial amino acid (AnaSpec, Fremont, CA) was used to synthesize Ac-SVAFS-COO^-. The amino termini were acetylated using acetic anhydride. The peptides were cleaved from the resin using a solution of 98% trifluoroacetic acid (TFA) and 2% deionized water. This was mixed at room temperature for 90 min. The slurry was filtered, and the liquid was poured into ice-cold diethyl ether to precipitate peptides. The peptides were then washed with diethyl ether three times and lyophilized. Once dried, the peptides were analyzed using reverse phase HPLC using a C18 column. Solvent A was 99.9% water and 0.1% TFA and Solvent B was 90% acetonitrile, 9.9% water, and 0.1% TFA. A 10% to 90% Solvent B gradient over 30 min was used to elute the peptides. Purity was shown to be over 80%. MALDI-

TOF MS was also used for confirmation of the correct mass on a Bruker Ultraflex II instrument (Billerica, MA). Lyophilized peptides were dissolved in 2, 2, 2-trifluoroethanol (TFE) before use.

Expression and purification of recombinant PAP3

A recombinant baculovirus stock for proPAP3 expression was obtained from Dr. Haobo Jiang (Wang et al., 2001) and amplified in Sf9 cells in suspension culture in Sf-900 II SFM (Thermo Fisher Scientific) medium. One liter of Sf9 cells (2×10^6/ml) was infected with the recombinant baculovirus at a multiplicity of infection of 2 and cultured at 27°C with shaking at 140 rpm for 72 h. The medium containing secreted proPAP was harvested by centrifugation at 4°C, 300 × g for 10 min. Ammonium sulfate (537 grams) was added to the medium, followed by incubation at 4°C for 2 days without disturbing. A brown precipitate was carefully collected from the surface of medium and then dialyzed against 5 L of 15 mM sodium phosphate, pH 8.0 three times at 4°C. Immunoblot analysis of this sample using PAP3 polyclonal antiserum (described below) indicated that proPAP3 was cleaved at a position consistent with its proteolytically activated form (Jiang et al., 2003), due to auto-activation or activation by other proteases in the medium. This sample (~150 ml) was then applied to a Ni-NTA column (1.5×14 cm, Qiagen), and after washing with buffer (10-30 mM imidazole, 50 mM sodium phosphate, 300 mM NaCl, pH 8.0), PAP3 was eluted with the same buffer supplemented with 250 mM imidazole. The fractions containing PAP3 were dialyzed against 5 L of 20 mM Tris-HCl, 20 mM NaCl, pH 8.0 three times and then concentrated to 3.5 ml by centrifugal ultrafiltration (Amicon 30K MWCO, Millipore). PAP3 was further purified by anion exchange chromatography on a UnoQ1 column (7×35 mm, Bio-Rad) using a linear gradient elution of 20-500 mM NaCl in 20 mM Tris-HCl, pH8.0. Fractions containing PAP3 were pooled, quantified, and stored at -80°C.

Expression and purification of recombinant serpin-3ΔN

Recombinant plasmid pET28a containing serpin-3 sequence encoding residues 31-435 was used to transfect *E. coli* strain BL21(DE3). Serpin-3ΔN expression in 1 L *E. coli* culture was induced at mid-log stage by 1 mM IPTG at 37°C for 6 h. Bacteria were then pelleted by centrifugation and lysed by sonication in cold 300 mM NaCl, 10 mM imidazole, 50 mM sodium phosphate, pH 8.0 at 4°C. After centrifugation, the pellet and supernatant were subjected to SDS-PAGE, which showed that the majority of serpin-3ΔN was insoluble, but also was present in

lower amounts in the soluble fraction. The supernatant (36 ml) was applied to a NiNTA (Qiagen) column (1×7 cm), and after washing with buffer (10-30 mM imidazole, 50 mM sodium phosphate, 300 mM NaCl, pH8.0), serpin-3ΔN was eluted with the same buffer supplemented with 250 mM imidazole. Fractions containing serpin-3ΔN were dialyzed against 4 L of 20 mM Tris-HCl, 20 mM NaCl, pH 8.0 three times at 4°C. Serpin-3ΔN was further purified by chromatography on a UnoQ1 column (7×35 mm, Bio-Rad) using a linear gradient of 20-500 mM NaCl in 20 mM Tris-HCl, pH 8.0. Fractions containing serpin-3ΔN were pooled, quantified, and stored at -80°C.

Expression and purification of recombinant serpin-1B

The plasmid pQE-60 containing full-length mature serpin-1B was used to transfect *E. coli* strain BL21 (Kanost et al., 1989). Serpin-1B expression in 1 L YT medium was induced at mid-log stage by 1 mM IPTG at 37°C for 3.5 h. Bacteria were then pelleted by centrifugation and lysed by sonication in cold 300 mM NaCl, 10 mM imidazole, 50 mM sodium phosphate, pH 8.0 at 4°C. After centrifugation, the supernatant (~20 ml) was incubated with 2 ml NiNTA beads at 4°C for 1.5 h, the mixture was then applied to column (1×7 cm), and after washing with buffer (10-30 mM imidazole, 50 mM sodium phosphate, 300 mM NaCl, pH8.0), serpin-1B was eluted with the same buffer supplemented with 250 mM imidazole. Fractions containing serpin-1B were dialyzed against 4 L of 20 mM Tris-HCl, 20 mM NaCl, pH 8.0 three times at 4°C. Serpin-1B was further purified by chromatography on a UnoQ1 column (7×35 mm, Bio-Rad) using a linear gradient of 20-500 mM NaCl in 20 mM Tris-HCl, pH 8.0. Fractions containing serpin-1B were pooled, quantified, and stored at -80°C.

Plasma preparation from naïve larvae

Hemolymph was collected from day 2 fifth instar larvae of *M. sexta*. Hemocytes were removed by centrifugation at 12,000 × g for 20 min at 4°C. Plasma samples from each larva were screened as follows: 2 µl of plasma was added to 97 µl of 50 mM sodium phosphate, pH 6.5, followed by addition of 1 µl of 1 mg/ml *Micrococcus luteus* to activate the proPO protease cascade or 1 µl filter-sterilized 0.85% NaCl as a control. These mixtures were incubated at room temperature for 10 min, and then PO activity was measured by adding 100 µl of 4 mM dopamine as substrate in 50 mM sodium phosphate, pH 6.5. PO activity was measured by detecting an increase in absorbance at 470 nm. One unit of PO activity was defined as $1000 \times \Delta A_{470}$/min.

Those plasma samples with low basal PO activity but significantly induced activity in response to *M. luteus* induction were stored at -80°C for future use.

SDS-PAGE and immunoblotting

Protein samples analyzed by SDS polyacrylamide gel electrophoresis were mixed with 2× or 6×SDS loading buffer (supplemented with β-mercaptoethanol) followed by heating at 95°C for 5 min. Samples were loaded into wells of 4-12% Bis-Tris NuPAGE gels and separated by electrophoresis using MES or MOPS buffer. The gels were stained using Instant Blue (Expedeon) or transferred to nitrocellulose in a semi-dry transfer cell (Bio-Rad). The presence of PAP3, serpin-3ΔN or serpin-1 on the membrane was detected using rabbit antisera to PAP3 (Wang et al., 2001), serpin-3 (Zhu et al., 2003) or serpin-1 (Kanost et al., 1989), followed by goat anti rabbit IgG conjugated to alkaline phosphatase (BioRad) and colorimetric detection of immobilized alkaline phosphatase activity.

Protein and peptide concentration assay

Protein concentration was measured using Coomassie Plus Protein Assay Reagent (Thermo Scientific), with bovine serum albumin as a standard. Concentration of RCL-derived peptides was determined spectrophotometrically at 257 nm using a molar extinction coefficient of phenylalanine, 195 $M^{-1} \bullet cm^{-1}$ (Mach et al., 1995).

Inhibitory activity of recombinant serpin-3ΔN against PAP3

Purified recombinant PAP3 (40 ng) was incubated with 0, 18, 36, 54, 72, 90, or 180 ng of recombinant serpin-3ΔN (molar ratio from 0 to 4.0) in 100 mM Tris, pH 8.0, supplemented with 5.8 μg bovine serum albumin (BSA) in a 96-well plate for 10 min at room temperature. The PAP3 substrate N-acetyl-Ile-Glu-Ala-Arg-p-nitroanilide (IEAR-*p*NA) at 50 μM in 0.1 M Tris, 0.1 M NaCl, 5 mM $CaCl_2$, pH 8.0 was then added, and residual PAP3 activity was measured by the change of absorbance at 405 nm over 20 min at room temperature.

Purified recombinant PAP3 (72 ng) was incubated with 81 ng or 40.5 ng purified recombinant serpin-3ΔN in 100 mM Tris, pH 8.0 at room temperature for 10 min, followed by analysis by SDS-PAGE and immunoblotting as described above.

Inhibition of PAP3 by serpin-3ΔN in the presence of RCL-derived peptides

Peptides (25 nmol) in TFE or TFE alone as a control were applied to wells of a 96-well plate and allowed to dry (>1 h). Serpin-3ΔN (135 ng) was then added to the wells and incubated at 37°C for 2 h. PAP3 (108 ng) supplemented with 18 μg BSA was then added to the wells and incubated for 10 min at room temperature. Substrate IEAR-*p*NA at 50 μM in 0.1 M Tris, 0.1 M NaCl, 5 mM $CaCl_2$, pH 8.0 was then added, and residual PAP3 activity was measured by the change of absorbance at 405 nm over 20 min at room temperature. Percentage of IEARase activity was defined as IEARase activity divided by IEARase activity of PAP3 in the absence of serpin. Data were analyzed by one-way ANOVA with Tukey's multiple comparison as post test using GraphPad Prism. Samples for analysis by reducing SDS-PAGE and immunoblotting were prepared in a similar way. Peptides or TFE alone were dried in 1.5 mL microcentrifuge tubes and incubated with 7.5 μl serpin-3ΔN (135 ng) at 37°C for 2 h, followed by addition of 46.5 μl PAP3 (108 ng) supplemented with 18 μg BSA and further incubated for 10 min at room temperature. Samples were then analyzed by reducing SDS-PAGE and immunoblotting as described above. To examine the time course of peptide interaction with serpin-3ΔN, pre-dried Ac-SVAFS-NH_2 (400 nmol), Ac-SVAFS-COO^- (400 nmol) and TFE alone as a control were incubated with 40 μl purified serpin-3ΔN (720 ng) supplemented with 40 μl BSA (80 μg) at 37°C for 1 h. At 0, 10, 20, 40 and 60 min, 12 μl aliquots were withdrawn and immediately incubated with 72 ng of PAP3 at room temperature for 10 min, followed by measuring residual PAP3 activity with 50 mM IEAR-*p*NA in 0.1 M Tris, 0.1 M NaCl, 5 mM $CaCl_2$, pH 8.0.

Inhibition of trypsin/elastase by *M. sexta* serpin-1A and 1B in the presence of Ac-SVAFS-COO^-

Recombinant serpin-1A was obtained from Dr. Chunju An and recombinant serpin-1B was purified in this work. Recombinant serpin-1A or 1B (2 μM) was incubated with pre-dried Ac-SVAFS-COO^- (0.4 μmol) or pre-dried TFE at 37°C for 2 h. Serpin-1A (1 μl, 2 μM) treated with or without Ac-SVAFS-COO^- was then incubated with 2 μl bovine trypsin (0.2 μM; Sigma) supplemented with 12 μg BSA in 20 m Tris, pH 8.0 for 10 min at room temperature. Serpin-1B (8 μl, 2 μM) treated with or without Ac-SVAFS-COO^- was then incubated with 2 μl porcine pancreatic elastase (4 μM; Sigma) supplemented with 12 μg BSA in 20 m Tris, pH 8.0 for 10 min at room temperature. Substrate IEAR-*p*NA (for trypsin) or AAA-*p*NA (elastase) at 50 μM in

0.1 M Tris, 0.1 M NaCl, 5 mM $CaCl_2$, pH 8.0 was then added, and residual amidase activity was measured by the change of absorbance at 405 nm over 20 min at room temperature. The same samples were analyzed by reducing SDS-PAGE and immunoblotting as described above.

Inhibition of PAP3 by *A. gambiae* SRPN2 in the presence of two pentapeptides

Ac-SVAFS-NH_2 or Ac-SVAFS-COO^- (25 nmol) in TFE or TFE alone as a control were applied to wells of a 96-well plate and allowed to dry (>1 h). Recombinant *A. gambiae* SRPN2 purified by Dr. David Meekins (80 ng) was then added to the wells and incubated at 37°C for 2 h. PAP3 (108 ng) supplemented with 18 μg BSA was then added to the wells and incubated for 10 min at room temperature. Substrate IEAR-*p*NA at 50 μM in 0.1 M Tris, 0.1 M NaCl, 5 mM $CaCl_2$, pH 8.0 was then added, and residual PAP3 activity was measured by the change of absorbance at 405 nm over 20 min at room temperature. Percentage of IEARase activity was defined as IEARase activity divided by IEARase activity of PAP3 in the absence of serpin.

Effects of RCL-derived peptides on pro-PO activation in plasma

Hemolymph was collected from day 2 fifth instar larvae and centrifuged at 12,000 rpm for 25 min at 4°C to remove hemocytes, to prepare plasma samples containing the proPO activation system. To examine the effect of pre-incubation of peptide with serpin before exposure to plasma, Ac-SVAFS-COO^- (10 nmol in TFE) or TFE alone were dried in wells of a 96-well plate and then incubated with 4 μl serpin-3ΔN (0.1 μg) at 37°C for 2 h, followed by incubation with 2 μl plasma at room temperature for 10 min. Then the proPO cascade was stimulated by addition of 1 μg *Micrococcus luteus* (Sigma) or filter-sterilized 0.85% NaCl as a control. These mixtures were incubated at room temperature for 10 min, and then PO activity was measured by adding 100 μl of 4 mM dopamine as substrate in 50 mM sodium phosphate, pH 6.5. PO activity was measured by detecting increase in absorbance at 470 nm. One unit of PO activity was defined as $1000 \times \Delta A_{470}$/min. Three replicates with four different larval plasma samples were examined. Paired one-way ANOVA with Tukey's multiple comparison as post test was performed in GraphPad Prism.

To test the effects of peptide mixed directly to plasma samples, pre-dried Ac-SVAFS-NH_2 (25 nmol) or TFE in wells of a 96-well plate were incubated with 5 μl plasma for 1 h at room temperature, followed by addition of 95 μl of 50 mM sodium phosphate buffer, pH 6.5 supplemented with or without 2 μg of *M. luteus* (Sigma). After incubation for 10 min at room

temperature, PO activity was measured as described above. Three replicates with four different larval plasma samples were examined. Statistical analysis was done as described above.

Circular dichroism analysis

To examine effects of RCL-derived peptides on serpin-3ΔN secondary structure, 600 µl serpin-3ΔN (150 µg) and 1.8 ml Ac-SVAFS-COO^- (25 µmol) were mixed and incubated at 37°C for 2 h to allow formation of a serpin-peptide binary complex. Then the mixture was subjected to gel permeation chromatography using Superdex 200 10/300 GL (Bio-Rad) in 20 mM Tris-HCl, 150 mM NaCl, pH 8.0 to separate binary complex from free peptide. The fractions containing serpin-3ΔN, presumed to be in complex with peptide, were pooled and quantified. Ellipticity of serpin-3ΔN (0.18 mg/ml) or purified binary complex (0.12 mg/ml) in 20 mM Tris, 10 mM NaCl, pH 8.0 was measured in a 0.02 cm cuvette from 190 nm to 260 nm at 20°C. The temperature was then increased in 10°C increments, and the spectra were measured at each temperature from 20°C to 90°C. The ellipticity of the buffer was also recorded and subtracted from that of serpin-3ΔN and binary complex. The data were smoothed by the method of Savitzky-Golay with value of 1533. Molar ellipticity was calculated as (ellipticity × molecular weight)/(10 × 0.02 cm × concentration).

Results

Expression and purification of PAP3, serpin-3ΔN and serpin-1B

PAP3 is present as a zymogen (proPAP3) in *M. sexta* plasma, and can be activated by hemolymph protease HP21 in response to microbial infection. *M. sexta* proPAP3 is composed of N-terminal dual clip domains (19 kDa) and a C-terminal protease domain (37 kDa) (Jiang et al., 2003). Cleavage of proPAP3 by HP21 between clip domains and protease domain generates active PAP3, while a disulfide bridge connects both parts after activation (Gorman et al., 2007). It was also reported that purified recombinant PAP3 can activate proPAP3 (Wang et al., 2014). I found that proPAP3 expressed in Sf9 cells became cleaved during ammonium sulfate precipitation or dialysis, observed as two bands that match the size of the dual clip domain and protease domain on reducing SDS-PAGE (Fig. 3-1). These bands are consistent with the sizes of the two products after activation of proPAP3 by HP21 (Gorman et al., 2007). Possibly the highly dense protein environment favored the activation of proPAP3 by a small amount of active PAP3

or other unknown PAP3-activating enzymes present in cell culture medium. The overall yield of PAP3 from 1.0 L of Sf9 cell culture was ~0.05 mg. Another way of activating proPAP3 was using proHP21[L→K], which is a constitutively active variant with the leucine P1 at the activation site replaced by lysine (Gorman et al., 2007). I found that proHP21[L→K] could activate proPAP3 at 1:10 molar ratio at 37°C after 18 h (data not shown). But this approach should be further optimized to avoid over-proteolysis of PAP3.

A majority of serpin-3ΔN (with deletion of a 30-residue amino-terminal extension to improve recombinant expression) expressed in *E. coli* remained insoluble, and lowering the temperature during expression (17, 23, 30°C rather than 37°C) did not lead to improvement of solubility (data not shown). Therefore, only the soluble portion of serpin-3ΔN expressed at 37°C was subjected to purification. From 2.0 L of bacterial culture, ~4.2 mg of recombinant serpin-3ΔN was obtained after purification (Fig. 3-1). Yield of recombinant serpin-1B was ~3.75 mg from 500 ml bacterial culture after purification (Fig. 3-1).

Serpin-blocking activities of four serpin-3 RCL-derived peptides

I sought to test whether short peptides derived from the serpin-3 RCL would block the inhibitory activity of serpin-3. Based on previous studies of mammalian serpins (Schulze et al., 1990; Carrell et al., 1991; Björk et al., 1992; Mast et al., 1992; Eitzman et al., 1995; Jankova et al., 2001; D'Amico et al., 2012; Mahadeva et al., 2002), I designed four peptides that began at the P14 residue of the serpin-3 RCL, with sizes of 5-8 amino acid residues (Fig. 3-2). These were initially synthesized with blocking groups at each end (acetyl block at the amino-terminus and amide block at the carboxyl-terminus) to avoid charged groups at the ends of the peptides. The effect of RCL-derived peptides on serpin-3ΔN was tested by treating the serpin with peptides and then measuring serpin-3ΔN inhibition of *M. sexta* PAP3, one of the main target serine proteases of serpin-3 in regulating *M. sexta* immune responses (Zhu et al., 2003; Christen et al., 2012). Serpin-3ΔN was an efficient inhibitor of PAP3, with ~100% inhibition of PAP3 activity at 1.6:1.0 molar ratio (serpin-3ΔN:PAP3) (Fig. 3-3A). The inhibitory complex formed by serpin-3ΔN and PAP3 was observed by immunoblotting (Fig. 3-3B). Incubation of RCL-derived peptides with serpin-3ΔN led to decreased inhibitory activity of serpin-3ΔN (Fig. 3-4A). The treatment of serpin-3ΔN with the pentapeptide, Ac-SVAFS-NH_2 (peptide 1, Fig. 3-1B), completely blocked its PAP3 inhibitory activity, whereas longer peptides had less effect, in a

size-dependent manner. The octapeptide, Ac-SVAFSATQ-NH_2 (peptide 4, Fig. 3-1B) showed about 50% blockage of serpin-3ΔN inhibition of PAP3. The peptides in the absence of serpin had no effect on PAP activity (data not shown).

To further examine molecular effects caused by the RCL-derived peptides, we analyzed samples of serpin-3ΔN after reaction with PAP3 in the presence or absence of the four RCL-derived peptides by SDS-PAGE and immunoblotting, using serpin-3 antiserum (Fig. 3-4B). In the absence of peptides, a major band of intact serpin-3ΔN at ~42 kDa was present, and a covalent inhibitory complex of serpin-3ΔN with PAP3 was detected at ~75 kDa (Fig. 3-3B and Fig. 3-4B) as previously observed (Zhu et al., 2003). A minor band at ~38 kDa was also present, consistent with some serpin-3ΔN undergoing cleavage in the RCL as a substrate rather than acting as an inhibitor. In contrast, the incubation of RCL-derived peptides with serpin-3ΔN resulted in an enhanced conversion of serpin-3ΔN from inhibitor to substrate, indicated by increased intensity of the 38 kDa cleaved serpin band, and decreased formation of the 75 kDa inhibitory complex (Fig. 3-4B). Consistent with effects on PAP3 amidase activity assay, Ac-SVAFS-NH_2, the shortest RCL-derived peptide, was the most efficient of the four RCL-derived peptides in inducing substrate-like property, with an intense band for the 38 kDa cleaved form, and absence of the ~75kDa complex. Therefore, this pentapeptide was used for further experiments.

Comparison of effects of Ac-SVAFS-COO^- and Ac-SVAFS-NH_2 on serpin-3

Peptide 1, Ac-SVAFS-NH_2, with amino-terminal and carboxyl-terminal blocking groups, had very low aqueous solubility. We synthesized a peptide with the same sequence but only an amino-terminal blocking group and a free carboxyl end, Ac-SVAFS-COO^-, which has a negative charge at neutral pH, for improved solubility. Ac-SVAFS-NH_2 and Ac-SVAFS-COO^- were evaluated for their effect on serpin-3ΔN as an inhibitor of PAP3 (Fig. 3-5). Inactivation of serpin-3ΔN began to occur by 10 min after incubating the serpin with either of the pentapeptides and increased to ~100% suppression of serpin-3ΔN inhibitory activity by 40 min. This result suggests that the difference in the solubility of these two peptides did not limit their effects on serpin function in this experiment, and that the peptides interact with serpin to cause its inactivation on the scale of minutes.

Specificity of serpin-3 RCL-derived peptides

A peptide based on the serpin-3 RCL was also tested with *M. sexta* serpin-1A and 1B, which are inhibitory serpins with a different hinge and RCL sequences (Fig. 3-6A). Amidase activity of trypsin was completely inhibited by serpin-1A at 1:4 molar ratio. Incubation of serpin-1A with Ac-SVAFS-COO^- completely blocked the inhibitory activity of serpin-1A (Fig. 3-6B). Serpin-1B showed 100% inhibition against elastase at 2:1 molar ratio, but 74% of elastase activity remained after incubation with Ac-SVAFS-COO^- treated serpin-1B (Fig. 3-6C). Immunoblotting results are consistent with the amidase activity assay. Incubation of Ac-SVAFS-COO^- with serpin-1A or 1B promoted the substrate-behavior of the serpins and abolished or attenuated the complex formation (Fig. 3-6D and E).

Specificity of serpin-3 based RCL peptides was also tested with *A. gambiae* SRPN2, which is orthologous to *M. sexta* serpin-3 (Fig. 3-7A) (Michel et al., 2005). Ac-SVAFS-NH_2 was able to block ~40% of the inhibitory activity of SRPN2, while Ac-SVAFS-COO^- did not show any inhibition of SRPN2 (Fig. 3-7B and C). Immunoblotting displayed a slight enhancement of the cleaved SRPN2 band and a less intense complex band when PAP3 was incubated with Ac-SVAFS-NH_2 treated SRPN2 (Fig. 3-7E). However, bands for Ac-SVAFS-COO^- treated SRPN2 did not appear different from those in the absence of the peptide (Fig. 3-7F).

Serpin-3 RCL-derived peptide promotes increased PO activation in plasma

Detection of microbes in hemolymph stimulates the initiation of a protease cascade that results in the activation of proPO by PAPs, leading to oxidation of catechols in hemolymph and subsequent reactions that produce melanin (Kanost et al., 2004). Serpin-3 in hemolymph regulates proPO activation by inhibiting PAPs (Zhu et al., 2003). To investigate whether the inactivation of serpin-3 by RCL-derived peptides can have an effect in hemolymph, Ac-SVAFS-COO^- was pre-incubated with serpin-3ΔN to allow formation of peptide-serpin complex, followed by the addition of plasma and stimulation of the protease cascade by *M. luteus* (Fig. 3-8A). *M. luteus* treatment stimulated activation of PO in plasma, which was suppressed by addition of free serpin-3ΔN. However, addition of serpin-3ΔN treated with Ac-SVAFS-COO^- to plasma did not significantly attenuate PO activation. This result is consistent with lack of inhibition of PAP activity by serpin-3ΔN complexed with the peptide.

To further confirm the inactivation of naturally occurring serpin-3 by the RCL-derived peptide in the complex protein mixture in hemolymph, plasma was incubated with Ac-SVAFS-NH_2 for 1 h to allow the association of RCL-derived peptides with endogenous serpin-3, followed by triggering the proPO cascade by addition of *M. luteus* (Fig. 3-8B). Addition of the bacteria to plasma led to increased PO activity, as expected, but in the presence of Ac-SVAFS-NH_2, PO activity was significantly greater after addition of bacteria than in control plasma (Fig. 3-8B), consistent with the hypothesis that the peptide blocked inhibition of PAPs by serpin-3.

Ac-SVAFS-COO^- alters conformation and increases thermal stability of serpin-3ΔN

The incorporation of RCL-derived peptides into β-sheet A was confirmed to mimic the relaxed state of human antithrombin, with increased thermodynamic stability (Björk et al., 1992). To compare the thermostability of serpin-3ΔN with that of the complex formed by serpin-3ΔN and RCL-derived peptide, I incubated serpin-3ΔN with Ac-SVAFS-COO^- and then separated the complex from free peptide by gel permeation chromatography. Analysis of serpin-3ΔN and the serpin-3ΔN•Ac-SVAFS-COO^- complex by circular dichroism spectroscopy (Fig. 3-9A) revealed a deeper trough at around 220 nm in the complex compared with the free serpin, indicating a slight change in secondary structure in the presence of Ac-SVAFS-COO^-. The effect of interaction of Ac-SVAFS-COO^- on the thermal stability of serpin-3ΔN was tested by measuring circular dichroism spectra at increasing temperatures. The spectrum of serpin-3ΔN changed significantly at temperatures of 60°C and above, whereas the serpin-3ΔN in complex with Ac-SVAFS-COO^- maintained its secondary structure, with little change in CD spectrum up to 90°C (Fig. 3-9B and C). Molar ellipticity of both native serpin-3ΔN and serpin-peptide complex at 215 nm was plotted as a function of temperature (Fig. 3-9D). The obvious conformational transition of native serpin-3ΔN occurred between 50°C and 70°C. In contrast, there was only small and gradual elevation of molar ellipticity of the serpin-3ΔN complexed with Ac-SVAFS-COO^- at higher temperatures, suggesting that the association of serpin with the RCL-derived peptide significantly increased the stability of the serpin molecule.

Discussion

M. sexta serpin-3 regulates proPO activation in response to bacteria by inhibiting PAP-1 and PAP-3 in hemolymph (Zhu et al., 2003). Complexes formed by serpin-3 with plasma

proteases, including PAP-1, PAP-2, PAP-3 and HP8, were previously identified in plasma by mass spectrometry, confirming the role serpin-3 plays in regulating immune protease cascades *in vivo* (Christen et al., 2012). RNA interference to decrease the expression of a mosquito ortholog of *M. sexta* serpin-3 (SRPN2 in *A. gambiae*) resulted in enhanced melanin deposition on implanted Sephadex beads and the appearance of melanotic pseudotumors on the abdominal wall, indicating that this serpin has a critical role in regulating proPO activation (Michel et al., 2006, An et al., 2011a). RNA interference has not been successfully used to decrease expression of plasma proteins in *M. sexta* (Terenius et al., 2011) and therefore it has not been possible to determine the effect of lowered serpin-3 concentrations *in vivo*. However, we hypothesized that blocking the inhibitory activity of serpin-3 would result in misregulated proPO activation. Modulation of mammalian serpin function by RCL-derived peptides has been studied through biochemical approaches and showed potential feasibility for application in a mouse model (Ambadapadi et al., 2016). In this study, experiments were carried out to use regulation of the melanization response by serpin-3 as a model system to investigate the potential for using RCL-derived peptides to probe the functions of insect serpins.

The proximal hinge region in the RCL of serpins tends to have small, hydrophobic residues, allowing this flexible sequence to drive the incorporation of the N-terminal RCL into β-sheet A during protease inhibition, whereas the distal region of the RCL has much more sequence variability in different serpins (Irving et al., 2000). Synthetic peptides with sequences spanning P15 or P14 to P1 of the RCL were the first to be described as a counterpart of incorporated strand A4, converting human serpins from an inhibitor to a substrate (Mast et al., 1992; Schulze et al., 1990; Björk et al., 1992; Eitzman et al., 1995; Jankova et al., 2001). Furthermore, research with human α_1-antitrypsin revealed that peptides representing the proximal RCL (P14-P4 and P14-P8) are sufficient to substantially inhibit antitrypsin activity, while those peptides representing the distal part of the RCL (P10-P1, P9-P1 and P8-P1) were much less efficient in blocking α_1-antitrypsin (Schulze et al., 1992). Therefore, we designed and synthesized peptides based on the RCL proximal hinge of serpin-3, with length of 5-8 residues (P14-P10, P14-P9, P14-P8 and P14-P7). These peptides did block serpin-3's ability to inhibit proteolytic activity of PAP3. We found that increasing the length of peptides decreased their efficiency in blocking serpin-3ΔN function, with the 5-residue peptide (P14-P10) having the greatest effect (Fig. 3-4A). This shorter peptide may have easier access for inserting into the

space between strand 3A and strand 5A (Fig. 3-1A). Such a difference was not observed between 11-residue (P14-P4) and 7-residue peptides (P14-P8) derived from the human α_1-antitrypsin RCL in blocking α_1-antitrypsin function (Schulze et al., 1992), perhaps because the longer incubation time they used may permit entry of longer peptides into β-sheet A.

In the natural RCL sequence of serpin-3, the amino acid residues from P14 to P2 are not charged, since they are participating in peptide bonds and lack ionizable side chains. In order to mimic the endogenous proximal RCL sequences, we synthesized peptides with ends blocked by N-terminal acetylation and C-terminal amidation, so that they would not contain charged groups at the ends. These peptides functioned in blocking serpin-3ΔN function, but they had low solubility due to the hydrophobic nature of this segment of the serpin sequence. For this reason, the five-residue peptide SVAFS was synthesized with only an N-terminal acetylated group and lacking the C-terminal amidation. This peptide with one negative charge was much more soluble and functioned equally as well as the uncharged peptide (Fig. 3-5). Therefore, it appears that negative charge at the C-terminus did not impede insertion of the peptide into β-sheet A of serpin-3ΔN.

The incorporation of an endogenous RCL into β-sheet A during a protease inhibition reaction is a complex process that requires opening of an existing β-sheet and insertion of a new strand (Björk et al., 1992). This involves coordinated movements of the RCL and regions of the serpin called the breach, the shutter, and the gate (Pearce et al., 2007). Long incubation times (15-48 h) at 37-48°C are necessary in many cases for inactivation of the human serpins α_1-antitrypsin, antithrombin, PAI-1 and PAI-2 by corresponding RCL-derived peptides, conditions which probably favor partial unfolding to promote accessibility of the peptides to insert into β-sheet A (Mast et al., 1992; Chang et al., 1996; Schulze et al., 1990; Björk et al., 1992; Skinner et al., 1998; Jankova et al., 2001). However, we found that the SVAFS peptide can block serpin-3ΔN function within 40 min at 37°C. The relatively small size of this peptide, compared to those investigated in studies of human serpins may contribute to more efficient insertion into β-sheet A. Furthermore, the three-dimensional structure of a mosquito ortholog of serpin-3, *A. gambiae* SRPN2 has the RCL hinge in a "partially inserted" conformation (An et al., 2011b; Zhang et al., 2015), which might contribute to more efficient insertion of the peptide as a new β-strand in these related insect serpins.

After serpin-3ΔN was incubated with the RCL peptides to allow formation of the complex, it lost activity as an inhibitor of PAP, and instead behaved as a substrate for the protease (Fig. 3-4B). This is consistent with observations of human serpins after insertion of RCL-derived peptides into β-sheet A, with increased vulnerability to cleavage in the RCL and lack of inhibitory reactions (Skinner et al., 1998; Xue et al., 1998; Jankova et al., 2001; Zhou et al., 2004; Eitzman et al., 1995; D'Amico et al., 2012).

At least 8 different serpins are present in the circulating plasma of *M. sexta*, including serpin-1, -3, -4, -5, -6, -9, -11 and -12 (He et al., 2016). It may be possible that some of these serpins would be unspecific targets of peptides based on the RCL of serpin-3. I tested the interaction of *M. sexta* serpin-1A and 1B with Ac-SVAFS-COO^- derived from serpin-3 RCL. Ac-SVAFS-COO^- was able to block >74% of the inhibitory activity of serpin-1A and 1B (Fig. 3-6B and C), indicating nonspecific interaction of this peptide with two isoforms of serpin-1. A few cases of unspecificity of RCL-derived peptides have been reported. P15-P1 peptide derived from α_1-antitrypsin had off-target effect on antichymotrypsin and antithrombin (Mast et al., 1992). P14-P3 peptide from antithrombin was able to inactivate α_1-antitrypsin (Chang et al., 1996). It seems that lack of specificity may result from a sequence rich in small hydrophobic residues in the hinge region of inhibitory serpins (Irving et al., 2000), without requirement of a specific sequence. This may impede the application of RCL-derived peptides in therapies for serpin related diseases. Ac-SVAFS-NH_2 displayed partial inhibition of a serpin-3 ortholog *A. gambiae* SRPN2, while Ac-SVAFS-COO^- did not have an effect on SRPN2 (Fig. 3-7). The charge on Ac-SVAFS-COO^- may have impeded the insertion into β-sheet A of *A. gambiae* SRPN2.

The CD spectrum of serpin-3ΔN complexed with Ac-SVAFS-COO^- differed slightly from that of serpin-3ΔN alone, with lower ellipticity at 220 nm, similar to observations of human α_1-antitrypsin and antithrombin in complex with their RCL-derived peptides (Schulze et al., 1990; Schulze et al., 1992; Carrell et al., 1991; Björk et al., 1992). The insertion of an RCL or RCL-derived peptide as a new strand (strand A4) in β-sheet A changes the configuration of that region of the β-sheet. Strands 3A and 5A are parallel in the native serpin before insertion of the RCL as strand A4, in a new antiparallel relationship with strands A3 and A5, which increases the stability of overall structure (Gettins and Olson, 2016). Native serpins are relatively unstable, with average melting temperature of around 58°C, while the forms that contain strand 4A have a

much higher melting temperature, such as cleaved serpins with >110°C melting temperature (Pearce et al., 2007). Similarly, we found that native serpin-3ΔN started to denature at ~60°C, whereas serpin-3ΔN in complex with Ac-SVAFS-COO^- showed little change in CD spectrum up to the highest temperature (90°C) tested (Fig. 3-9B and C). This result is quite similar to an experiment with human antithrombin, with change in CD at 220 nm revealing a melting temperature of 58°C for native antithrombin, but no elliptical change of an antithrombin•P14-P1 complex up to 85°C (Björk et al., 1992). These results support the hypothesis that the RCL peptides are functioning in *M. sexta* serpin-3 in a manner similar that that shown by previous structural and biochemical studies of human serpins.

Because serpin-3 is a negative modulator of the proPO cascade by inhibiting PAPs in hemolymph (Zhu et al., 2003), we hypothesized that interfering with serpin-3 activity would lead to a higher level of proPO activation in response to a microbial challenge. The results demonstrated that addition of recombinant serpin-3ΔN to plasma samples stimulated by *M. luteus* caused a significant reduction in PO activity, likely due to inhibition of PAPs. In contrast, when serpin-3ΔN treated with Ac-SVAFS-COO^- was added to the same plasma, PO activity was as high as in the absence of added serpin, indicating that the Ac-SVAFS-COO^- peptide blocked the inhibition of PAPs by serpin-3ΔN, resulting in unregulated proPO activation (Fig. 3-8A). Similar results were observed when the RCL peptide was mixed with plasma, to allow it to interact with endogenous serpin-3 in the complex mixture of hemolymph proteins.

Future Directions

The work presented in this chapter explored the potential use of RCL-derived peptides as serpin inhibitors in *M. sexta*. A foundation was laid for future study involving serpin regulation by RCL mimicking peptides and potentially the physiological functions of *M. sexta* serpins. Some questions arose from the current data:

(1) Is the pentapeptide derived from *M. sexta* serpin-3 able to block the inhibitory activity of other serpins besides serpin-1A, serpin-1B and *A. gambiae* SRPN2 *in vitro* by being incorporated into β-sheet A?

(2) Ac-SVAFS-NH_2 and Ac-SVAFS-COO^- behaved differently in blocking *A. gambiae* SRPN2 (Fig. 3-7), which indicates that one negative charge on the C-terminus is sufficient to

alter the efficiency of serpin blocking. The mechanism underlining this difference remains to be revealed.

(3) The addition of Ac-SVAFS-NH_2 to *M. sexta* plasma caused misregulation of PO activation (Fig. 3-8B), but this effect was not seen when Ac-SVAFS-COO^- was added to plasma. Current data and literature could not give a good explanation, and I generally believe the complicated environment in plasma likely reduced the accessibility of Ac-SVAFS-COO^- to serpin-3. But more study should be done to solve this puzzle.

(4) Molecular Dynamics or crystal structure of RCL-derived peptide and serpin-3 complex could be performed or solved to have a look at the binding interaction at the angstrom level.

(5) RCL peptides have been shown to decrease serpin function in regulating mammalian blood clotting. RCL peptides from plasminogen activator inhibitor-1 (PAI-1) suppress activity of this serpin and result in decreased blood clot lysis *in vitro* (Eitzman et al., 1995; D'Amico et al., 2012; Van De Craen et al., 2012). A series of RCL-derived peptides from mammalian neuroserpin and a myxomavirus serpin displayed anti-inflammatory, anti-atherogenic and pro-thrombotic functions in mice (Ambadapadi et al., 2016), indicating that RCL peptides can have biological activity *in vivo*. Another application of RCL-derived peptides is to depolymerize or deaccelerate aberrant polymerization of serpin monomers, as a potential treatment for human serpinopathies (Fitton et al., 1997; Chang et al., 1997). Modulating activity of arthropod serpins by RCL-derived peptides may be a useful tool for investigating the biological roles of serpins with unknown functions. Therefore, injection of Ac-SVAFS-NH_2 or Ac-SVAFS-COO^- into the hemocoel of larvae was carried out, but no effect of PO activation was observed (data not shown), possibly due to the high variability of tested larvae. Determinants of efficient *in vivo* application of serpin RCL-derived peptides in insects require further investigation.

(6) Another application of RCL-derived peptides is to depolymerize or deaccelerate aberrant polymerization of serpin monomers, as a potential treatment for human serpinopathies (Fitton et al., 1997; Chang et al., 1997). Whether serpin-3 RCL derived peptides are able to play a role in depolymerization may be worth studying.

Acknowledgements

I would like to thank Dr. Daisuke Takahashi for providing some purified serpin-3ΔN and larval plasma samples. I thank Susan Whitaker in the KSU Biotechnology/Proteomics Core Laboratory for help with synthesizing peptides. And my thanks are also expressed to Dr. Haobo Jiang for providing baculovirus of proPAP3. I really appreciate Dr. Maureen Gorman for advice on protein purification and providing recombinant HP21 variant, Dr. Michal Zolkiewski for advice on circular dichroism analysis, Dr. Di Wu for making the construct of serpin-3ΔN, Dr. David Meekins for providing recombinant *A. gambiae* SRPN2, Dr. Chunju An for providing recombinant serpin-1B, and Lisa Brummett for supplying *M. sexta* larvae. This work was supported by National Institutes of Health Grants GM041247.

Figures

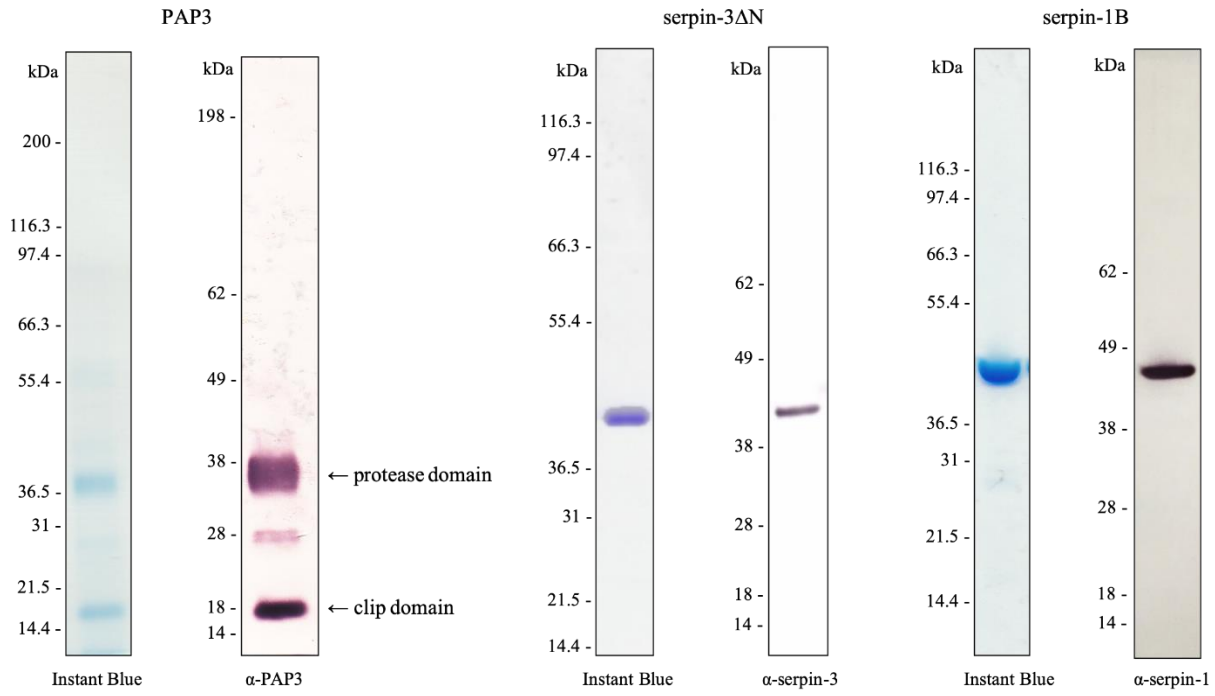

Figure 3-1. Purification results of PAP3, serpin-3ΔN and serpin-1B.

Purified recombinant PAP3, serpin-3ΔN, or serpin-1B with reducing SDS loading buffer was subjected to 4-12% Bis-Tris NuPAGE gel. Instant blue staining and immunoblotting using diluted antiserum against PAP3, serpin-3 or serpin-1 as the primary antibody were performed for each protein.

A

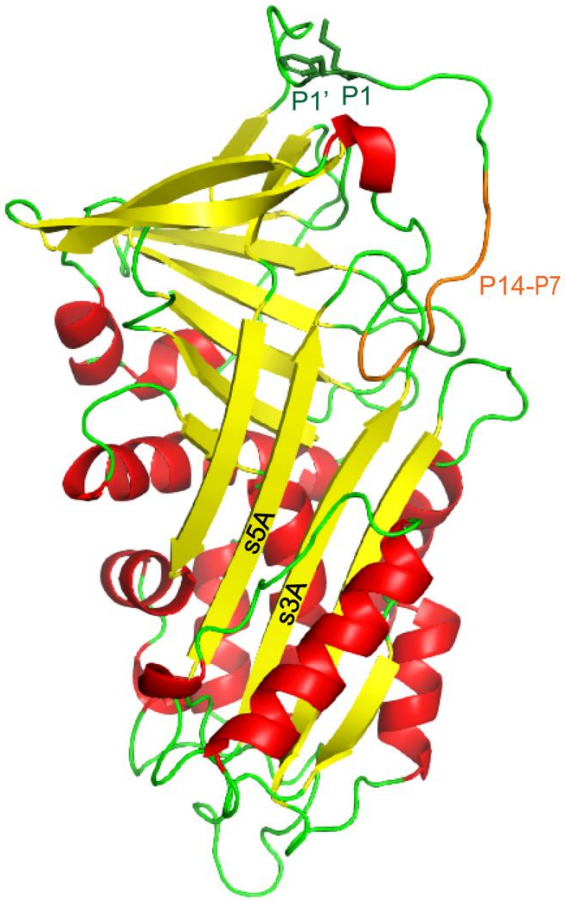

B

		P14	P13	P12	P11	P10	P9	P8	P7	P6	P5	P4	P3	P2	P1	P1'
		S	V	A	F	S	A	T	Q	I	G	I	Q	N	K	F
peptide	1	S	V	A	F	S										
	2	S	V	A	F	S	A									
	3	S	V	A	F	S	A	T								
	4	S	V	A	F	S	A	T	Q							

Figure 3-2. RCL derived peptide design.

(A) Homology model of serpin-3. P1 and P1' side chains are indicated as stick drawings and P14-P7 residues are in orange. (B) Sequences of RCL derived peptides aligned with P14-P1' of the serpin-3 RCL.

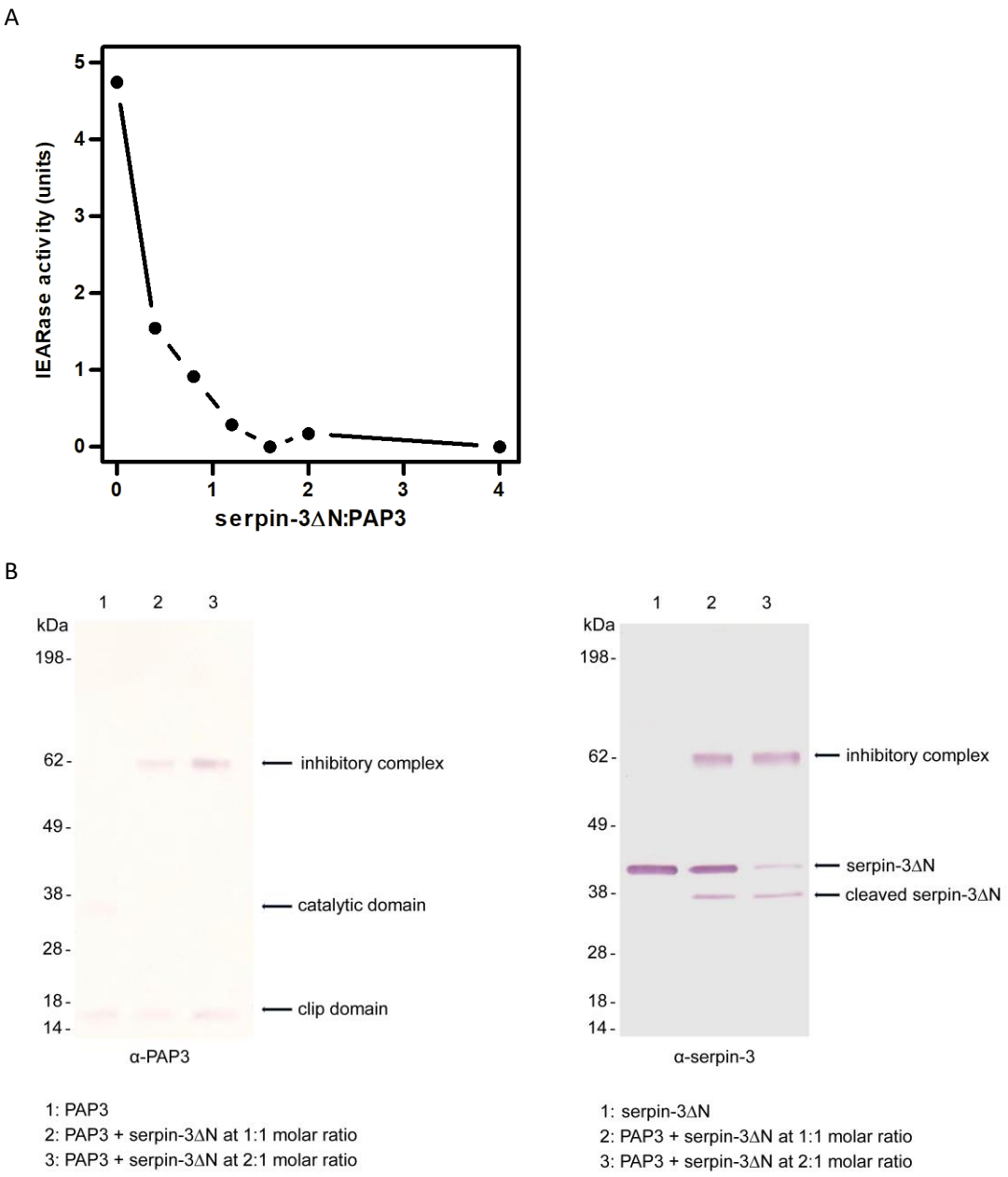

Figure 3-3. Inhibition of PAP3 by serpin-3ΔN.

(A) Purified recombinant PAP3 (40 ng) was incubated with 0, 18, 36, 54, 72, 90, or 180 ng of recombinant serpin-3ΔN (molar ratio: 0, 0.4, 0.8, 1.2, 1.6, 2.0 and 4.0) in 100 mM Tris, pH 8.0 at room temperature for 10 min, followed by residual amidase activity determination of PAP3 by using 50 μM IEAR-*p*NA as substrate. (B) Purified recombinant PAP3 was incubated with serpin-3ΔN at 0:1, 1:1 and 2:1 molar ratio in 100 mM Tris, pH 8.0 at room temperature for 10 min, followed by analyzing with reducing 4-12% Bis-Tris NuPAGE gel and immunoblotting using diluted antiserum against PAP3 (left) or serpin-3 (right) as the primary antibody.

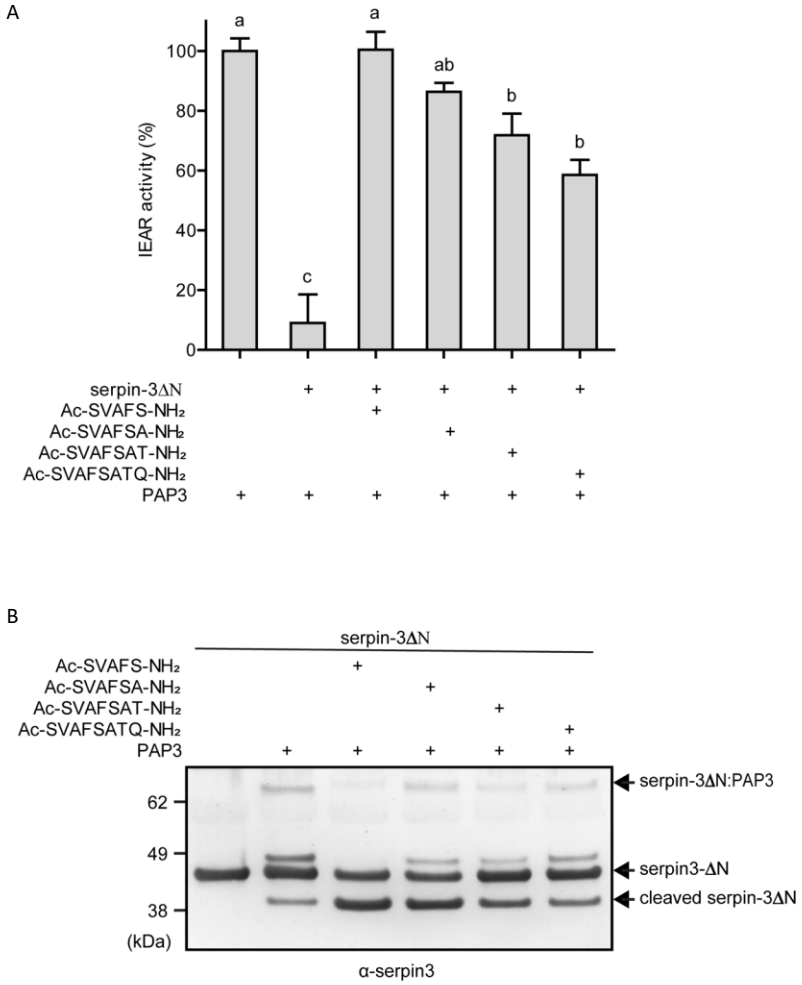

Figure 3-4. Effects of RCL peptides on inhibitory activity of serpin-3ΔN.

Pre-dried peptides (25 nmol) or dried TFE as a control were incubated with purified serpin-3ΔN (135 ng) at 37°C for 2 h, followed by addition of PAP3 (108 ng) and further incubation for 10 min at room temperature. (A) Residual amidase activitiy of PAP3 was determined by using IEAR-*p*NA (50 μM) as the substrate. Data are means ± standard deviation (n=3). Results of statistical analysis (one-way ANOVA followed by Tukey's multiple comparison test, $P<0.05$) are indicated. Means with the same letter are not significantly different. (B) Samples prepared as described above were analyzed by reducing SDS-PAGE followed by immunoblotting using diluted antiserum against serpin-3 as the primary antibody.

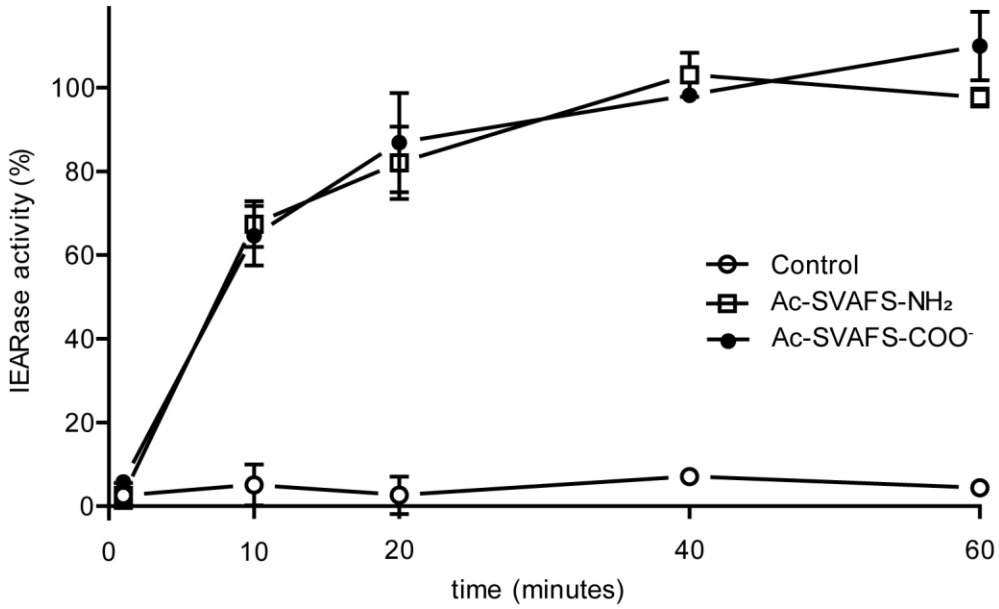

Figure 3-5. Inactivation of serpin-3ΔN by Ac-SVAFS-NH_2 and Ac-SVAFS-COO^- over the time.

Pre-dried Ac-SVAFS-NH_2, Ac-SVAFS-COO^- (400 nmol) and TFE alone as control were incubated with purified serpin-3ΔN (720 ng) at 37°C for 2 h. A portion of sample was withdrawn at the indicated time intervals and added PAP3 to react at room temperature for 10 min, followed by IEARase activity measurement in 0.1 M Tris, 0.1 M NaCl, 5 mM $CaCl_2$, pH 8.0. Percentage of IEARase activity is defined as individual IEARase activity over gross PAP3 activity.

A

	P14												P1	P1'
M. sexta serpin-3	S	V	A	F	S	A	T	Q	I	G	I	Q	N	K	F
M. sexta serpin-1A	A	E	A	A	A	A	N	A	F	F	I	T	-	R	Q
M. sexta serpin-1B	A	E	A	A	A	A	N	A	F	G	I	V	P	A	S

B

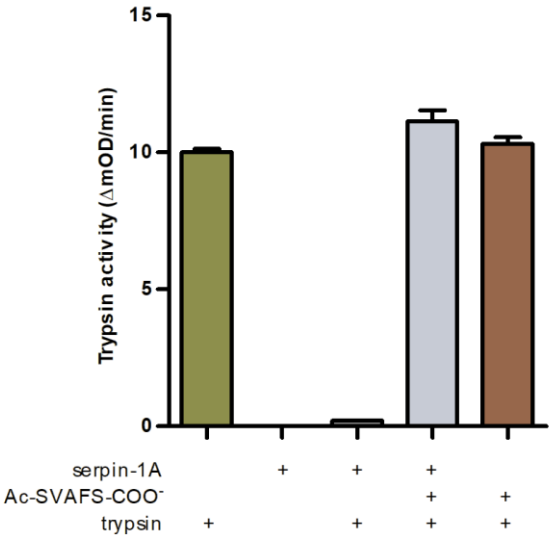

C

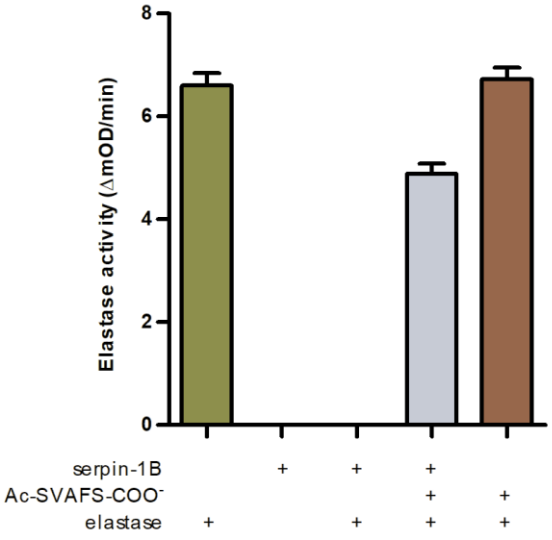

D

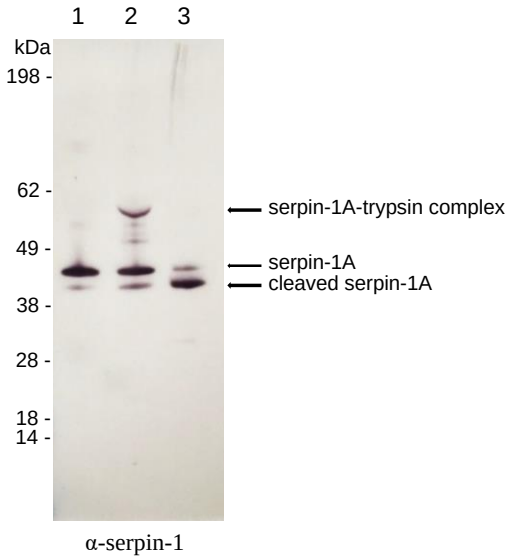

α-serpin-1

1: serpin-1A
2: serpin-1A + trypsin
3: Ac-SVAFS-COO- treated serpin-1A + trypsin

E

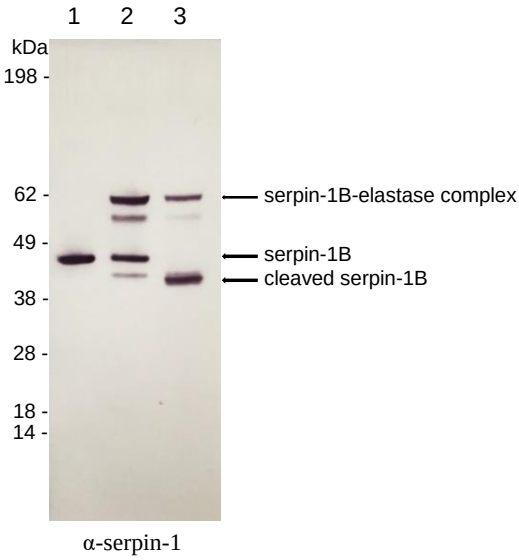

α-serpin-1

1: serpin-1B
2: serpin-1B + elastase
3: Ac-SVAFS-COO- treated serpin-1B + elastase

Figure 3-6. Effects of Ac-SVAFS-COO- on inhibitory activity of serpin-1A and 1B.
(A) N-terminal RCL sequence alignment of serpin-3, serpin-1A and 1B. P1 and P1' residues flanking the scissile bond are indicated. (B) serpin-1A (1 µl, 2 µM) treated with or without Ac-SVAFS-COO- was incubated with 2 µl trypsin (0.2 µM) for 10 min at room temperature, followed by residual amidase activitiy determination of trypsin by using IEAR-*p*NA (50 µM) as the substrate. Data are means ± standard deviation (n=3). (C) serpin-1B (8 µl, 2 µM) treated with or without Ac-SVAFS-COO- was incubated with 2 µl elastase (4 µM) for 10 min at room temperature, followed by residual amidase activity determination of elastase using AAA-*p*NA (50 µM) as the substrate. Data are means ± standard deviation (n=3). (D) and (E) Samples prepared as described above were analyzed by reducing SDS-PAGE followed by immunoblotting using diluted antiserum against serpin-1 as the primary antibody.

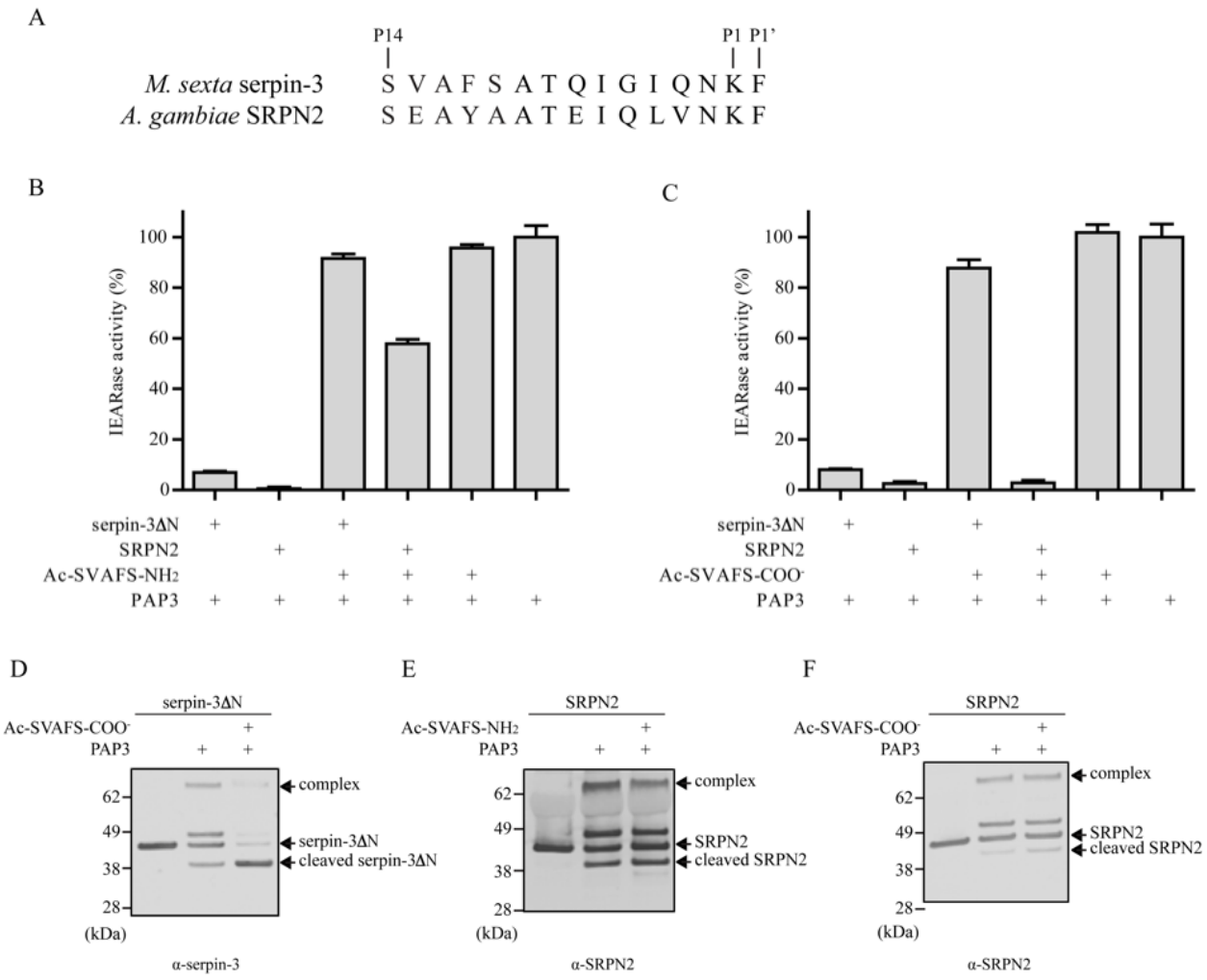

Figure 3-7. Effects of Ac-SVAFS-NH_2 and Ac-SVAFS-COO^- on inhibitory activity of *A. gambiae* SRPN2.

(A) N-terminal RCL sequence alignment of serpin-3 and *A. gambiae* SRPN2. P1 and P1' residues flanking the scissile bond are indicated. (B) and (C) Recombinant serpin-3ΔN (108 ng) or SRPN2 (80 ng) treated by pre-dried Ac-SVAFS-NH_2 or Ac-SVAFS-COO^- was incubated with PAP3 (108 ng) at room temperature for 10 min, followed by residual amidase activitiy determination by using IEAR-*p*NA (50 μM) as the substrate. Data are means ± standard deviation (n=3). (D), (E) and (F) Immunoblotting was performed using indicated antisera as the primary antibody.

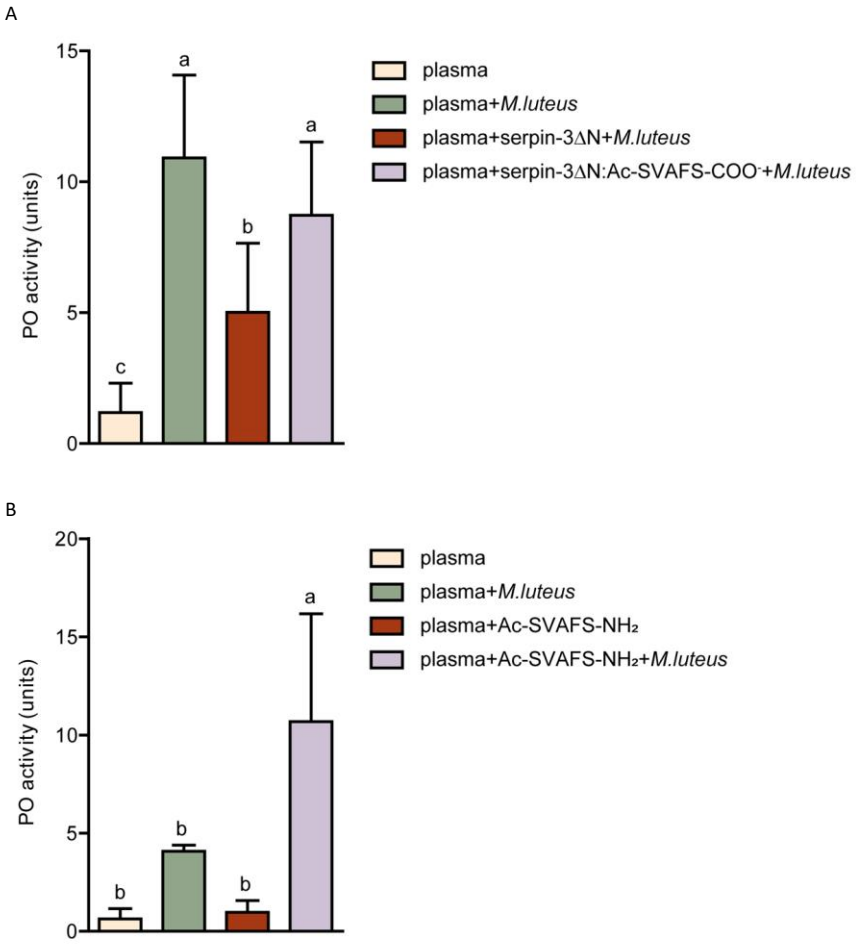

Figure 3-8. Interference of proPO activation in *M. sexta* plasma by RCL-derived peptides. (A) Ac-SVAFS-COO^- treated serpin-3ΔN (0.1 µg) or untreated serpin-3ΔN (0.1 µg) was incubated with 2 µl plasma at room temperature for 10 min, followed by addition of 2 µg *M. luteus* or sterile saline and further incubation for 10 min at room temperature. PO activities were measured by adding 2 mM dopamine. (B) 1 µl plasma was incubated with pre-dried Ac-SVAFS-NH_2 (5 nmol) or TFE in 50 mM sodium phosphate, pH 6.5 at room temperature for 1 h, followed by addition of 2 µg *M. luteus* or sterile saline and further incubation for 10 min at room temperature. PO activities were measured after adding 2 mM dopamine. The graphs represent results using plasma from four different larvae. One unit of PO activity is defined as 0.001 change of OD_{470} per minute. Data are means ± standard deviation (n=4). Results of statistical analysis (paired one-way ANOVA followed by Tukey's multiple comparison test, $P<0.05$) are indicated with different letters.

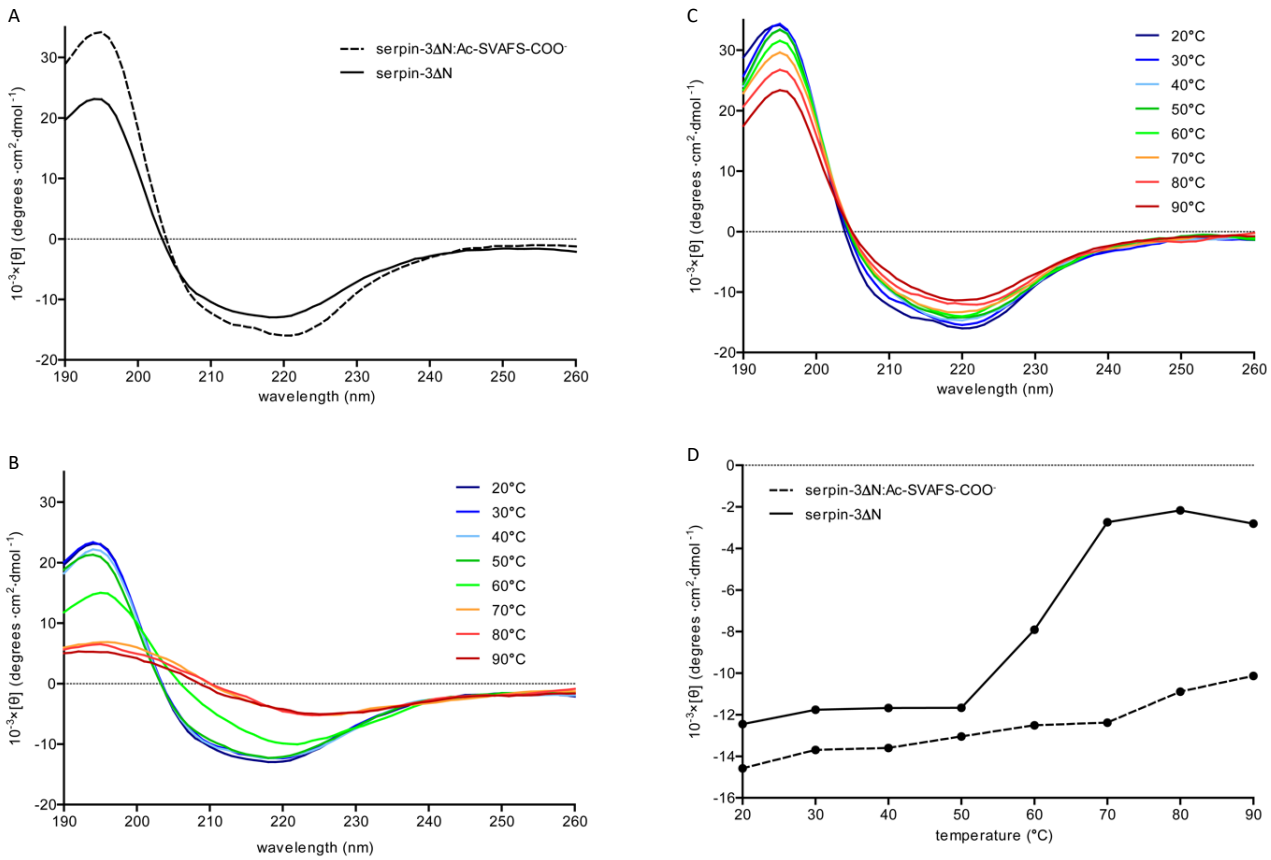

Figure 3-9. Circular dichroism of serpin-3ΔN and binary complex formed by serpin-3ΔN and Ac-SVAFS-COO$^-$.

CD spectra were measured with serpin-3ΔN and binary complex formed by serpin-3ΔN and Ac-SVAFS-COO$^-$ in 20 mM Tris, 10 mM NaCl, pH 8.0 at different temperatures. (A) CD spectra of serpin-3ΔN and binary complex at 20°C. (B) CD spectrum of serpin-3ΔN at different temperatures. (C) CD spectrum of binary complex formed by serpin-3ΔN and Ac-SVAFS-COO$^-$ at different temperatures. (D) Molar ellipticity of serpin-3ΔN and binary complex at 215 nm at different temperatures

References

Ambadapadi, S., G. Munuswamy-Ramanujam, D. Zheng, C. Sullivan, E. Dai, S. Morshed, B. McFadden, E. Feldman, M. Pinard & R. McKenna (2016) Reactive center loop (RCL) peptides derived from serpins display independent coagulation and immune modulating activities. *Journal of Biological Chemistry*, 291, 2874-2887.

An, C., A. Budd, M. R. Kanost & K. Michel (2011a) Characterization of a regulatory unit that controls melanization and affects longevity of mosquitoes. *Cellular and Molecular Life Sciences*, 68, 1929-1939.

An, C., S. Lovell, M. R. Kanost, K. P. Battaile & K. Michel (2011b) Crystal structure of native *Anopheles gambiae* serpin-2, a negative regulator of melanization in mosquitoes. *Proteins*, 79, 1999.

Björk, I., K. Ylinenjärvi, S. T. Olson & P. E. Bock (1992) Conversion of antithrombin from an inhibitor of thrombin to a substrate with reduced heparin affinity and enhanced conformational stability by binding of a tetradecapeptide corresponding to the P1 to P14 region of the putative reactive bond loop of the inhibitor. *Journal of Biological Chemistry*, 267, 1976-1982.

Carrell, R. & J. Travis (1985) α_1-Antitrypsin and the serpins: variation and countervariation. *Trends in biochemical sciences*, 10, 20-24.

Carrell, R. W., D. L. Evans & P. E. Stein (1991) Mobile reactive centre of serpins and the control of thrombosis. *Nature*, 353, 576.

Chang, W.-S. W., M. R. Wardell, D. A. Lomas & R. W. Carrell (1996) Probing serpin reactive-loop conformations by proteolytic cleavage. *Biochemical Journal*, 314, 647-653.

Chang, W. S. W., J. Whisstock, P. C. R. Hopkins, A. M. Lesk, R. W. Carrell & M. R. Wardell (1997) Importance of the release of strand 1C to the polymerization mechanism of inhibitory serpins. *Protein Science*, 6, 89-98.

Christen, J. M., Y. Hiromasa, C. An & M. R. Kanost (2012) Identification of plasma proteinase complexes with serpin-3 in *Manduca sexta*. *Insect biochemistry and molecular biology*, 42, 946-955.

D'Amico, S., J. A. Martial & I. Struman (2012) A peptide mimicking the C-terminal part of the reactive center loop induces the transition to the latent form of plasminogen activator inhibitor type-1. *FEBS letters*, 586, 686-692.

Eitzman, D. T., W. P. Fay, D. A. Lawrence, A. M. Francis-Chmura, J. D. Shore, S. T. Olson & D. Ginsburg (1995) Peptide-mediated inactivation of recombinant and platelet plasminogen activator inhibitor-1 *in vitro*. The *Journal of clinical investigation*, 95, 2416-2420.

Fitton, H. L., R. N. Pike, R. W. Carrell & W. S. W. Chang (1997) Mechanisms of antithrombin polymerisation and heparin activation probed by the insertion of synthetic reactive loop peptides. *Biological chemistry*, 378, 1059-1064.

Gettins, P. G. & S. T. Olson (2016) Inhibitory serpins. New insights into their folding, polymerization, regulation and clearance. *The Biochemical journal*, 473, 2273-2293.

Gooptu, B. & D. A. Lomas (2009) Conformational pathology of the serpins: themes, variations, and therapeutic strategies. *Annual Review of Biochemistry*, 78, 147-176.

Gorman, M. J., Y. Wang, H. Jiang & M. R. Kanost (2007) *Manduca sexta* hemolymph proteinase 21 activates prophenoloxidase-activating proteinase 3 in an insect innate immune response proteinase cascade. *Journal of Biological Chemistry*, 282, 11742-11749.

He, Y., X. Cao, S. Zhang, J. Rogers, S. Hartson & H. Jiang (2016) Changes in the plasma proteome of *Manduca sexta* Larvae in relation to the transcriptome variations after an immune challenge: evidence for high molecular weight immune complex formation. *Molecular & Cellular Proteomics*, 15, 1176-1187.

Irving, J. A., R. N. Pike, A. M. Lesk & J. C. Whisstock (2000) Phylogeny of the serpin superfamily: implications of patterns of amino acid conservation for structure and function. *Genome research*, 10, 1845-1864.

Irving, J. A., P. J. M. Steenbakkers, A. M. Lesk, H. J. M. Op den Camp, R. N. Pike & J. C. Whisstock (2002) Serpins in prokaryotes. *Molecular biology and evolution*, 19, 1881-1890.

Jankova, L., S. J. Harrop, D. N. Saunders, J. L. Andrews, K. C. Bertram, A. R. Gould, M. S. Baker & P. M. G. Curmi (2001) Crystal structure of the complex of plasminogen activator inhibitor 2 with a peptide mimicking the reactive center loop. *Journal of Biological Chemistry*, 276, 43374-43382.

Jendrny, C. & A. G. Beck-Sickinger. 2015. Peptides as modulators of serpin action. In *The Serpin Family*, 29-45. Springer.

Jiang, H., Y. Wang, X. Q. Yu, Y. Zhu & M. Kanost (2003) Prophenoloxidase-activating proteinase-3 (PAP-3) from *Manduca sexta* hemolymph: a clip-domain serine proteinase regulated by serpin-1J and serine proteinase homologs. *Insect biochemistry and molecular biology*, 33, 1049-1060.

Kanost, M. R. & M. J. Gorman (2008) Phenoloxidases in insect immunity. *Insect immunology*, 1, 69-96.

Kanost, M. R. & H. Jiang (2015) Clip-domain serine proteases as immune factors in insect hemolymph. *Current opinion in insect science*, 11, 47-55.

Kanost, M. R., H. Jiang & X. Q. Yu (2004) Innate immune responses of a lepidopteran insect, *Manduca sexta*. *Immunological reviews*, 198, 97-105.

Kanost, M. R., S. V. Prasad & M. A. Wells (1989) Primary structure of a member of the serpin superfamily of proteinase inhibitors from an insect, *Manduca sexta*. *The Journal of Biological Chemistry*, 264, 965-972.

Li, M., J. M. Christen, N. T. Dittmer, X. Cao, X. Zhang, H. Jiang & M. R. Kanost (2018) The *Manduca sexta* serpinome: analysis of serpin genes and proteins in the tobacco hornworm. *Insect biochemistry and molecular biology*, 102, 21-30.

Mach, H., D. B. Volkin, C. J. Burke & C. R. Middaugh. 1995. Ultraviolet absorption spectroscopy. In *Protein stability and folding*, 91-114. Springer.

Mahadeva, R., T. R. Dafforn, R. W. Carrell & D. A. Lomas (2002) 6-mer Peptide selectively anneals to a pathogenic serpin conformation and blocks polymerization: implications for the prevention of Z α_1-antitrypsin-related cirrhosis. *Journal of Biological Chemistry*, 277, 6771-6774.

Mast, A. E., J. J. Enghild & G. Salvesen (1992) Conformation of the reactive site loop of α_1-proteinase inhibitor probed by limited proteolysis. *Biochemistry*, 31, 2720-2728.

Meekins, D. A., M. R. Kanost & K. Michel. 2017. Serpins in arthropod biology. In *Seminars in cell & developmental biology*, 105-119. Elsevier.

Michel, K., A. Budd, S. Pinto, T. J. Gibson & F. C. Kafatos (2005) *Anopheles gambiae* SRPN2 facilitates midgut invasion by the malaria parasite Plasmodium berghei. *EMBO reports*, 6, 891-897.

Michel, K., C. Suwanchaichinda, I. Morlais, L. Lambrechts, A. Cohuet, P. H. Awono-Ambene, F. Simard, D. Fontenille, M. R. Kanost & F. C. Kafatos (2006) Increased melanizing activity in *Anopheles gambiae* does not affect development of *Plasmodium falciparum*. *Proceedings of the National Academy of Sciences of the United States of America*, 103, 16858-16863.

Pearce, M. C., R. N. Pike, A. M. Lesk & S. P. Bottomley. 2007. *Serpin conformations*. World Scientific.

Roberts, T. H. & J. Hejgaard (2008) Serpins in plants and green algae. *Functional & integrative genomics*, 8, 1-27.

Schulze, A. J., U. Baumann, S. Knof, E. Jaeger, R. Huber & C. B. Laurell (1990) Structural transition of α_1-antitrypsin by a peptide sequentially similar to β-strand s4A. *European journal of biochemistry*, 194, 51-56.

Schulze, A. J., P. W. Frohnert, R. A. Engh & R. Huber (1992) Evidence for the extent of insertion of the active site loop of intact α_1-proteinase inhibitor in β-sheet A. *Biochemistry*, 31, 7560-7565.

Shin, J. S. & M. H. Yu (2002) Kinetic dissection of α_1-antitrypsin inhibition mechanism. *Journal of Biological Chemistry*, 277, 11629-11635.

Silverman, G. A., P. I. Bird, R. W. Carrell, F. C. Church, P. B. Coughlin, P. G. Gettins, J. A. Irving, D. A. Lomas, C. J. Luke, R. W. Moyer, P. A. Pemberton, E. Remold-O'Donnell, G. S. Salvesen, J. Travis & J. C. Whisstock (2001) The serpins are an expanding superfamily of structurally similar but functionally diverse proteins. Evolution, mechanism of inhibition, novel functions, and a revised nomenclature. *The Journal of Biological Chemistry*, 276, 33293-33296.

Skinner, R., W. S. W. Chang, L. Jin, X. Pei, J. A. Huntington, J. P. Abrahams, R. W. Carrell & D. A. Lomas (1998) Implications for function and therapy of a 2.9 Å structure of binary-complexed antithrombin. *Journal of Molecular Biology*, 283, 9-14.

Terenius, O., A. Papanicolaou, J. S. Garbutt, I. Eleftherianos, H. Huvenne, S. Kanginakudru, M. Albrechtsen, C. An, J. L. Aymeric & A. Barthel (2011) RNA interference in Lepidoptera: an overview of successful and unsuccessful studies and implications for experimental design. *Journal of insect physiology*, 57, 231-245.

Turner, P. C., P. F. McAuliffe, A. L. MacNeill & R. W. Moyer (2007) New lessons from poxvirus serpins. *Molecular and Cellular Aspects of the Serpinopathies and Disorders in Serpin Activity*, 163.

Van De Craen, B., P. J. Declerck & A. Gils (2012) The biochemistry, physiology and pathological roles of PAI-1 and the requirements for PAI-1 inhibition *in vivo*. *Thrombosis research*, 130, 576-585.

Wang, Y., H. Jiang & M. R. Kanost (2001) Expression and purification of *Manduca sexta* prophenoloxidase-activating proteinase precursor (proPAP) from baculovirus-infected insect cells. *Protein expression and purification*, 23, 328-337.

Wang, Y., Z. Lu & H. Jiang (2014) *Manduca sexta* proprophenoloxidase activating proteinase-3 (PAP3) stimulates melanization by activating proPAP3, proSPHs, and proPOs. *Insect biochemistry and molecular biology*, 50, 82-91.

Xue, Y., P. Björquist, T. Inghardt, M. Linschoten, D. Musil, L. Sjölin & J. Deinum (1998) Interfering with the inhibitory mechanism of serpins: crystal structure of a complex formed between cleaved plasminogen activator inhibitor type 1 and a reactive-centre loop peptide. *Structure*, 6, 627-636.

Yang, F., Y. Wang, N. Sumathipala, X. Cao, M. R. Kanost & H. Jiang (2018) *Manduca sexta* serpin-12 controls the prophenoloxidase activation system in larval hemolymph. *Insect biochemistry and molecular biology*.

Yang, J. & Y. Zhang (2015) I-TASSER server: new development for protein structure and function predictions. *Nucleic Acids Research*, 43, W174-W181.

Zhang, X., D. A. Meekins, C. An, M. Zolkiewski, K. P. Battaile, M. R. Kanost, S. Lovell & K. Michel (2015) Structural and inhibitory effects of hinge loop mutagenesis in serpin-2 from the malaria vector *Anopheles gambiae*. *Journal of Biological Chemistry*, 290, 2946-2956.

Zhou, A., P. E. Stein, J. A. Huntington, P. Sivasothy, D. A. Lomas & R. W. Carrell (2004) How small peptides block and reverse serpin polymerisation. *Journal of Molecular Biology*, 342, 931-941.

Zhu, Y., Y. Wang, M. J. Gorman, H. Jiang & M. R. Kanost (2003) *Manduca sexta* serpin-3 regulates prophenoloxidase activation in response to infection by inhibiting prophenoloxidase-activating proteinases. *The Journal of Biological Chemistry*, 278, 46556-46564.

Chapter 4 - Characterization of Diapausin, an Antifungal Peptide from *Manduca sexta*

Introduction

Production of antimicrobial peptides (AMPs) is an essential strategy for multicellular organisms, including insects, to combat infectious bacteria, fungi and parasites (Zasloff, 2002). AMPs found in insects are typically synthesized in fat body in response to foreign microbes and secreted into hemolymph (Kanost et al., 2004). They are diverse in size and molecular structure, but a majority of them cause damage to pathogens by disrupting the cell membrane and subsequent leakage of cell contents (Rautenbach et al., 2016). Because of this mode of action, some AMPs are active against both bacteria and fungi, such as defensins from mammalians (Ganz, 2003), plants (Thomma et al., 2002) and insects (Yi et al., 2014), histatins from primates (Kavanagh and Dowd, 2004), LL-37 from mammals (Dürr et al., 2006), cecropins from insects (Yi et al., 2014).

Antifungal peptides refer to those AMPs with fungistatic or fungicidal activity. The fungal cell wall can be a target for some antifungal peptides, such as rabbit defensin NP-1 targeting chitin (Levitz et al., 1986), tobacco defensin NaD1 binding to mannoproteins on the cell wall (van der Weerden et al., 2010), and human histatin-5 binding to *Candida albicans* cell wall protein Ssa1/2 (Li et al., 2003). Cell wall synthesis-related enzymes localized at the membrane can be the targets as well, such as β-1,3 glucan synthase targeted by a family of cyclic lipopeptides, echinocandins (Cappelletty and Eiselstein-McKitrick, 2007). Glycerophospholipids in the cell membrane interact with a group of antifungal peptides with single linear α-helical structure, such as LL-37 from mammals (den Hertog et al., 2005) and cecropins from *Hyalophora cecropia* (De Lucca et al., 1998a). Specific lipids on the cell membrane are preferred for some antifungal peptides to bind, such as phosphatidylinositol(4,5)-bisphosphate (PIP_2) targeted by NaD1 from tobacco and TPP3 from tomato (Payne et al., 2016; Baxter et al., 2015).

Several antifungal peptides have been isolated from insects and their properties were characterized. The only described fungi-specific peptides from insects, lacking antibacterial activity, are drosomycin from *Drosophila melanogaster* (Landon et al., 1997), heliomicin from

Heliothis virescens (Lamberty et al., 1999), gallerimycin from *Galleria mellonella* (Schuhmann et al., 2003), defensin from *G. mellonella* (Lee et al., 2004), defensin-like peptide (Btdef) from *Bemisia tabaci* (Wang et al., 2013), and diapausin-1 from *Manduca sexta*. Drosomycin is composed of an α-helix and three β-strands, stabilized by four pairs of disulfide bonds (Landon et al., 1997) and has potent antifungal activity, with IC_{50} 0.9-12 μM against various fungi (Tian et al., 2008). Diapausin was first discovered in *Gastrophysa atrocyanea* (leaf beetle) hemolymph as diapause-specific peptide (DSP), composed of 2 α-helices and 3 β-strands stabilized by 3 pairs of disulfide bonds (Kouno et al., 2007). DSP was observed to inhibit the growth of a dermatophytic fungus *Trichophyton rubrum* and an entomopathogenic fungus *Beauveria bassiana* (Tanaka et al., 2003). It was proposed that DSP might be a Ca^{2+} channel blocker based on experimental and structural evidence. DSP reduced Ca^{2+} influx into bovine adrenal chromaffin cells in a dose-dependent manner (Tanaka et al., 2003). NMR structure of DSP revealed a similar surface residue distribution with ω-conotoxins, which inhibit N-type voltage-dependent calcium channels (Kouno et al., 2007).

Diapausin-1 was isolated from *M. sexta* hemolymph, demonstrating antifungal activity against *Saccharomyces cerevisiae*, *Magnaporthe oryzae*, *Fusarium culmorum* and *Fusarium graminearum*, with no antibacterial activity (Al Souhail et al., 2016). Germination tubes of *M. oryzae* became curled and cockscrew-like in the presence of 15 μM diapausin-1. Hyphal growth of *Fusarium* was reduced and morphologically altered. Diapausin-1 mRNA levels significantly increased (>100-fold) after larvae were injected with *S. cerevisiae*, suggesting its protective role during fungal infection (Al Souhail et al., 2016). Genome analysis of *M. sexta* annotated 14 diapausin genes with 65-100% amino acid sequence identity (He et al., 2015).

To further investigate the diapausin family in *M. sexta*, regarding antifungal activity and modes of action, we expressed and purified recombinant diapausin-1 and diapausin-2. They were tested against *S. cerevisiae*, *Candida*, a genus of yeast that causes human fungal infections, as well as an entomopathogenic fungus, *B. bassiana*. Diapausin-1 was shown to bind to β-1,3-glucan on the yeast cell wall and to interrupt cell separation after cell division, leading to cell clusters.

Materials and Methods

I-TASSER models of diapausin-1 and diapausin-2

Full sequences of diapausin-1(INNWVRVPPCDQVCSRSNPEKDECCRAHGHAFHAHCNGGMNCYRR) and diapausin-2 (VRVPPCDEVCNRIPRERDECCRAHGHSGYSSCSGGMYCY) were uploaded to I-TASSER server (https://zhanglab.ccmb.med.umich.edu/I-TASSER/) with default settings for structure prediction (Yang and Zhang, 2015).

Expression and purification of recombinant diapausin-1 and diapausin-2

The plasmid pHis-GB1 containing full-length mature diapausin-1 or diapausin-2 was kindly provided by Dr. Bindiya Sachdev and used to transfect *Escherichia coli* strain Rosetta-gami (Novagen). Expression of fusion proteins 6His-GB1-diapausin-1 and 6His-GB1-diapausin-2 was induced in 1 L LB medium at mid-log stage by 0.4 mM IPTG at 37°C for 4 h. Bacteria were then pelleted by centrifugation and lysed by sonication in 20 ml cold 300 mM NaCl, 10mM imidazole, 50 mM sodium phosphate, pH 8.0 at 4°C. After centrifugation, 17 ml supernatant containing fusion 6His-GB1-diapausin-1 was incubated with 4.25 ml NiNTA beads and 12 ml supernatant containing fusion 6His-GB1-diapausin-2 was incubated with 3 ml NiNTA beads at 4°C for 1 h. The mixture was then applied to a column (1×7 cm), and after washing with buffer (300 mM NaCl, 20mM imidazole, 50 mM sodium phosphate, pH 8.0), 6His-GB1-diapausin-1 or 6His-GB1-diapausin-2 were eluted with the same buffer supplemented with 250 mM imidazole. Fractions containing 6His-GB1-diapausin-1 or 6His-GB1-diapausin-2 were dialyzed against 4 L of 20 mM Tris-HCl, 20 mM NaCl, pH 8.0 three times at 4°C. The amino-terminal 6His-GB1 tag was removed by incubating the fusion proteins with Tobacco Etch Virus (TEV) protease (from Dr. Brian Geisbrecht) at 800:1 (fusion protein:TEV) mass ratio for 2 or 7 days at 30°C. To separate the 6His-GB1 tag from the mature diapausin-1 or diapausin-2, the sample was applied to an UnoQ1 column (7×35 mm, Bio-Rad) and eluted with a linear gradient of 20-1000 mM NaCl in 20mM Tris, pH 8.0. Fractions containing mature diapausin-1 or diapausin-2 were pooled, concentrated using Pall Corp Microsep Advance device 1K, and quantified. MALDI-TOF was also used for confirmation of the correct masses of diapausin-1 and diapausin-2 on a

Bruker Ultraflex II instrument (Billerica, MA). Recombinant diapausins used for antifungal assays were sterilized using SPIN-X centrifuge tube filters (0.22 μm).

SDS-PAGE and protein concentration assay

Protein samples analyzed by SDS polyacrylamide gel electrophoresis were mixed with 2× or 6×SDS loading buffer (supplemented with β-mercaptoethanol) followed by heating at 95°C for 5 min. Samples were loaded into wells of 4-12% Bis-Tris NuPAGE gels and separated by electrophoresis using MES buffer. The gels were stained using Instant Blue (Expedeon). Protein concentration was measured using Coomassie Plus Protein Assay Reagent (Thermo Scientific), with bovine serum albumin (BSA) as a standard.

Antifungal assay of diapausin-1 and diapausin-2 against *Saccharomyces cerevisiae*

A single colony of *S. cerevisiae* wild type diploid strain BY4743 was inoculated into 3 ml YPD medium and cultured overnight with shaking at 200 rpm at 30°C. Then the overnight culture was diluted with YPD medium to OD_{600}=0.1. Sterile recombinant diapausin-1 (9.4 μl/6.3 μl, 1.27 mM) or diapausin-2 (2.8 μl/1.9 μl, 4.23 mM) was added to 200 μl of yeast sample to a final concentration of 60 μM or 40 μM in a sterile 96-well plate, followed by 2-fold serial dilution, resulting in 60, 40, 30, 20, 15, 10, 7.5, 5, 2.5 μM final concentration of diapausin-1/2. The plate was covered by Breathe-Easy sealing membrane (Sigma) and cultured at 30°C for 8 h, followed by measurement of OD_{600} using an Epoch2 microplate reader (BioTek).

Spot assay of diapausin-1 against *S. cerevisiae*

An overnight culture of *S. cerevisiae* wildtype BY4743 cells was diluted to OD_{600}=0.1 in YPD medium, followed by incubation with 0, 40, 80, 120, 160, or 200 μM of sterile diapausin-1 at 30°C. After 2, 4, 6, 8, 10 and 20 h, a 5 μl of sample was collected from each treatment and serially diluted 5-fold. Then 2 μl from each dilution was spotted onto a YPD agar plate, followed by incubation at 30°C for 2 days.

Time course microscopic observations of *S. cerevisiae* treated by diapausin-1

An overnight culture of *S. cerevisiae* wild type BY4743 cells was diluted to OD_{600}=1.0 in YPD medium, followed by mixing with 19 μl of cell suspension with 1 μl sterile diapausin-1 (1.67 mM) or 1 μl sterile deionized water, and incubation at 30°C. After 0, 1, 2, 3 and 4 h, a 2 μl

sample from treatment and control was collected and applied to a 12-well glass slide. Then the cells were examined using a differential interference contrast microscope (ZEISS 30 B) and imaged by camera (AxioCam MRc5). Cells were categorized into four groups: single (a cell without a bud), double (a mother cell with a bud), triple (a mother cell with probably two buds) and cluster (with four or more cells stuck to each other). The number of cells in each group was counted (n>60).

Antifungal assay of diapausin-1 against *Beauveria bassiana*

B. bassiana conidia were kindly provided by Patil Tawidian and Dr. Kristin Michel from the Division of Biology, KSU. Conidia were suspended in sterile medium (2% yeast extract, 2% sucrose) to 3.5×10^4/ml. Then 24 μl of conidia suspension was mixed with 16 μl of 5 mM sterile diapausin-1 in a 96-well plate, followed by 2-fold serial dilution, resulting in 400, 200, 100, 50, 25, and 12.5 μM final concentration of diapausin-1 and included a control with no diapausin-1. The plate was covered by Breathe-Easy sealing membrane (Sigma) and cultured at 30°C for 8 h, followed by examination and imaging using an inverted phase contrast microscope. Lengths of the germination tubes were measured by using Image J (Abràmoff et al., 2004). A conidium with a germination tube more than two times longer than the conidial diameter was defined as germinated, otherwise as non-germinated.

Antifungal assay of diapausin-1 and diapausin-2 against *Candida*

C. albicans and *C. krusei* were cultured overnight in YPD medium at 30°C, followed by dilution to 1×10^6 cells/ml in YPD medium. Sterile diapausin-1 (40 μl, 1.44 mM) or diapausin-2 (40 μl, 2.52 mM) were added to 200 μl cell suspension in a 96-well plate to a final concentration of 240 μM and 420 μM respectively, followed by 2-fold serial dilution. The plate was incubated at 30°C for 8 h, and OD_{600} was measured using an Epoch2 microplate reader (BioTek).

Staining and visualization of *C. albicans* treated by diapausin-1

C. albicans was cultured overnight in YPD medium at 30°C, followed by dilution to 1×10^6/ml in YPD medium. In a 96-well plate, sterile diapausin-1 (2.2 μl, 5.45 mM) was added to 100 μl cell suspension to a final concentration of 120 μM. Sterile deionized water (2.2 μl) was added as control, followed by incubation at 30°C. After 8 h, the cells were transferred to 1.5 ml centrifuge tubes and fixed in 3.7 % formaldehyde for 30 min with agitation at room temperature,

followed by centrifugation at 4,000 rpm for 5 min and washing twice in 600 μl PBS. Then the cells were stained in 0.1 mg/ml Alexa Fluor® 594 conjugate of Concanavalin A (Invitrogen) for 15 min at room temperature in the dark, followed by washing twice in 600 μl PBS. The pellet was resuspended in 400 μl PBS, and 2 μl cell suspension was mounted on one well in a 12-well glass slide with fluoromount-G (Southern Biotech). Examination of fluorescence was performed using an LSM airyscan 880 microscope.

Labeling of diapausin-1 with FITC

Recombinant diapausin-1 (500 μl, 11 mg/ml) or BSA (500 μl, 11 mg/ml) were incubated with 100 μl of 10 mg/ml fluorescein isothiocyanate (FITC, Sigma) in 0.1 M sodium bicarbonate, pH 9.0 for 1 h at room temperature in the dark. Sephadex™ G-25 (Amersham Bioscience AB) was swelled in water and packed in an Econo column (1×7 cm). The protein-FITC was applied to the column and 1 ml fractions were collected. The fractions were analyzed by measuring OD_{280} and OD_{494}. The concentration of the labeled protein and degree of labeling were calculated according to the manufacturer's manual.

Staining and visualization of *S. cerevisiae* by ConA-Alexa Fluor 594, calcofluor white M2R, and FITC-diapausin-1

This experiment was based on the protocol from Okada and Ohya (Okada and Ohya, 2016) with modifications. An overnight culture of *S. cerevisiae* wildtype BY4743 cells was diluted to OD_{600}=1.0 in YPD medium. The cell suspension (38 μl) was incubated with 2 μl sterile deionized water/FITC-BSA (11mg/ml)/FITC-diapausin-1 (11mg/ml) at 30°C. After 2 h, the cells were collected by centrifugation and washed twice in sterile deionized water. The cells were resuspended and incubated with sterile 2.5 mg/ml fluorescent brightener 28 (synonym: calcofluor white M2R; Sigma) at room temperature for 10 min in the dark. The cells were collected by centrifugation, washed twice in sterile PBS and incubated with sterile 0.1 mg/ml Alexa Fluor® 594 conjugate of Concanavalin A (Invitrogen) for 10 min at room temperature in the dark, followed by washing twice in sterile PBS. Cells were resuspended in 40 μl sterile PBS and examined in 35 mm dishes (MatTek) using an LSM airyscan 880 microscope.

Cell wall components pull-down assay

Curdlan (from *Alcaligenes faecalis*; Sigma), zymosan (from *Saccharomyces cerevisiae*; Sigma), chitin (from shrimp shell; Sigma), starch (from wheat; MGP, Midsol 50), and peptidoglycan (from *Micrococcus luteus*; Sigma) were each suspended in 10 mM sodium phosphate, pH 7.4 to a final concentration of 5 mg/ml. Each polysaccharide (20 μl) was incubated with 0.5 μg/ml recombinant diapausin-1 or diapausin-2 at room temperature for 10 min, followed by centrifugation at 14,000 rpm for 5 min and collection of supernatant as unbound fraction. Pellets were washed with 50 μl buffer (10 mM sodium phosphate, pH 7.4), followed by centrifugation at 14,000 rpm for 5 min and collection of supernatant. Each pellet was mixed with 20 μl 2×SDS loading buffer supplemented with β-mercaptoethanol and heated at 95°C for 5 min, followed by centrifugation at 14,000 rpm for 5 min and collection of supernatant as elution fraction. Unbound (20 μl), wash (20 μl) and elution fractions (20 μl) were analyzed with SDS-PAGE as described above.

Morphological changes of *S. cerevisiae* induced by diapausin-1

This experiment was based on the protocol from Okada and Ohya (Okada and Ohya, 2016) with modifications. An overnight culture of *S. cerevisiae* wildtype BY4741 cells was diluted to OD_{600}=1.0 in YPD medium. Cell suspension (19 μl) was incubated with 1 μl sterile recombinant diapausin-1 (1.67 mM) or 1 μl sterile deionized water at 30°C for 2 h, followed by fixation in 3.7% formaldehyde at room temperature for 30 min. The cells were collected by centrifugation and washed twice in sterile PBS. Then the pellet was resuspended and incubated with 0.1 mg/ml Alexa Fluor® 594 conjugate of Concanavalin A (Invitrogen) for 10 min at room temperature in the dark, followed by washing twice in sterile PBS. Cells were resuspended in 40 μl sterile PBS, and 2 μl cell suspension was mounted in one well in a 12-well glass slide with fluoromount-G (Southern Biotech). Examination of fluorescence was performed by using an LSM airyscan 880 microscope. Pictures (696×520 pixel size) were processed to grayscale (256 gradation) and 8- bit depth using Zen and Photoshop. CalMorph 2.0 was used to quantify the parameters relevant to cell shape (Ohya et al., 2005). Triplicates were performed with more than 490 cells being analyzed in each replicate. Wilcoxon rank-sum test (synonym: Mann–Whitney *U* test) (Nachar 2008) was performed to test whether there was a significant difference between control and diapausin-1-treated yeast cells regarding each parameter given by CalMorph. Violin

plots, which display the kernel density along the vertical axis, were made by jjplot for those parameters which had significant differences ($p<0.05$) between control and diapausin-1 treatment.

Search of single gene deletion mutants with "clover" phenotype

Diapausin-1disrupted the *S. cerevisiae* daughter cell separation after cell division, resulting in cell clusters after a few cell cycles. This "clover" phenotype was observed frequently after 2 h (1-2 cell cycles) treatment with diapausin-1, so we were seeking to find yeast mutants with similar "clover" phenotype. Saccharomyces Cerevisiae Morphological Database (https://scmd.gi.k.u-tokyo.ac.jp/datamine/) provides photos from 4782 haploid MATa strains with single non-essential gene deletions. Photos of *S. cerevisiae* mutants with deleted genes that are required for cell wall polymer synthesis/remodeling and in cell wall relevant Gene Ontology (GO) terms (GO:0006075, (1->3)-beta-D-glucan biosynthetic process; GO: 0005199, structural constituent of cell wall; GO: 0042546, cell wall biogenesis; GO: 0097271, protein localization to bud neck; GO: 0070880, fungal-type cell wall beta-glucan biosynthetic process; GO: 0009986, cell surface; GO: 0009272, fungal-type cell wall biogenesis; GO: 0031505, fungal-type cell wall organization) were screened visually for a high proportion of "clover" cell clusters.

Results

Diapausin-1 and diapausin-2 homology models

To examine a predicted three-dimensional structure of *M. sexta* diapausins, we produced homology models for diapausin-1 and diapausin-2. The top threading templates used by I-TASSER to model diapausin-1 and diapausin-2 was diapausin-specific peptide (DSP) (PDB ID: 2E2F) from *Gastrophysa atrocyanea*, which also belongs to diapausin family of antimicrobial peptides (Kouno et al., 2007; Tanaka et al., 2003). The homology models of diapausin-1 and diapausin-2 have three disulfide bonds to stabilize the compact structure comprised of two α-helices and two β-strands (Fig. 4-1A). The arrangement of the disulfide bonds is consistent with that in GaDSP (Kouno et al., 2007), but different from defensins or drosomycin (Yi et al., 2014; Landon et al., 1997). Diapausin-1 has four more neutral amino acid residues at the amino-terminus and two more arginines at the carboxyl-terminus compared to diapausin-2 (Fig. 4-1B).

Expression and purification of diapausin-1 and diapausin-2

Recombinant diapausin-1 and diapausin-2 were expressed with an amino-terminal 6His-GB1 tag, which was removed by TEV protease after NiNTA chromatography. The trials in small batches (20 μl) of TEV processing took 1-2 days to show complete cleavage between the 6His-GB1 tag and diapausin. However, complete processing of 6His-GB1-diapausin-2 with TEV in large batches (1 ml) required 7 days. Mass spectrometry indicated the actual cleavage site on 6His-GB1-diapausin-2 during TEV processing was 3 residues away from expected site (Fig. 4-2A, Fig. C-1). This unexpected cleavage shift might be caused by contaminating proteases which were not successfully removed during NiNTA column and the long reaction time. The fusion 6His-GB1-diapausin-1 was properly processed by TEV according to MS data (Fig 4-2A, Fig. C-1). I used NiNTA chromatography attempting to retain the 6His-GB1 tag and collect diapausins after TEV processing, but the tag did not bind to column. Unexpected protease processing might have occurred to 6His-GB1 tag by removing 6His, resulting in reduced affinity to the NiNTA column. Therefore, a UnoQ1 ion exchange column was utilized for separating the tag from diapausins (Fig 4-2B). The yield of recombinant diapausin-1 was 4.5 mg, and diapausin-2 was 0.37 mg from 1 L bacterial culture.

Antifungal activities of diapausins against *S. cerevisiae, B. bassiana* and *Candida*

Recombinant diapausin-1 and diapausin-2 exhibited antifungal activity against a *S. cerevisiae* wildtype strain in a dose dependent manner, with IC_{50} of 30 μM and 60 μM, respectively based on optical density measurement (Fig. 4-3A). A colony spot assay was performed with *S. cerevisiae* after 2, 4, 6, 8, 10 and 20 h treatment with recombinant diapausin-1 at various concentrations, as well as 0 h at 0 μM diapausin-1 as control (Fig. 4-3B). All treatment samples demonstrated a comparable or higher colony densities on the plate compared to control (0 h at 0 μM diapausin-1). The treatment of *S. cerevisiae* with diapausin-1 apparently caused the inhibition of cell growth, rather than cell death.

It was previously reported that diapausin-1 did not have antifungal activity against *B. bassiana*, an entomopathogenic fungus (Al Souhail et al., 2016). But this result may have been due to the limitation of the assay using measurement by optical density. Therefore, I used measurement of the germination tube length for anti-*B. bassiana* assay (Fig. 4-4). 82% of conidia germinated in the absence of diapausin-1 after 8 h, but germination was reduced in a dose-

dependent manner in the presence of diapausin-1 (Fig. 4-4). Only 32% conidia were germinated in the medium supplemented with 200 μM diapausin-1 after 8 h. The growth of germination tubes was impaired by diapausin-1 as well. The median length of germination tubes reduced from 16 μm to 7 μm when concentration of diapasuin-1 increased from 0 μM to 200 μM (Fig. 4-4).

Antifungal activity of diapausins was also determined against *C. albicans* and *C. krusei*, which are human pathogenic fungi. In YPD medium, the growth of *C. albicans* and *C. krusei* was inhibited by recombinant diapausin-1 with IC_{50} of 60 μM and 20 μM respectively (Fig. 4-5). Inhibitory activity of recombinant diapausin-2 against *C. albicans* and *C. krusei* was less potent than that of diapausin-1, with IC_{50} of 240 μM and >600 μM respectively (Fig. 4-5).

Diapausin-1 binds to the *S. cerevisiae* cell surface, likely to β-1,3-glucan

Recombinant diapausin-1was labeled with FITC and incubated with *S. cerevisiae*. Calcofluor white M2R and Alexa Fluor® 594 conjugate of Con-A were used to stain chitin and mannoproteins, respectively on the cell wall (Fig. 4-6). FITC-diapausin-1 only appeared at the surface of the yeast cells, with an even appearance similar to mannoprotein labeling. In contrast, chitin appeared mostly at bud necks of dividing yeast. FITC-BSA as a control did not label the yeast (Fig. 4-6). This result indicates that diapausin-1 likely binds to a component on the surface of yeast cells and does not enter the cells.

To further investigate the potential molecule on the cell wall that might bind to diapausin, a pull-down assay was performed to test binding of diapausin to different fungal cell wall components, bacterial peptidoglycan, and starch as a polysaccharide control (Fig. 4-7, Fig. C-2). Recombinant diapausin-1 was present predominantly in the unbound fraction from chitin (β-1,4-N-acetylglucosamine), starch (α-1,4-glucose with α-1,6 branches), and peptidoglycan (alternating N-acetylglucosamine and N-acetylmuramic acid with peptide chain crosslinking), indicating little affinity of diapausin-1 to those polysaccharides or peptidoglycan (Fig. 4-7). In contrast, curdlan (β-1,3-glucan) from *Alcaligenes faecalis* and zymosan (β-1,3-glucan) from *S. cerevisiae* retained diapausin-1 until elution with SDS (Fig. 4-7). Recombinant diapausin-2 exhibited the same results (Fig. C-2). These results suggest that diapausins bind specifically to β-1,3-glucans in fungal cell walls. We also intended to test β-1,3-glucan as the target of diapausin-1 by using mutants of *FKS1*, a gene encoding β-1,3-glucan synthase catalytic subunit (Nogami

and Ohya, 2009). However, the growth of both homozygous *fks1/fks1* and heterozygous *FKS1/fks1* yeast was still inhibited by 80 μM diapausin-1 after 24 h (Fig. C-3), probably due to the presence of β-1,3-glucan synthesized by redundant homologous genes *FKS2* and *FKS3*.

Failure of cell separation after cell division caused by diapausin-1

S. cerevisiae yeast cells were incubated with recombinant diapausin-1 and examined using differential interference contrast (DIC) microscopy every hour. Control yeast cells in YPD medium are rich in double-cell form with a mother cell and a bud (>60%), which is consistent with proportions of double-cell appearance in the active cell cycle (Hartwell 1974). In contrast, after 1 h incubation with diapausin-1, a triple-cell form was frequently seen, and after 2 h cell clusters started to dominate (Fig. 4-8). After incubation with 80 μM diapausin-1 for 4 h, nearly 90% of yeast cells were in cell clusters. In contrast, yeast cells did not display prevalent abnormal triple-cell form or clumps when treated by diapausin-1 in YP medium, which limits the cell growth due to lack of carbon source (Fig. C-4). Recombinant diapausin-1 was also incubated with *S. cerevisiae* strain GFY-42 with mCherry-labeled Cdc10p, which is one of the septins mediating cytokinesis and cell septation (Finnigan et al., 2015). The control in absence of diapausin-1 had typical dividing cells, with mCherry-Cdc10p localized at the bud neck between a mother cell and a budding daughter cell (Fig. C-5). However, diapausin-1 treatment caused a frequent triple-cell form with a single mCherry-Cdc10p labeled septum between two of the cells (Fig. C-5), implying no concurrence of the cell cycle in the triple-cell form. These observations verified that the appearance of the triple-cell form and cell clusters was the consequence of failed cell separation after completion of cytokinesis. Cell clusters were also observed in *C. albicans* treated with diapausin-1, as well as abnormal cell swelling (Fig. 4-9), which is often seen with drugs affecting the cell wall (Okada et al., 2014).

Morphological changes of *S. cerevisiae* caused by diapausin-1

Phenotypic analysis was carried out on control and diapausin-1-treated *S. cerevisiae* (BY4741) cells by utilizing CalMorph, a software package for quantification of yeast cell morphology (Fig. 4-10) (Ohya et al., 2005). Parameters describing mother cell, daughter cell and the overall cell shape were output for every individual cell (Table 4-1, Fig. C-6). Cells in control and diapausin-1 treatment had significant differences regarding 20/24 parameters. In mother cells, diapausin-1 treatment caused a longer long axis, shorter short axis and less elliptical shape

(Fig. 4-11A). In daughter cells, the long axis was shorter, short axis was longer and overall size was smaller in the presence of diapausin-1 (Fig. 4-11B). The ratio of daughter cell size to mother cell size was decreased, and the neck was wider in diapausin treatment compared with control (Fig. 4-11C). Overall, the morphometric analysis revealed that diapausin-1 caused appearance of an elongated mother cell with a flattened bud and wider neck, as well as less elliptical shape (Fig. 4-11D).

We performed morphological comparison of diapausin-1-treated *S. cerevisiae* with single gene deletion mutants in the Saccharomyces Cerevisiae Morphological Database (SCMD), aiming to find mutants with similar morphology, which might provide hints of diapausin-1 mode of action. However, not much valuable information resulted from this method (data not shown). This strategy was originally developed to screen target genes of antifungal drugs with no evidence of modes of action, based on correlation between morphological phenotypes and gene functions (Ohya et al., 2005). Since we were aware that diapausin-1 interacts with the cell surface without penetrating into the cell cytosol, the genes which are involved in cell wall biogenesis and maintenance are of interest in the study of the mode of action of diapausin-1. Considering the observation of cell clusters caused by diapausin-1, I screened by visual inspection of available micrographs the mutants deficient in cell-wall associated genes for those exhibiting triple-cell forms ("clover-like") (Table 4-2). Additionally, Pearson's chi-square test indicated SWA2, SWI4 and GUP1 with the similar bud size distribution in diapasuin-1-treated yeast cells (Table 4-3). Of note, these three mutants also display frequent triple-cell forms.

Discussion

In response to invading bacteria, fungi, and parasites in the hemolymph, insects transduce the message to nuclei and trigger the synthesis of AMPs as effectors to eliminate foreign microbes (Yi et al., 2014). Most insect AMPs were characterized with antibacterial activity, while some of them also have antifungal activity (Faruck et al., 2016). Only a few AMPs were previously reported to have fungi-specific activity (Landon et al., 1997; Lamberty et al., 1999; Schuhmann et al., 2003; Lee et al., 2004; Al Souhail et al., 2016; Wang et al., 2013). These antifungal specific peptides all have cysteine-stabilized alpha beta structure (CSαβ). *Galleria* defensin, gallerimycin, heliomycin and Btdef have a conserved defensin structure composed of one α-helix and an antiparallel β-sheet, with six cysteines forming three disulfide bridges as

follows: Cys (1)-Cys (4), Cys (2)-Cys (5) and Cys (3)-Cys (6) (Lamberty et al., 1999; Schuhmann et al., 2003; Lee et al., 2004). Drosomycin contains eight cysteines with four disulfide bonds, Cys (1)-Cys (8), Cys (5)-Cys (5), Cys (3)-Cys (6), and Cys (4)-Cys (7) (Landon et al., 1997). Based on GaDSP structure (Kouno et al., 2007), *M. sexta* diapausins were predicted to have a disulfide array as following: Cys (1)-Cys (3), Cys (2)-Cys (5) and Cys (4)-Cys (6), a topology different from the CSαβ structures mentioned above (Fig. 4-1).

Antifungal activity of recombinant diapausins against *S. cerevisiae* and *Candida* species was measured in YPD growth medium and expressed as IC_{50}. Recombinant diapausin-1 was more potent than diapausin-2 against Saccharomycetes with IC_{50} of 20-60 μM (Fig. 4-3, 4-5), a higher concentration than some anti-Saccharomycetes peptides. Heliomicin has minimun inhibitory concentration (MIC) of 2.5-5 μM against *C. albicans* and *C. neoformans* (Lamberty et al., 1999), drosomycins have IC_{50} of 1.5-12 μM against *S. cerevisiae* and *Geotrichum candidum* (Fehlbaum et al., 1994; Tian et al., 2008), *Galleria* defensin has MIC of 1.6-50 μM against *C. albicans, G. candidum* and *C. neoformans* (Lee et al., 2004). Btdef has MIC of 1.9-7.6 μM against *C. albicans* and *Pichia pastoris* (Wang et al., 2013). Heliomicin and gallerimycin did not show any inhibitory activity against *S. cerevisiae* up to 50 μM (Lamberty et al., 1999; Lee et al., 2004).

Previously it was thought that diapausin-1 did not have activity against *B. bassiana*, an entomopathogenic fungus (Al Souhail et al., 2016). But this was probably due to the limitation of measurement by optical density as an assay. Therefore, I measured germination ratio and length of germination tubes of *B. bassiana* and found that recombinant diapausin-1 inhibited the germination and growth of germination tubes (Fig. 4-4). Btdef showed strong activity against *B. bassiana* with IC_{50} of 0.48 μM and germination rate was 0% after 24 h incubation with 0.96 μM Btdef (Wang et al., 2013). In contrast, diapausin-1 demonstrated less potency against *B. bassiana* with 31% germination rate caused by 200 μM diapausin-1 (Fig. 4-4).

Diapausin-1 showed activity against fungi tested in this work, but did not show evidence of fungi killing (Fig. 4-3). Viability of blastospores from the entomopathogenic fungi *Metarhizium anistropliae* was 55% after the treatment of 50 μM Btdef (Schuhmann et al., 2003). But viability data is lacking for other fungi-specific AMPs. Those peptides with both antibacterial and antifungal activity likely cause cell death by interrupting the integrity of the cell membrane and subsequent cell leakage (Faruck et al., 2016). The observation of cell growth

inhibition without causing significant cell death suggests that diapausin-1 does not disrupt the cell membrane integrity.

Distortion of *S. cerevisiae* cell shape occurred upon diapausin-1 treatment (Table. 4-1), probably due to binding of diapausin-1 to β-1,3-glucan on the cell wall. The median neck width in diapausin-1 treated yeast cells is 1.68 μm, significantly greater than 1.51 μm in control cells (Table 4-1). Of note, wider neck was reported as a common phenotype induced by wall-associated drugs, such as echinocandin B, tunicamycin, and nikkomycin Z (Okada et al., 2014).

Recombinant diapausins showed affinity to β-1,3 glucan, which is the major component for ascomycete cell walls (Fig. 4-7). Poacic acid, a diferulate found primarily in grasses (Poaceae), also showed binding to β-1,3 glucan and inhibited the incorporation of β-1,3 glucan into cell wall (Piotrowski et al., 2015). Other targets might be involved in poacic acid activity, considering the observation of rapid cell leakage caused by poacic acid (Piotrowski et al., 2015). Binding to cell wall components occurs with some non-insect antifungal peptides and is always associated with further actions. Histatin-5 discovered in humans specifically binds to cell wall proteins Ssa1/2, followed by cell membrane permeabilization and subsequent intracellular actions leading to mitochondrial depletion and induction of reactive oxygen species (Li et al., 2003; Vylkova et al., 2006; Helmerhorst et al., 2001). NaD1 from tobacco anchors to mannoproteins on the cell wall, which is necessary for further interaction with PIP_2 on the cell membrane and subsequent cell lysis (van der Weerden et al., 2010; Payne et al., 2016). Rather than cell permeabilization, blocking the cell separation after cell division was observed as the direct effect triggered by *M. sexta* diapausin (Fig. 4-8, 4-9). By looking through the morphology of 214 mutants of cell wall biogenesis and maintenance-related genes in SCMD, I found a few genes whose absence leads to a “clover”-like phenotype, suggesting the inefficient cell separation (Table 4-2). Additionally, the mutants that showed similar bud size distribution with diapausin-1-treated cells, exhibit “clover”-like phenotype as well (Table 4-3). By taking advantage of the correlation between phenotype and gene function, diapausin-1 mode of action might be relevant to these gene products, whose gene deletion manifests “clover”-like cell cluster morphology.

Future Directions

Characterization of *M. sexta* antifungal peptide, diapausin, regarding activity and morphology leads to some open questions for the future study:

(1) Antifungal activity of recombinant diapausin-2 was not potent, which was probably caused by incorrect TEV cleavage or wrong disulfide bonds formed in *E. coli*. Future purification could include the verification of the correct disulfide bond pattern. If the inefficiency did not come from incorrect disulfide bonds, it would be interesting to look at the different amino acid residues between diapausin-1 and diapausin-2, especially the longer N- and C-terminal parts in diapausin-1.

(2) The abundance of β-1,3-glucan varies among different fungal Divisions. For example, zygomycota and chytridiomycota cell wall is rich in chitin and chitosan (Faruck et al., 2016). Testing antifungal activity of diapausins against non-ascomycete fungi is another direction that should be pursued.

(3) Binding of diapausin-1 to β-1,3-glucan is worth further study. The N-terminal binding domain of *Plodia interpunctella* and *M. sexta* βGRP interacts with laminarihexaoses through side chains of Agr^{29}, D^{49}, Y^{78} and R^{87} on the β-sheet (Kanagawa et al., 2011; Takahashi et al., 2014). A glycoside hydrolase family 149 protein Pro_7066 was revealed to form hydrogen bonds with laminarihexaoses through side chains of K^{831}, E^{838}, E^{990}, E^{994} E^{982}, and R^{1062} (Kuhaudomlarp et al., 2019). Electrostatic interactions in glucan binding was believed to be critical (Takahashi et al., 2014). Therefore, several charged resides in diapausins, especially a two-arginine C-terminal tail in diapausin-1, might be responsible for glucan binding.

(4) Synergistic effects can be test by using diapausin-1 with other antifungal peptides.

(5) Information of deleted genes in the mutants with “clover”-like phenotype was collected from Saccharomyces Genome Database and I notice three genes (DSE2, EGT2 and SCW3) encode glucanase/glucanase-like proteins, which might participate in septum degradation (Lesage and Bussey, 2006; Mouassite et al., 2000). Two of them (OCH1, ANP1 and MNN10) encode enzymes critical for N-mannosylation (Nakanishi-Shindo et al., 1993; Nakayama et al., 1992). SWI4 and SWI5 are transcription factors associated with cell cycle regulation (Harrington and Andrews 1996; Cosma et al., 1999). GAS1 encodes a GPI-anchored β-1,3-glucan elongase (Tomishige et al., 2003). It is interesting to test whether diapausin-1 interferes with glucan degradation during cell septation.

Acknowledgements

I would like to thank Dr. Govindsamy Vediyappan from Biology Division for collaborating on *Candida* assays. And my appreciation is expressed to Dr. Greg Finnigan for his advice and suggestions on *S. cerevisiae* assays, as well as his generous gifts of yeast strains (BY4741, BY4742, BY4741; *cdc10Δ::CDC10::mCherry::SpHIS5*). I also want to thank Joel Sanneman from KSU CVM Confocal Facility for training and assistance on use of the LSM airyscan 880 microscope. I would give thanks to Dr. Kristin Michel and her graduate student Patil Tawidian from the KSU Division of Biology for their support and advice on *B. bassiana* assay. And my appreciation is also expressed to Chenshuang Lu, a former graduate student in the KSU Statistics Department, for helping with the statistical analysis. I really appreciate undergraduate student Gina Reyes for measuring the length of germination tubes. I want to thank Dr. Yoshikazu Ohya and Dr. Shinsuke Ohnuki from the University of Tokyo for advice and suggestions on yeast morphological analysis. And appreciation is expressed to Dr. Bindiya Sachdev for making the construct of recombinant diapausin-1 and 2. Besides, I would like to thank Dr. Brian Geisbrecht for providing TEV enzyme, Dr. Kunyan Zhu for providing calcofluor white, and Zhenhua Sun for providing starch.

Figures

A

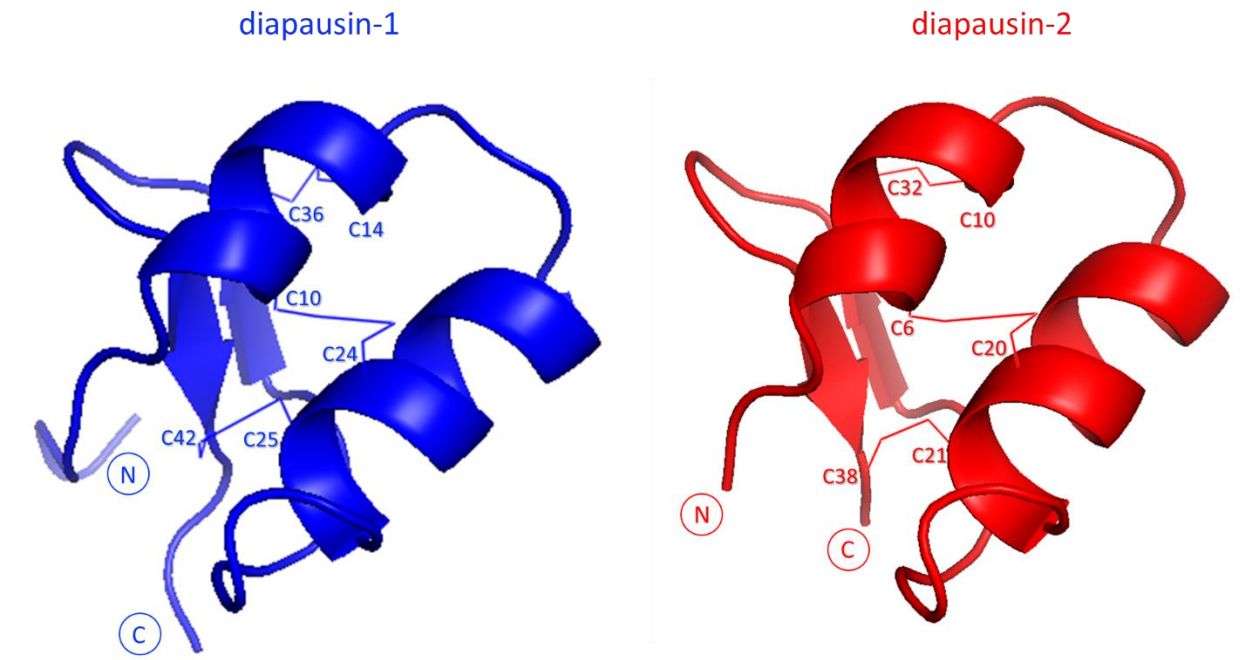

B

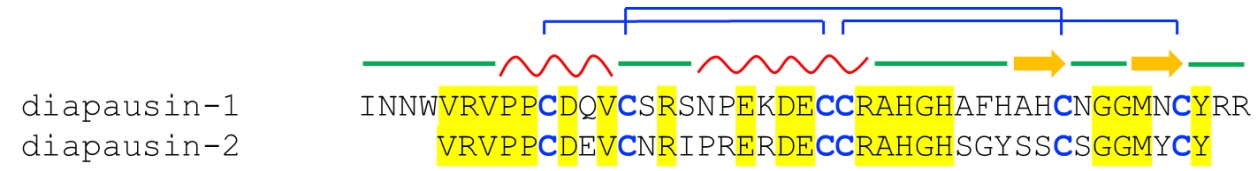

Figure 4-1. Structural models of *M. sexta* diapausins.

(A) I-TASSER homology models of diapausin-1 and diapausin-2 were made using DSP from *Gastrophysa atrocyanea* (PDB ID: 2E2F) as template. Three disulfide bonds formed by six cysteins are indicated in each model. (B) Sequence alignment of diapausin-1 and diapausin-2 with identical amino acid residues highlighted. Secondary structures are marked above corresponding sequence: loop (green line), α-helix (red curled line), and β-strand (yellow arrow). Disulfide bridges are indicated by blue brackets, and cystines forming disulfide bonds are in blue.

A

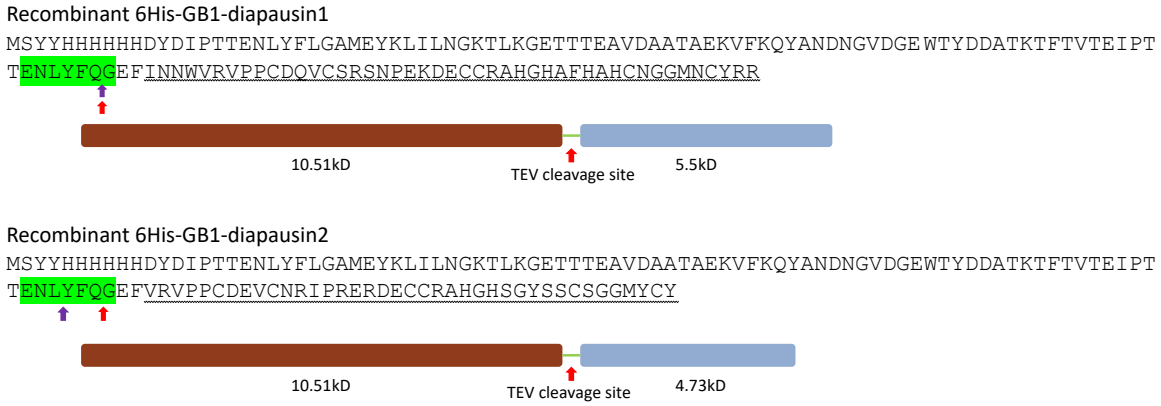

B

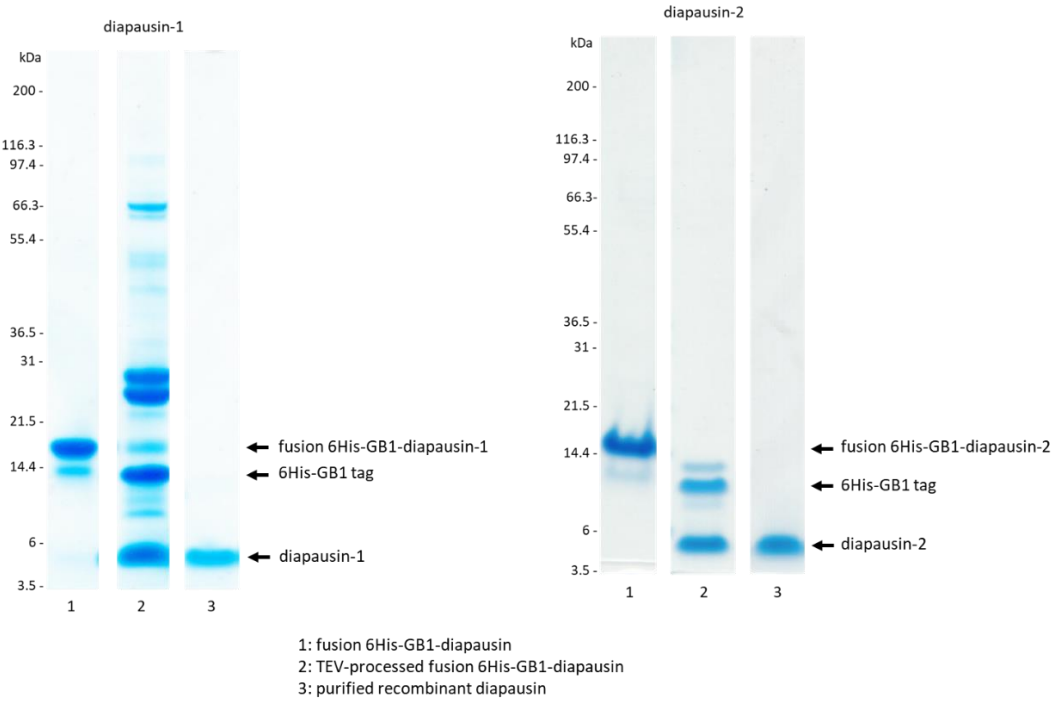

Figure 4-2. Purification of recombinant diapausin-1 and diapausin-2.

(A) Sequences of fusion 6His-GB1-diapausin-1 and 6His-GB1-diapausin-2 are shown with diapausin-1 and diapausin-2 sequences underlined. The sizes of 6His-GB1 tag and diapausins are illustrated by cartoon. The TEV protease recognition site is highlighted in green, TEV theoretical cleavage site is indicated with red arrow and actual cleavage site in indicated with purple arrow. (B) Fusion 6His-GB1-diapausins were processed by TEV protease and further purified by ion exchange chromatography. Samples with reducing SDS loading buffer were subjected to 4-12% Bis-Tris NuPAGE gel, followed by Instant Blue staining.

A

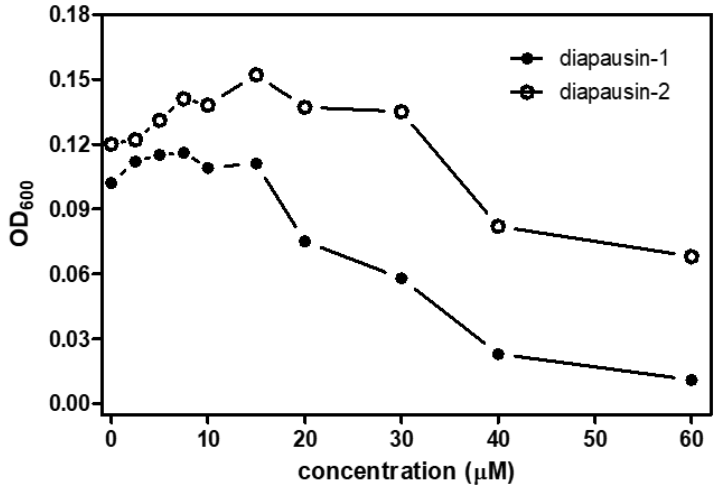

B

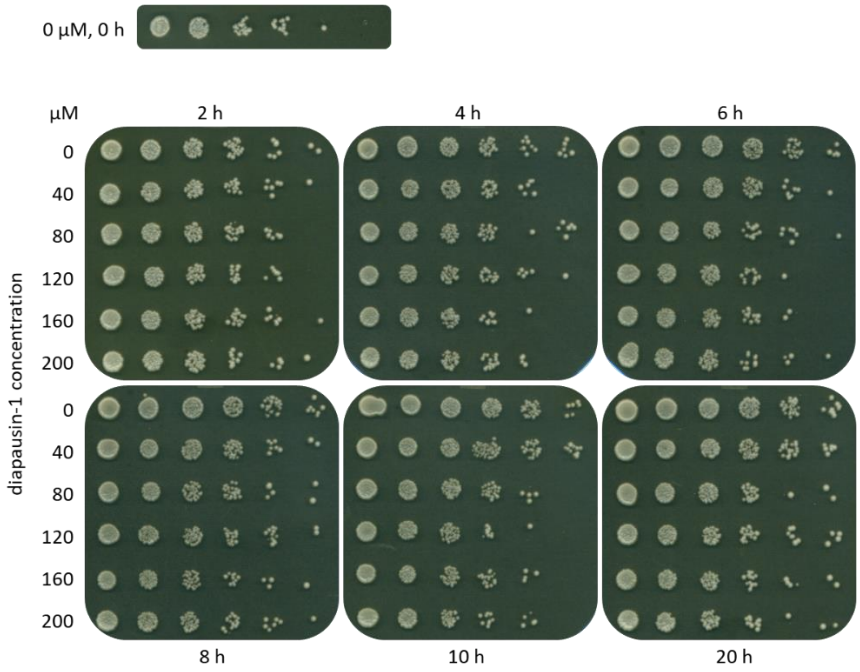

Figure 4-3. Antifungal activity of diapausins against *S. cerevisiae*.

(A) OD_{600} was measured after 8 h of incubation of recombinant diapausin-1/2 with yeast cells at different diapausin concentrations. IC_{50} values of recombinant diapausin-1 and diapausin-2 against *S. cerevisiae* are 30 μM and 60 μM, respectively. (B) Spot assay was performed with 5-fold serial dilutions after 2, 4, 6, 8, 10, and 20 h treatment of yeast cells with various concentrations of recombinant diapausin-1 prior to spotting on the plate. Control (0 μM) was spotted at 0 h. Pictures of plates were scanned after 2 days of incubation at 30°C.

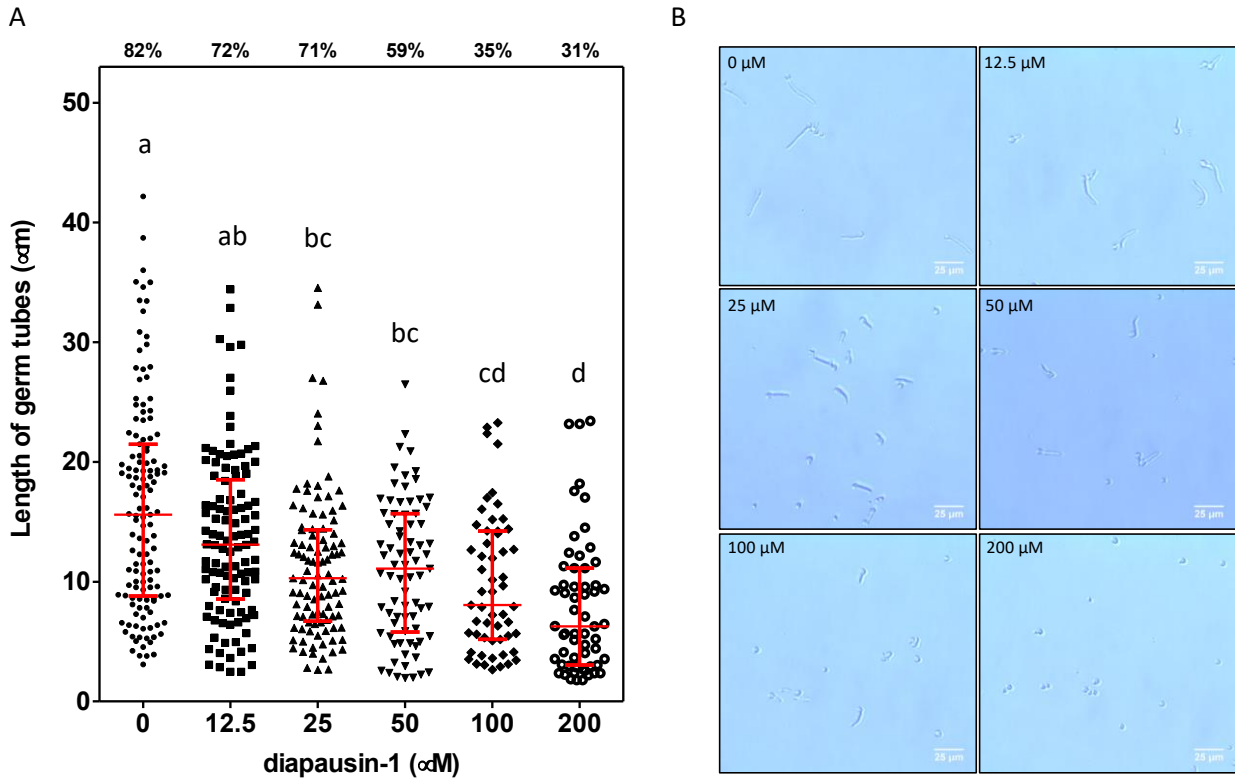

Figure 4-4. Inhibition of germination and hyphal growth of *B. bassiana* by diapausin-1.

B. bassiana conidia (3.5×10^4/ml) were incubated with recombinant diapausin-1 at different concentrations at 30°C for 8 h. (A) The percentage of conidia germinated was calculated and marked above the figure. Median and interquartile range of lengths of germination tubes are indicated in red (n=131, 110, 97, 77, 55, 51). Results of statistical analysis (Kruskal-Wallis test followed by Dunns multiple comparison test, $p<0.05$) are indicated with different letters. (B) Representative pictures show the conidial status in the presence of diapausin-1 at different concentrations.

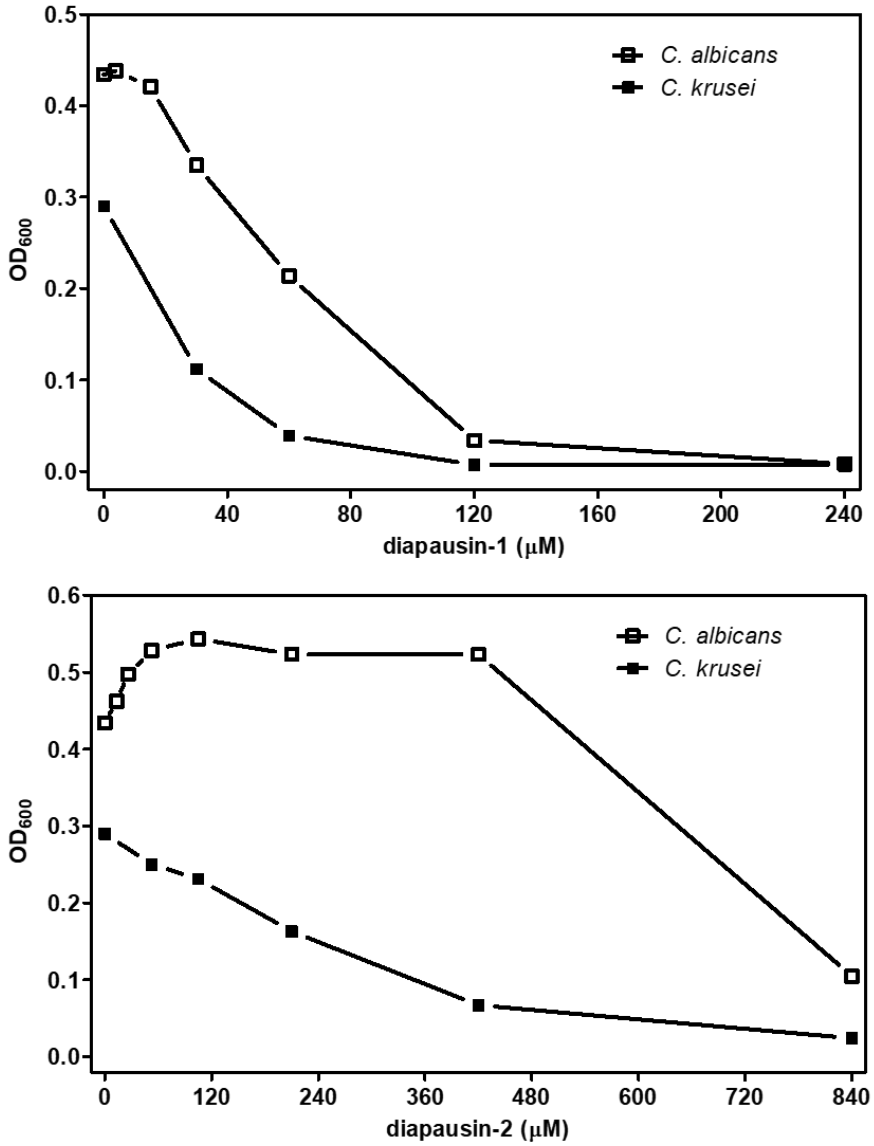

Figure 4-5. Antifungal activity of diapausins against *Candida* species.

Recombinant diapausin-1 or diapausin-2 at different concentrations were incubated with *C. albicans* and *C. krusei* at 30°C for 8 h in YPD medium, followed by measurement of OD_{600}. The growth of *C. albicans* and *C. krusei* was inhibited by recombinant diapausin-1 with IC_{50} of 60 μM and 20 μM respectively, and by diapausin-2 with IC_{50} of 240 μM and >600 μM respectively.

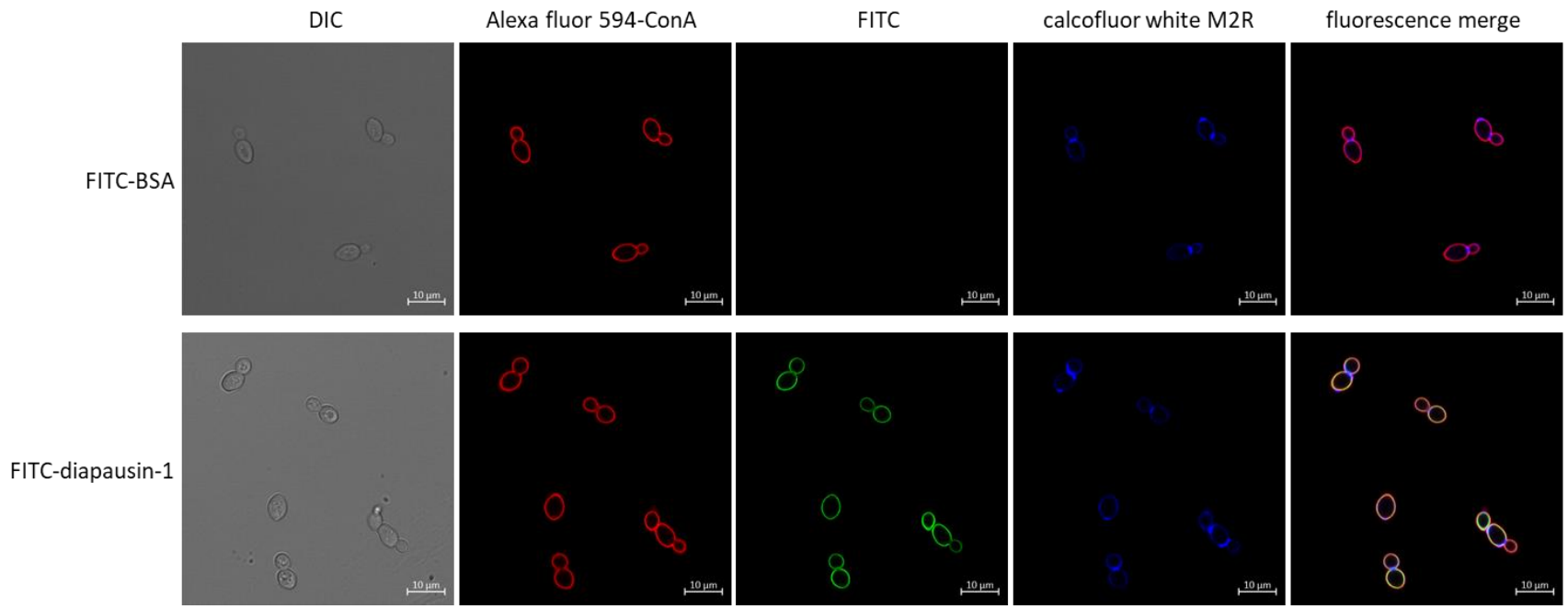

Figure 4-6. FITC-diapausin-1 binds to yeast cell surface.

Wildtype *S. cerevisiae* cells were incubated with 80 µM FITC-diapausin-1 and FITC-BSA at 30°C for 2 h, respectively, followed by staining with Alexa Fluor 594-ConA to label mannoproteins and calcofluor white M2R to mark chitin on the cell wall. Pictures were obtained using an LSM airyscan 880 microscope.

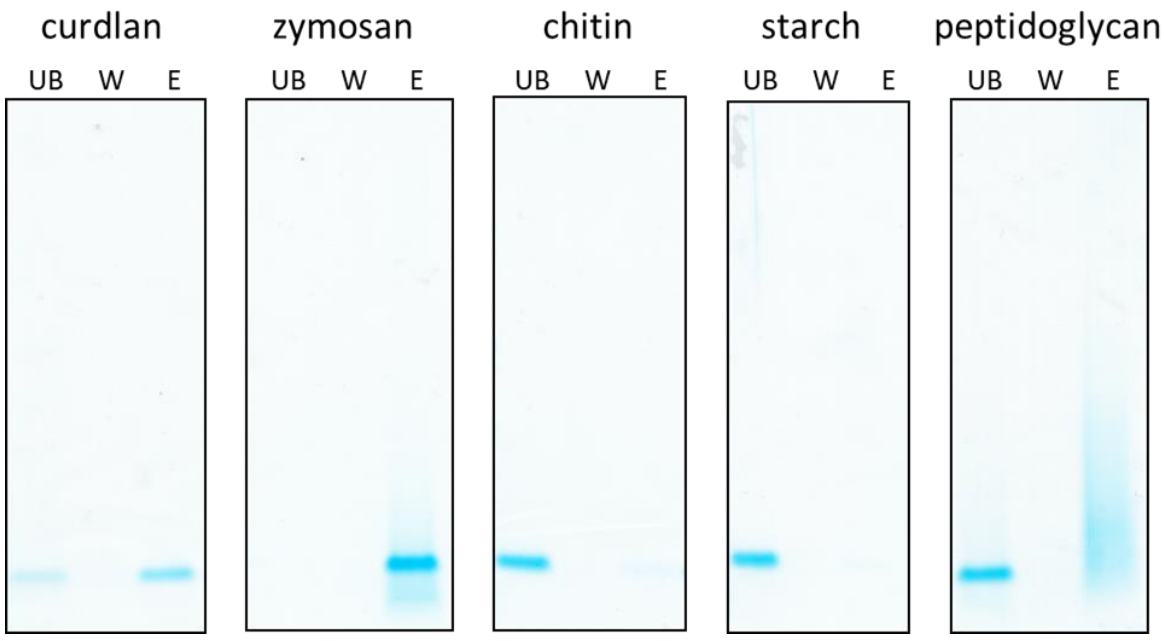

Figure 4-7. Binding of recombinant diapausin-1 to β-1,3-glucan.

Recombinant diapausin-1 (10 ng) was incubated with 100 μg polysaccharides (curdlan, zymosan, chitin, starch and peptidoglycan) at room temperature for 10 min in 1.5 ml centrifuge tubes. Supernatant was collected as unbound (UB) fraction by centrifugation. The polysaccharides were washed with 10 mM sodium phosphate, pH 7.4 and subjected to centrifugation for collecting supernatant as wash (W) fraction. Bound diapausin-1 was eluted by heating the polysaccharides in 2×SDS loading buffer supplemented with β-mercaptoethanol at 95°C for 5 min and collecting the supernatant as elution (E) fraction after centrifugation. Each fraction with reducing SDS loading buffer was subjected to 4-12% Bis-Tris NuPAGE gel, followed by Instant Blue staining.

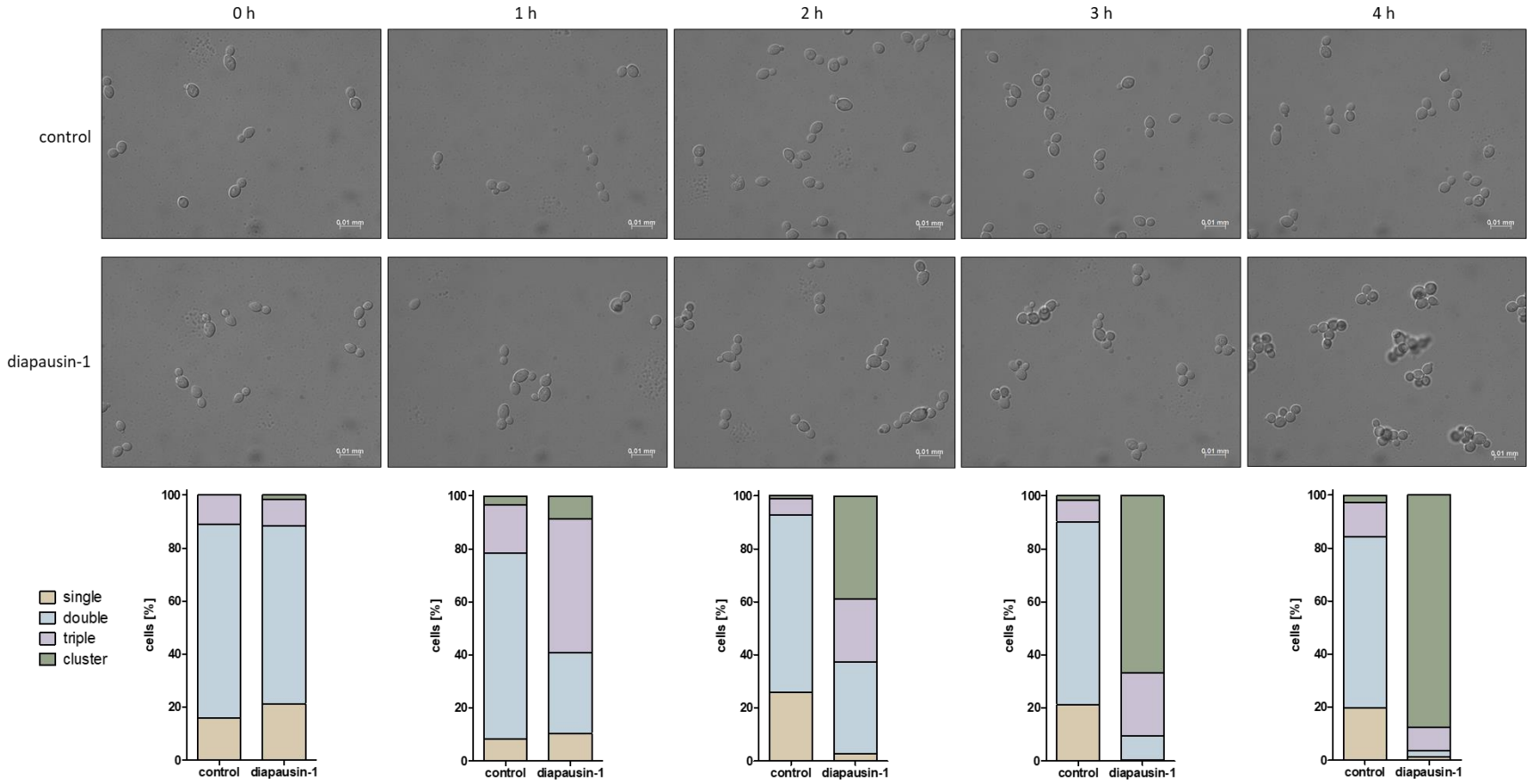

Figure 4-8. Time course microscopic observations of *S. cerevisiae* treated by diapausin-1.

Wildtype *S. cerevisiae* cells were incubated with recombinant diapausin-1 (80 μM) or sterile water as a control at 30°C. Cells were observed after 0, 1, 2, 3 and 4 h of incubation using a DIC microscope and captured by camera. The number of single (a cell without a bud), double (a mother cell with a bud), triple (a mother cell with probably two buds) and cluster (with four or more cells sticking to each other) was counted in each sample (n>74) and reflected by percentage in bar graph.

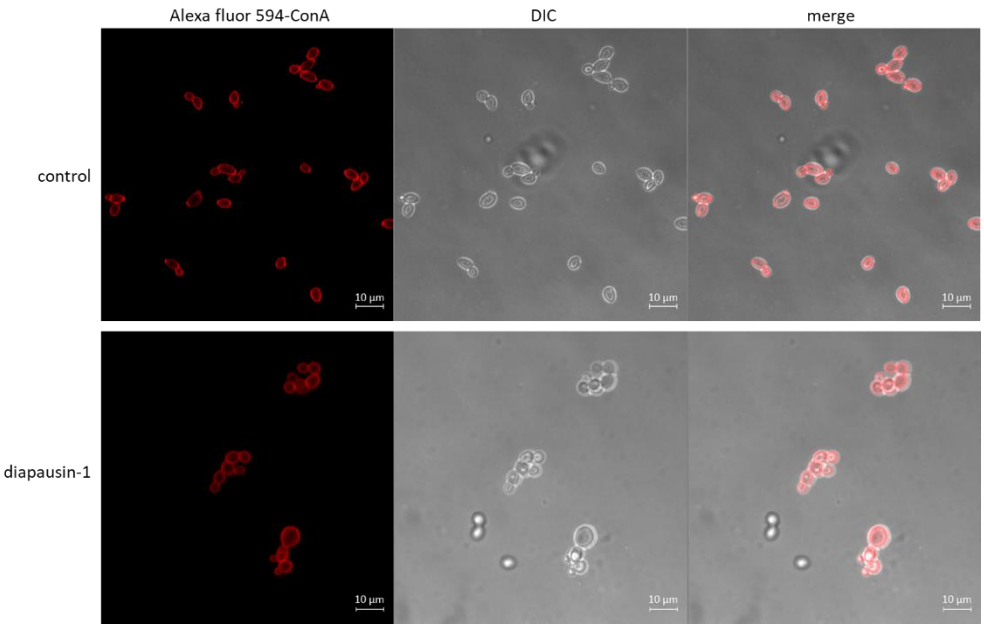

Figure 4-9. Microscopic observations of *C. albicans* caused by diapausin-1.

C. albicans cells were incubated in YPD medium with recombinant diapausin-1 (80 μM) or sterile water as a control at 30°C for 8 h, followed by fixation in 3.7% formaldehyde and staining with Alexa Fluor 594-ConA. Pictures were obtained using an LSM airyscan 880 microscope.

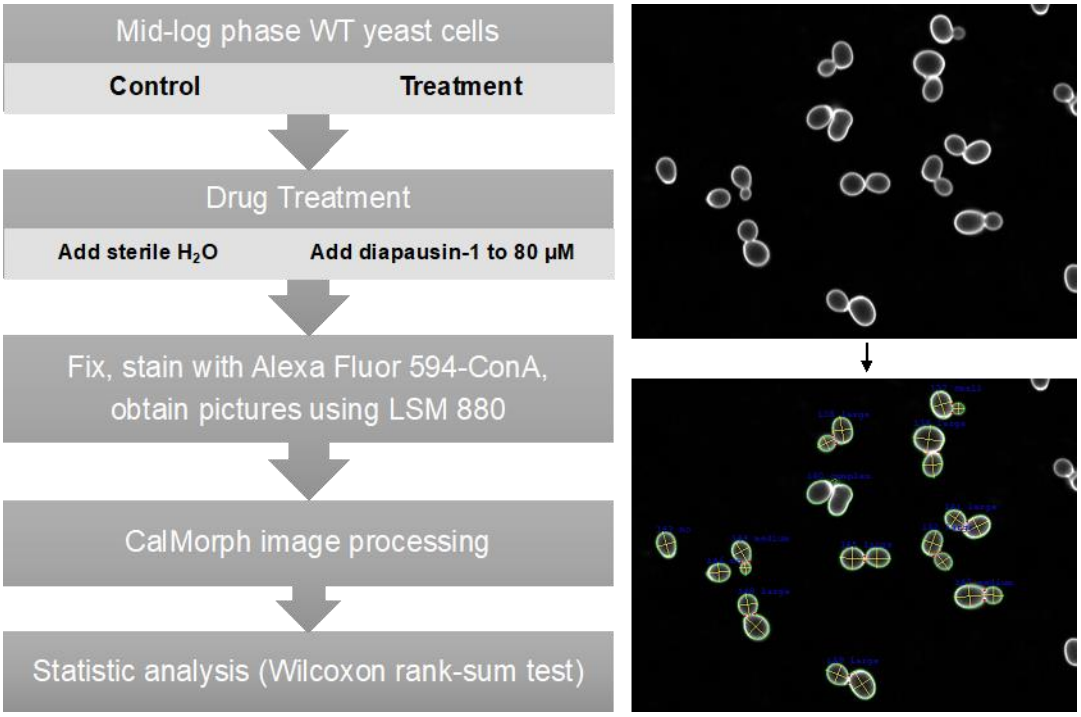

Figure 4-10. Demonstration of morphological analysis of *S. cerevisiae* caused by diapausin-1.

S. cerevisiae wildtype BY4741 cells were incubated with 80 μM diapausin-1 or sterile water as a control at 30°C for 2 h, followed by fixation in 3.7% formaldehyde and staining with Alexa Fluor 594-ConA. Pictures were obtained using an LSM airyscan 880 microscope, followed by morphological quantification of yeast cells using CalMorph (n>490). Difference between control and diapausin-1-treated yeast cells regarding each parameter was tested by Wilcoxon rank-sum test. An example picture of morphological quantification by CalMorph was shown.

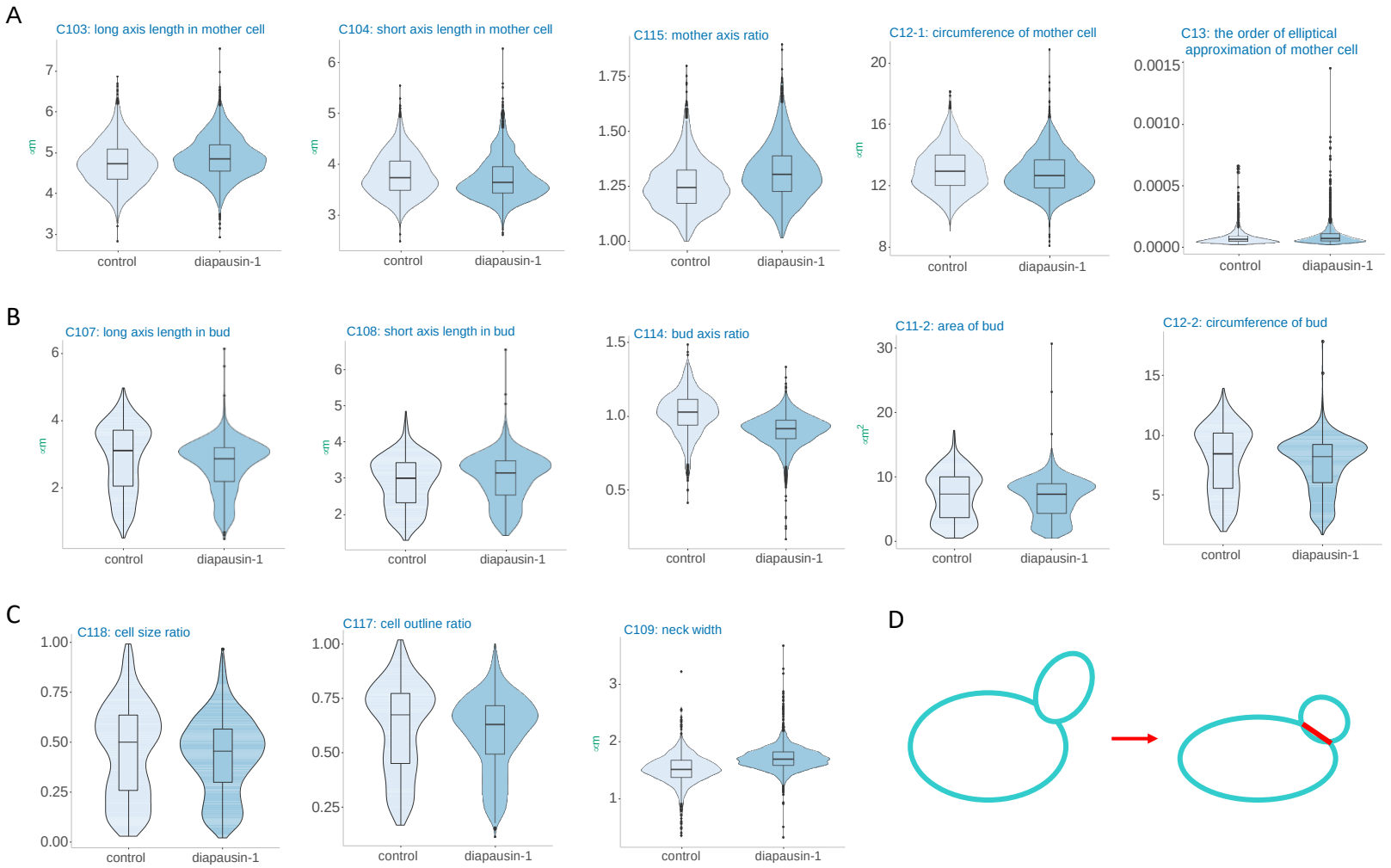

Figure 4-11. Morphological changes of *S. cerevisiae* caused by diapausin-1.

Morphological parameters in mother cell (A), bud (B) and other (C), which have significant difference ($p<0.05$) between control (sterile H_2O treatment) and diapausin-1 treatment are shown using violin plots. (D) A sketch of general morphological differences of control and diapausin-1-treated yeast cells.

Tables

Table 4-1. Morphological analysis of *S. cerevisiae* cells treated with diapausin-1.

Morphology of control (sterile H_2O treatment) and diapausin-1-treated cells was quantified by CalMorph by measuring parameters listed below. Parameters which have significant difference ($p<0.05$; Wilcoxon rank-sum test) between control and diapausin-1 treatment are in red.

parameter	control		diapausin-1		p value	definition of parameter
	median	interquartile	median	interquartile		
C11-1	14.465	4.127	14.490	3.566	0.05219243	mother cell size (μm²)
C11-2	7.264	6.382	7.220	4.574	0.0015091	bud cell size (μm²)
C12-1	12.893	1.981	12.614	1.813	1.24E-05	mother cell circumference (μm)
C12-2	8.397	4.616	8.172	3.141	2.52E-07	bud cell circumference (μm)
C13	6.103E-05	4.656E-05	6.855E-05	6.006E-05	5.03E-10	order of the elliptical approximation of mother cell
C101	18.850	9.778	20.399	7.976	5.69E-07	whole cell size (μm²)
C102	18.738	8.032	19.992	5.636	1.89E-05	whole cell outline length (μm)
C103	4.718	0.736	4.841	0.643	4.09E-16	long axis length in mother cell (μm)
C104	3.733	0.570	3.653	0.511	2.37E-05	short axis length in mother cell (μm)
C105	28.794	24.020	28.926	21.693	0.2667755	neck position (°)
C106	43.141	32.632	40.903	30.928	0.00070258	bud direction (°)
C107	3.094	1.674	2.843	1.007	3.37E-16	long axis length in bud (μm)
C108	2.985	1.110	3.138	0.950	1.62E-05	short axis length in bud (μm)
C109	1.511	0.299	1.685	0.235	8.09E-96	neck width (μm)
C110	2.873	2.231	2.683	1.686	1.57E-05	distance between bud tip and mother long axis extension (μm)
C111	3.648	1.977	3.834	1.787	0.42192479	distance between bud tip and mother short axis extension (μm)
C112	2.160	0.336	2.160	0.303	0.86131183	distance between middle point of neck and mother center (μm)
C113	4.540	1.845	4.386	1.331	5.17E-05	distance between bud tip and mother long axis through middle point of neck (μm)
C114	1.026	0.174	0.914	0.125	1.51E-106	bud axis ratio
C115	1.244	0.150	1.303	0.160	4.00E-42	mother axis ratio
C116	0.821	0.174	0.701	0.123	3.66E-114	axis ratio ratio
C117	0.674	0.325	0.632	0.222	1.23E-05	cell outline ratio
C118	0.498	0.377	0.453	0.265	0.00088629	cell size ratio
C128	4.450	0.625	4.492	0.555	0.002436651	distance between middle point of neck and mother hip (μm)

Table 4-2. Mutants with "clover" phenotype.

systematic name	gene name	description of the gene product (from Saccharomyces Genome Database)
YDR245w	MNN10	Subunit of a Golgi mannosyltransferase complex; complex mediates elongation of the polysaccharide mannan backbone; membrane protein of the mannosyltransferase family; other members of the complex are Anp1p, Mnn9p, Mnn11p, and Hoc1p
YEL036c	ANP1	Subunit of the alpha-1,6 mannosyltransferase complex; type II membrane protein; has a role in retention of glycosyltransferases in the Golgi; involved in osmotic sensitivity and resistance to aminonitrophenyl propanediol
YHR143w	DSE2	Daughter cell-specific secreted protein with similarity to glucanases; degrades cell wall from the daughter side causing daughter to separate from mother; expression is repressed by cAMP; encodes a putative GPI-anchored cell surface protein
YMR307w	GAS1	Beta-1,3-glucanosyltransferase; required for cell wall assembly and also has a role in transcriptional silencing; localizes to cell surface via a glycosylphosphatidylinositol (GPI) anchor; also found at nuclear periphery; genetic interactions with histone H3 lysine acetyltransferases GCN5 and SAS3 indicate previously unsuspected functions for Gas1 in DNA damage response and cell cycle regulation.
YNL327w	EGT2	Glycosylphosphatidylinositol (GPI)-anchored cell wall endoglucanase; required for proper cell separation after cytokinesis; expression is activated by Swi5p and tightly regulated in a cell cycle-dependent manner
YNL066w	SCW3	Cell wall protein related to glucanases; possibly involved in cell wall septation; member of the SUN family; SUN4 has a paralog, SIM1, that arose from the whole genome duplication
YDR146c	SWI5	Transcription factor that recruits Mediator and Swi/Snf complexes; activates transcription of genes expressed at the M/G1 phase boundary and in G1 phase; required for expression of the HO gene controlling mating type switching; localization to nucleus occurs during G1 and appears to be regulated by phosphorylation by Cdc28p kinase; SWI5 has a paralog, ACE2, that arose from the whole genome duplication
YLR038c	OCH1	Och1, α-1,6-manno-syltransferase catalyzes the transfer of a mannose residue to the $Man_8GlcNAc_2$ structure. Glycoproteins produced by a null *och1* mutant lack α-1,6-polymannose, indicating that the addition of this initial mannose residue is critical for other reactions to take place and/or that Och1 is involved in the catalysis of subsequent α-1,6 linkages
YNL233w	BNI4	Targeting subunit for Glc7p protein phosphatase; localized to the bud neck, required for localization of chitin synthase III to the bud neck via interaction with the chitin synthase III regulatory subunit Skt5p; phosphorylation by Slt2p and Kss1p involved in regulating Bni4p in septum assembly
YPL158c	AIM44/GPS1	Protein that regulates Cdc42p and Rho1p; functions in the late steps of cytokinesis and cell separation; sustains Rho1p at the cell division site after actomyosin ring contraction; inhibits the activation of Cdc42-Cla4 at the cell division site to prevent budding inside the old bud neck; transcription is regulated by Swi5p; null mutant displays elevated frequency of mitochondrial genome loss; relocalizes from bud neck to cytoplasm upon DNA replication stress

Table 4-3. Mutants with similar bud size distributions in diapausin-1-treated cells.

Cells were categorized to "no bud" (a single cell without bud), "small bud" (0<bud size/mother cell size<0.5), "medium bud" (0.5≤bud size/mother cell size<0.7), "large bud" (0.7≤bud size/mother cell size), and "complex" (too complicated to be analyzed by CalMorph). Pearson's chi-square test was performed between diapausin-1 treatment and mutants provided by SCMD regarding bud size distribution. Listed three mutants don't have significant difference with diapausin-1 treatment ($p<0.05$).

	no bud	small bud	medium bud	large bud	complex
diapausin-1-treated	**14.20%**	**17.62%**	**31.55%**	**36.62%**	**28.6%**
YDR320c (SWA2)	15.79%	12.75%	23.89%	23.48%	24.09%
YER111c (SWI4)	13.18%	15.19%	13.47%	32.66%	25.50%
YGL084c (GUP1)	13.91%	11.26%	13.91%	31.12%	29.80%

References

Abràmoff, M. D., P. J. Magalhães & S. J. Ram (2004) Image processing with ImageJ. *Biophotonics international*, 11, 36-42.

Al Souhail, Q., Y. Hiromasa, M. Rahnamaeian, M. C. Giraldo, D. Takahashi, B. Valent, A. Vilcinskas & M. R. Kanost (2016) Characterization and regulation of expression of an antifungal peptide from hemolymph of an insect, *Manduca sexta*. *Developmental & Comparative Immunology*, 61, 258-268.

Baxter, A., M. Hulett & I. Poon (2015) The phospholipid code: a key component of dying cell recognition, tumor progression and host-microbe interactions. *Cell Death and Differentiation*, 22, 1893-1905.

Cappelletty, D. & K. Eiselstein-McKitrick (2007) The Echinocandins. *Pharmacotherapy: The Journal of Human Pharmacology and Drug Therapy*, 27, 369-388.

Cosma, M. P., T. Tanaka & K. Nasmyth (1999) Ordered recruitment of transcription and chromatin remodeling factors to a cell cycle–and developmentally regulated promoter. *Cell*, 97, 299-311.

De Lucca, A., J. Bland, T. Jacks, C. Grimm & T. Walsh (1998a) Fungicidal and binding properties of the natural peptides cecropin B and dermaseptin. *Medical Mycology*, 36, 291-298.

De Lucca, A., T. Jacks & W. Broekaert (1998b) Fungicidal and binding properties of three plant peptides. *Mycopathologia*, 144, 87-91.

De Samblanx, G. W., I. J. Goderis, K. Thevissen, R. Raemaekers, F. Fant, F. Borremans, D. P. Acland, R. W. Osborn, S. Patel & W. F. Broekaert (1997) Mutational analysis of a plant defensin from radish (*Raphanus sativus* L.) reveals two adjacent sites important for antifungal activity. *Journal of Biological Chemistry*, 272, 1171-1179.

den Hertog, A. L., van Marle, J., Bolscher, J. G., Veerman, E. C., & Arie, V. (2005) Candidacidal effects of two antimicrobial peptides: histatin 5 causes small membrane defects, but LL-37 causes massive disruption of the cell membrane. *Biochemical Journal*, 388, 689-695.

Dürr, U. H., U. Sudheendra & A. Ramamoorthy (2006) LL-37, the only human member of the cathelicidin family of antimicrobial peptides. *Biochimica et Biophysica Acta (BBA)-Biomembranes*, 1758, 1408-1425.

Faruck, M., F. Yusof & S. Chowdhury (2016) An overview of antifungal peptides derived from insect. *Peptides*, 80, 80-88.

Fehlbaum, P., P. Bulet, L. Michaut, M. Lagueux, W. Broekaert, C. Hetru & J. Hoffmann (1994) Insect immunity. Septic injury of *Drosophila* induces the synthesis of a potent antifungal peptide with sequence homology to plant antifungal peptides. *Journal of Biological Chemistry*, 269, 33159-33163.

Finnigan, G., J. Takagi, C. Cho & J. Thorner (2015) Comprehensive Genetic Analysis of Paralogous Terminal Septin Subunits Shs1 and Cdc11 in *Saccharomyces cerevisiae*. *Genetics*, 200(3), 821-841.

Ganz, T. (2003) Defensins: antimicrobial peptides of innate immunity. *Nature reviews immunology*, 3, 710.

Harrington, L. A. & B. J. Andrews (1996) Binding to the yeast Swi4, 6-dependent cell cycle box, CACGAAA, is cell cycle regulated in vivo. *Nucleic acids research*, 24, 558-565.

Hartwell, L. H. (1974) *Saccharomyces cerevisiae* cell cycle. *Bacteriological reviews*, 38, 164.

He, Y., X. Cao, K. Li, Y. Hu, Y. R. Chen, G. Blissard, M. R. Kanost & H. Jiang (2015) A genome-wide analysis of antimicrobial effector genes and their transcription patterns in *Manduca sexta*. *Insect biochemistry and molecular biology*, 62, 23-37.

Helmerhorst, E., R. Troxler & F. Oppenheim (2001) The human salivary peptide histatin 5 exerts its antifungal activity through the formation of reactive oxygen species. *Proceedings of the National Academy of Sciences of the United States of America*, 98, 14637-14642.

Kanagawa, M., T. Satoh, A. Ikeda, Y. Adachi, N. Ohno & Y. Yamaguchi (2011) Structural insights into recognition of triple-helical β-glucans by an insect fungal receptor. *Journal of Biological Chemistry*, 286, 29158-29165.

Kanost, M. R., H. Jiang & X. Q. Yu (2004) Innate immune responses of a lepidopteran insect, *Manduca sexta*. Immunological reviews, 198, 97-105.

Kavanagh, K. & S. Dowd (2004) Histatins: antimicrobial peptides with therapeutic potential. *Journal of pharmacy and pharmacology*, 56, 285-289.

Kouno, T., M. Mizuguchi, H. Tanaka, P. Yang, Y. Mori, H. Shinoda, K. Unoki, T. Aizawa, M. Demura, K. Suzuki & K. Kawano (2007) The structure of a novel insect peptide explains its $Ca2^{+}$ channel blocking and antifungal activities. *Biochemistry*, 46, 13733-13741.

Kuhaudomlarp, S., C. E. Stevenson, D. M. Lawson & R. A. Field (2019) The structure of a GH149 β-(1→3) glucan phosphorylase reveals a new surface oligosaccharide binding site and additional domains that are absent in the disaccharide-specific GH94 glucose-β-(1→3)-glucose (laminaribiose) phosphorylase. *Proteins: Structure, Function, and Bioinformatics*.

Lamberty, M., S. Ades, S. Uttenweiler-Joseph, G. Brookhart, D. Bushey, J. A. Hoffmann & P. Bulet (1999) Insect Immunity: isolation from the lepidopteran heliothis virescensof a novel insect defensin with potent antifungal activity. *Journal of Biological Chemistry*, 274, 9320-9326.

Landon, C., P. Sodano, C. Hetru, J. Hoffmann & M. Ptak (1997) Solution structure of drosomycin, the first inducible antifungal protein from insects. *Protein Science*, 6, 1878-1884.

Lee, Y., E. Yun, W. Jang, I. Kim, J. Lee, S. Park, K. Ryu, S. Seo, C. Kim & I. Lee (2004) Purification, cDNA cloning and expression of an insect defensin from the great wax moth, *Galleria mellonella*. *Insect Molecular Biology*, 13, 65-72.

Lesage, G. & H. Bussey (2006) Cell wall assembly in *Saccharomyces cerevisiae*. *Microbiology and Molecular Biology Reviews*, 70(2), 317-343.

Levitz, S. M., M. E. Selsted, T. Ganz, R. I. Lehrer & R. D. Diamond (1986) *In vitro* killing of spores and hyphae of *Aspergillus fumigatus* and *Rhizopus oryzae* by rabbit neutrophil cationic peptides and bronchoalveolar macrophages. *The Journal of Infectious Diseases*, 154, 483-489.

Li, X., M. Reddy, D. Baev & M. Edgerton (2003) *Candida albicans* Ssa1/2p is the cell envelope binding protein for human salivary histatin 5. *Journal of Biological Chemistry*, 278, 28553-28561.

Mouassite, M., N. Camougrand, E. Schwob, G. Demaison, M. Laclau & M. Guérin (2000) The 'SUN'family: yeast SUN4/SCW3 is involved in cell septation. *Yeast*, 16, 905-919.

Nachar, N. (2008) The Mann-Whitney U: A test for assessing whether two independent samples come from the same distribution. *Tutorials in quantitative Methods for Psychology*, 4, 13-20.

Nakanishi-Shindo, Y., K. I. Nakayama, A. Tanaka, Y. Toda & Y. Jigami (1993) Structure of the N-linked oligosaccharides that show the complete loss of alpha-1, 6-polymannose outer chain from och1, och1 mnn1, and och1 mnn1 alg3 mutants of *Saccharomyces cerevisiae*. *Journal of Biological Chemistry*, 268, 26338-26345.

Nakayama, K. I., T. Nagasu, Y. I. Shimma, J. R. Kuromitsu & Y. Jigami (1992) OCH1 encodes a novel membrane bound mannosyltransferase: outer chain elongation of asparagine-linked oligosaccharides. The EMBO journal, 11, 2511-2519.

Nogami, S. & Y. Ohya. 2009. Biosynthetic enzymes for (1-3)-β-glucans,(1-3; 1-6)-β-glucans from yeasts: biochemical properties and molecular biology. In *Chemistry, Biochemistry, and Biology of 1-3 Beta Glucans and Related Polysaccharides*, 259-282. Elsevier.

Ohya, Y., J. Sese, M. Yukawa, F. Sano, Y. Nakatani, T. Saito, A. Saka, T. Fukuda, S. Ishihara, S. Oka, G. Suzuki, M. Watanabe, A. Hirata, M. Ohtani, H. Sawai, N. Fraysse, J. Latge, J. Francois, M. Aebi, S. Tanaka, S. Muramatsu, H. Araki, K. Sonoike, S. Nogami & S. Morishita (2005) High-dimensional and large-scale phenotyping of yeast mutants. *Proceedings of the National Academy of Sciences of the United States of America*, 102, 19015-19020.

Okada, H., S. Ohnuki, C. Roncero, J. Konopka & Y. Ohya (2014) Distinct roles of cell wall biogenesis in yeast morphogenesis as revealed by multivariate analysis of high-dimensional morphometric data. *Molecular Biology of the Cell*, 25, 222-233.

Okada, H. & Y. Ohya (2016) Fluorescent labeling of yeast cell wall components. *Cold Spring Harbor Protocols, 2016*, pdb. prot085241.

Payne, J., M. Bleackley, T. Lee, T. Shafee, I. Poon, M. Hulett, M. Aguilar, N. van der Weerden & M. Anderson (2016) The plant defensin NaD1 introduces membrane disorder through a specific interaction with the lipid, phosphatidylinositol 4,5 bisphosphate. *Biochimica Et Biophysica Acta-Biomembranes*, 1858, 1099-1109.

Piotrowski, J. S., H. Okada, F. Lu, S. C. Li, L. Hinchman, A. Ranjan, D. L. Smith, A. J. Higbee, A. Ulbrich & J. J. Coon (2015) Plant-derived antifungal agent poacic acid targets β-1, 3-glucan. *Proceedings of the National Academy of Sciences*, 112, E1490-E1497.

Rautenbach, M., A. Troskie & J. Vosloo (2016) Antifungal peptides: to be or not to be membrane active. *Biochimie*, 130, 132-145.

Schuhmann, B., V. Seitz, A. Vilcinskas & L. Podsiadlowski (2003) Cloning and expression of gallerimycin, an antifungal peptide expressed in immune response of greater wax moth larvae, *Galleria mellonella*. *Archives of Insect Biochemistry and Physiology*, 53, 125-133.

Takahashi, D., H. Dai, Y. Hiromasa, R. Krishnamoorthi & M. R. Kanost (2014) Self-association of an insect β-1, 3-glucan recognition protein upon binding laminarin stimulates prophenoloxidase activation as an innate immune response. *Journal of Biological Chemistry*, 289, 28399-28410.

Tanaka, H., K. Sato, Y. Saito, T. Yamashita, M. Agoh, J. Okunishi, E. Tachikawa & K. Suzuki (2003) Insect diapause-specific peptide from the leaf beetle has consensus with a putative iridovirus peptide. *Peptides*, 24, 1327-1333.

Thomma, B. P., B. P. Cammue & K. Thevissen (2002) Plant defensins. *Planta*, 216, 193-202.

Tian, C., B. Gao, M. Rodriguez, H. Lanz-Mendoza, B. Ma & S. Zhu (2008) Gene expression, antiparasitic activity, and functional evolution of the Drosomycin family. *Molecular Immunology*, 45, 3909-3916.

Tomishige, N., Y. Noda, H. Adachi, H. Shimoi, A. Takatsuki & K. Yoda (2003) Mutations that are synthetically lethal with a gas1Δ allele cause defects in the cell wall of *Saccharomyces cerevisiae*. *Molecular genetics and genomics*, 269, 562-573.

van der Weerden, N., R. Hancock & M. Anderson (2010) Permeabilization of fungal hyphae by the plant defensin NaD1 occurs through a cell wall-dependent process. *Journal of Biological Chemistry*, 285, 37513-37520.

Vylkova, S., X. Li, J. Berner & M. Edgerton (2006) Distinct antifungal mechanisms: beta-defensins require *Candida albicans* Ssa1 protein, while Trk1p mediates activity of cysteine-free cationic peptides. *Antimicrobial Agents and Chemotherapy*, 50, 324-331.

Wang, Z. Z., M. Shi, X. Q. Ye, M. Y. Chen & X. X. Chen (2013) Identification, characterization and expression of a defensin-like antifungal peptide from the whitefly *Bemisia tabaci* (G ennadius) (Hemiptera: Aleyrodidae). *Insect molecular biology*, 22, 297-305.

Yang, J. & Y. Zhang (2015) I-TASSER server: new development for protein structure and function predictions. *Nucleic Acids Research*, 43, W174-W181.

Yi, H. Y., M. Chowdhury, Y. D. Huang & X. Q. Yu (2014) Insect antimicrobial peptides and their applications. *Appl Microbiol Biotechnol*, 98, 5807-22.

Zasloff, M. (2002) Antimicrobial peptides of multicellular organisms. *Nature*, 415, 389.

Appendix A – Copyright Permissions

Published work – Chapter 2 (Li et al., 2018)

Elsevier Copyright Policy: as the author of this Elsevier article, you retain the right to include it in a thesis or dissertation, provided it is not published commercially. Permission is not required, but please ensure that you reference the journal as the original source. Non-commercial Creative Commons user license (CC-BY-NC-ND) is attached as below.

https://doi.org/10.1016/j.ibmb.2018.09.008

Copyright Clearance Center RightsLink®

Home | Account Info | Help

Title: The Manduca sexta serpinome: Analysis of serpin genes and proteins in the tobacco hornworm

Author: Miao Li,Jayne M. Christen,Neal T. Dittmer,Xiaolong Cao,Xiufeng Zhang,Haobo Jiang,Michael R. Kanost

Publication: Insect Biochemistry and Molecular Biology

Publisher: Elsevier

Date: November 2018

Logged in as:
Miao Li
LOGOUT

Appendix B – Chapter 2 Supplementary Materials

Figure B-1. Complete sequence alignment of *M. sexta* serpin proteins.

Conserved amino acid residues in regions that are critical for the inhibition mechanism (Irving et al., 2000) are highlighted. Residues conserved in the shutter region are in blue, residues conserved in the breach region are in yellow, residues conserved in the hinge region are in green, residues conserved in the gate region are in magenta and other conserved residues are in grey. Predicted secondary structures, α-helix and β-strand, and reactive center loop (RCL) marked above the sequences are based on crystal structures of human α_1-antitrypsin and *M. sexta* serpin-1K (Irving et al., 2000; Li et al., 1999).

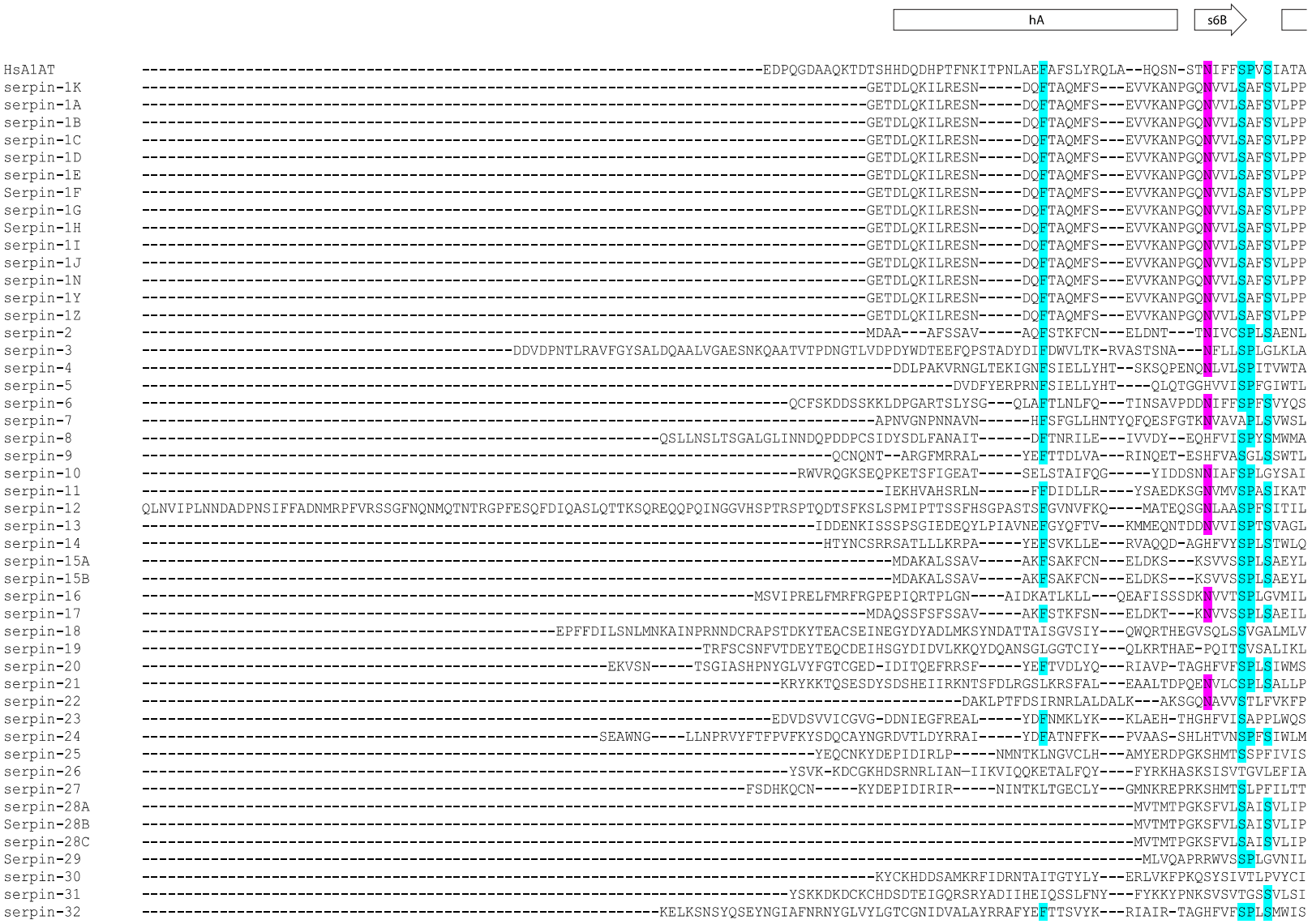
hA
s6B
HsA1AT
serpin-1K
serpin-1A
serpin-1B
serpin-1C
serpin-1D
serpin-1E
Serpin-1F
serpin-1G
Serpin-1H
serpin-1I
serpin-1J
serpin-1N
serpin-1Y
serpin-1Z
serpin-2
serpin-3
serpin-4
serpin-5
serpin-6
serpin-7
serpin-8
serpin-9
serpin-10
serpin-11
serpin-12
serpin-13
serpin-14
serpin-15A
serpin-15B
serpin-16
serpin-17
serpin-18
serpin-19
serpin-20
serpin-21
serpin-22
serpin-23
serpin-24
serpin-25
serpin-26
serpin-27
serpin-28A
Serpin-28B
serpin-28C
Serpin-29
serpin-30
serpin-31
serpin-32

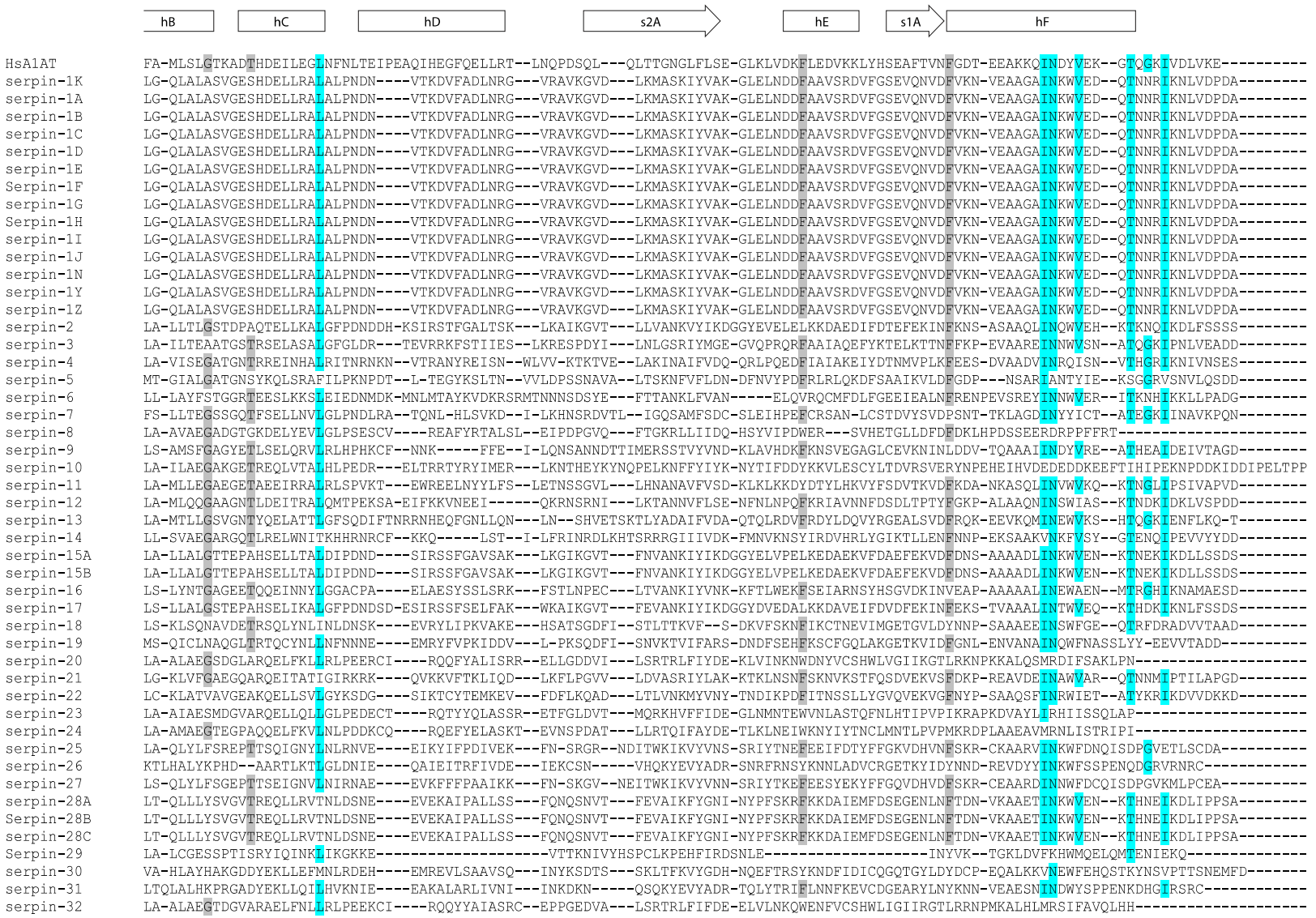
hB
hC
hD
s2A
hE
s1A
hF
HsA1AT FA-MLSLGTKADTHDEILEGLNFNLTEIPEAQIHEGFQELLRT--LNQPDSQL---QLTTGNGLFLSE-GLKLVDKFLEDVKKLYHSEAFTVNFGDT-EEAKKQINDYVEK--GTQGKIVDLVKE----------
serpin-1K LG-QLALASVGESHDELLRALALPNDN----VTKDVFADLNRG---VRAVKGVD---LKMASKIYVAK-GLELNDDFAAVSRDVFGSEVQNVDFVKN-VEAAGAINKWVED--QTNNRIKNLVDPDA--------
serpin-1A LG-QLALASVGESHDELLRALALPNDN----VTKDVFADLNRG---VRAVKGVD---LKMASKIYVAK-GLELNDDFAAVSRDVFGSEVQNVDFVKN-VEAAGAINKWVED--QTNNRIKNLVDPDA--------
serpin-1B LG-QLALASVGESHDELLRALALPNDN----VTKDVFADLNRG---VRAVKGVD---LKMASKIYVAK-GLELNDDFAAVSRDVFGSEVQNVDFVKN-VEAAGAINKWVED--QTNNRIKNLVDPDA--------
serpin-1C LG-QLALASVGESHDELLRALALPNDN----VTKDVFADLNRG---VRAVKGVD---LKMASKIYVAK-GLELNDDFAAVSRDVFGSEVQNVDFVKN-VEAAGAINKWVED--QTNNRIKNLVDPDA--------
serpin-1D LG-QLALASVGESHDELLRALALPNDN----VTKDVFADLNRG---VRAVKGVD---LKMASKIYVAK-GLELNDDFAAVSRDVFGSEVQNVDFVKN-VEAAGAINKWVED--QTNNRIKNLVDPDA--------
serpin-1E LG-QLALASVGESHDELLRALALPNDN----VTKDVFADLNRG---VRAVKGVD---LKMASKIYVAK-GLELNDDFAAVSRDVFGSEVQNVDFVKN-VEAAGAINKWVED--QTNNRIKNLVDPDA--------
Serpin-1F LG-QLALASVGESHDELLRALALPNDN----VTKDVFADLNRG---VRAVKGVD---LKMASKIYVAK-GLELNDDFAAVSRDVFGSEVQNVDFVKN-VEAAGAINKWVED--QTNNRIKNLVDPDA--------
serpin-1G LG-QLALASVGESHDELLRALALPNDN----VTKDVFADLNRG---VRAVKGVD---LKMASKIYVAK-GLELNDDFAAVSRDVFGSEVQNVDFVKN-VEAAGAINKWVED--QTNNRIKNLVDPDA--------
Serpin-1H LG-QLALASVGESHDELLRALALPNDN----VTKDVFADLNRG---VRAVKGVD---LKMASKIYVAK-GLELNDDFAAVSRDVFGSEVQNVDFVKN-VEAAGAINKWVED--QTNNRIKNLVDPDA--------
serpin-1I LG-QLALASVGESHDELLRALALPNDN----VTKDVFADLNRG---VRAVKGVD---LKMASKIYVAK-GLELNDDFAAVSRDVFGSEVQNVDFVKN-VEAAGAINKWVED--QTNNRIKNLVDPDA--------
serpin-1J LG-QLALASVGESHDELLRALALPNDN----VTKDVFADLNRG---VRAVKGVD---LKMASKIYVAK-GLELNDDFAAVSRDVFGSEVQNVDFVKN-VEAAGAINKWVED--QTNNRIKNLVDPDA--------
serpin-1N LG-QLALASVGESHDELLRALALPNDN----VTKDVFADLNRG---VRAVKGVD---LKMASKIYVAK-GLELNDDFAAVSRDVFGSEVQNVDFVKN-VEAAGAINKWVED--QTNNRIKNLVDPDA--------
serpin-1Y LG-QLALASVGESHDELLRALALPNDN----VTKDVFADLNRG---VRAVKGVD---LKMASKIYVAK-GLELNDDFAAVSRDVFGSEVQNVDFVKN-VEAAGAINKWVED--QTNNRIKNLVDPDA--------
serpin-1Z LG-QLALASVGESHDELLRALALPNDN----VTKDVFADLNRG---VRAVKGVD---LKMASKIYVAK-GLELNDDFAAVSRDVFGSEVQNVDFVKN-VEAAGAINKWVED--QTNNRIKNLVDPDA--------
serpin-2 LA-LLTLGSTDPAQTELLKALGFPDNDDH-KSIRSTFGALTSK---LKAIKGVT---LLVANKVYIKDGGYEVELELKKDAEDIFDTEFEKINFKNS-ASAAQLINQWVEH--KTKNQIKDLFSSSS--------
serpin-3 LA-ILTEAATGSTRSELASALGFGLDR---TEVRRKFSTIIES--LKRESPDYI---LNLGSRIYMGE-GVQPRQRFAAIAQEFYKTELKTTNFFKP-EVAARENNNWVSN--ATQGKIPNLVEADD--------
serpin-4 LA-VISEGATGNTRREINHALRITNRNKN--VTRANYREISN--WLVV-KTKTVE--LAKINAIFVDQ-QRLPQEDFIAIAKEIYDTNMVPLKFEES-DVAADVINRQISN--VTHGRIKNIVNSES--------
serpin-5 MT-GIALGATGNSYKQLSRAFILPKNPDT--L-TEGYKSLTN--VVLDPSSNAVA--LTSKNFVFLDN-DFNVYPDFRLRLQKDFSAAIKVLDFGDP---NSARIANTYIE--KSGGRVSNVLQSDD--------
serpin-6 LL-LAYFSTGGRTEESLKKSLEIEDNMDK-MNLMTAYKVDKRSRMTNNNSDSYE---FTTANKLFVAN-----ELQVRQCMFDLFGEEIEALNFRENPEVSREYINNWVER--ITKNHIKKLLPADG--------
serpin-7 FS-LLTEGSSGQTFSELLNVLGLPNDLRA--TQNL-HLSVKD--I-LKHNSRDVTL--IGQSAMFSDC-SLEIHPEFCRSAN-LCSTDVYSVDPSNT-TKLAGDINYYICT--ATEGKIINAVKPQN--------
serpin-8 LA-AVAEGADGTGKDELYEVLGLPSESCV----REAFYRTALSL--EIPDPGVQ---FTGKRLLIIDQ-HSYVIPDWER---SVHETGLLDFDFDKLHPDSSEERDRPPFFRT----------------------
serpin-9 LS-AMSFGAGYETLSELQRVLRLHPHKCF--NNK-----FFE--I-LQNSANNDTTIMERSSTVYVND-KLAVHDKFKNSVEGAGLCEVKNINLDDV-TQAAAIINDYVRE--ATHEAIDEIVTAGD--------
serpin-10 LA-ILAEGAKGETREQLVTALHLPEDR---ELTRRTYRYIMER---LKNTHEYKYNQPELKNFFYIYK-NYTIFDDYKKVLESCYLTDVRSVERYNPEHEIHVDEDEDDKEEFTIHIPEKNPDDKIDDIPELTPP
serpin-11 LA-MLLEGAEGETAEEIRRALRLSPVKT---EWREELNYYLFS--LETNSSGVL---LHNANAVFVSD-KLKLKKDYDTYLHKVYFSDVTKVDFKDA-NKASQLINVWVKQ--KTNGLIPSIVAPVD--------
serpin-12 LA-MLQQGAAGNTLDEITRALQMTPEKSA-EIFKKVNEEI------QKRNSRNI---LKTANNVFLSE-NFNLNPQFKRIAVNNFDSDLTPTYFGKP-ALAAQNINSWIAS--KTNDKIDKLVSPDD--------
serpin-13 LA-MTLLGSVGNTYQELATTLGFSQDIFTNRRNHEQFGNLLQN---LN--SHVETSKTLYADAIFVDA-QTQLRDVFRDYLDQVYRGEALSVDFRQK-EEVKQMINEWVKS--HTQGKIENFLKQ-T--------
serpin-14 LL-SVAEGARGQTLRELWNITKHHRNRCF--KKQ-----LST--I-LFRINRDLKHTSRRRGIIIVDK-FMNVKNSYIRDVHRLYGIKTLLENFNNP-EKSAAKVNKFVSY--GTENQIPEVVYYDD--------
serpin-15A LA-LLALGTTEPAHSELLTALDIPDND----SIRSSFGAVSAK---LKGIKGVT---FNVANKIYIKDGGYELVPELKEDAEKVFDAEFEKVDFDNS-AAAADLINKWVEN--KTNEKIKDLLSSDS--------
serpin-15B LA-LLALGTTEPAHSELLTALDIPDND----SIRSSFGAVSAK---LKGIKGVT---FNVANKIYIKDGGYELVPELKEDAEKVFDAEFEKVDFDNS-AAAADLINKWVEN--KTNEKIKDLLSSDS--------
serpin-16 LS-LYNTGAGEETQQEINNYLGGACPA----ELAESYSSLSRK---FSTLNPEC---LTVANKIYVNK-KFTLWEKFSEIARNSYHSGVDKINVEAP-AAAAALINEWAEN--MTRGHIKNAMAESD--------
serpin-17 LS-LLALGSTEPAHSELIKALGFPDNDSD-ESIRSSFSELFAK---WKAIKGVT---FEVANKIYIKDGGYDVEDALKKDAVEIFDVDFEKINFEKS-TVAAALINTWVEQ--KTHDKIKNLFSSDS--------
serpin-18 LS-KLSQNAVDETRSQLYNLINLDNSK----EVRYLIPKVAKE---HSATSGDFI--STLTTKVF--S-DKVFSKNFIKCTNEVIMGETGVLDYNNP-SAAAEEINSWFGE--QTRFDRADVVTAAD--------
serpin-19 MS-QICLNAQGLTRTQCYNLLNFNNNE----EMRYFVPKIDDV---L-PKSQDFI--SNVKTVIFARS-DNDFSEHFKSCFGQLAKGETKVIDFGNL-ENVANAINQWFNASSLYY-EEVVTADD----------
serpin-20 LA-ALAEGSDGLARQELFKLLRLPEERCI----RQQFYALISRR--ELLGDDVI----LSRTRLFIYDE-KLVINKNWDNYVCSHWLVGIIKGTLRKNPKKALQSMRDIFSAKLPN----------------------
serpin-21 LG-KLVFGAEGQARQEITATIGIRKRK----QVKKVFTKLIQD---LKFLPGVV---LDVASRIYLAK-KTKLNSNFSKNVKSTFQSDVEKVSFDKP-REAVDEINAWVAR--QTNNMIPTILAPGD--------
serpin-22 LC-KLATVAVGEAKQELLSVLGYKSDG----SIKTCYTEMKEV---FDFLKQAD---LTLVNKMYVNY-TNDIKPDFITNSSLLYGVQVEKVGFNYP-SAAQSFINRWIET--ATYKRIKDVVDKKD--------
serpin-23 LA-AIAESMDGVARQELLQLLGLPEDECT----RQTYYQLASSR--ETFGLDVT---MQRKHVFFIDE-GLNMNTEWVNLASTQFNLHTIPVPIKRAPKDVAYLIRHIISSQLAP----------------------
serpin-24 LA-AMAEGTEGPAQQELFKVLNLPDDKCQ----RQEFYELASKT--EVNSPDAT---LLRTQIFAYDE-TLKLNEIWKNYIYTNCLMNTLPVPMKRDPLAAEAVMRNLISTRIPI----------------------
serpin-25 LA-QLYLFSREPTTSQIGNYLNLRNVE----EIKYIFPDIVEK---FN-SRGR--NDITWKIKVYVNS-SRIYTNEFEEIFDTYFFGKVDHVNFSKR-CKAARVINKWFDNQISDPGVETLSCDA----------
serpin-26 KTLHALYKPHD--AARTLKTLGLDNIE----QAIEITRFIVDE---IEKCSN-----VHQKYEVYADR-SNRFRNSYKNNLADVCRGETKYIDYNND-REVDYYINKWFSSPENQDGRVRNRC----------
serpin-27 LS-QLYLFSGEPTTSEIGNVLNIRNAE----EVKFFFPAAIKK---FN-SKGV--NEITWKIKVYVNN-SRIYTKEFEESYEKYFFGQVDHVDFSKR-CEAARDINNWFDCQISDPGVKMLPCEA----------
serpin-28A LT-QLLLYSVGVTREQLLRVTNLDSNE----EVEKAIPALLSS---FQNQSNVT---FEVAIKFYGNI-NYPFSKRFKKDAIEMFDSEGENLNFTDN-VKAAETINKWVEN--KTHNEIKDLIPPSA--------
Serpin-28B LT-QLLLYSVGVTREQLLRVTNLDSNE----EVEKAIPALLSS---FQNQSNVT---FEVAIKFYGNI-NYPFSKRFKKDAIEMFDSEGENLNFTDN-VKAAETINKWVEN--KTHNEIKDLIPPSA--------
serpin-28C LT-QLLLYSVGVTREQLLRVTNLDSNE----EVEKAIPALLSS---FQNQSNVT---FEVAIKFYGNI-NYPFSKRFKKDAIEMFDSEGENLNFTDN-VKAAETINKWVEN--KTHNEIKDLIPPSA--------
Serpin-29 LA-LCGESSPTISRYIQINKLIKGKKE----------VTTKNIVYHSPCLKPEHFIRDSNLE----------INYVK--TGKLDVFKHWMQELQMTENIEKQ----------
serpin-30 VA-HLAYHAKGDDYEKLLEFMNLRDEH----EMREVLSAAVSQ---INYKSDTS---SKLTFKVYGDH-NQEFTRSYKNDFIDICQGQTGYLDYDCP-EQALKKVNEWFEHQSTKYNSVPTTSNEMFD-------
serpin-31 LTQLALHKPRGADYEKLLQILHVKNIE----EAKALARLIVNI---INKDKN-----QSQKYEVYADR-TQLYTRIFLNNFKEVCDGEARYLNYKNN-VEAESNINDWYSPPENKDHGIRSRC----------
serpin-32 LA-ALAEGTDGVARAELFNLLRLPEEKCI----RQQYYAIASRC--EPPGEDVA---LSRTRLFIFDE-ELVLNKQWENFVCSHWLIGIIRGTLRRNPMKALHLMRSIFAVQLHH----------

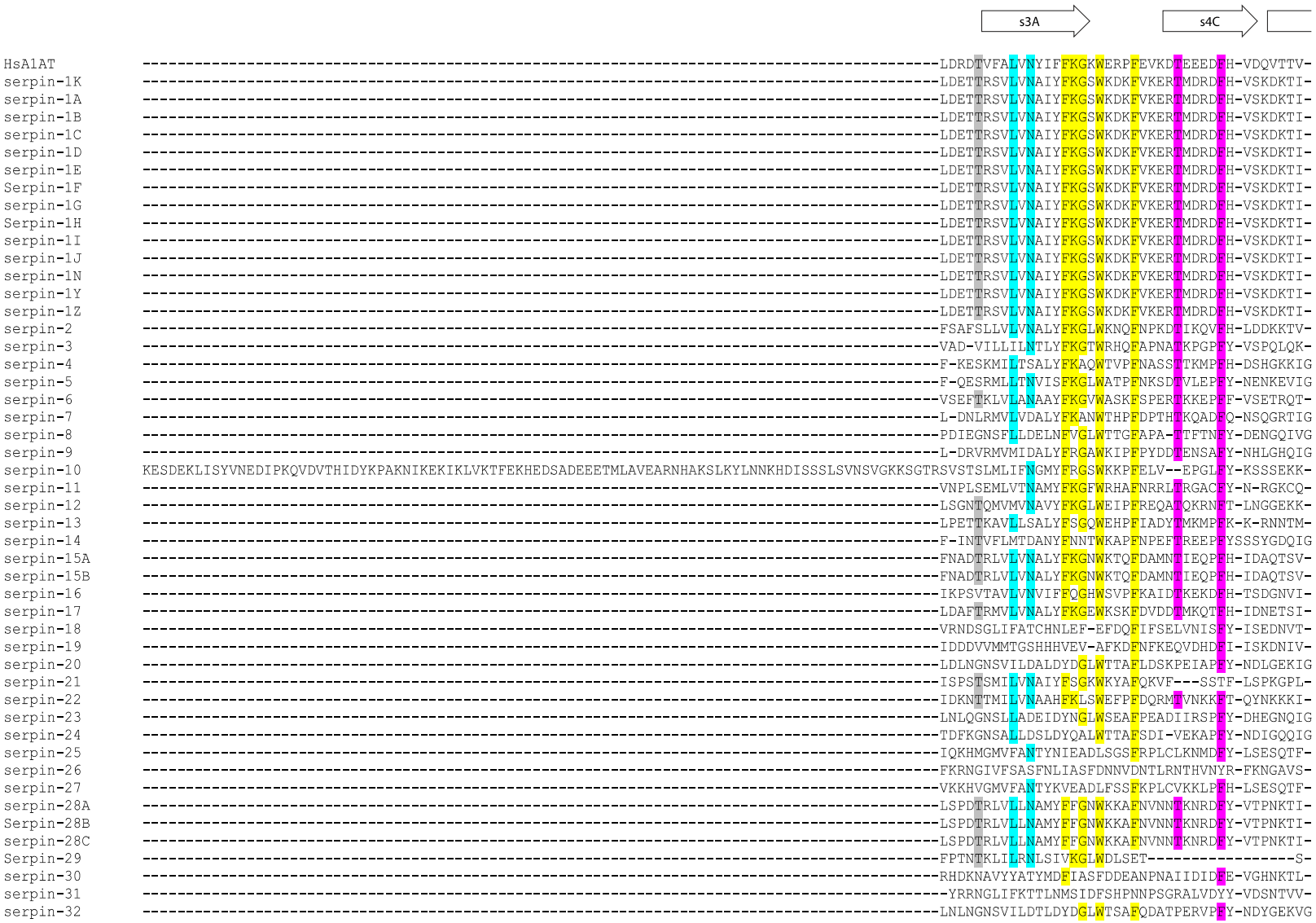
s3A
s4C
HsA1AT
serpin-1K
serpin-1A
serpin-1B
serpin-1C
serpin-1D
serpin-1E
Serpin-1F
serpin-1G
Serpin-1H
serpin-1I
serpin-1J
serpin-1N
serpin-1Y
serpin-1Z
serpin-2
serpin-3
serpin-4
serpin-5
serpin-6
serpin-7
serpin-8
serpin-9
serpin-10
serpin-11
serpin-12
serpin-13
serpin-14
serpin-15A
serpin-15B
serpin-16
serpin-17
serpin-18
serpin-19
serpin-20
serpin-21
serpin-22
serpin-23
serpin-24
serpin-25
serpin-26
serpin-27
serpin-28A
Serpin-28B
serpin-28C
Serpin-29
serpin-30
serpin-31
serpin-32

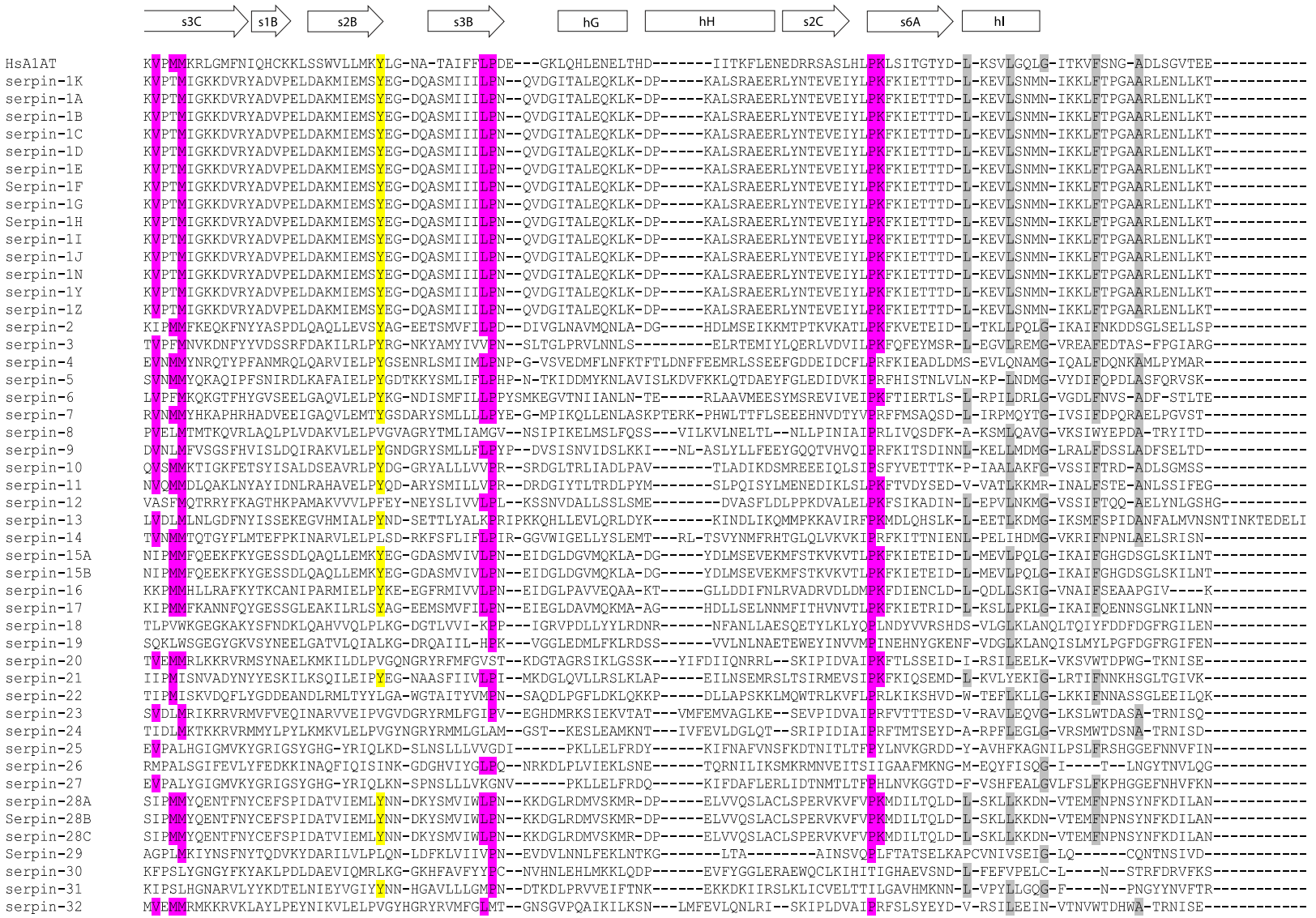
s3C
s1B
s2B
s3B
hG
hH
s2C
s6A
hI
HsA1AT KVPMMKRLGMFNIQHCKKLSSWVLLMKYLG-NA-TAIFFLPDE---GKLQHLENELTHD-------IITKFLENEDRRSASLHLPKLSITGTYD-L-KSVLGQLG-ITKVFSNG-ADLSGVTEE----------
serpin-1K KVPTMIGKKDVRYADVPELDAKMIEMSYEG-DQASMIIILPN--QVDGITALEQKLK-DP-----KALSRAEERLYNTEVEIYLPKFKIETTTD-L-KEVLSNMN-IKKLFTPGAARLENLLKT----------
serpin-1A KVPTMIGKKDVRYADVPELDAKMIEMSYEG-DQASMIIILPN--QVDGITALEQKLK-DP-----KALSRAEERLYNTEVEIYLPKFKIETTTD-L-KEVLSNMN-IKKLFTPGAARLENLLKT----------
serpin-1B KVPTMIGKKDVRYADVPELDAKMIEMSYEG-DQASMIIILPN--QVDGITALEQKLK-DP-----KALSRAEERLYNTEVEIYLPKFKIETTTD-L-KEVLSNMN-IKKLFTPGAARLENLLKT----------
serpin-1C KVPTMIGKKDVRYADVPELDAKMIEMSYEG-DQASMIIILPN--QVDGITALEQKLK-DP-----KALSRAEERLYNTEVEIYLPKFKIETTTD-L-KEVLSNMN-IKKLFTPGAARLENLLKT----------
serpin-1D KVPTMIGKKDVRYADVPELDAKMIEMSYEG-DQASMIIILPN--QVDGITALEQKLK-DP-----KALSRAEERLYNTEVEIYLPKFKIETTTD-L-KEVLSNMN-IKKLFTPGAARLENLLKT----------
serpin-1E KVPTMIGKKDVRYADVPELDAKMIEMSYEG-DQASMIIILPN--QVDGITALEQKLK-DP-----KALSRAEERLYNTEVEIYLPKFKIETTTD-L-KEVLSNMN-IKKLFTPGAARLENLLKT----------
Serpin-1F KVPTMIGKKDVRYADVPELDAKMIEMSYEG-DQASMIIILPN--QVDGITALEQKLK-DP-----KALSRAEERLYNTEVEIYLPKFKIETTTD-L-KEVLSNMN-IKKLFTPGAARLENLLKT----------
serpin-1G KVPTMIGKKDVRYADVPELDAKMIEMSYEG-DQASMIIILPN--QVDGITALEQKLK-DP-----KALSRAEERLYNTEVEIYLPKFKIETTTD-L-KEVLSNMN-IKKLFTPGAARLENLLKT----------
Serpin-1H KVPTMIGKKDVRYADVPELDAKMIEMSYEG-DQASMIIILPN--QVDGITALEQKLK-DP-----KALSRAEERLYNTEVEIYLPKFKIETTTD-L-KEVLSNMN-IKKLFTPGAARLENLLKT----------
serpin-1I KVPTMIGKKDVRYADVPELDAKMIEMSYEG-DQASMIIILPN--QVDGITALEQKLK-DP-----KALSRAEERLYNTEVEIYLPKFKIETTTD-L-KEVLSNMN-IKKLFTPGAARLENLLKT----------
serpin-1J KVPTMIGKKDVRYADVPELDAKMIEMSYEG-DQASMIIILPN--QVDGITALEQKLK-DP-----KALSRAEERLYNTEVEIYLPKFKIETTTD-L-KEVLSNMN-IKKLFTPGAARLENLLKT----------
serpin-1N KVPTMIGKKDVRYADVPELDAKMIEMSYEG-DQASMIIILPN--QVDGITALEQKLK-DP-----KALSRAEERLYNTEVEIYLPKFKIETTTD-L-KEVLSNMN-IKKLFTPGAARLENLLKT----------
serpin-1Y KVPTMIGKKDVRYADVPELDAKMIEMSYEG-DQASMIIILPN--QVDGITALEQKLK-DP-----KALSRAEERLYNTEVEIYLPKFKIETTTD-L-KEVLSNMN-IKKLFTPGAARLENLLKT----------
serpin-1Z KVPTMIGKKDVRYADVPELDAKMIEMSYEG-DQASMIIILPN--QVDGITALEQKLK-DP-----KALSRAEERLYNTEVEIYLPKFKIETTTD-L-KEVLSNMN-IKKLFTPGAARLENLLKT----------
serpin-2 KIPMMFKEQKFNYYASPDLQAQLLEVSYAG-EETSMVFILPD--DIVGLNAVMQNLA-DG-----HDLMSEIKKMTPTKVKATLPKFKVETEID-L-TKLLPQLG-IKAIFNKDDSGLSELLSP----------
serpin-3 TVPFMNVKDNFYYVDSSRFDAKILRLPYRG-NKYAMYIVVPN--SLTGLPRVLNNLS---------ELRTEMIYLQERLVDVILPKFQFEYMSR-L-EGVLREMG-VREAFEDTAS-FPGIARG----------
serpin-4 EVNMMYNRQTYPFANMRQLQARVIELPYGSENRLSMIIMLPNP-G-VSVEDMFLNFKTFTLDNFFEEMRLSSEEFGDDEIDCFLPRFKIEADLDMS-EVLQNAMG-IQALFDQNKAMLPYMAR----------
serpin-5 SVNMMYQKAQIPFSNIRDLKAFAIELPYGDTKKYSMLIFLPHP-N-TKIDDMYKNLAVISLKDVFKKLQTDAEYFGLEDIDVKIPRFHISTNLVLN-KP-LNDMG-VYDIFQPDLASFQRVSK----------
serpin-6 LVPFMKQKGTFHYGVSEELGAQVLELPYKG-NDISMFILLPPYSMKEGVTNIIANLN-TE-----RLAAVMEESYMSREVIVEIPKFTIERTLS-L-RPILDRLG-VGDLFNVS-ADF-STLTE----------
serpin-7 RVNMMYHKAPHRHADVEEIGAQVLEMTYGSDARYSMLLLLPYE-G-MPIKQLLENLASKPTERK-PHWLTTFLSEEEHNVDTYVPRFFMSAQSD-L-IRPMQYTG-IVSIFDPQRAELPGVST----------
serpin-8 PVELMTMTKQVRLAQLPLVDAKVLELPVGVAGRYTMLIAMGV--NSIPIKELMSLFQSS---VILKVLNELTL--NLLPINIAIPRLIVQSDFK-A-KSMLQAVG-VKSIWYEPDA-TRYITD----------
serpin-9 DVNLMFVSGSFHVISLDQIRAKVLELPYGNDGRYSMLLFLPYP--DVSISNVIDSLKKI---NL-ASLYLLFEEYGQQTVHVQIPRFKITSDINNL-KELLMDMG-LRALFDSSLADFSELTD----------
serpin-10 QVSMMKTIGKFETSYISALDSEAVRLPYDG-GRYALLLVVPR--SRDGLTRLIADLPAV-------TLADIKDSMREEEIQLSIPSFYVETTTK-P-IAALAKFG-VSSIFTRD-ADLSGMSS----------
serpin-11 NVQMMDLQAKLNYAYIDNLRAHAVELPYQD-ARYSMILLVPR--DRDGIYTLTRDLPYM-------SLPQISYLMENEDIKLSLPKFTVDYSED-V-VATLKKMR-INALFSTE-ANLSSIFEG----------
serpin-12 VASFMQTRRYFKAGTHKPAMAKVVVLPFEY-NEYSLIVVLPL--KSSNVDALLSSLSME--------DVASFLDLPPKDVALELPKFSIKADIN-L-EPVLNKMG-VSSIFTQQ-AELYNLGSHG----------
serpin-13 LVDLMLNLGDFNYISSEKEGVHMIALPYND-SETTLYALKPRIPKKQHLLEVLQRLDYK-------KINDLIKQMMPKKAVIRFPKMDLQHSLK-L-EETLKDMG-IKSMFSPIDANFALMVNSNTINKTEDELI
serpin-14 TVNMMTQTGYFLMTEFPKINARVLELPLSD-RKFSFLIFLPIR-GGVWIGELLYSLEMT---RL-TSVYNMFRHTGLQLVKVKIPRFKITTNIENL-PELIHDMG-VKRIFNPNLAELSRISN----------
serpin-15A NIPMMFQEEKFKYGESSDLQAQLLEMKYEG-GDASMVIVLPN--EIDGLDGVMQKLA-DG-----YDLMSEVEKMFSTKVKVTLPKFKIETEID-L-MEVLPQLG-IKAIFGHGDSGLSKILNT----------
serpin-15B NIPMMFQEEKFKYGESSDLQAQLLEMKYEG-GDASMVIVLPN--EIDGLDGVMQKLA-DG-----YDLMSEVEKMFSTKVKVTLPKFKIETEID-L-MEVLPQLG-IKAIFGHGDSGLSKILNT----------
serpin-16 KKPMMHLLRAFKYTKCANIPARMIELPYKE-EGFRMIVVLPN--EIDGLPAVVEQAA-KT------GLLDDIFNLRVADRVDLDMPKFDIENCLD-L-QDLLSKIG-VNAIFSEAAPGIV----K----------
serpin-17 KIPMMFKANNFQYGESSGLEAKILRLSYAG-EEMSMVFILPN--EIEGLDAVMQKMA-AG-----HDLLSELNNMFITHVNVTLPKFKIETRID-L-KSLLPKLG-IKAIFQENNSGLNKILNN----------
serpin-18 TLPVWKGEGKAKYSFNDKLQAHVVQLPLKG-DGTLVVI-KPP---IGRVPDLLYYLRDNR------NFANLLAESQETYLKLYQPLNDYVVRSHDS-VLGLKLANQLTQIYFDDFDGFRGILEN----------
serpin-19 SQKLWSGEGYGKVSYNEELGATVLQIALKG-DRQAIIL-HPK---VGGLEDMLFKLRDSS------VVLNLNAETEWEYINVVMPINEHNYGKENF-VDGLKLANQISLMYLPGFDGFRGIFEN----------
serpin-20 TVEMMRLKKRVRMSYNAELKMKILDLPVGQNGRYRFMFGVST--KDGTAGRSIKLGSSK---YIFDIIQNRRL--SKIPIDVAIPKFTLSSEID-I-RSILEELK-VKSVWTDPWG-TKNISE----------
serpin-21 IIPMISNVADYNYYESKILKSQILEIPYEG-NAASFIIVLPI--MKDGLQVLLRSLKLAP-----EILNSEMRSLTSIRMEVSIPKFKIQSEMD-L-KVLYEKIG-LRTIFNNKHSGLTGIVK----------
serpin-22 TIPMISKVDQFLYGDDEANDLRMLTYYLGA-WGTAITYVMPN--SAQDLPGFLDKLQKKP-----DLLAPSKKLMQWTRLKVFLPRLKIKSHVD-W-TEFLKLLG-LKKIFNNASSGLEEILQK----------
serpin-23 SVDLMRIKRRVRMVFVEQINARVVEIPVGVDGRYRMLFGIPV--EGHDMRKSIEKVTAT---VMFEMVAGLKE--SEVPIDVAIPRFVTTTESD-V-RAVLEQVG-LKSLWTDASA-TRNISQ----------
serpin-24 TIDLMKTKKRVRMMYLPYLKMKVLELPVGYNGRYRMMLGLAM--GST--KESLEAMKNT---IVFEVLDGLQT--SRIPIDIAIPRFTMTSEYD-A-RPFLEGLG-VRSMWTDSNA-TRNISD----------
serpin-25 EVPALHGIGMVKYGRIGSYGHG-YRIQLKD-SLNSLLLVVGDI------PKLLELFRDY------KIFNAFVNSFKDTNITLTFPYLNVKGRDD-Y-AVHFKAGNILPSLFRSHGGEFNNVFIN----------
serpin-26 RMPALSGIFEVLYFEDKKINAQFIQISINK-GDGHVIYGLPQ--NRKDLPLVIEKLSNE------TQRNILIKSMKRMNVEITSIIGAAFMKNG-M-EQYFISQG-I----T--LNGYTNVLQG----------
serpin-27 EVPALYGIGMVKYGRIGSYGHG-YRIQLKN-SPNSLLLVKGNV------PKLLELFRDQ------KIFDAFLERLIDTNMTLTFPHLNVKGGTD-F-VSHFEALGVLFSLFKPHGGEFNHVFKN----------
serpin-28A SIPMMYQENTFNYCEFSPIDATVIEMLYNN-DKYSMVIWLPN--KKDGLRDMVSKMR-DP-----ELVVQSLACLSPERVKVFVPKMDILTQLD-L-SKLLKKDN-VTEMFNPNSYNFKDILAN----------
Serpin-28B SIPMMYQENTFNYCEFSPIDATVIEMLYNN-DKYSMVIWLPN--KKDGLRDMVSKMR-DP-----ELVVQSLACLSPERVKVFVPKMDILTQLD-L-SKLLKKDN-VTEMFNPNSYNFKDILAN----------
serpin-28C SIPMMYQENTFNYCEFSPIDATVIEMLYNN-DKYSMVIWLPN--KKDGLRDMVSKMR-DP-----ELVVQSLACLSPERVKVFVPKMDILTQLD-L-SKLLKKDN-VTEMFNPNSYNFKDILAN----------
Serpin-29 AGPLMKIYNSFNYTQDVKYDARILVLPLQN-LDFKLVIIVPN--EVDVLNNLFEKLNTKG-------LTA--------AINSVQPLFTATSELKAPCVNIVSEIG-LQ------CQNTNSIVD----------
serpin-30 KFPSLYGNGYFKYAKLPDLDAEVIQMRLKG-GKHFAVFYYPC--NVHNLEHLMKKLQDP------EVFYGGLERAEWQCLKIHITIGHAEVSND-L-FEFVPELC-L----N--STRFDRVFKS----------
serpin-31 KIPSLHGNARVLYYKDTELNIEYVGIYYNN-HGAVLLLGMPN--DTKDLPRVVEIFTNK------EKKDKIIRSLKLICVELTTILGAVHMKNN-L-VPYLLGQG-F----N--PNGYYNVFTR----------
serpin-32 MVEMMRMKKRVKLAYLPEYNIKVLELPVGYHGRYRVMFGLMT--GNSGVPQAIKILKSN---LMFEVLQNLRI--SKIPLDVAIPRFSLSYEYD-V-RSILEEIN-VTNVWTDHWA-TRNISE----------

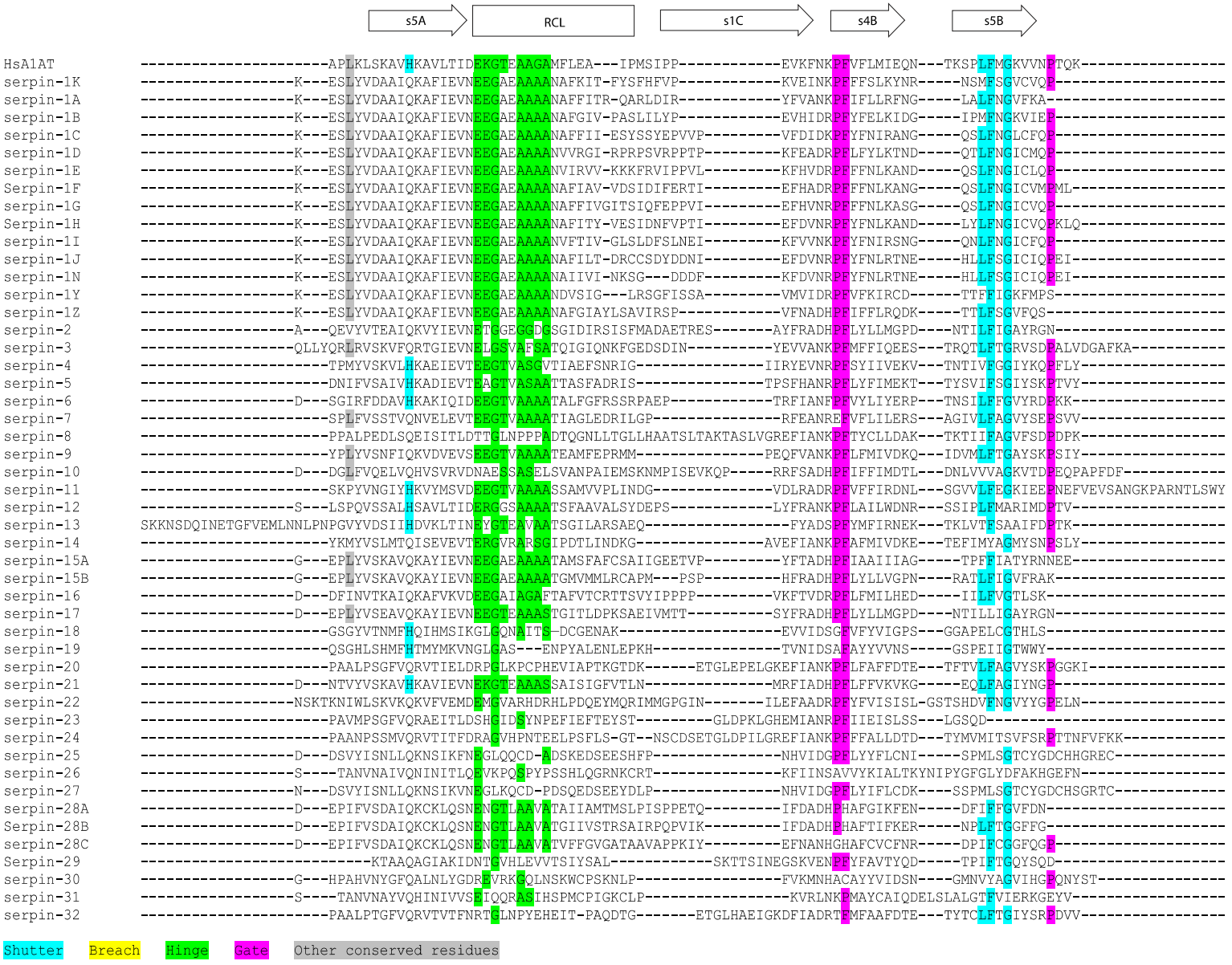
s5A
RCL
s1C
s4B
s5B
HsA1AT
serpin-1K
serpin-1A
serpin-1B
serpin-1C
serpin-1D
serpin-1E
Serpin-1F
serpin-1G
Serpin-1H
serpin-1I
serpin-1J
serpin-1N
serpin-1Y
serpin-1Z
serpin-2
serpin-3
serpin-4
serpin-5
serpin-6
serpin-7
serpin-8
serpin-9
serpin-10
serpin-11
serpin-12
serpin-13
serpin-14
serpin-15A
serpin-15B
serpin-16
serpin-17
serpin-18
serpin-19
serpin-20
serpin-21
serpin-22
serpin-23
serpin-24
serpin-25
serpin-26
serpin-27
serpin-28A
Serpin-28B
serpin-28C
Serpin-29
serpin-30
serpin-31
serpin-32
Shutter
Breach
Hinge
Gate
Other conserved residues

Table B-1. Annotation of serpin gene clusters on scaffold.

Locations of serpin genes were obtained from *M. sexta* JBrowse/Apollo (Poelchau et al., 2015).

scaffold number	serpin gene	Location on scaffold	length (bp)
00101	serpin-2	488980..496460 (- strand)	7481
	serpin-17	503779..514944 (- strand)	11166
00559	serpin-12	44567..50075 (- strand)	5509
	serpin-10	69198..85271 (- strand)	16074
	serpin-11	93634..104693 (- strand)	11060
	serpin-3[a]	108941..117428 (- strand)	8488
00170	serpin-6	212220..222394 (+ strand)	10175
	serpin-15	504696..517545 (+ strand)	12850
00024	serpin-23	119237..125940 (+ strand)	6704
	serpin-24	126242..129331 (- strand)	3090
	serpin-8	128602..131566 (+ strand)	2965
00304	serpin-14	135952..137163 (- strand)	1212
	serpin-9	167191..168399 (+ strand)	1209
00258	serpin-16	113210..117691 (- strand)	4482
	serpin-29	131185..134857 (- strand)	3673
00379	serpin-28	117090..122676 (+ strand)	5587
	serpin-19	135525..138905 (+ strand)	3381
	serpin-18	140554..149737 (- strand)	9184
	serpin-26	159939..167504 (- strand)	7566
	serpin-31	175404..182306 (- strand)	6932
	serpin-30	183177..190063 (- strand)	6887
	serpin-27	200810..208208 (- strand)	7399
	serpin-25	210586..216389 (- strand)	5804
00125	serpin-32	67811..70348 (+ strand)	2538
	serpin-20	72329..74807 (+ strand)	2479

[a] incomplete sequence with only N-terminal fragment

Table B-2. Gene structure annotation of alternative splicing variants.

Information of serpin-15 and serpin-28 exons and CDS were obtained from *M. sexta* JBrowse/Apollo (Poelchau et al., 2015).

	exon	length (bp)	position on scaffold 00170	position in gene	serpin-15A_CDS	serpin-15B_CDS
serpin-15	1	46	212210-212255(+)	1-46	none	none
	2	98	212363-212460(+)	154-251	195-251	195-251
	3	135	214445-214579(+)	2236-2370	2236-2370	2236-2370
	4	207	215126-215332(+)	2917-3123	2917-3123	2917-3123
	5	99	215413-215511(+)	3204-3302	3204-3302	3204-3302
	6	141	215601-215741(+)	3392-3532	3392-3532	3392-3532
	7	210	217130-217339(+)	4921-5130	4921-5130	4921-5130
	8	145	217602-217746(+)	5393-5537	5393-5537	5393-5537
	9A	147	219513-219659(+)	7304-7450	7304-7431	N/A
	9B	1518	220877-222394(+)	8668-10185	N/A	8668-8807

	exon	length (bp)	position on scaffold 00379	position in gene	serpin-28A_CDS	serpin-28B_CDS	serpin-28C_CDS
serpin-28	1	144	117090-117233(+)	1-144	1-144	1-144	1-144
	2	204	117857-118060(+)	768-971	768-971	768-971	768-971
	3	99	118466-118564(+)	1377-1475	1377-1475	1377-1475	1377-1475
	4	141	118708-118848(+)	1619-1759	1619-1759	1619-1759	1619-1759
	5	210	119458-119667(+)	2369-2578	2369-2578	2369-2578	2369-2578
	6	145	120199-120343(+)	3110-3254	3110-3254	3110-3254	3110-3254
	7A	132	121258-121389(+)	4169-4300	4169-4299	N/A	N/A
	7B	139	121633-121771(+)	4544-4682	N/A	4544-4674	N/A
	7C	135	122164-122298(+)	5075-5209	N/A	N/A	5075-5208
	8	73	122604-122676(+)	5515-5587	none	none	none

Table B-3. Changes of *M. sexta* serpin transcript abundance in response to immune challenge.

The data was retrieved from previous work (Zhang et al., 2011). nCF, nCH, nIF and nIH are normalized read numbers. When nIF or IH is zero, nIF/nCF=nIF×825/1618, nIH/nCH=nIH×3980/3352 (Zhang et al., 2011).

	contig#	CF	CH	IF	IH	nCF	nCH	nIF	nIH	nIF/nCF	nIH/nCH
Serpin-1	07639	651	0	1237	14	7713.36	0.00	7473.22	40.83	0.97	16.62
Serpin-2	05255	6	102	24	159	71.09	250.52	144.99	463.67	2.04	1.85
	05821	1	37	6	198	11.85	90.87	36.25	577.40	3.06	6.35
	14248	0	6	0	196	0.00	14.74	0.00	571.57	0.00	38.79
	14456	0	0	1	52	0.00	0.00	6.04	151.64	3.08	180.05
	15111	1	48	8	800	11.85	117.89	48.33	2332.94	4.08	19.79
	15910	1	31	4	472	11.85	76.14	24.17	1376.43	2.04	18.08
	16917	0	40	2	519	0.00	98.24	12.08	1513.49	6.16	15.41
	17048	0	1	0	95	0.00	2.46	0.00	277.04	0.00	112.80
	17058	0	32	4	545	0.00	78.59	24.17	1589.31	12.32	20.22
	17751	0	24	1	269	0.00	58.94	6.04	784.45	3.08	13.31
	18441	0	1	0	65	0.00	2.46	0.00	189.55	0.00	77.18
	sum	9	322	50	3370	106.64	790.84	302.07	9827.49	2.83	12.43
Serpin-3	02693	21	7	310	19	248.82	17.19	1872.84	55.41	7.53	3.22
Serpin-4	04422	47	136	370	211	556.88	334.02	2235.32	615.31	4.01	1.84
	01873	51	141	355	160	604.27	346.30	2144.70	466.59	3.55	1.35
	sum	98	277	725	371	1161.15	680.32	4380.02	1081.90	3.77	1.59
Serpin-5	05831	3	8	97	25	35.55	19.65	586.02	72.90	16.49	3.71
	13453	5	4	58	7	59.24	9.82	350.40	20.41	5.91	2.08
	13454	0	1	17	10	0.00	2.46	102.70	29.16	52.37	11.87
	sum	8	13	172	42	94.79	31.93	1039.12	122.48	10.96	3.84
Serpin-6	01706	7	34	27	81	82.94	83.51	163.12	236.21	1.97	2.83
Serpin-7	08071	14	2	75	2	165.88	4.91	453.11	5.83	2.73	1.19
	08076	18	1	53	1	213.27	2.46	320.19	2.92	1.50	1.19
	sum	32	3	128	3	379.15	7.37	773.30	8.75	2.04	1.19
Serpin-9	08071	14	2	75	2	165.88	4.91	453.11	5.83	2.73	1.19
	08076	18	1	53	1	213.27	2.46	320.19	2.92	1.50	1.19
	10218	12	2	34	2	142.18	4.91	205.41	5.83	1.44	1.19
	14528	29	2	62	1	343.61	4.91	374.57	2.92	1.09	0.59
	sum	73	7	224	6	864.94	17.19	1353.28	17.50	1.56	1.02
Serpin-11	06359	0	2	6	11	0.00	4.91	36.25	32.08	18.48	6.53

Serpin-12	03776	109	5	579	31	1291.48	12.28	3497.98	90.40	2.71	7.36
	06215	29	1	108	8	343.61	2.46	652.47	23.33	1.90	9.50
	06531	45	2	199	11	533.18	4.91	1202.24	32.08	2.25	6.53
	17814	21	0	74	1	248.82	0.00	447.06	2.92	1.80	3.46
	sum	204	8	960	51	2417.09	19.65	5799.75	148.72	2.40	7.57
Serpin-13	02184	53	2	111	1	627.97	4.91	670.60	2.92	1.07	0.59
Serpin-14	09363	0	5	2	4	0.00	12.28	12.08	11.66	6.16	0.95
Serpin-15	05255	6	102	24	159	71.09	250.52	144.99	463.67	2.04	1.85
	05821	1	37	6	198	11.85	90.87	36.25	577.40	3.06	6.35
A	09533	3	26	5	37	35.55	63.86	30.21	107.90	0.85	1.69
B	17895	0	9	4	13	0.00	22.10	24.17	37.91	12.32	1.72
	sum	10	174	39	407	118.48	427.35	235.61	1186.88	1.99	2.78
Serpin-17	05821	1	37	6	198	11.85	90.87	36.25	577.40	3.06	6.35
	16684	0	22	0	100	0.00	54.03	0.00	291.62	0.00	5.40
	05255	6	102	24	159	71.09	250.52	144.99	463.67	2.04	1.85
	14456	0	0	1	52	0.00	0.00	6.04	151.64	3.08	180.05
	15111	1	48	8	800	11.85	117.89	48.33	2332.94	4.08	19.79
	18549	0	0	0	8	0.00	0.00	0.00	23.33	0.00	27.70
	sum	8	209	39	1317	94.79	513.31	235.61	3840.60	2.49	7.48
Serpin-18	03224	98	0	477	0	1161.15	0.00	2881.75	0.00	2.48	0.00
Serpin-19	09511	11	0	1	0	130.33	0.00	6.04	0.00	0.05	0.00
Serpin-22	03224	98	0	477	0	1161.20	0.00	2881.80	0.00	2.48	0.00

CF, control fat body; CH, control hemocyte; IF, induced fat body; IH, induced hemocyte.

References

Irving, J. A., R. N. Pike, A. M. Lesk & J. C. Whisstock (2000) Phylogeny of the serpin superfamily: implications of patterns of amino acid conservation for structure and function. *Genome research,* 10**,** 1845-1864.

Li, J., Z. Wang, B. Canagarajah, H. Jiang, M. Kanost & E. J. Goldsmith (1999) The structure of active serpin 1K from *Manduca sexta*. *Structure,* 7**,** 103-109.

Poelchau, M., C. Childers, G. Moore, V. Tsavatapalli, J. Evans, C. Y. Lee, H. Lin, J. W. Lin & K. Hackett (2015) The i5k Workspace@NAL-enabling genomic data access, visualization and curation of arthropod genomes. *Nucleic Acids Research,* 43**,** D714-D719.

Zhang, S., R. T. Gunaratna, X. Zhang, F. Najar, Y. Wang, B. Roe & H. Jiang (2011) Pyrosequencing-based expression profiling and identification of differentially regulated genes from *Manduca sexta*, a lepidopteran model insect. *Insect biochemistry and molecular biology,* 41**,** 733-746.

Appendix C – Chapter 4 Supplementary Materials

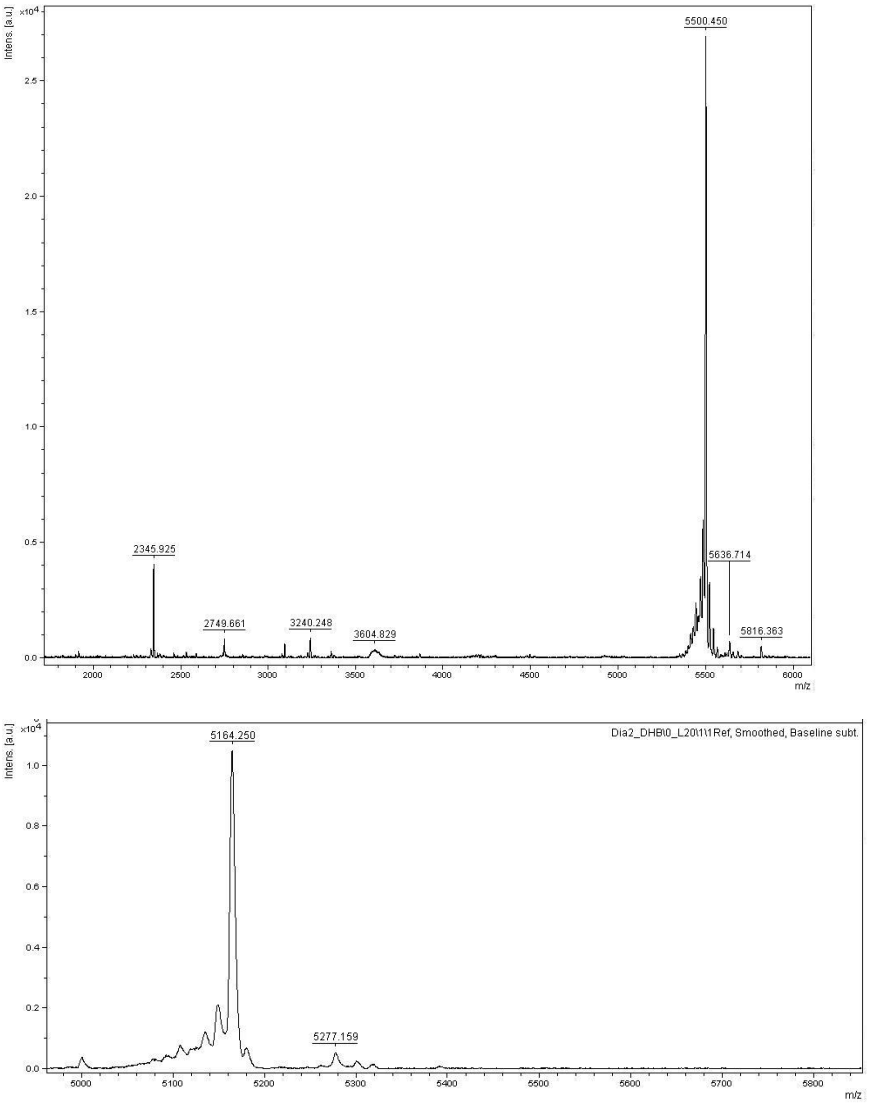

Figure C-1. Mass Spectrometry of purified recombinant diapausin-1 and diapausin-2. MALDI-TOF was also used for confirmation of the correct mass of diapausin-1 (above) and diapausin-2 (below).

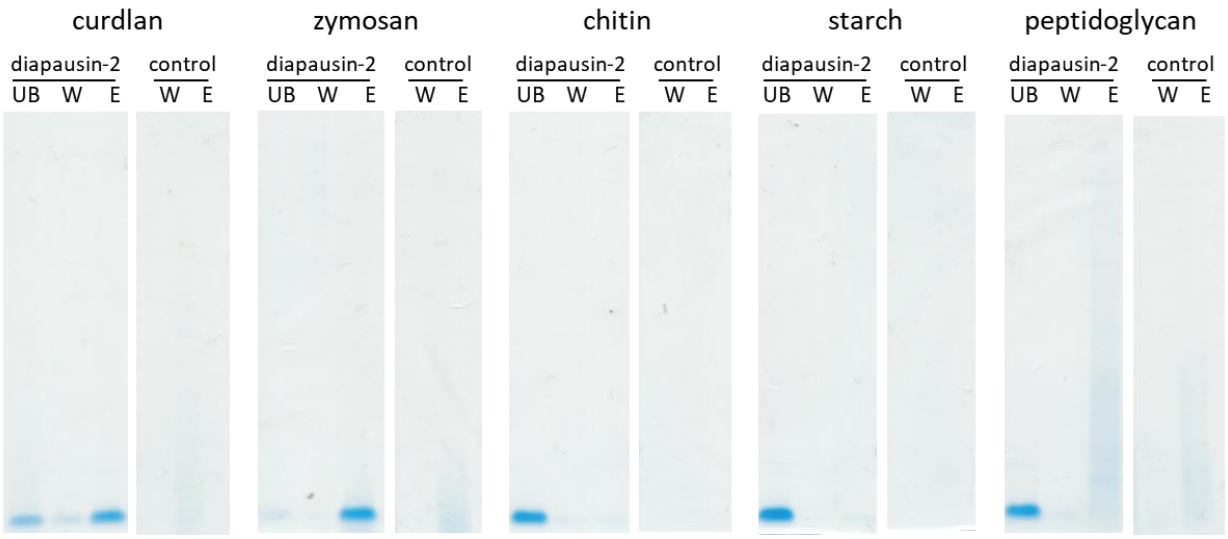

Figure C-2. Binding of recombinant diapausin-2 to β-1,3-glucan.

Recombinant diapausin-2 (10 ng) or deionized water as a control was incubated with 100 μg polysaccharides (curdlan, zymosan, chitin, starch and peptidoglycan) at room temperature for 10 min in 1.5 ml centrifuge tubes. Supernatant was collected as unbound (UB) fraction by centrifugation. The polysaccharides were washed by 10 mM sodium phosphate, pH 7.4 and subjected to centrifugation for collecting supernatant as wash (W) fraction. Bound diapausin-2 was eluted by heating the polysaccharides in 2×SDS loading buffer supplemented with β-mercaptoethanol at 95°C for 5 min and colleting supernatant as elution (E) fraction after centrifugation. Each fraction with reducing SDS loading buffer was subjected to 4-12% Bis-Tris NuPAGE gel, followed by Instant Blue staining.

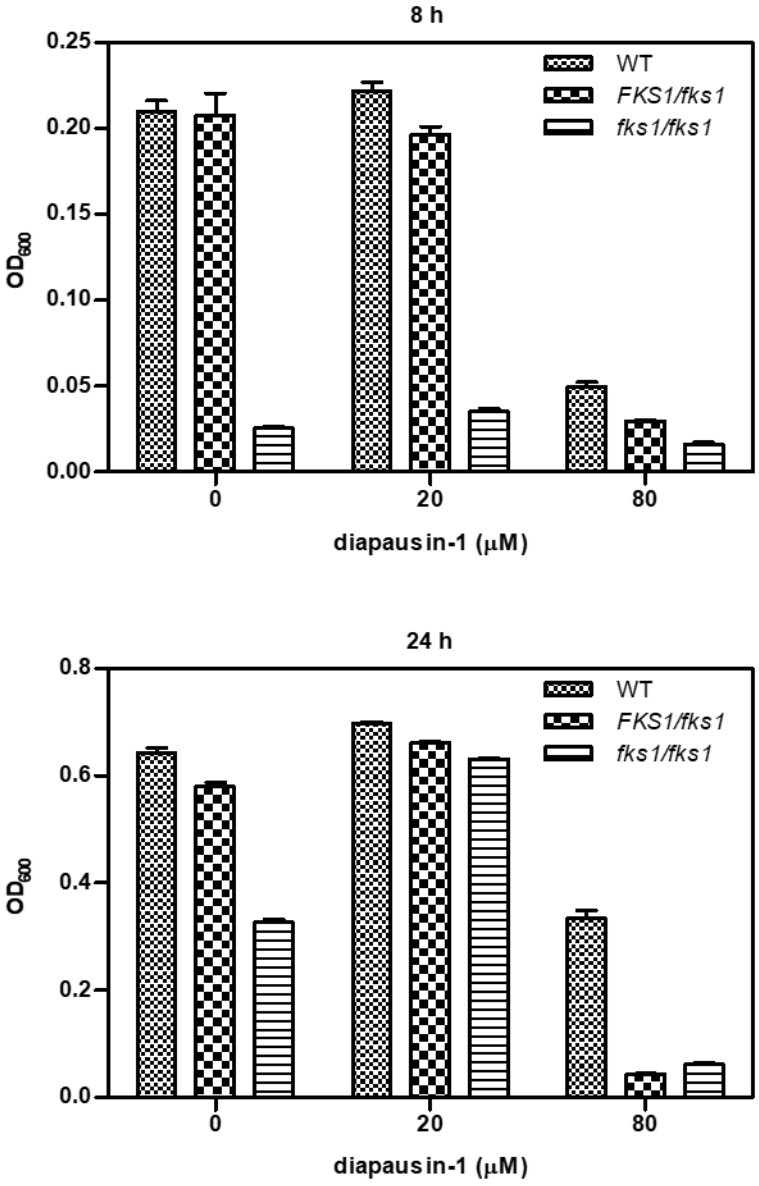

Figure C-3. Antifungal assay of diapausin-1 against FKS1 mutants.

Antifungal assay was performed by using WT (BY4743), *FKS1/fks1* (hom dip; MATa/MATα; YLR342w::kanMX4/YLR342w::kanMX4), and *fks1/fks1* (BY4743; MATa/MATα; YLR342w/YLR342w::kanMX4). OD_{600} was measured after 8 h and 24 h of incubation of recombinant diapausin-1 at 0, 20 and 80 μM with three yeast strains.

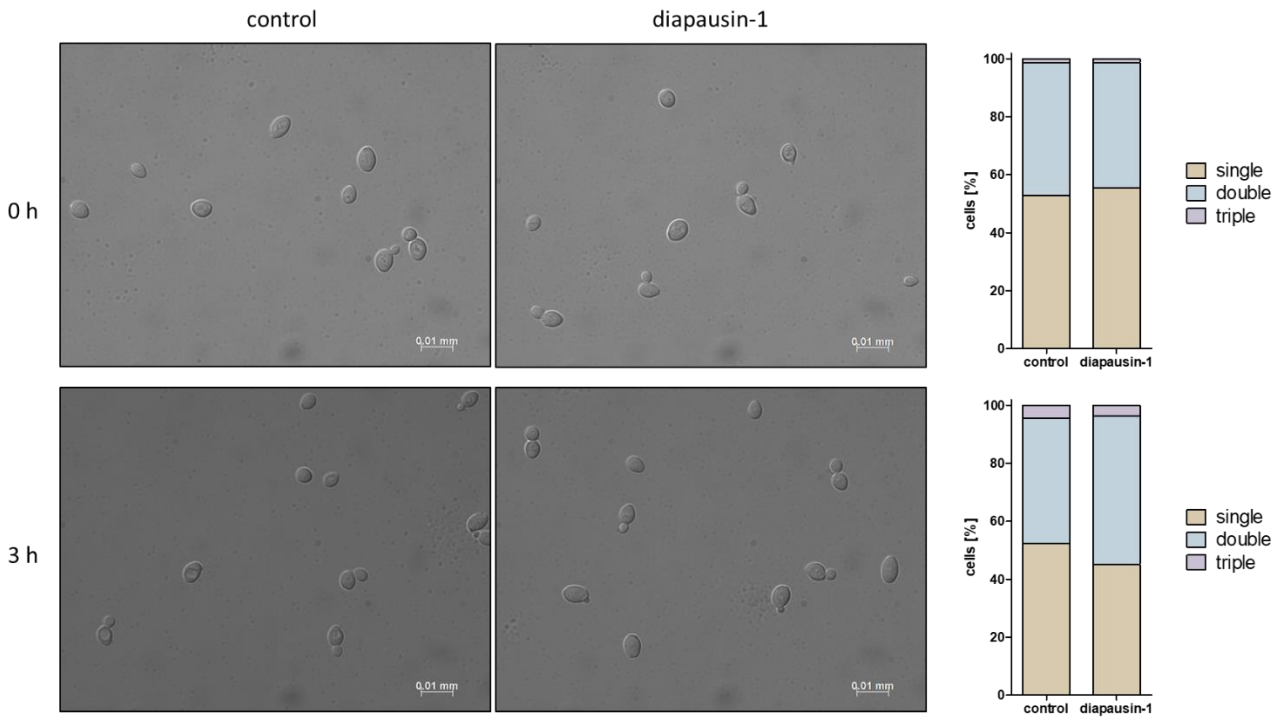

Figure C-4. Microscopic observation of *S. cerevisiae* treated by diapausin-1 in YP medium. Yeast cells were incubated at 30°C in YP medium, which restrains the cell growth due to lack of carbon source, supplemented with or without 80 μM recombinant diapausin-1. Samples were examined and imaged by DIC microscope at 0 h and after 3 h of incubation. The number of single (a cell without a bud), double (a mother cell with a bud), triple (a mother cell with probably two buds) and cluster (with four or more cells sticking to each other) was counted in each sample (n>60) and reflected by percentage in bar graph.

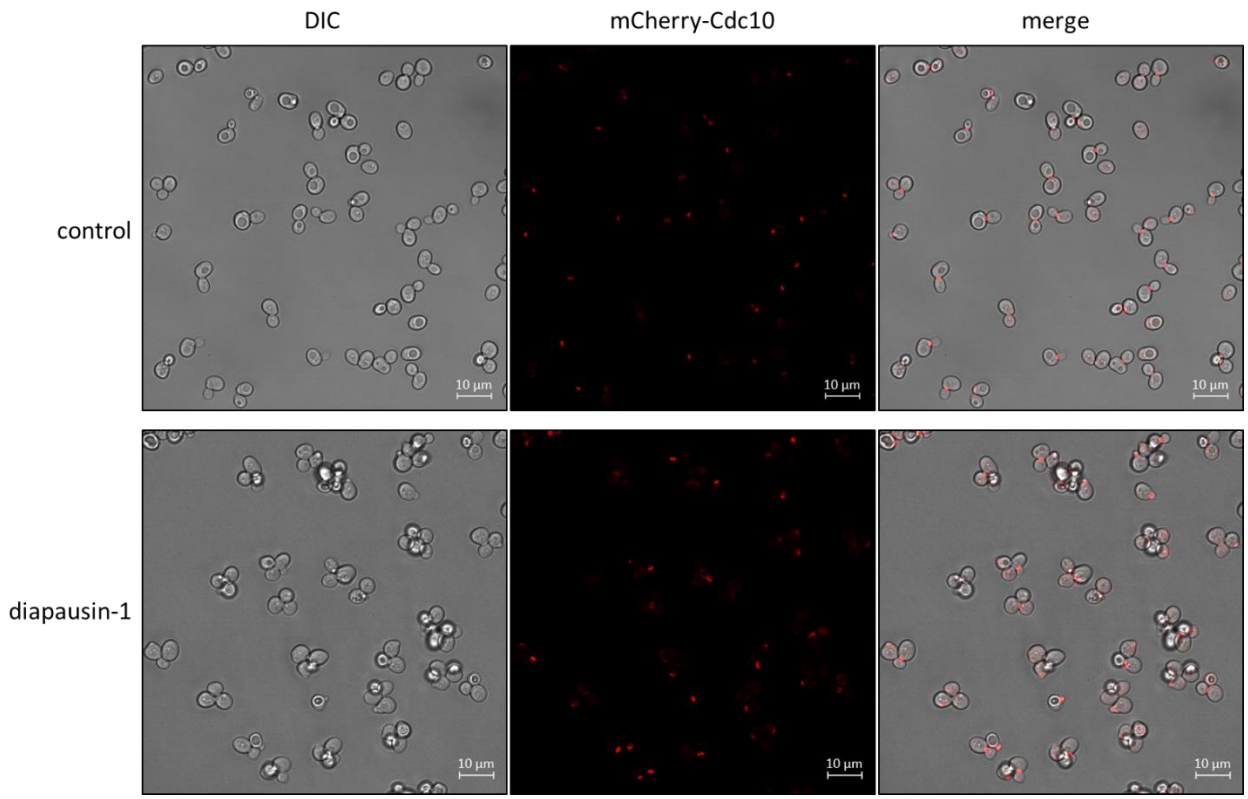

Figure C-5. Microscopic observations of GFY-42 treated by diapausin-1.

S. cerevisiae strain GFY-42 (BY4741; *cdc10Δ::CDC10::mCherry::SpHIS5)* (Finnigan et al., 2015) was cultured overnight and diluted to OD_{600}=1.0, followed by incubation with 80 μM recombinant diapausin-1 or sterile water as a control at 30°C for 2 h. Then the cells were examined and imaged using an LSM airy scan 880 microscope.

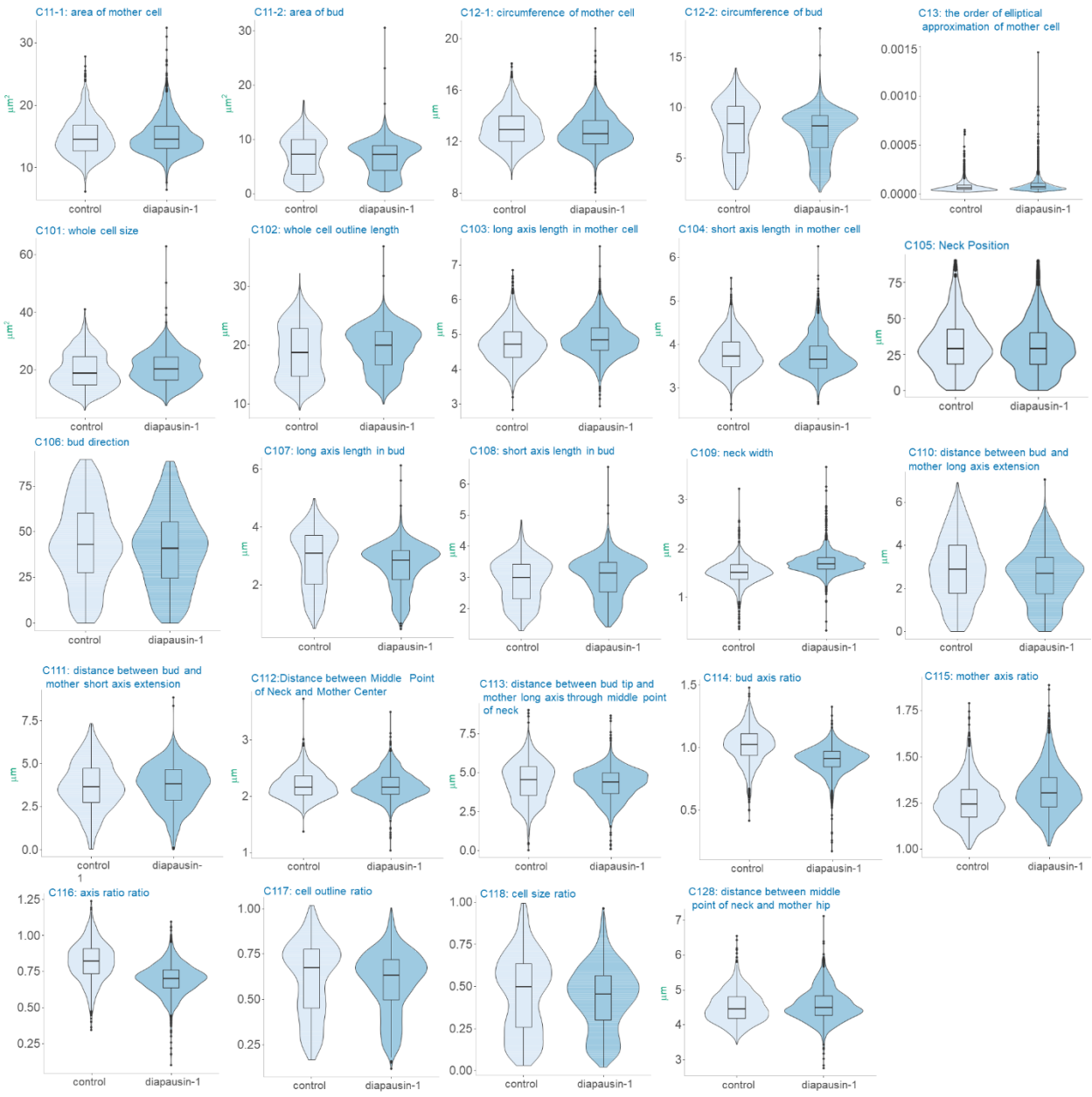

Figure C-6. Morphological changes of *S. cerevisiae* treated by diapausin-1 (complete). Morphological parameters which have a significant difference ($p<0.05$) between control (sterile H_2O treatment) and diapausin-1 treatment were shown using violin plots.

References

Finnigan, G., J. Takagi, C. Cho & J. Thorner (2015) Comprehensive genetic analysis of paralogous terminal septin subunits Shs1 and Cdc11 in *Saccharomyces cerevisiae*. *Genetics*, 200(3)**,** 821-841.